ANTIOXIDANT AND ANTI-INFLAMMATORY EFFECTS OF
OROXYLUM INDICUM (L.) KURZ AND *GYMNEMA INODORUM*
(LOUR.) DECNE. EXTRACTS ON RAW264.7 MACROPHAGES

BENJAWAN   DUNKHUNTHOD

A Thesis Submitted in Partial Fulfillment of the Requirements for the

Degree of Doctor of Philosophy in Biomedical Sciences

Suranaree University of Technology

Academic Year 2021

ผลการต้านอนุมูลอิสระและต้านการอักเสบของสารสกัดจากเพกาและผักเชียงดาในเซลล์แมโครฟาจ (RAW264.7)
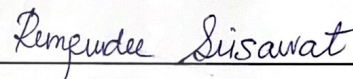
นางสาวเบญจวรรณ ดุนขุนทด

วิทยานิพนธ์นี้เป็นส่วนหนึ่งของการศึกษาตามหลักสูตรปริญญาวิทยาศาสตรดุษฎีบัณฑิต

สาขาวิชาชีวเวชศาสตร์

มหาวิทยาลัยเทคโนโลยีสุรนารี

ปีการศึกษา 2564

ANTIOXIDANT AND ANTI-INFLAMMATORY EFFECTS OF *OROXYLUM INDICUM* (L.) KURZ AND *GYMNEMA INODORUM* (LOUR.) DECNE. EXTRACTS ON RAW264.7 MACROPHAGES
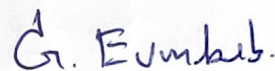
Suranaree University of Technology has approved this thesis submitted in partial fulfillment of the requirements for the Degree of Doctor of Philosophy.

Thesis Examining Committee

_____

(Asst. Prof. Dr. Rungrudee Srisawat)

Chairperson

_____

(Prof. Dr. Griangsak Eumkeb)
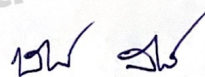
Member (Thesis Advisor)

_____

(Asst. Prof. Dr. Chutima Talabnin)

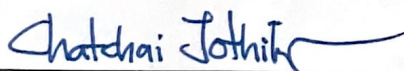Member (Thesis Co-Advisor)

_____

(Asst. Prof. Dr. Panida Khunkaewla)
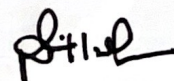
Member

_____

(Asst. Prof. Dr. Patcharawan Sittisart)

Member

_____ _____

(Assoc. Prof. Dr. Chatchai Jothityangkoon)   (Prof. Dr. Santi Maensiri)

Vice Rector for Academic Affairs   Dean of Institute of Science

and Quality Assurance

เบญจวรรณ ดุนขุนทด : ผลการต้านอนุมูลอิสระและต้านการอักเสบของสารสกัดจากเพกา และผักเชียงดาในเซลล์แมโครฟาจ (RAW264.7) (ANTIOXIDANT AND ANTI-INFLAMMATORY EFFECTS *OF OROXYLUM INDICUM* (L.) KURZ AND *GYMNEMA INODORUM* (LOUR.) DECNE. EXTRACTS ON RAW264.7 MACROPHAGES) อาจารย์ที่ปรึกษา : ศาสตราจารย์ เภสัชกร ดร.เกรียงศักดิ์ เอื้อมเก็บ, 148 หน้า.

คำสำคัญ: เพกา/ ผักเชียงดา/ พฤกษเคมี/ ต้านอนุมูลอิสระ/ ต้านการอักเสบ/ เซลล์แมโครฟาจ (RAW264.7)

การค้นพบทางการแพทย์ที่สำคัญที่สุดอย่างหนึ่งในช่วงสองทศวรรษที่ผ่านมาคือการที่ระบบภูมิคุ้มกันและกระบวนการอักเสบมีส่วนเกี่ยวข้องกับโรคต่างๆ การใช้สมุนไพรเพื่อเป็นยาแผนโบราณในการรักษาโรคต่างๆ รวมทั้งโรคที่เกี่ยวข้องกับการอักเสบมีมาอย่างยาวนาน หลายประเทศในแถบเอเชียนิยมบริโภคเพกาและผักเชียงดา เพื่อใช้เป็นอาหารและยาสมุนไพรมาเป็นเวลาหลายพันปีโดยไม่พบผลข้างเคียงที่เป็นอันตรายต่อร่างกาย การศึกษานี้มีวัตถุประสงค์เพื่อตรวจสอบสารพฤกษเคมี ฤทธิ์ต้านอนุมูลอิสระและฤทธิ์ต้านการอักเสบของสารสกัดหยาบจากเพกา (OIE) และผักเชียงดา (GIE) ในเซลล์แมโครฟาจ (RAW264.7) ที่ถูกกระตุ้นด้วย LPS ร่วมกับ IFN-γ การตรวจสอบสารพฤกษเคมีพบว่า สารสกัดจากเพกามีองค์ประกอบของสารกลุ่มฟลาโวนอยด์ 5 ชนิด (ลิวทิโอลิน เอพิเจนิน ไบคาลีน ออโรไซลินเอ และเคอซิติน) และสารจำพวกน้ำมันระเหย 27 ชนิด ในสารสกัดหยาบผักเชียงดาพบองค์ประกอบของน้ำมันระเหย 16 ชนิด ทั้งสารสกัดหยาบจากเพกาและผักเชียงดาสามารถลดการสร้างอนุมูลอิสระและกระตุ้นการแสดงออกของยีนต้านอนุมูลอิสระในเซลล์แมโครฟาจ (RAW264.7) ที่ถูกกระตุ้นด้วย LPS ร่วมกับ IFN-γ นอกจากนี้ยังพบว่า ทั้งสารสกัดหยาบจากเพกาและผักเชียงดามีฤทธิ์ต้านการอักเสบโดยการยับยั้งการหลั่งไนตริกออกไซด์ (NO) และอินเตอร์ลิวคิน 6 (IL-6) และลดการแสดงออกของยีนไซโคลออกซิจิเนส 2 (COX-2) ไนตริกออกไซด์ซินเทส (iNOS) และ อินเตอร์ลิวคิน 6 ในเซลล์แมโครฟาจ (RAW264.7) ที่ถูกกระตุ้นด้วย LPS ร่วมกับ IFN-γ การศึกษากลไกการออกฤทธิ์ในการต้านการอักเสบแสดงให้เห็นว่าทั้งสารสกัดหยาบจากเพกาและผักเชียงดา มีฤทธิ์ยับยั้งการเคลื่อนที่เข้าสู่นิวเคลียสของทรานสคริปชันแฟคเตอร์ NF-kB (NF-kB p65) และลดการฟอสโฟรีเลชั่นของโปรตีน NF-kB p65 (p-NF-kB p65) ได้เล็กน้อย ดังนั้นจึงเป็นไปได้ที่ฤทธิ์การต้านอนุมูลอิสระของทั้งสารสกัดหยาบจากเพกาและผักเชียงดาจะส่งผลในการควบคุมกระบวนการอักเสบโดยผ่านการควบคุมระดับของอนุมูลอิสระภายในเซลล์ ซึ่งนำไปสู่การยับยั้งการหลั่งของไซโตไคน์และยีนที่เกี่ยวข้องกับการอักเสบ ดังนั้นโดยภาพรวม ทั้งสารสกัดหยาบจากเพกาและผักเชียงดาอาจใช้เป็น

แหล่งอาหารเสริมที่มีศักยภาพในการพัฒนาผลิตภัณฑ์เสริมอาหารเพื่อสุขภาพหรือยาสมุนไพรต้าน
การอักเสบในอนาคตได้

สาขาวิชาปรีคลินิก   ลายมือชื่อนักศึกษา _เบญจวรรณ ดุนขุนทด_

ปีการศึกษา 2564   ลายมือชื่ออาจารย์ที่ปรึกษา _____

BENJAWAN DUNKHUNTHOD : ANTIOXIDANT AND ANTI-INFLAMMATORY EFFECTS OF *OROXYLUM INDICUM* (L.) KURZ AND *GYMNEMA INODORUM* (LOUR.) DECNE. EXTRACTS ON RAW264.7 MACROPHAGES. THESIS ADVISOR : PROF. GRIANGSAK EUMKEB, Ph.D. 148 PP.

Keyword: *OROXYLUM INDICUM / GYMNEMA INODORUM* / PHYTOCHEMICAL / ANTI-OXIDANT/ ANTI-INFLAMMATION/ RAW264.7 MACROPHAGES

One of the most important medical discoveries of the past two decades has been that the immune system and inflammatory processes are involved in many diseases. Herbs, like traditional medicine, have a long history of treating various conditions, including inflammatory diseases. *Oroxylum indicum* (*O. indicum*) and *Gymnema inodorum* (*G. inodorum*) have been used in many Asian countries as plant-based food and herbal medicine for thousands of years without any known adverse effects. The present study aimed to investigate the phytochemicals and explore the antioxidant and anti-inflammatory activities of *O. indicum* extract (OIE) and *G. inodorum* extract (GIE) on LPS plus IFN-γ-induced RAW264.7 cells. Five flavonoids (luteolin, apigenin, baicalein, oroxylin A, and quercetin) and 27 volatile compounds were found in OIE. Sixteen volatile compounds were found in GIE. Both OIE and GIE could also effectively attenuate intracellular reactive oxygen species (ROSs) generation and upregulate anti-oxidant genes expression in LPS plus IFN-γ-induced RAW264.7. Both OIE and GIE possessed the potent anti-inflammatory action through suppressing nitric oxide (NO) and IL-6 secretion and also downregulation of the expression of cyclooxygenase-2 (COX-2), inducible nitric oxide synthase (iNOS), and IL-6 mRNA levels in LPS plus IFN-γ-induced RAW264.7 cells. Mechanism studies showed that both OIE and GIE suppressed the NF-kB p65 nuclear translocation and slightly decreased the phosphorylation of the NF-kB p65 (p-NF-kB p65) protein. Therefore, it is possible that the antioxidant properties of both OIE and GIE could modulate the inflammation process by regulating the ROS levels, which lead to the suppression of proinflammatory cytokines and genes. Collectively, *O. indicum* and *G.*

inodorum may be used as a potential nutraceutical source for the development of health food supplements or a novel anti-inflammatory herbal medicine.

School of Preclinical Sciences

Academic Year 2021

Student's Signature _Benjawan Dunkhunthod_

Advisor's Signature _G. Eumkeb._

ACKNOWLEDGEMENTS

Benjawan Dunkhunthod

CONTENTS

CONTENTS (Continued)

CONTENTS (Continued)

CONTENTS (Continued)

LIST OF TABLES

LIST OF FIGURES

LIST OF FIGURES (Continued)

LIST OF ABBREVIATIONS

µg/mL	=	Microgram per milliliter
µL	=	Microliter
µM	=	Micromolar
g	=	Gravitational acceleration
ANOVA	=	Analysis of variance
BSA	=	Bovine serum albumin
COX-2	=	Cyclooxygenase-2
DCFH-DA	=	2',7'-dichlorofluorescin-diacetate
DI water	=	Distilled water
DMSO	=	Dimethylsulfoxide
DNA	=	Deoxyribonucleic acid
DPPH	=	2,2-diphenyl-1-picrylhydrazyl
ECL	=	Enhanced chemiluminescence system
EDTA	=	Ethylenediaminetetraacetic acid
ELISA	=	Enzyme-linked immunosorbent assay
FBS	=	Fetal bovine serum
FRAP	=	Ferric reducing antioxidant power
GCLC	=	Glutamate-Cysteine Ligase Catalytic Subunit
GCLM	=	Glutamate-Cysteine Ligase Modifier Subunit
GIE	=	*G. inodorum* extract
GSTP1	=	Glutathione S-Transferase Pi 1
g	=	Gram
h	=	Hour
HBSS	=	Hank's balanced salt solution
HEPES	=	4-(2-hydroxylethyl)-1-piperazineethanesulfonic acid
IC_{50}	=	Median inhibition concentration
IFN-γ	=	Interferon-γ

LIST OF ABBREVIATIONS (Continued)

IL-6	=	Interleukin-6
IL-10	=	Interleukin-10
iNOS	=	Inducible nitric oxide synthase
kg	=	Kilogram
L	=	Liter
LPS	=	Lipopolysaccharide
M	=	Molar
mAb	=	Monoclonal antibody
min	=	Minute
mg	=	Milligram
mg/mL	=	Milligram per milliliter
mL	=	Milliliter
mM	=	Millimolar
MTT	=	3-(4,5-dimethythiazol-2-yl)-2,5-diphenyltetrazolium bromide
NF-kB	=	Nuclear factor-kappaB
nm	=	Nanometer
NO	=	Nitric oxide
NQO1	=	NADPH quinone oxidoreductase
NOS	=	Nitric oxide synthase
OD	=	Optical density
OIE	=	*O. indicum* extract
PBS	=	Phosphate buffered saline
p-NF-kB	=	Phosphorylated-nuclear factor-kappaB
PMSF	=	Phenylmethanesulfonyl fluoride
RNA	=	Ribonucleic acid
RNS	=	Reactive nitrogen species
ROS	=	Reactive oxygen species
rpm	=	Revolution per minute
RPMI 1640	=	Roswell Park Memorial Institute number 1640

LIST OF ABBREVIATIONS (Continued)

RT	=	Room temperature
SOD2	=	Superoxide dismutase 2
TEMED	=	N, N, N´, N´-tetramethylethylenediamine
TLR4	=	Toll-like receptor 4
TNF-α	=	Tumor necrosis factor-alpha
TREA	=	Trolox equivalent antioxidant capacity
Trolox	=	6-Hydroxy-2, 5, 7, 8-tetramethylchroman-2-carboxylic acid
VCEAC	=	Vitamin C equivalent antioxidant capacity
SD	=	Standard deviation
SDS-PAGE	=	Sodium dodecyl sulfate-polyacrylamide gel electrophoresis
VH	=	Vehicle
v/v	=	volume by volume
w/v	=	weight by volume

CHAPTER I

INTRODUCTION

1.1 Introduction

Noncommunicable chronic diseases such as inflammatory bowel diseases, cancer, diabetes, obesity, pulmonary, cardiovascular, rheumatoid arthritis, and neurodegenerative diseases are becoming the leading cause of death worldwide. An Unhealthy diet, smoking, lack of exercise, stress, radiation exposure, and environmental pollution are among the common causes of chronic diseases. Most of these risk factors are closely linked to chronic inflammation, leading to various chronic diseases.

Inflammation is the immune system's response to injury, irritation, or infection caused by invading pathogens, radiation exposure, very high or low temperatures, or autoimmune processes. Lipopolysaccharide (LPS), an outer membrane component of Gram-negative bacteria, has been reported as one of the major causes of septic shock (Raetz et al., 1991). In response to endotoxin stimulation, a variety of immune cells can be activated. In the innate immunity system, macrophages play pivotal roles in the cellular host's defense against infection and tissue injury (Calandra and Roger, 2003; T.-L. Chen et al., 2009). Inflammation is considered beneficial when short-term and under control within the immune system (acute inflammation). However, if the inflammatory process goes on for too long (chronic inflammation) or if the inflammatory response occurs in places where it is not needed, it can become problematic (Aggarwal et al., 2009).

Mast cells, monocytes, macrophages, lymphocytes, and other immune cells are first activated during inflammation responses. The cells are recruited to the site of damage, resulting in the generation of reactive oxygen species (ROS) that damage macromolecules, including DNA. At the same time, these inflammatory cells also produce large amounts of inflammatory mediators such as metabolites of

arachidonic acid, nitric oxide (NO), proinflammatory cytokines, chemokines, prostaglandins, inducible enzymes, and growth factors (Calixto et al., 2003). Excessive production of intracellular ROS can cause oxidative stress associated with redox unbalance (Ye et al., 2014). This imbalance leads to damage of essential biomolecules and cells, with potential impact on the whole organism (Durackova, 2010). Accordingly, excessive oxidative stress and chronic inflammation can cause chronic diseases such as cancer, aging, diabetes, obesity, cardiovascular diseases, Alzheimer's, and Parkinson's disease (W. J. Huang et al., 2016; Khansari et al., 2009; Li et al., 2015; Maiese, 2015; Mathieu et al., 2010; Reuter et al., 2010; Rinnerthaler et al., 2015). Therefore, oxidative stress and inflammation must be adequately controlled to prevent the progressions of chronic diseases.

The nuclear factor kappa light chain enhancer of activated B cells (NF-kB) plays a key role in regulating many genes responsible for the generation of inflammatory mediators. NF-kB activation involves the rapid phosphorylation of I$\varkappa$Bs in response to proinflammatory stimuli. Free NF-kB produced by this process translocates into the nucleus, where it induces the expression of inducible nitric oxide synthase (iNOS), inducible cyclooxygenase-2 (COX-2), tumor necrosis factor α (TNF-α), interleukin-6 (IL-6), interleukin-1β (IL-1β), and prostaglandin E2 (PGE2) mRNA (Oeckinghaus and Ghosh, 2009; Taniguchi and Karin, 2018), the activation of NF-kB is closely linked with ROS generation during inflammation (Taniguchi and Karin, 2018). ROS were found to mediate inhibitor of NF-kB α (IKBα) kinase (IKKα and IKKβ) phosphorylation and release of free NF-kB dimers (Kamata et al., 2002). Studies further support the importance of ROS on NF-kB activation that activation of NF-kB by nearly all stimuli can be blocked by antioxidants, such as L-cysteine, N-acetylcysteine (NAC), thiols, green tea polyphenols, and vitamin E (Nomura et al., 2000; Schulze-Osthoff et al., 1997).

The nuclear factor (erythroid-derived 2)-like 2 (Nrf2) regulates the expression of phase II detoxifying enzymes, including NADPH, NAD(P)H quinone oxidoreductase 1 (NQO1), glutathione peroxidase, ferritin, heme oxygenase-1 (HO-1), and antioxidant genes that protect cells from various injuries via their anti-inflammatory effects, thus influencing the course of many diseases (Arisawa et al., 2007; Braun et al., 2002; X.-L.

Chen et al., 2006). It has been reported that activation of Nrf2 prevents LPS-induced transcriptional upregulation of pro-inflammatory cytokines, including IL-6 and IL-1β (Kobayashi et al., 2016). Numerous studies have demonstrated that protein phosphorylation of the IKK complex is a potential mechanism for activating Nrf2 and NF-kB pathways (O. J. Kwon et al., 2015; Lampiasi and Montana, 2018; S. C. Lee et al., 2017). Therefore, in response to inflammatory stimuli, upregulation of Nrf2 signaling inhibits the overproduction of pro-inflammatory cytokines and chemokines and limits the activation of NF-kB.

Over the past few decades, studies have investigated the possible protective role of plant foods against chronic diseases. Several epidemiological studies have revealed that higher consumption of fruits and vegetables is associated with a lower risk of chronic diseases (Ames and Wakimoto, 2002). The usages of herbs or traditional herbal medicines that are complementary and alternative medicines for managing inflammation have increased because of concerns about the adverse side effects of nonsteroidal anti-inflammatory drugs (Khansari et al., 2009). These indigenous vegetables can be readily available in the local area. Consequently, consuming these vegetables would be appropriate to control and reduce the cost of inflammatory management.

Gymnema inodorum Decne (*G. inodorum*) is one of the local Thai vegetables belonging to the family Asclepiadaceae. The leaves of *G. inodorum* have been known to be effective for some diseases, including diabetes mellitus, rheumatic arthritis, and gout (Bespinyowong et al., 2013). It is widely used in traditional Thai cuisines and healthy herbal products to prevent diabetes. Recently, this plant has been reported to contain phenolics, flavonoids, a mixture of steroids containing stigmasterol, saponins, triterpenoid, and gymnemic acid, also possessed antioxidant activity (Chanwitheesuk et al., 2005; Tiamyom et al., 2019).

Oroxylum indicum (L.) Kurz (*O. indicum*) is a species of flowering plant belonging to the Bignoniaceae family. It has been used as an essential medicinal plant in several Asian countries for the treatment of a variety of diseases such as wounds, diabetes, jaundice, gastric ulcers, diarrhea, cancer, rheumatoid arthritis, and osteoarthritis (Bhushan and Kumar, 2013; Chhetri et al., 2005; Laupattarakasem et al.,

2003; Devanathan, 2001; Ripunjoy, 2013). This medicinal tree is also an important source of several medicinally essential flavonoids, including baicalein, chrysin, and oroxylin A, which have a large number of therapeutic potentials. The crude extracts and their isolates exhibit a wide spectrum of *in vitro* and *in vivo* pharmacological activities involving antioxidant, anti-diabetic, anti-adipogenesis, hepatoprotective, and anti-inflammatory activities (Dunkhunthod et al., 2017; Hengpratom et al., 2018; Singh and Kakkar, 2013; Siriwatanametanon et al., 2010; Tenpe et al., 2009; Tripathy et al., 2011). *O. indicum* possessed high antioxidant activity against DPPH radicals, lipid peroxidation, superoxide, and nitric oxide (Palasuwan et al., 2005; Tenpe et al., 2009). The stem bark extracts of *O. indicum* showed the anti-inflammatory effects on PMA-induced activation of NF-kB in HeLa cells and LPS-induced IL-1β, IL-6, TNF-α, and PGE2 release in human monocytes (Siriwatanametanon et al., 2010).

However, no further work has been carried out on the anti-inflammatory and antioxidant activities of *G. inodorum* extract (GIE) and *O. indicum* extract (OIE) on RAW264.7 macrophage cells and the mechanisms responsible for its effects. Thus, it was chosen for this investigation.

1.2 Research objectives

1. To investigate the phytochemical composition of OIE and GIE.
2. To investigate the antioxidant and anti-inflammatory activities of OIE and GIE in RAW264.7 macrophage cells.
3. To investigate the effect of OIE and GIE on the anti-oxidant gene expression.
4. To investigate the anti-inflammatory mechanism of OIE and GIE mediate through NF-kB suppression.

1.3 Scope and limitation of the study

The research was only focused on the antioxidant, anti-inflammatory activities and its mechanism of action of OIE and GIE. The antioxidant activity of OIE and GIE were investigated in uninduced- and LPS plus IFN-γ-induced RAW264.7 macrophage cells. The anti-inflammatory properties of OIE and GIE were investigated *in vitro* using LPS plus IFN-γ-induced RAW264.7 macrophage cells.

1.4 Expected results

OIE and GIE could have possessed the antioxidant and anti-inflammatory activity in RAW264.7 macrophage cells. The underlying mechanism of anti-inflammation mediates through NF-kB suppression.

CHAPTER II

LITERATURE REVIEW

2.1 Immune system

The immune system consists of a series of effector mechanisms that destroy pathogenic organisms like bacteria, fungi, viruses, and parasites. The immune system consists of two responses: an innate immune response and adaptive immunity (Figure 2.1) (Koenderman et al., 2014).
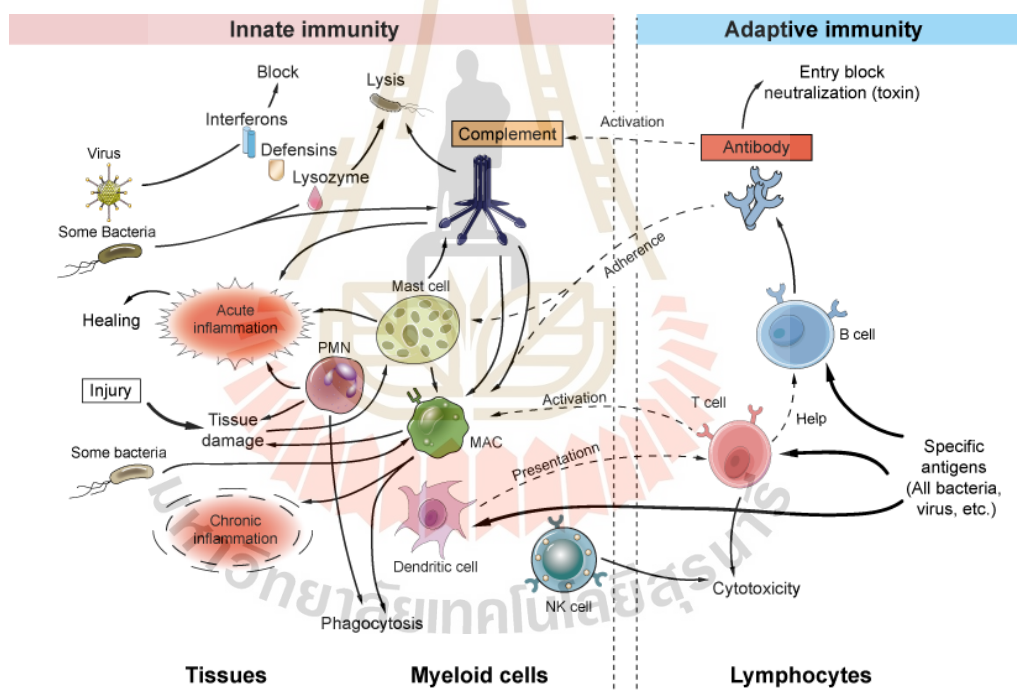
Figure 2.1 Innate immunity and adaptive immunity.

(Source: https://www.creative-diagnostics.com/innate-and-adaptive-immunity.htm)

Innate immunity (also called natural or native immunity) provides the first line of defense against microbes. It consists of cellular and biochemical defense mechanisms that are in place before the infection and are poised to respond rapidly to infections. The mechanisms of innate immunity are specifically for structures that are common to groups of related microbes and may not distinguish

subtle differences between microbes. Innate immunity is activated when cells use specialized sets of receptors (Pattern recognition receptor, PRR) to recognize different microorganisms (bacteria, viruses, etc.) that have managed to penetrate the host. Binding to these receptors activates a limited number of basic microbial disposal mechanisms, such as phagocytosis of bacteria by macrophages and neutrophils or the release of antiviral interferons. Many of the mechanisms involved in innate immunity are mostly the same as those responsible for non-specifically reacting to tissue damage, with the production of inflammation.

The adaptive immunity (also called specificity or acquired immunity) system recognizes and reacts to many microbial and nonmicrobial substances. The defining characteristics of adaptive immunity are the ability to distinguish different substances, called specificity, and respond more vigorously to repeated exposures to the same microbe, known as memory. The unique components of adaptive immunity are cells called lymphocytes and their secreted products, such as antibodies. Foreign substances that induce specific immune responses or are recognized by lymphocytes or antibodies are called antigens. Adaptive immunity is based on the unique properties of lymphocytes (T and B cells), which can respond selectively to thousands of different non-self-materials, or 'antigens', leading to a specific memory and a permanently altered pattern of response and then adapt to the animal's surroundings. Adaptive mechanisms can function on their own against specific antigens, but the majority of their effects are exerted using the interaction of antibodies with complement and the phagocytic cells of innate immunity and T cells with macrophages.

2.2   Inflammation

Inflammation is an essential immune response that enables survival during infection or injury and maintains tissue homeostasis under various harmful conditions (Medzhitov, 2010). Inflammation can be classified into acute and chronic. Acute inflammation is a short-term inflammatory response to an insult to the body. Acute inflammation is usually characterized by pain, swelling, redness, heat, or even loss of function. If the cause of the inflammation is not resolved; however, it can lead to

chronic inflammation, which is associated with major tissue destruction and fibrosis. This chronic inflammation can play a role in various health conditions, including metabolic syndrome, non-alcoholic fatty liver disease, type 2 diabetes, cancer, asthma, Alzheimer's disease, rheumatoid arthritis, and heart disease. The release of damaged cellular contents into the injury site is enough to stimulate the response, even in the absence of breaks in physical barriers that would allow pathogens to enter. The inflammatory reaction brings phagocytic cells to the damaged area to clear cellular debris and set the stage for wound repair (Figure 2.2).
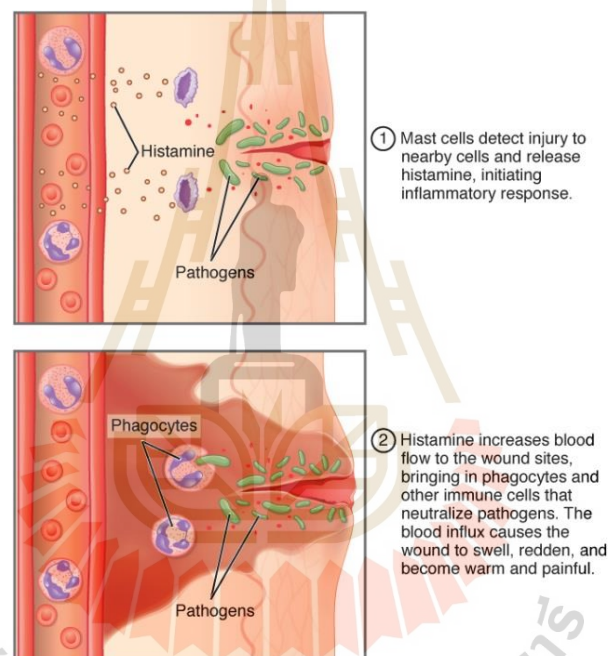
Figure 2.2 Inflammatory response.
(Source: https://opentextbc.ca/anatomyandphysiology /chapter/ 21-2-barrier-defenses-and-the-innate-immune-response/)

This reaction also brings in the innate immune system cells, allowing them to get rid of the sources of a possible infection. Inflammation is part of a basic form of the immune response. The process not only brings fluid and cells into the site to destroy the pathogen and remove it and debris from the site but also helps isolate the site, limiting the pathogen's spread. Intrinsic to the efficacy of such a system is the ability to mount a rapid response appropriate to the particular type of

inflammatory trigger while limiting the damaging aspects of inflammation as much as possible. Thus, the ideal inflammatory response is quick and destructive (when necessary), yet specific and self-limiting. The observations demonstrate the importance of this balance that in certain chronic infections or inflammatory disorders, the inflammatory response causes more damage to the host than the microbe (Maizels et al., 2012; Nathan, 2002; Segal et al., 2000).

2.3   Inflammation mechanism

The inflammatory response processes depend on the precise nature of sharing a common mechanism, which can be summarized as follows: 1) cell surface pattern receptors recognize harmful stimuli; 2) inflammatory pathways are activated; 3) inflammatory markers are released; and 4) inflammatory cells are recruited (L. Chen et al., 2018).

2.3.1   Activation of cell surface pattern-recognition receptor

Microbial structures known as pathogen-associated molecular patterns (PAMPs) can trigger the inflammatory response through the activation of germline-encoded pattern-recognition receptors (PRRs) expressed in both immune and non-immune cells (Brusselle and Bracke, 2014). Some PRRs also recognize various endogenous signals activated during tissue or cell damage and are known as a danger-associated molecular pattern (DAMPS) (Gudkov and Komarova, 2016). DAMPs are host biomolecules that can initiate and perpetuate a noninfectious inflammatory response (Seong and Matzinger, 2004). Disrupted cells can also recruit innate inflammatory cells without pathogens by releasing DAMPs (Ozinsky et al., 2000).

Classes of PRR families include the Toll-like receptors (TLRs), C-type lectin receptors (CLRs), retinoic acid-inducible gene (RIG)-I-like receptors (RLRs), and NOD-like receptors (NLRs) (Takeuchi and Akira, 2010). Amongst the innate immune PRRs, Toll-like receptors (TLRs) have the unique capacity to sense the initial infection and are the most potent inducers of the inflammatory responses. Depending on their cellular localization or respective PAMPs they identify, TLRs can be divided into two subgroups as transmembrane (TLR1, TLR2, TLR4, TLR5, TLR6, and TLR11) and intracellular (TLR3, TLR7, TLR8, and TLR9) (Kawai and Akira, 2011).

The best possible explanation of cell surface TLR activation is the presentation and binding of lipopolysaccharide (LPS) to TLR4. TLR4 is expressed in various immune cells, including neutrophils, monocytes/macrophages, and dendritic cells. Amongst these, neutrophils first migrate to the site of infection, sense to the pathogen, and elicit an immune response. However, coordinated adaptive response activation is mediated by the binding of a specific ligand to monocytes or dendritic cells that are also mediated principally by TLR4. Moreover, these TLRs are also expressed on classical adaptive immune cells viz. B and T lymphocytes. LPS is a principal outer membrane component of Gram-negative bacteria, potently activating the innate immune system (Lu et al., 2008). Under the pathogenic conditions, a soluble plasma protein, namely LPS-binding protein (LBP) interacts and binds with LPS. The entire LPS-LBP complex handed over to glycosylphosphatidylinositol-linked CD14 firstly and then on to the TLR4-MD2 complex. TLR4 forms a complex with MD2 on the cell surface, which serves as the main LPS-binding component. Five out of the six lipid chains of LPS occupy the hydrophobic pocket of MD2 and the remaining lipid chain exposed to the surface on MD2 associated with TLR4. The phosphate groups on sugar moieties also interact with the positively charged residues of TLR4. The multimeric receptor is composed of two copies of the TLR4-MD2-LPS complex resulting in the initiation of signal transduction by recruiting intracellular adaptor molecules such as Myeloid differentiation factor 88 (MyD88), TIR-related adaptor protein inducing interferon (TRIF), TRIF-related adaptor molecule (TRAM), TIR domain-containing adaptor protein (TIRAP) or MyD88 adaptor-like (MAL), and Sterile-alpha and Armadillo motif-containing protein (SARM). The summary of the mode of ligand recognition by TLR4 has been depicted in Figure 2.3.
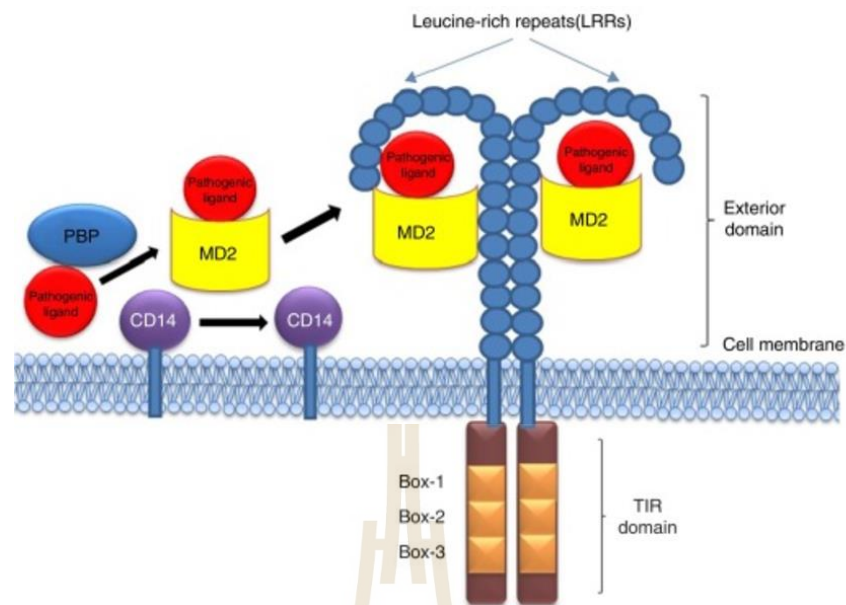
Figure 2.3 Presentation of ligand (LPS) to TLR4 through the coordinated actions of serum LBP, membrane-bound CD14, and MD2 (Mukherjee et al., 2016).

2.3.2 Inflammatory pathways are activated

Activation of these TLRs triggers two distinct signaling pathways viz. MyD88 dependent and MyD88 independent or TRIF dependent pathways. Signaling through TLRs activates an intracellular signaling cascade that leads to nuclear translocation of transcription factors, such as activator protein-1 (AP-1) and NF-kB or interferon regulatory factor 3 (IRF3) (Mukherjee et al., 2016). The mechanism of signaling induced from the TLR-ligand interface to mediate the inflammatory response is presented in Figure 2.4.
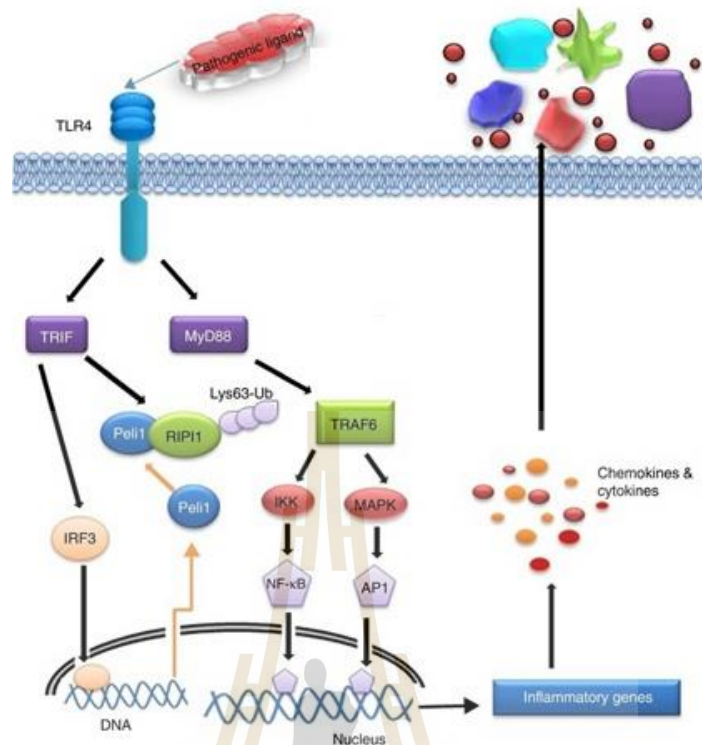
Figure 2.4 Toll-like receptor signaling pathways (Mukherjee et al., 2016).

Inflammatory stimuli activate intracellular signaling pathways that then trigger the production of inflammatory mediators. Primary inflammatory stimuli, including microbial products and cytokines such as interleukin-1β (IL-1β), interleukin-6 (IL-6), and tumor necrosis factor-α (TNF-α), mediate inflammation through interaction with the TLRs, IL-1 receptor (IL-1R), IL-6 receptor (IL-6R), and the TNF receptor (TNFR) (Kaminska, 2005). Receptor activation triggers crucial intracellular signaling pathways, including the nuclear factor kappa-B (NF-kB), mitogen-activated protein kinase (MAPK), and Janus kinase (JAK) signal transducer and activator of transcription (STAT) pathways (Hendrayani et al., 2016; Kyriakis and Avruch, 2001).

Nuclear factor kappa-B (NF-kB) signaling pathway, NF-kB is expressed ubiquitously in the cytoplasm of almost all cell types. Many diseases, including cancer, and inflammatory and autoimmune diseases, are associated with dysregulation of NF-kB. NF-kB can be activated via two distinct pathways, the classical or canonical NF-kB pathway and the alternative or non-canonical NF-kB pathway (Noort et al., 2015; Haisong Zhang and Sun, 2015).

The most extensively studied NF-kB activation pathway is the canonical pathway (Figure 2.5), which can be activated by stimulation of a variety of cell membrane receptors, including tumor necrosis factor (TNF) receptor, interleukin (IL)-1 receptor, and Toll-like receptors, in response to pro-inflammatory stimuli like lipopolysaccharide, IL-1, and TNF, as well as via triggering of the T-cell receptor or B-cell receptor. Activation of the canonical pathway via Toll-like receptor or cytokine receptor signaling depends on the inhibitor of the kB kinase (IKK) complex, which is composed of the kinases IKKα and IKKβ, and the regulatory subunit IKKγ (NEMO). Activated IKK phosphorylates the inhibitory subunit IkBα to induce its degradation, allowing NF-kB dimers (p50-p65) to translocate to the nucleus and bind to DNA to induce NF-kB target gene transcription.

In the past decade, a second alternative NF-kB activation pathway was identified, the so-called non-canonical NF-kB pathway (Figure 2.6). This pathway can be triggered by the activation of members of the TNF-receptor superfamily, including the lymphotoxin β (LTβ) receptor (LTβR), CD40, B cell-activating factor (BAFF) belonging to the TNF family receptor, and receptor activator of NF-kB (RANK). The NF-kB inducing kinase (NIK) is stabilized and activates and recruits IKKα into the p100 complex to phosphorylate p100, leading to p100 ubiquitination. Processing of p100 generates the p52/RelB NF-kB complex, which can translocate to the nucleus and induce gene expression. Of note, these receptors not only trigger the non-canonical NF-kB pathway but simultaneously also the canonical pathway.
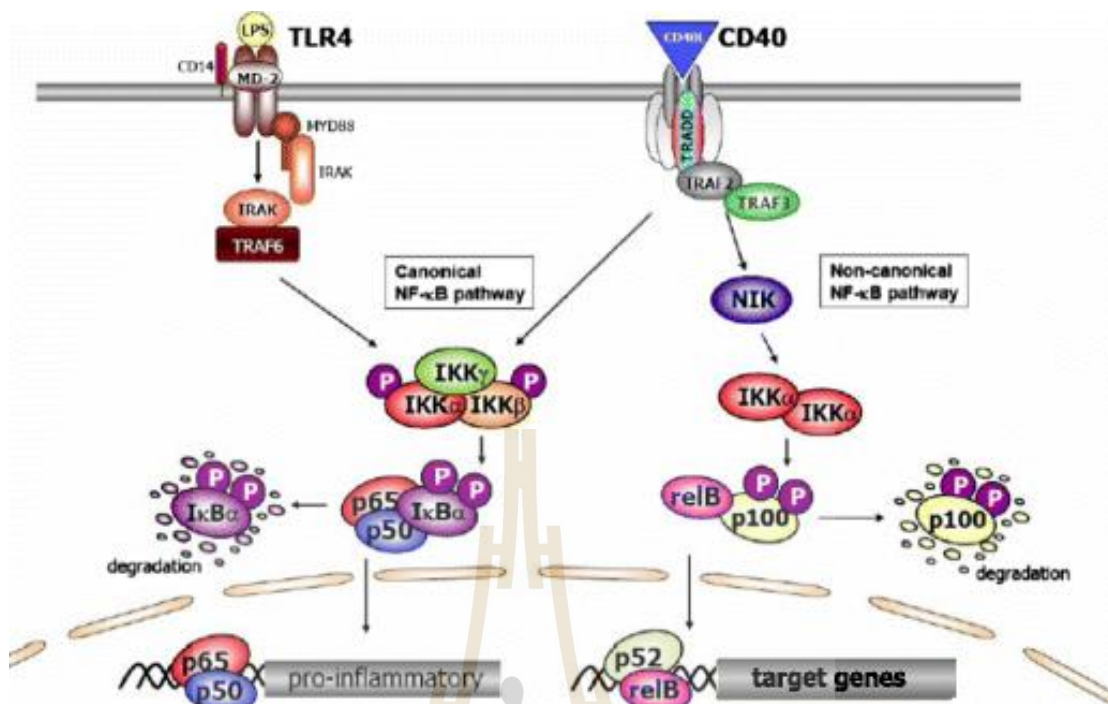
Figure 2.5 The canonical and non-canonical NF-kB pathways (Noort et al., 2015).

2.3.3 Inflammatory markers are released

Markers are used in clinical applications to indicate normal versus pathogenic biological processes and assess responses to therapeutic interventions. Inflammatory markers may be predictive of inflammatory diseases and correlate with the causes and consequences of various inflammatory diseases, such as cardiovascular diseases, endothelial dysfunctions, and infection (Bhowmik et al., 2000; Cesari et al., 2003; Kotas and Medzhitov, 2015). Stimuli activate inflammatory cells, such as macrophages and adipocytes, and induce production of inflammatory cytokines, such as IL-1β, IL-6, TNF-α, inflammatory proteins and enzymes, such as high-mobility group box 1 (HMGB1), inducible nitric oxide synthase (iNOS) and cyclooxygenase (COX)-2, and antioxidant defense biomarkers, such as superoxide dismutase (SOD), glutathione peroxidase (GPx), and NADPH oxidase (NOX) (Lopresti et al., 2014; Murakami and Ohigashi, 2007). These molecules can potentially serve as biomarkers for disease diagnosis, prognosis, and therapeutic decision-making.

Tumor necrosis factor-alpha (TNF-α), TNF-α is a cell-signaling protein (cytokine) involved in systemic inflammation. It is one of the cytokines that make up

the acute phase reaction. It is produced chiefly by activating macrophages, although it can be produced by many other cell types such as CD4+ lymphocytes, NK cells, neutrophils, mast cells, eosinophils, and neurons. The primary role of TNF is in the regulation of immune cells. TNF, being an endogenous pyrogen, can induce fever, apoptotic cell death, cachexia, inflammation and to inhibit tumorigenesis and viral replication, and respond to sepsis via IL-1 and IL-6 producing cells. Dysregulation of TNF production has been implicated in various human diseases, including Alzheimer's disease, cancer, major depression, psoriasis, and inflammatory bowel disease (IBD) (Armaka et al., 2008; Bradley, 2008). TNF-α mediates its effect through two different receptors: TNF-α receptor I (TNF-R1; p55 or p60) and TNF-α receptor II (TNF-R2; p75 or p80) (Levine, 2006). The TNF-R1 and TNF-R2 belong to the TNF superfamily receptors that have structurally related cysteine-rich extracellular domains. The TNF-R2 is expressed only on endothelial and immune cells. The TNF-R1 is universally expressed in all cell types and has a broader role in NF-kB activation versus that of TNF-R2. The TNF-α can activate different pathways to induce apoptosis, cell survival, or inflammation (Figure 2.6). TNF binding to TNFR1 mediates the translocation of TNFR1 to lipid rafts, where it recruits the adaptor proteins TRADD, RIP1, and TRAF2, which can activate the NF-kB pathway via an I-kB kinase complex composed of IkB kinase-a, IkB kinase-b, and IkB kinase-g (NEMO). Alternatively, TNFR1 signaling through TRAF2 can activate the c-Jun N-terminal kinase (JNK) pathway through the MAPK kinase, MKK7, which results in the phosphorylation of c-Jun, with resultant increases in AP-1 activity. Both the NF-kB and JNK pathways stimulate inflammation. Furthermore, activation of the NF-kB pathway inhibits apoptosis due to the increased expression of anti-apoptotic genes (i.e., c-FLIP, cIAP1, and cIAP2). TNFR1 signaling can induce apoptosis in the absence of NF-kB activation. A model proposed that the formation of a TNFR1-associated death-inducing signaling complex (DISC) is dependent on receptor internalization within endocytic vesicles, termed TNF receptosomes. Internalized receptors recruit TRADD, FADD, and caspase-8 to form a TNFR1-associated DISC. This results in the rapid activation of caspase-8, which initiates apoptosis.
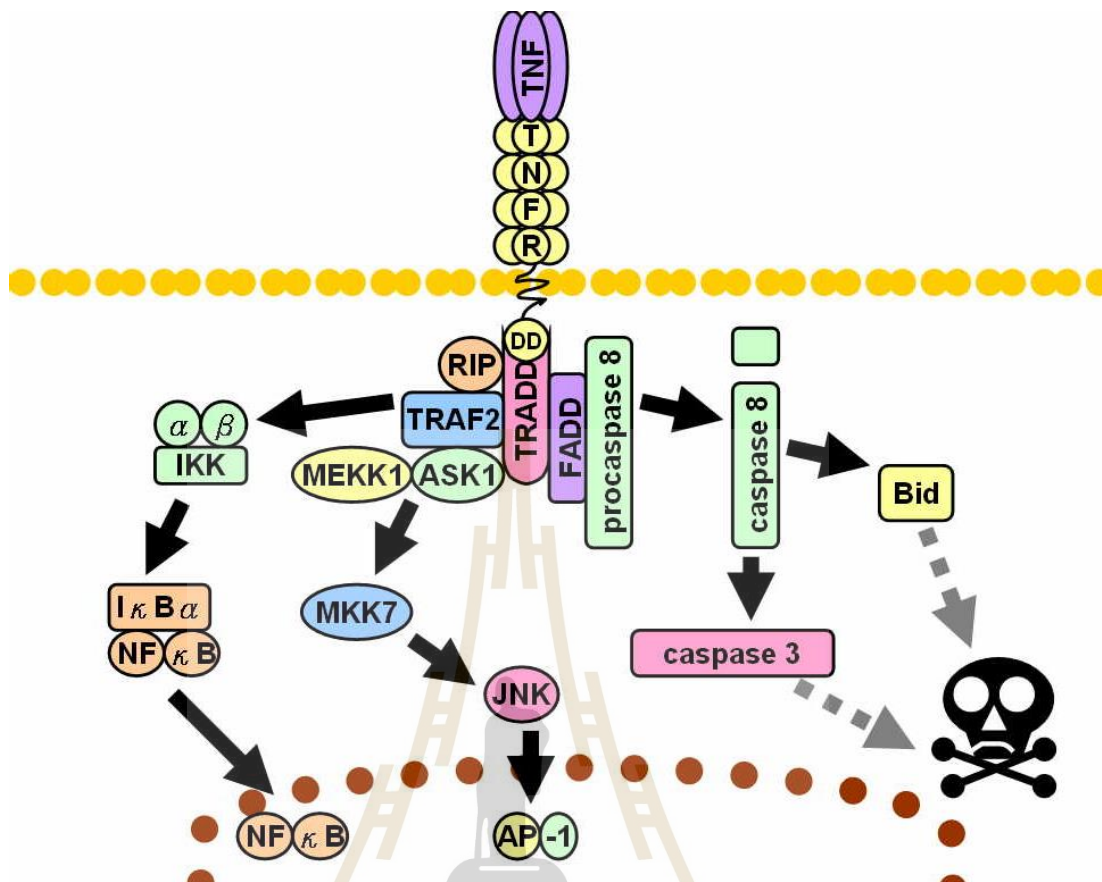
Figure 2.6 Signaling pathways of TNFR1.

(Source: https://en.wikipedia.org/wiki/Tumor_necrosis_factor_alpha)

Interleukin-6 (IL-6), initially designated as a B cell differentiation factor, is a representative cytokine featuring redundancy and pleiotropic activity (Hirano et al., 1986; Kishimoto, 2005). In the early phase of infectious inflammation, IL-6 is produced by monocytes and macrophages immediately after the stimulation of Toll-like receptors (TLRs) with distinct pathogen-associated molecular patterns (PAMPs) (Janeway Jr and Medzhitov, 2002). In non-infectious inflammations, such as a burn or traumatic injury, damage-associated molecular patterns (DAMPs) from damaged or dying cells stimulate TLRs to produce IL-6 (Matzinger, 2002). This acute IL-6 expression plays a central role in host defense by promoting various cell populations. When acting on hepatocytes, IL-6 strongly induces a broad spectrum of acute-phase proteins such as C-reactive protein (CRP), serum amyloid A (SAA), fibrinogen, hepcidin, haptoglobin, and anti-chymotrypsin, whereas it reduces albumin,

cytochrome P450, fibronectin, and transferrin (Figure 2.7) (Heinrich et al., 1990; Siewert et al., 2000). CRP is the best biomarker of inflammation, and its expression mainly depends on IL-6. IL-6 combined with TGF-β preferentially induces the differentiation of naïve CD4 positive T cells into Th17 cells, whereas IL-6 inhibits TGF-β induced regulatory T cell (Treg) development. Consequently, Th17/Treg imbalance may cause the onset and progression of autoimmune and chronic inflammatory diseases. In the bone marrow, IL-6 induces the maturation of megakaryocytes into platelets and the activation of hematopoietic stem cells. IL-6 also promotes the differentiation of osteoclasts and angiogenesis, the proliferation of keratinocytes and mesangial cells, and the growth of myeloma and plasmacytoma cells (Tanaka and Kishimoto, 2012). Thus, the dysregulated continuous IL-6 production has been demonstrated to play a pathological role in various autoimmune and chronic inflammatory diseases.
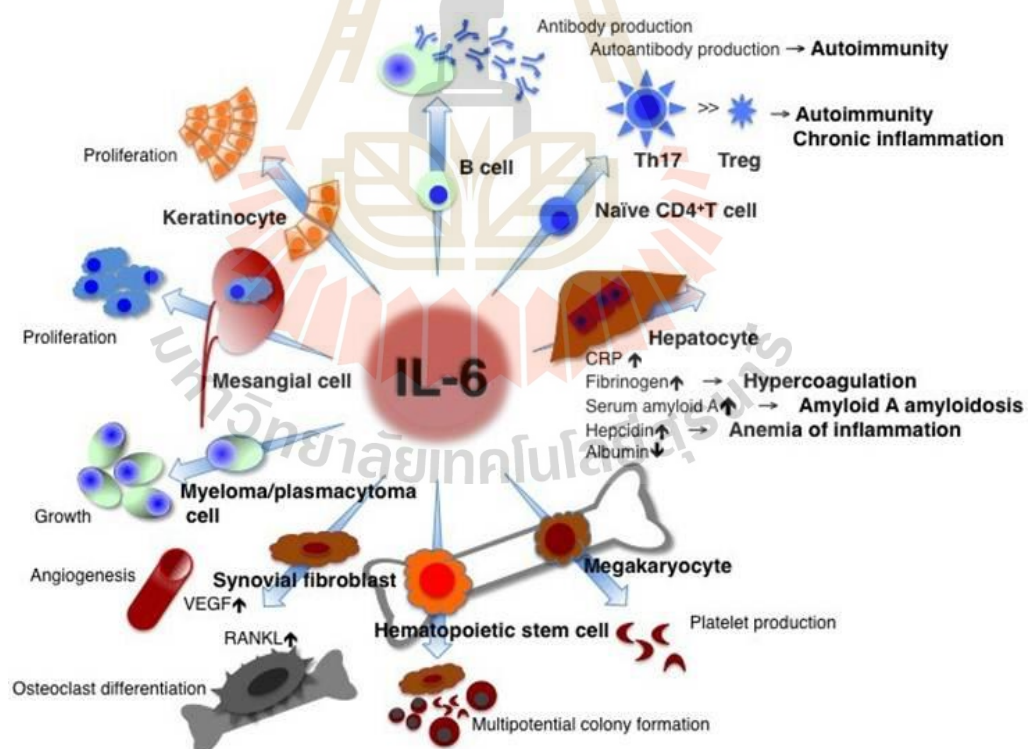
Figure 2.7   IL-6 has a pleiotropic effect, but its dysregulated persistent production causes the onset and development of various autoimmune and chronic inflammatory diseases (Tanaka and Kishimoto, 2012).

Nitric oxide synthases (NOS) are a family of isoforms responsible for synthesizing the potent dilator nitric oxide (NO). There are three isoforms of nitric oxide synthase (NOS) named according to their activity or the tissue type in which each isoform is first characterized. The neuronal form (nNOS, NOS-1, Type I) is a Ca^{2+}-dependent enzyme found in neuronal tissue and skeletal muscle. A second isoform of NOS (iNOS, NOS-2, Type II) is inducible in various cells and tissues in response to cytokine or endotoxin activation. NOS binds Ca^{2+}/calmodulin so tightly that at normal physiologic levels, its activity is functionally Ca^{2+}-independent. A third form, first found in vascular endothelial cells (eNOS, NOS-3, Type III), is also Ca^{2+} dependent. iNOS is expressed typically in response to immunological stimuli, bacterial lipopolysaccharide (LPS), and a variety of proinflammatory cytokines and produces nanomoles rather than picomoles of NO (Cuzzocrea et al., 2001). Macrophages can produce wide ranges of NO concentrations depending on the source of stimulus, such as LPS, proinflammatory cytokines, or LPS plus proinflammatory cytokines. Interestingly, macrophages are stimulated by LPS plus IFN-γ. The amount of NO generation is higher when compared to stimulation with LPS alone or LPS plus TNF-α or IL-1β (Cheng et al., 2010). Biosynthetic NO is derived from the amino acid arginine in an oxidative reaction that consumes molecular oxygen and reduces equivalents in NADPH. The products of the reaction are NO, $NADP^+$, and citrulline. The general mechanism of NO production from NOS is illustrated below (Figure 2.8).
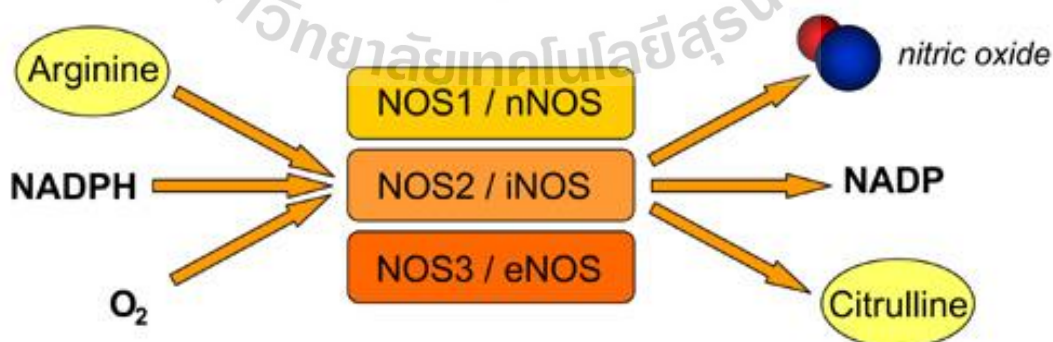
Figure 2.8 The general mechanism of NO production from NOS.

(Source: http://www.reading.ac.uk/cellmigration/synthesis.htm)

Nitric oxide (NO) is synthesized by many cell types involved in immunity and inflammation. NO is vital as a toxic defense molecule against infectious organisms. It also regulates the functional activity, growth, and death of many immune and inflammatory cell types, including macrophages, T lymphocytes, antigen-presenting cells, mast cells, neutrophils, and natural killer cells. NO is a reactive molecule that has various effects depending on the relative concentrations of NO and the surrounding milieu in which NO is produced. There are both direct effects of NO-mediated by the NO molecule itself and indirect effects of NO-mediated by reactive nitrogen species produced by the interaction of NO with superoxide anion or oxygen. The cGMP produced by the interaction of NO with soluble guanylate cyclase mediates many of the physiological effects. It is also an essential example of the direct effects (Korhonen et al., 2005). The molecular mechanisms that mediate the biological activities of NO can be divided into three categories. Firstly, NO reacts readily with transition metals, such as iron, copper, and zinc. These metals are abundantly present in prosthetic groups of enzymes and other proteins, and by that mechanism, NO regulates the activity of various enzymes. Secondly, NO can induce the formation of S-nitrosothiols from cysteine residues in a reaction called S-nitrosylation. Nitrosylation has been shown to modify the activity of several proteins involved in cellular regulatory mechanisms (Stamler et al., 2001). Thirdly, NO reacts very quickly with superoxide anion (O_2^-), resulting in peroxynitrite ($ONOO^-$). Peroxynitrite is a nitrating agent and a powerful oxidant that can modify proteins, lipids, and nucleic acids.

Cyclooxygenase (COX), officially known as prostaglandin-endoperoxide synthase (PTGS), is an enzyme responsible for forming prostanoids, including thromboxane and prostaglandins such as prostacyclin, from arachidonic acid. Two closely related forms of COX known as COX-1 and COX-2 have been identified. Prostaglandin production (Figure 2.9) depends on the activity of prostaglandin G/H synthases, colloquially known as COXs, bifunctional enzymes that contain both cyclooxygenase and peroxidase activity and which exist as distinct isoforms referred to as COX-1 and COX-2. COX-1, expressed constitutively in most cells, is the dominant prostanoid source that subserves housekeeping functions, such as gastric

epithelial cytoprotection and homeostasis (Dubois et al., 1998). COX-2, induced by inflammatory stimuli, hormones, and growth factors, is the most crucial source of prostanoid formation in inflammation and proliferative diseases, such as cancer. However, both enzymes contribute to the generation of autoregulatory and homeostatic prostanoids, and both can contribute to prostanoids released during inflammation. During an inflammatory response, both the level and the profile of prostaglandin production change dramatically. Prostaglandin production is generally deficient in uninflamed tissues but increases immediately in acute inflammation before the recruitment of leukocytes and the infiltration of immune cells. PGH_2 is produced by both COX isoforms, and it is the common substrate for a series of specific isomerase and synthase enzymes that produce PGE_2, PGI_2, PGD_2, $PGF2\alpha$, and TXA_2. COX-1 couples preferred, but not exclusively, with thromboxane synthase (TXS), prostaglandin F synthase, and the cytosolic (c) prostaglandin E synthase (PGES) isozymes. COX-2 prefers prostaglandin I synthase (PGIS) and the microsomal (m) PGES isozymes, both of which are often co-induced along with COX-2 by cytokines and tumor promoters (Smyth et al., 2009). The profile of prostanoid production is determined by the differential expression of these enzymes within cells present at sites of inflammation. For example, mast cells predominantly generate PGD_2 while macrophages produce PGE_2 and TXA_2 (Tilley et al., 2001). Also, alterations in the profile of prostanoid synthesis can occur upon cellular activation. While resting macrophages produce TXA_2 over PGE_2, this ratio changes to favor PGE_2 production after bacterial lipopolysaccharide (LPS) activation.
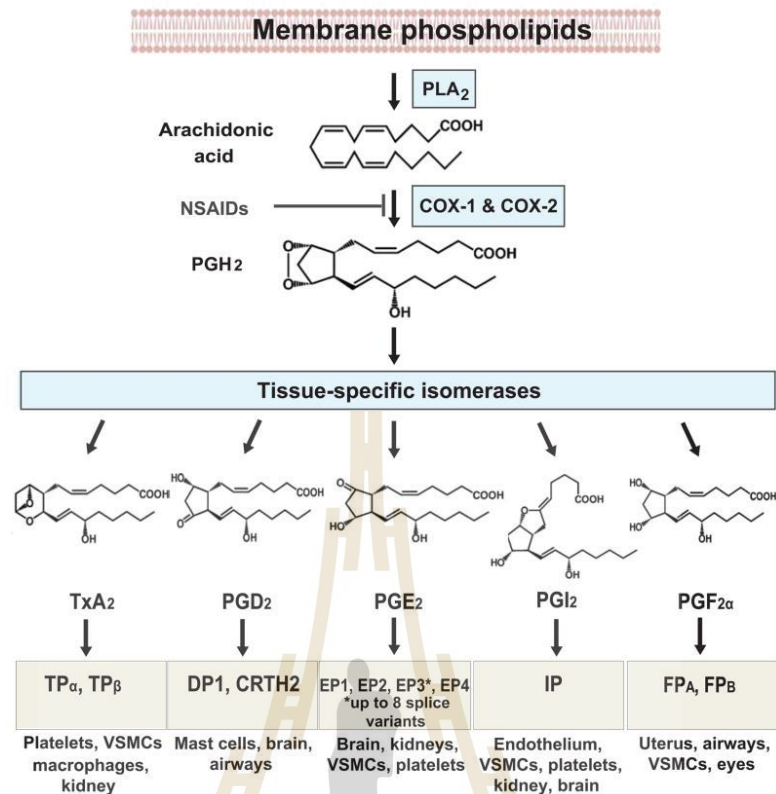
Figure 2.9 Biosynthetic pathways of prostanoids (Ricciotti and FitzGerald, 2011).

2.3.4 Inflammatory cells are recruited

The inflammatory response involves a highly coordinated network of many cell types. Activated macrophages, monocytes, and other cells mediate local responses to tissue damage and infection. Upon tissue injury, damaged epithelial and endothelial cells release factors that trigger the inflammatory cascade, along with chemokines and growth factors, which attract circulating neutrophils and monocytes to the site of the damaged tissue. Neutrophils are the first circulating inflammatory cells to be recruited to the area of injury, followed by monocytes, lymphocytes [natural killer cells (NK cells), T cells, and B cells], and mast cells (Stramer et al., 2007; Van Linthout et al., 2014). Monocytes can differentiate into macrophages and dendritic cells and are recruited via chemotaxis into damaged tissues. Inflammation-mediated immune cell alterations are associated with many diseases, including asthma, cancer, chronic inflammatory diseases, atherosclerosis, diabetes, and autoimmune and degenerative diseases. Neutrophils, which target microorganisms in

the body, can damage host cells and tissues (Nathan, 2006). Neutrophils are key mediators of the inflammatory response and program antigen-presenting cells to activate T cells and release localized factors to attract monocytes and dendritic cells. Macrophages are essential components of the mononuclear phagocyte system and are critical in inflammation initiation, maintenance, and resolution (Fujiwara and Kobayashi, 2005). During inflammation, macrophages present antigens, undergo phagocytosis, and modulate the immune response by producing cytokines and growth factors. Mast cells, which reside in connective tissue matrices and on epithelial surfaces, are effector cells that initiate inflammatory responses. Activated mast cells release various inflammatory mediators, including cytokines, chemokines, histamine, proteases, prostaglandins, leukotrienes, and serglycin proteoglycans (C. Huang et al. Multiple groups have demonstrated that platelet impacts the inflammatory process, from atherosclerosis to infection. Platelet interactions with inflammatory cells may mediate pro-inflammatory outcomes. The acute phase response (APR) is the earliest response to disease or injury, and some studies have indicated that platelets induce the APR (Aggrey et al., 2013). After being recruited by inflammatory stimuli, immune cells amplify and sustain the APR by releasing local inflammatory mediators at the recruitment site.

Leukocytes called monocytes and macrophages eat bacteria and digest cellular debris. They use a process called phagocytosis, in which cellular materials or bacteria are engulfed when the leukocyte forms a pocket on its surface and pinches off the "swallowed" piece. Monocytes are precursor cells that are produced in the bone marrow, which are mobilized into the bloodstream and then differentiate into macrophages at the site of inflammation (Gordon, 1976). Macrophages are a very heterogeneous cell population, such as effector cells of the innate immune system, which play an essential role in host defense and inflammation. In general, macrophages can be divided into two populations: resident and inflammatory macrophages (Raggatt et al., 2014). Resident macrophages are found in almost all tissues and contribute to their development and immunological surveillance, homeostasis, and tissue repair. On the other hand, inflammatory macrophages are derived from circulating monocytes and rapidly infiltrate tissues compromised by

injury or infection. In response to several signals from the microenvironment, macrophages can be activated and adopt different functions: M1 macrophages (classically activated macrophages) and M2 macrophages (alternatively activated macrophages) (Wynn et al., 2013). M1 macrophages have proinflammatory functions and participate in host defense against pathogens and tumoral cells, and it is considered that they promote the Th1 immune response (Tan et al., 2016). When M1 macrophages are activated by interferon (IFN)-γ, granulocyte-macrophage colony-stimulating factor (GM-CSF), or other ligands of Toll-like receptor, these macrophages produce proinflammatory cytokines such as interleukin (IL)-1β, IL-12, and tumor necrosis factor (TNF)-α, chemokine, and reactivate species of nitrogen and oxygen, increase the complement-mediated phagocytosis as their main purpose is to kill intracellular pathogens (Suzuki et al., 2017). In contrast, M2 macrophages are associated with tissue remodeling and tumor progression and have an immunoregulatory effect. M2 macrophages express IL-10, IL-1 receptor antagonist, chemokines, transforming growth factor (TGF)-β, mannose, and galactose receptors and possess efficient phagocytic activity. M2 macrophages are considered to promote the Th2 immune response and antagonize the inflammatory response and its mediators (Gordon and Martinez, 2010). Macrophages possess a wide range of surface receptors, which gives them the ability to recognize a wide range of endogenous/exogenous ligands to respond adequately, which is critical in these cells. These receptors include Toll-like receptors (TLRs), NOD-like receptors, retinoic acid-inducible gene (RIG)-I family, lectins, and scavenger receptors, which recognize PAMPs, DAMPs, foreign substances, and dead or damaged cells. During the inflammatory response by pathogens, macrophages activated with an inflammatory phenotype produce several inflammatory mediators, such as TNF-α, IL-1, IL-6, and IFN-γ, which are involved in the activation of microbicidal mechanisms contributing to the pathogen elimination.

2.4   Inflammation and oxidative stress

Acute inflammatory responses are essential for eliminating infections during wound healing but become detrimental if they are not resolved and become self-

perpetuating. This chronic response is sometimes observed under sterile conditions when no pathogens are present to attack, but the inflammatory response persists, resulting in damage to the body's cells and tissues. The mechanisms underlying the chronic inflammatory response are unclear; however, ROS are thought to be involved. The term ROS encompasses the superoxide anion ($O_2^{\bullet-}$), hydroxyl radical ($OH^\bullet$), and hydrogen peroxide (H_2O_2), amongst others. ROS are the intermediate breakdown products of molecular oxygen, and as aerobic organisms, we are constantly breaking down oxygen and produce ROS as we respire. As well as being formed routinely during cell metabolism, ROS are important in pathogen defense during respiratory bursts. However, inflammatory cells generate more soluble inflammatory mediators such as cytokines, arachidonic acid, and chemokines, which act through active inflammatory cells in the area of infection and release more reactive species. Increased ROS can trigger immune responses via two main mechanisms: (1) by incorrectly oxidizing proteins, lipids or DNA, which immune cells then do not recognize as safe and launch an immune response against, or (2) by activating redox-sensitive proteins inside cells which can then partake in inflammatory signaling. ROS can stimulate signal transduction cascades in addition to alterations in transcription factors, like nuclear factor kappa B (NF-kB), signal transducer and activator of transcription 3, activator protein-1, NF-E2 related factor-2 (Nrf2), nuclear factor of activated T cells, and hypoxia-inducible factor-1α (HIF1-α), which mediate vital cellular stress reactions. Initiation of cyclooxygenase-2 (COX-2), inducibility of nitric oxide synthase (iNOS), and high expression of inflammatory cytokines, including tumor necrosis factor-α (TNF-α), interleukin-1β (IL-1β), IL-6, and chemokines (CXC chemokine receptor 4), in addition to changes in the expression of specific microRNAs, have also been exhibited to have a role in oxidative stress-induced inflammation (Federico et al., 2007; Perwez Hussain and Harris, 2007). This inflammatory/oxidative environment triggers an unhealthy circle, harming healthy stromal cells and neighboring epithelial cells, leading to inflammatory diseases (Figure 2.10).
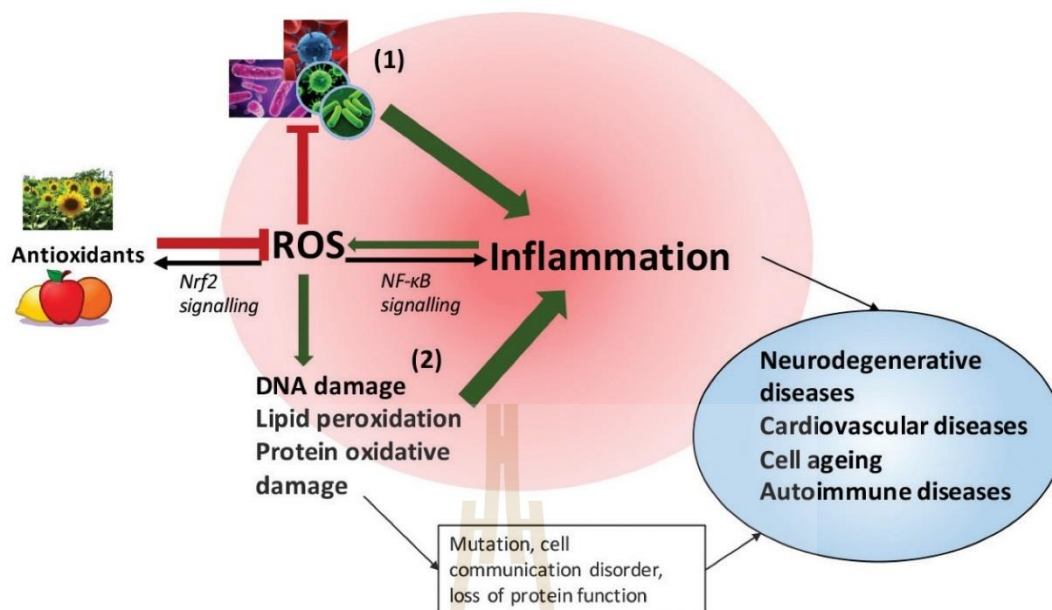
Figure 2.10 The multiple roles of ROS in inflammation (Ingram and Diotallevi, 2017).

2.5 Natural compounds as convenient antioxidant and anti-inflammatory agents

The World Health Organization (WHO) has estimated that 80% of its inhabitants utilize traditional medicine for their primary health care needs. The majority of this therapy requires the use of herbal extracts and their active components. Various medicinal plant bioactive extracts and their identified/isolated active constituents have shown various medicinal pharmacological properties against various acute and chronic diseases (Rajasekaran et al., 2007; S. Subramanian et al., 2006). Currently, the impact of oxidative stress and its associated factors has become an important issue of human health (Krishnaiah et al., 2011). When the body is under much stress, the production of ROS is amplified. Endogenous enzymatic and nonenzymatic antioxidant substances cannot handle the overload of ROS and lead to imbalances in the process, cell damage, and health problems. Lack of antioxidant compounds in the daily diet can lead to degenerative diseases such as cancers, cardiovascular diseases, Alzheimer's disease, neurodegenerative diseases, and various inflammatory illnesses (Matteo and Esposito, 2003; Steer et al., 2002). Incorporating antioxidant compounds by consuming natural plant sources in the daily diet can be

a suitable solution to human health issues. These natural antioxidant sources can be used as preventive medicine. A Recent investigation suggested an inverse link between the dietary consumption of antioxidant-rich foods and the prevalence of human illness.

Numerous studies exhibited that flavonoids and phenolic content have contributed to the antioxidant activities of natural compounds. In addition, other studies also reported that trace metals such as Cu, Zn, Mg, Mn, and Se perform a significant function in the antioxidant system (Ravipati et al., 2012). Moreover, dietary antioxidants, including tocopherols, carotenoids, and ascorbic acid, have been investigated (Krishnaiah et al., 2011). Several synthetic antioxidant supplements have been produced to remediate oxidative stress. Nevertheless, factors such as lack of availability, high cost, and side effects remain the main challenge in dealing with oxidative stress. However, natural antioxidants are abundant in several plant sources, free from side effects, and less expensive. The natural compound-based antioxidant substances perform a preventive role in protecting against the generation of free radicals, and therefore natural-based antioxidants are one of the most valuable therapeutic agents to reduce the illnesses triggered by oxidative stress (Arulselvan et al., 2016).

Besides having antioxidant activities, flavonoids and phenolic compounds also exert an effective role as anti-inflammatory factors. The anti-inflammatory actions of natural compounds have been reported in several studies and observed in numerous preclinical studies. The findings from anti-inflammatory researches have proven that bioactive extracts and their natural compounds exert their biological properties by blocking two major signaling pathways such as NF-kB and mitogen-activated protein kinases (MAPKs) which have the main role in the production of various proinflammatory mediators.

2.6   Plant material

2.6.1   *Oroxylum indicum* (L.) Kurz

Oroxylum indicum (L.) Kurz is a species of flowering plant belonging to the monotypic genus *Oroxylum* and the family Bignoniaceae. The plant is widely

distributed throughout India, Nepal and South East Asia, Indonesia, Sri Lanka, Philippines, China, Japan, Bhutan, Malaysia, Taiwan, Thailand, and Vietnam. In Thailand, it is called "Phe kaa" (central), "Litmai" (northern), or "Linfaa" (northeastern) (Devanathan, 2001). *O. indicum* is a small to medium-sized deciduous tree by height 12-15 m. The plant's bark is light grayish brown in color and soft, spongy in texture, having corky lenticels. Leaves are 90-180 cm long, bipinnate or tripinnate ovate or elliptical, broad; leaflets are 2-4 pairs ovate or elliptic, 5 inches long and 2-3 inches broad, having sharp edges, glabrous and acuminate. Leafstalks of the adjacent leaflets are 6-15 mm long. The flowers are numerous. Corolla is fleshy and dark purple from outside, pale and pinkish-yellow within, 10 cm long, multiple, in large erect racemes; calyx 4 cm long, leathery, oblongcampanulate and glabrous; stamens 5, slightly exserted beyond the corolla tube, one of them little shorter than the 4, filaments cottony at the base. Fruits are woody, winged, large and flat, capsule or sword-shaped. The fresh root bark is creamish yellow to greyish and has a soft and juicy texture. Seeds are numerous, round, flat, and thin, having broad silvery papery wings (Figure 2.11).
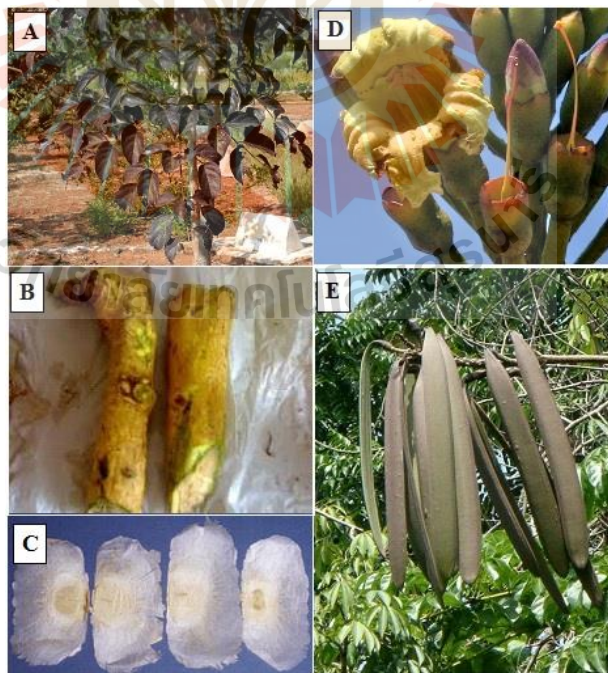
Figure 2.11 The different parts of *O. indicum* (A) leaf, (B) root, (C) seed, (D) flower, (E) fruit.

The different parts of the plant, mainly the fruits, seeds, stem-bark, and roots, have been used for centuries as an important herbal medicine in many Asian countries to cure various diseases. The root and stem bark are used for fever, bronchitis, intestinal worms, leucoderma, asthma, inflammation, anal troubles, diarrhea, and dysentery. The phytochemicals with chemical structures have been reported from different parts of *O. indicum* to date. These include the following: 50 flavonoids, 6 iso-flavonoids, 14 napthalenoids, 3 phenylethanoids, 9 cyclohexyletha-noids, 3 triterpenoids, 4 steroids, 5 stilbenoids, and 17 miscellaneous compounds. Among them, flavonoids are the major storage components. Among the flavonoids, baicalein, chrysin, and oroxylin A are the significant flavones present in stem bark (Babu et al., 2010; Dinda et al., 2007). Baicalein, chrysin, baicalein 7-O-glucoside, baicalein 7-O-diglucoside, and chrysin 7-O-diglucoside are the major chemical constituents of seeds (Yan et al., 2011). In fruits, baicalein was present as the antigen-presenting constituent and represented approximately 4% of freeze-dried fruits (Roy et al., 2007). In root bark, oroxylin A and baicalein are the major constituents (Ali et al., 1998; Khandhar et al., 2006). In leaves, the major chemical components are baicalein, scutellarein, and their 7-O-glucuronides (Subramanian, 1972). Many previous studies have reported antioxidant, anti-inflammatory, anti-diabetic, anticancer, antiulcer, and hepatoprotective properties for *O. indicum* and its isolated compounds. In 2010, Siriwatanametanon found that the ethyl acetate extract of *O. indicum* derived from the plant's stem bark showed the inhibitory effect on PMA-induced activation of NF-kB in HeLa cells and on LPS-induced IL-1β and PGE2 release in human monocytes (Siriwatanametanon et al., 2010). Furthermore, the stem bark extract showed a high level of antioxidant activity by inhibiting lipid peroxidation. Tran (2015) reported that oroxylin A isolated from *O. indicum* stem bark contributes to the NF-kB inhibitory activity in the HEK293/NF-kB-Luc cell system (Tran et al., 2015). In addition, the major flavonoids in *O. indicum*, baicalein, chrysin, and oroxylin A are known for their anti-inflammatory effects attributed at least partially through the suppression of NF-kB activation (Y.-C. Chen et al., 2000; B. Y. Kang et al., 2003; Sala et al., 2011; Shin et al., 2009).

2.6.2 *Gymnema inodorum* (Lour.) Decne.

Gymnema inodorum (Lour.) Decne is one of the local Thai vegetables belonging to the family Asclepiadaceae. It is found ubiquitously in Southeastern Asia, including Thailand, especially in the northern region. In Thailand, its local name is "Phak chin da" or "Phak chiang da". *G. inodorum* is a climbing plant with slender but vigorous woody stems that can be up to 25 meters long. Its stems are 0.5-5 cm in diameter, 5-10 cm long. Leaves are simple, ovate, acuminate, dark green in the upper part, coming out from the water opposite decussate. Flowers are small, round tight clusters, 5-6 cm in diameter (Figure 2.12). It has been known to have therapeutic effects in curing certain diseases, including diabetes mellitus, rheumatic arthritis, and gout. Nowadays, commercial products made from *G. inodorum* leaves, including powder decoctions, herbal tea bags, and capsules, have been developed and claimed to cure diabetes. These products are available in the Thailand market. The literature survey suggested that the leaves *G. inodorum* has many phytochemical compounds such as phenolics, flavonoids, terpenoids, and glycosides. Moreover, its antioxidant, anti-adipogenesis, antidiabetic, and hypoglycemic effects property was also reported (Arisawa et al., 2007; K. Shimizu et al., 2001; Tiamyom et al., 2019). However, there are minimal published studies of *G. inodorum*, and most of them are written in Thai.

Figure 2.12 The different parts of *G. inodorum* (A) whole plant, (B) flower, (C) leaf, (D) fruit.

CHAPTER III

MATERIALS AND METHODS

3.1   Overview of the study
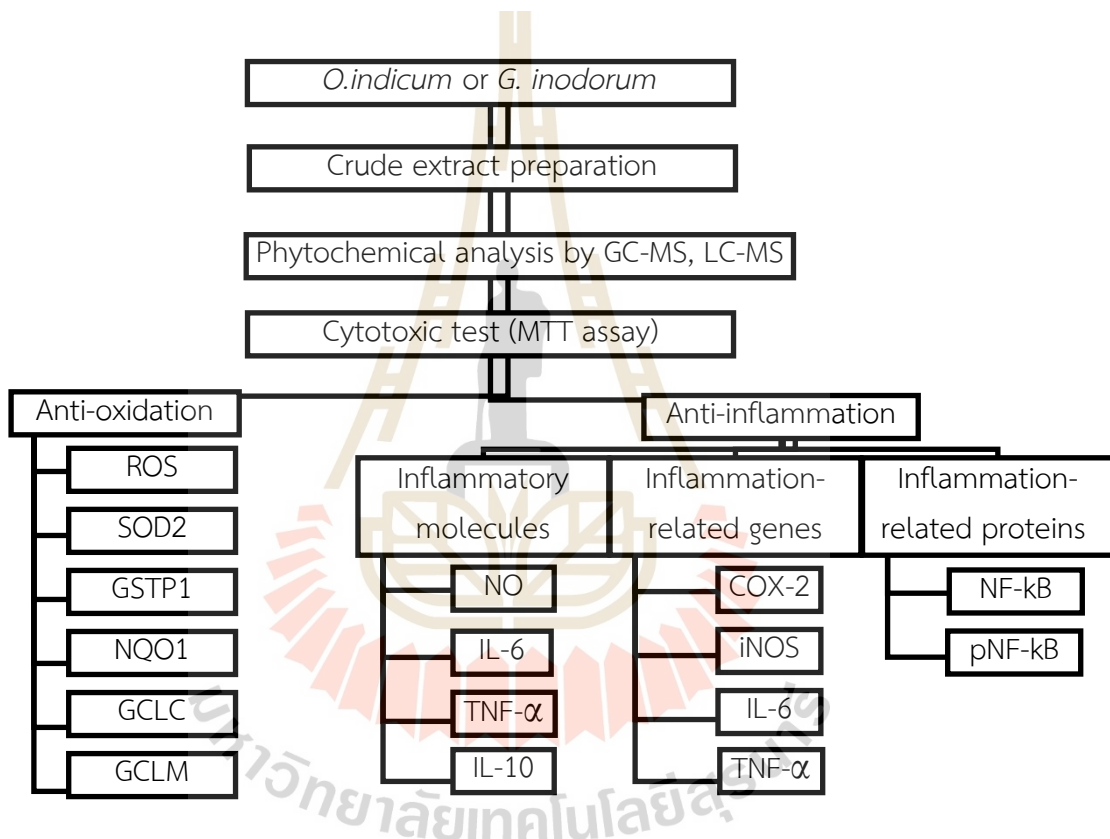
Figure 3.1 Overview of the study.

3.2   Materials

3.2.1   Cell lines

The RAW264.7 macrophage cells (Cell Lines Service, Eppelheim, Germany) were cultured at 37°C, 5% CO_2 in RPMI-1640 medium supplemented with 10% heat-inactivated FBS, and 100 U/mL penicillin-streptomycin. Exponentially growing cells were used for experiments when they reached about 80% confluence.

3.2.2 Chemicals and instruments

The chemicals and instruments employed in the present studies are summarized in Tables 3.1 and 3.2.

Tables 3.1 List of chemicals.

Name	Source
Absolute ethanol	Carlo erba
Agarose	Gibco
Ammonium sodium phosphate tetrahydrate	Acros organics
Ascorbic acid (Vitamin C)	Fluka
Dimethyl sulfoxide (DMSO)	Amresco
EDTA (Ethylenediaminetetraacetic acid)	Sigma
Folin & Ciocalteu's Phenol Reagent	Sigma
Gallic acid	Riedel-de Haen®
HEPES	Invitrogen
Magnesium chloride	Analar Normapur
Magnesium sulfate	Carlo erba
Methyl alcohol	Fisher Scientific
Potassium chloride	Carlo erba
Potassium phosphate, dibasic (anhydrous)	Univar
RPMI 1640	Invitrogen
Sodium acetate	Aldrich
Sodium ammonium phosphate	Acros organics
Sodium hydroxide	Carlo erba
Sodium monohydrogen phosphate heptahydrate	Merck
Streptomycin solution sulfate	Sigma-Aldrich
Tris base	Carlo erba
Triton X-100	Aldrich
Trolox	Sigma
Trypan blue	Fluka
Tween-20	Sigma

Table 3.2 List of instruments.

Name	Source
Bruker Vertex 70 spectrometer coupled with a Bruker-Hyperion 2000 microscope	Bruker Optics
Centrifuge (modelCT15RT)	Techcomp
CO_2 incubator	Thermo fisher scientific
Confocal microscopy	Nikon
Electrophoresis power supply (EPS 601)	Amersham
Electrophoresis system (model HE33)	Hoefer
Gemini EM fluorescence microplate reader	Molecular Devices
Inverted microscope (model CKX41)	Olympus
Laminar flow hood (Model CLASS II Biohazard safety cabinet)	ESCO
Light microscope (model CX21)	Olympus
Lyophilizer (model Freeze-zone 12 plus)	Labconco Corporation
Microplate reader	Benchmark

3.3 Methods

3.3.1 Preparation of *O. indicum* extract (OIE)

O. indicum (fruit pods) fresh samples were purchased from the local market at Wang Nam Khiao District, Nakhon Ratchasima province, Thailand. Fresh fruit pods were washed and cut into small pieces and then dried in the oven at 40 °C for 2 days. The dried pieces were pulverized using a mechanical grinder. The *O. indicum* dry powder (500 g) was extracted with 95% ethanol by a soxhlation for 8 h and then filtered through Whatman filter paper. The ethanolic extract was concentrated and lyophilized to obtain the powder of *O. indicum* crude extract. The extract was stored at -20 °C till use in subsequent experiments. The *O. indicum* extract (OIE) was dissolved in DMSO and diluted to 0.1% (v/v) in the cell culture medium.

3.3.2 Preparation of *G. inodorum* extract (GIE)

G. inodorum (dried leaves) was purchased from commercial products (Chiangda organic company garden, Chiangmai, Thailand). A 250-g dried powder of *G.*

inodorum was soaked in 750 mL 95% ethanol at room temperature (25 ± 1 °C) for 7 days with occasional stirring and then filtered through Whatman filter paper. The ethanolic extract was concentrated and lyophilized to obtain the powder of *G. inodorum* crude extract. The extract was stored at -20 °C till use in subsequent experiments. The *G. inodorum* extract (GIE) was dissolved in DMSO and diluted to 0.1% (v/v) in the cell culture medium.

3.3.3 Determination of phytochemicals and antioxidant activity

3.3.3.1 Gas Chromatograph-Mass Spectrometer (GC-MS)

GC-MS analysis of OIE and GIE was performed using a Bruker 450-GC/Bruker 320-MS equipped with Rtx-5MS fused silica capillary column (30 m length × 250 μm diameter × 0.25 μm film thickness). An electron ionization system was operated in the electron impact mode for GC-MS detection with ionization energy of 70 eV. The injector temperature was maintained at 250 °C, and the ion-source temperature was 200 °C; the oven temperature was programmed from 110 °C (2 min), with an increase of 10 °C/min to 200°C (3 min), then 5 °C/min to 280°C, ending with a 20 min isothermal at 280 °C. The MS scan range was 45-500 atomic mass units (amu), and helium was used as the carrier gas with a 1.0 mL/min flow rate. The chemical components were identified by matching their mass spectra with those recorded in the NIST mass spectral library 2008.

3.3.3.2 The 2, 2-diphenyl-1-picrylhydrazyl (DPPH) assay

This assay is based on the measurement of the scavenging ability of antioxidants towards the stable radical DPPH, and hence the decreasing absorbance at 515-528 nm. The free radical DPPH (purple) is reduced to the corresponding hydrazine (no color) when it reacts with hydrogen donors from antioxidant compounds.

The DPPH˙ scavenging activity was determined by following the method of Sánchez-Moreno (2002) (Sánchez-Moreno, 2002). Briefly, one milliliter of the extracts at different concentrations was added to 3.9 ml of DPPH solution (63 mM). The mixture was shaken vigorously at room temperature for 45 min in the dark and measured absorbance at 515 nm using a spectrophotometer. The free radical scavenging activity was calculated as shown below. The IC_{50} of DPPH˙ was

determined from a dose-response curve using linear regression analysis. Decreasing DPPH solution absorption indicates an increase in DPPH radical scavenging activity.

$$\text{DPPH inhibition (\%)} = \frac{[(A_{control} - A_{sample}) \times 100}{A_{control}}$$

Where $A_{control}$ = The absorbance of control

A_{sample} = The absorbance of different concentrations of sample extracts

3.3.3.3 FRAP assay

The ferric reducing capacity of OIE and GIE was determined by using the colorimetric method as described by Rupasinghe (2018) (Rupasinghe et al., 2008). Briefly, 20 µL of each of the samples and 180 µL of FRAP reagent (300 mM acetate buffer (pH 3.6), 10 mM 2, 4, 6-tripyridyl-s-triazine (TPTZ) and 20 mM $FeCl_3 \bullet 6H_2O$ solution) were mixed in a 96-well plate for 6 min. The absorbance was recorded at 595 nm using a microplate reader (Bio-Rad Laboratories, Inc., Hercules, CA, USA). The different concentrations of Trolox and vitamin C were used to develop the standard calibration curve. FRAP values were expressed as a milligram of Trolox equivalent antioxidant capacity (TREA) or ascorbic equivalent antioxidant capacity (VCEA) per gram of dry extract.

3.3.4 Cytotoxic test (MTT assay)

The cytotoxic effect of OIE and GIE on RAW264.7 macrophage cell viability was determined by 3-(4, 5-dimethylthiazol-2-yl)-2, 5-diphenyltetrazolium bromide (MTT) assay (Sittisart and Chitsomboon, 2014). Briefly, cells were plated at a density of 2×10^4 cells/well in a 96-well plate and incubated overnight. Cells were treated with OIE and GIE at concentrations ranging from 0 to 1000 µg/mL and then incubated at 37 °C under 5% CO_2 for 24 h. After incubation, the culture medium was removed, and 0.5 mg/mL (final concentration) MTT solution was added. Then, cells were further incubated for 4 h at 37 °C. Formazan crystals formed by viable cells were dissolved in DMSO, and absorbance was measured at 540 nm with a microplate spectrophotometer (Benchmark Plus, Bio-Rad, Japan).

3.3.5 Cell treatment

To investigate the anti-oxidant and anti-inflammatory activities of OIE and GIE in RAW264.7 macrophage cells, the cells were seeded at a density of 2×10^4 cells/well in a 96-well plate or 6×10^5 cells/well in a 6-well plate and then incubated overnight. After incubation, the culture medium was removed, and the cells were treated with various concentrations of OIE (50, 100, or 200 µg/mL) or GIE (50, 100, 200, or 300 µg/mL) or the anti-inflammatory agent, Dexamethasone (1 µM) for 3 h. Then, the cells were activated with 1 µg/mL LPS plus 10 ng/mL IFN-γ and incubated for 24 h. The cells were collected to investigate the anti-oxidant or anti-inflammatory activities of the extracts on the cell-based assay.

3.3.6 Anti-oxidant study

3.3.6.1 Measurement of intracellular ROS

A fluorescent dichlorofluorescein diacetate (DCFH-DA) assay accessed intracellular ROS concentrations (Sittisart and Chitsomboon, 2014). RAW264.7 macrophage cells were seeded in a 96-well black plate at 2.5×10^4 cells/well and incubated overnight. Then, the culture medium was removed, and the cells were treated with various concentrations of OIE (50, 100, or, 200 µg/mL) or GIE (50, 100, 200, or 300 µg/mL) or a selective ROS scavenger, N-acetyl-cysteine (NAC) for 3 h. Then, the cells were activated with 1 µg/mL LPS plus 10 ng/mL IFN-γ and incubated for 24 h. After removing the medium, the cells were treated with 20 µM DCFH-DA in Hank's Balanced Salt Solution (HBSS) for 30 min at 37°C. The DCFH-DA was removed by washing the cells with HBBS twice. The intensity of the fluorescence signaling was detected with an excitation wavelength of 485 nm and an emission wavelength of 535 nm using a Gemini EM fluorescence microplate reader (Molecular Devices, Sunnyvale, CA).

3.3.6.2 Quantitative reverse transcription PCR (RT-qPCR)

To determine the level of mRNA expression of antioxidant genes, including SOD2, glutathione S-transferase pi 1 (GSTP1), NAD(P)H quinone dehydrogenase 1 (NQO1), cysteine ligase catalytic subunit (GCLC), and glutamate-cysteine ligase regulatory subunit (GCLM) in RAW264.7 macrophage cells after treating with OIE or GIE, the cells were seeded in 6-well plate and allowed to grow overnight. Then, the

cells were treated with various concentrations of OIE (50, 100, or 200 μg/mL) or GIE (50, 100, 200, or 300 μg/mL) for 3 h. Total RNA was isolated using TRIzol reagent (Invitrogen, Carlsbad, CA, USA), and 2 μg of total RNA was reverse transcribed to single-stranded cDNA using the SuperScript VILO cDNA Synthesis Kit (Invitrogen™, California, USA) at 42 °C for 1 h.

qPCR was performed in a LightCycler® 480 Real-Time PCR System (Roche Diagnostics, Mannheim, Germany) using SYBR green master mix. The PCR was performed in a final volume of 20 μL containing 1 μL of primer mixture (10 μM), 10 μL of 2X SYBR Green Master Mix (Roche Diagnostics, Mannheim, Germany), 5 μL of cDNA template (5 μg), and 4 μL of nuclease-free distilled water. Real-time PCR cycles included: initial denaturation at 95 °C for 5 min; 95 °C for 10 s, annealing at 60 °C for 20 s, and extension at 72 °C for 30 s through 40 cycles. The specificity of each of the PCR products was confirmed by melting curve analysis. The fold change in mRNA expression was calculated by comparing the GAPDH normalized threshold cycle numbers (Ct) in the untreated- and GIE treated-LPS plus IFN-γ-induced cells to the uninduced cells using the $2^{-\Delta\Delta Ct}$ method. Triplicate wells were run for each experiment, and two independent experiments were performed. The primer sequences designed for qRT-PCR analysis are listed in Table 3.3.

Table 3.3 Oligomeric nucleotide primer sequence of qRT-PCR.

Gene	Forward primer (5′-3′)	Reverse primer (5′-3′)
iNOS	CAGCACAGGAAATGTTTCAGC	TAGCCAGCGTACCGGATGA
COX-2	TTTGGTCTGGTGCCTGGTC	CTGCTGGTTTGGAATAGTTGCTC
IL-6	CTGCAAGAGACTTCCATCCAG	AGTGGTATAGACAGGTCTGTTGG
SOD2	TTAACGCGCAGATCATGCA	GGTGGCGTTGAGATTGTTCA
GSTP1	TGGGCATCTGAAGCCTTTTG	GATCTGGTCACCCACGATGAA
NQO1	TTCTGTGGCTTCCAGGTCTT	AGGCTGCTTGGAGCAAAATA
GCLC	GATGATGCCAACGAGTCTGA	GACAGCGGAATGAGGAAGTC
GCLM	CTGACATTGAAGCCCAGGAT	GTTCCAGACAACAGCAGGTC
GAPDH	AACGACCCCTTCATTGAC	TCCACGACATACTCAGCAC

3.3.7 Anti-inflammatory study

3.3.7.1 Nitrite assay

The Griess solution is a chemical analysis test that detects the presence of organic nitrite compounds. The Griess reaction was first described in 1879, and this assay has also been used extensively to analyze numerous biological samples, including cell culture media. In this assay, nitrite is first treated with a diazotizing reagent, sulfanilamide (SA) in acidic media to form a transient diazonium salt. This intermediate is then allowed to treat with a coupling reagent, naphthylethylenediamine dihydrochloride (NED), to form a stable compound (Sun et al., 2003).

The NO level in the culture media was detected as nitrite, a primary stable NO product, using Griess reagent as described by Sittisart and Chitsomboon (2014) (Sittisart and Chitsomboon, 2014), with slight modifications. Briefly, 100 µL of supernatant was transferred to an equal volume of Griess reagent in a 96-well plate. After 10 min of incubation in the dark, the absorbance of samples was measured at 540 nm using a microplate reader (Bio-Rad Laboratories, Inc.). The amount of nitrite in the samples was derived from a standard curve of sodium nitrite at the concentration range of 2.5-100 µM.

3.3.7.2 Enzyme-linked immunosorbent assay (ELISA)

ELISA is a prevalent technique in clinical diagnosis, biological, and medical, scientific research. ELISA can be used to detect and quantify the antigens, antibodies, hormones, or cytokines presented in the sample.

Cytokine levels (TNF-α, IL-6 or IL-10) were quantified by DuoSet® ELISA Kits (R&D system). Briefly, Immunolon strip plates (Thermo, York, PA) were coated with 100 µL per well of the diluted Capture Antibody (anti-Mouse TNF-α, anti-Mouse IL-6, or anti-Mouse IL-10) and incubated overnight at 4 °C. After incubation, each well was washed three times with 400 µL wash buffer (0.05% Tween 20 in phosphate-buffered saline, pH 7.2-7.4) to remove excess unbound antibodies. Then, the non-specific sites were blocked with 300 µL of Reagent Diluent (1% BSA in PBS, pH 7.2-7.4) for 1 h at room temperature, followed by three additional washes. After blocking, one hundred microliters of the cell supernatant or standard (mouse TNF-α, mouse IL-6, or mouse

IL-10 standard) was added to respective wells and incubated for 2 h. After washing, one hundred microliters of the Detection Antibody were added to the corresponding wells and allowed to incubate at room temperature for 2 h. After washing, 100 μL of the working dilution of Streptavidin-HRP was added, followed by incubation at room temperature for 20 min. After washing, 100 μL of TMB substrate [12.5 mL citric phosphate buffer pH 5.0 + 200 μL of 3, 3', 5, 5'-tetramethyl-benzidine stock solution (6 mg/mL in DMSO) + 50 μL 1% H_2O_2] was added to each well for 20 min at room temperature. The reaction was stopped by the addition of 50 μL 6 N H_2SO_4. Optical density was determined at 450 nm with a microplate spectrophotometer (Benchmark Plus, Bio-Rad, Japan). The concentration of cytokine (TNF-α, IL-6, and IL-10) was determined from a standard curve prepared from the known concentration of standard cytokine.

3.3.7.3 Western blot analysis

RAW264.7 cells were treated with the same protocol as described in section 3.3.5 Cell treatment. After treatment, the cells were washed three times with PBS. The whole-cell lysates were performed, the cell pellets were resuspended in 150 μL of ice-cold lysis buffer (1 mL RIPA buffer supplemented with 2mM PMSF, 2 μM leupeptin, and 1 μM E-64) for 20 min. Then the disrupted cells were transferred to microcentrifuge tubes and centrifuged at 14,000 g at 4 °C for 30 min. The supernatant, consisting of the whole-cell fraction, was immediately frozen for Western blot analysis. Protein concentration was determined using the Lowry method (Lowry et al., 1951).

Cell lysate was boiled for 5 min in a 6X sample buffer (50 mM Tris-base, pH 7.4, 4% SDS, 10% glycerol, 4% 2-mercaptoethanol, and 0.05 mg/mL of bromophenol blue). Thirty micrograms of cellular proteins were separated by sodium dodecyl sulfate-polyacrylamide gel electrophoresis (SDS-PAGE) using 10% polyacrylamide gels (125 volts, 120 min). The proteins in the gel were transferred onto a nitrocellulose membrane (Amersham, Pittsburgh, PA, USA) at 80 volts for 1 h. The membrane was blocked with 5% bovine serum albumin (BSA) in 0.1% Tween 20 in a PBS buffer (0.1% PBST) at retention time (RT) for 1 h. The membranes were then incubated with a 1: 1,000 dilution of the mouse monoclonal anti-NF-kB p65 antibody (F-6, sc-8008),

anti-p-NF-kB p65 (27.Ser 536, sc136548), α-tubulin (B-7, sc-5286) (Santa Cruz Biotechnology, Inc., Dallas, TX, USA) at 4 ℃ overnight. After extensive washing with 0.1% PBST, the membranes were incubated with a 1: 5,000 dilution of the secondary antibody mouse IgGk light chain binding protein (m-IgGk BP) conjugated to horseradish peroxidase (HRP) at RT for 1 h. The membranes were washed three times for 5 min each time, with 0.1% PBST. The membranes were incubated for 3 min in ECL Western blotting substrate (Thermo Scientific, Waltham, MA, USA) and exposed to film. The relative expression of NF-kBp65 and p-NF-kBp65 proteins was quantified densitometrical using the software image J. The α-tubulin was used as a housekeeping protein.

3.3.7.4 Immunofluorescence staining

As a marker of NF-kB activation, the nuclear translocation of the p65 NF-kB subunit was visualized in RAW264.7 cells by immunofluorescence microscopy. Cells were seeded at a density of 6×10^4 cells/well in an 8-well cell culture slide (Invitrogen, Waltham, MA, USA). After 24 h of incubation, cells were pretreated with OIE or GIE or 1 μM of DEX for 3 h. Then, cells were co-incubated with 1 μg/mL LPS+10 ng/mL IFN-γ for another 24 h. After incubation, cells were fixed with 4% paraformaldehyde for 15 min and then permeabilized with 0.1%Triton-X100 for 10 min at room temperature. After washing with PBS, the samples were blocked in 0.1% PBST containing 4% bovine serum albumin (BSA), and then incubated overnight at 4 ℃ with the mouse monoclonal anti-NF-kB p65 antibody (F-6), sc-8008 (Santa Cruz Biotechnology, Inc., Dallas, TX, USA) diluted 1:200 in 0.1% PBST containing 1% BSA. After washing with 0.1% PBST, each reaction was followed by incubation for 1 h with anti-mouse conjugated to Alexa 488-conjugated goat anti-mouse IgG (1:250 in 0.1% PBST containing 1% BSA; Abcam, Cambridge, UK). After washing with 0.1% PBST, the cells were incubated with 10 mg/mL Hoechst 33258 diluted 1:2000 in 0.1 % PBST (Invitrogen, Waltham, MA, USA) for 10 min at room temperature and then washed with 0.1% PBST. Slides were mounted with Bio Mount HM mounting medium (Bio-Optica Milano S.p.a., Milano, Italy). The fixed RAW264.7 cells were taken with confocal microscopy (Nikon, Melville, NY, USA).

3.3.8   Statistical analysis

All statistical significances (Statistical Package for the Social Sciences, version 19) were determined by performing a one-way analysis of variance (ANOVA) with a Tukey's post hoc analysis to determine differences among each treated and control group. Values were considered statistically significant when $p < 0.05$, and data was representative of at least three independent experiments.

CHAPTER IV

RESULT AND DISCUSSION

4.1   Anti-oxidation and anti-inflammation of *O. indicum* extract (OIE)

4.1.1 Phytochemicals and antioxidant activity

4.1.1.1   Extraction yield

A 1.0 kg weight of fruit pods from *O. indicum* was extracted with 95% ethanol by a soxhlation for 8 h. The ethanol extract was evaporated and lyophilized to obtain a final yield of 18.41% (w/w) *O. indicum* extract (OIE).

4.1.1.2   GC-MS analysis of volatile oil constituents of OIE

GC/MS analysis of OIE enabled the identification of 27 volatile compounds, as shown in Table 4.1. The data in Table 4.1 illustrate retention time, chemical formula, and the relative amount of each component detected in OIE. Based on abundance, the top five major compounds present in OIE were γ-sitosterol (17.19%), 2-Cyclohexen-1-one, 2-methyl- (15.28%), benzeneethanol, 4-hydroxy- (13.33%), 3-Hydroxy-2-methylbenzaldehyde (11.18%), and cyclobutanecarboxylic acid, decyl ester (8.82%). These compounds exhibit important pharmacological activity, such as antidiabetic, antioxidant, anticancer, and anti-inflammatory activities. The sterol compounds, namely stigmasterol and β-sitosterol, isolated from the methanol extract of *Achillea ageratum* have been shown to possess anti-inflammatory activity against 12-0-tetradecanoylphorbol acetate- (TPA-) induced mouse ear edema (Gomez et al., 1999). Therefore, the presence of phytosterols in OIE is considered to be of great importance for the curing of diseases.

Table 4.1 GC-MS analysis of OIE.

No.	Compound Name	Formula	RT	%Area
1	2-Furancarboxaldehyde,5-(hydroxymethyl)-	$C_6H_6O_3$	4.88	4.86
2	Nonanoic acid	$C_9H_{18}O_2$	5.30	2.28

Table 4.1 GC-MS analysis of OIE (Continued).

No.	Compound Name	Formula	RT	%Area
3	n-Decanoic acid	$C_{10}H_{20}O_2$	6.55	2.82
4	2-Cyclohexen-1-one, 2-methyl-	$C_7H_{10}O$	7.13	15.28
5	2-Dodecenoic acid	$C_{12}H_{22}O_2$	7.30	1.33
6	Benzeneethanol, 4-hydroxy-	$C_8H_{10}O_2$	7.54	13.33
7	3-Hydroxy-2-methylbenzaldehyde	$C_8H_8O_2$	7.88	11.18
8	Cyclobutanecarboxylic acid, decyl ester		8.89	8.82
9	Dodecanoic acid	$C_{12}H_{24}O_2$	8.98	1.15
10	Ethyl N-(o-anisyl)formimidate	$C_{10}H_{13}NO_2$	9.59	0.40
11	1,6-Dihydro-5-(2-hydroxyethyl)-4-methyl-6-oxopyrimidine	$C_7H_{10}N_2O_2$	10.99	1.39
12	Tetradecanoic acid	$C_{14}H_{28}O_2$	11.26	0.21
13	Hexadecanoic acid, methyl ester	$C_{17}H_{34}O_2$	13.58	0.28
14	n-Hexadecanoic acid	$C_{16}H_{32}O_2$	14.28	0.66
15	Hexadecanoic acid, ethyl ester	$C_{18}H_{36}O_2$	14.82	0.99
16	Phytol	$C_{20}H_{40}O$	17.09	0.39
17	Linoleic acid ethyl ester	$C_{20}H_{36}O_2$	17.95	0.58
18	Linolenic acid ethyl ester	$C_{20}H_{34}O_2$	18.08	0.57
19	Glycerol 1,3-dipalmitate	$C_{35}H_{68}O_5$	20.36	1.13
20	Linolelaidic acid, methyl ester	$C_{19}H_{34}O_2$	23.30	0.79
21	9,12,15-Octadecatrienoic acid, 2-phenyl-1,3-dioxan-5-yl ester	$C_{28}H_{42}O_4$	23.44	0.52
22	Dotriacontane	$C_{32}H_{66}$	23.67	1.29
23	Glycerol 1-monopalmitate	$C_{19}H_{38}O_4$	23.93	4.37
24	beta-Monolinolein	$C_{21}H_{38}O_4$	26.70	4.09

Table 4.1 GC-MS analysis of OIE (Continued).

No.	Compound Name	Formula	RT	%Area
25	Campesterol	C28H48O	35.57	2.48
26	Stigmasterol	C29H48O	36.33	1.48
27	γ-Sitosterol	C29H52O2	37.88	17.19

4.1.1.3 LC-MS analysis of volatile oil constituents of OIE

The LC-MS chromatograms obtained from OIE are shown in Figure 4.1. Corresponding standards of scutellarin, daidzein, luteolin, apigenin, genistein, baicalein, and oroxylin A were used to identify and quantify the flavonoids composition in OIE. The predominant compounds were identified in OIE, namely, luteolin (peaks 14, RT 11.4 min) at m/z = 285, apigenin (peaks 16, RT 14.6 min) at m/z = 269, baicalein (peaks 19, RT 16.2 min) at m/z = 269, and oroxylin A (peaks 23, RT 22.0 min) m/z = 283. The identified compounds were quantified by comparisons of their retention time to known amounts of authentic standards. The largest amount of baicalein was detected in OIE with a concentration of 25,498.16 μg/g, while oroxylin A, luteolin, and apigenin were estimated in OIE at the level of 266.70, 209.98, and 77.54 μg/g, respectively. The previous investigation reported that OIE also contained quercetin as another flavonoid (Hengpratom et al., 2018). Many studies have shown the high biological and pharmacological activity of flavonoid compounds. Baicalein, oroxylin, luteolin, apigenin, and quercetin, the flavonoid compounds found in OIE, contributed to the anti-adipogenesis, anticancer, antioxidant, and anti-inflammatory proprieties of plants (Moon et al., 2006).
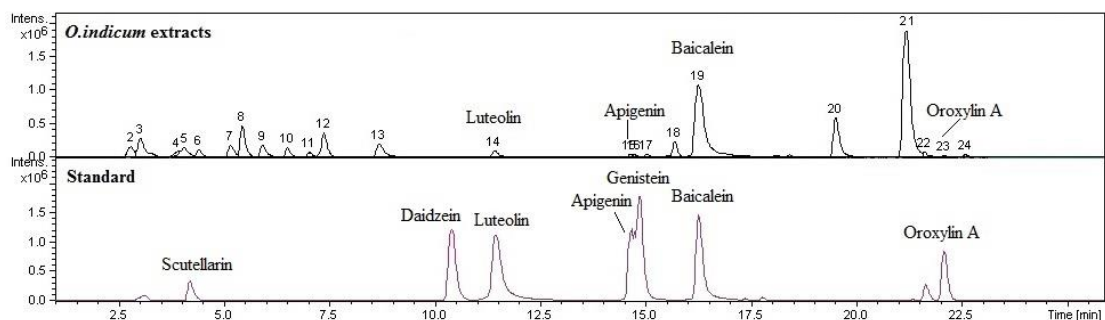
Figure 4.1 LC-MS chromatograms of OIE and standard compounds (scutellarin, daidzein, luteolin, apigenin, naringenin, genistein, baicalein, and oroxylin (A)).

4.1.1.4 Free radical scavenging and antioxidant activities of OIE

The antioxidative potential of OIE was assessed *in vitro* by DPPH and FRAP assays. The obtained results are shown in Table 4.2. This study determined the free radical scavenging activity of OIE and standard compound, vitamin C and Trolox, using the DPPH-based method. The results showed that the DPPH scavenging ability of OIE and standard compound, vitamin C, were comparable and both significantly stronger than Trolox ($p < 0.05$). The ferric reducing antioxidant power (FRAP) was used to assess whether OIE had an electron-donating capacity. OIE exhibited a degree of electron-donating capacity by 57.14±4.39 µgVCEA/mg and 65.77±4.99 µgTREA/mg of dry extract. These results indicate that OIE displays an antioxidant activity based on the reducing ability to reduce ferric ion (Fe^{3+}) to ferrous ion (Fe^{2+}). Therefore, it could be concluded that OIE displays strong antioxidant activity in the assay used in this study. This finding is in accordance with several studies that the antioxidant activity of OIE is caused by scavenging free radical DPPH and ferric reducing antioxidant power (FRAP) (Saha et al., 2017; Siriwatanametanon et al., 2010; Trang et al., 2018).

Table 4.2 Total antioxidant (FRAP) and DPPH scavenging activities of OIE and standard compounds.

Sample	FRAP values		DPPH scavenging activity
	(µgVCEA/mg)	(µgTREA/mg)	(IC$_{50}$) µg/mL
OIE	57.14±4.39	65.77±4.99	43.28±0.67[a]
Vitamin C	-	-	44.57±0.59[a]
Trolox	-	-	67.19±4.82[b]

Values are mean ± SD (n = 3) and represent three independent experiments with similar results. Different letters within the same column are significantly different at *p* < 0.05.

4.1.2 Effects of OIE on cell viability in RAW264.7 cells

The effects of OIE on cell viability in RAW264.7 cells were comprehensively investigated, as shown in Figure 4.2. The cell viability of RAW264.7 cells treated with OIE at a concentration range of 50-1,000 µg/mL was evaluated by using MTT assay. The viability of RAW264.7 cells was not significantly affected by OIE when concentrations of OIE were not greater than 300 µg/mL (*p* > 0.05). This result suggests further investigation to proceed with OIE at 50, 100, and 200 µg/mL concentrations in all subsequent experiments.
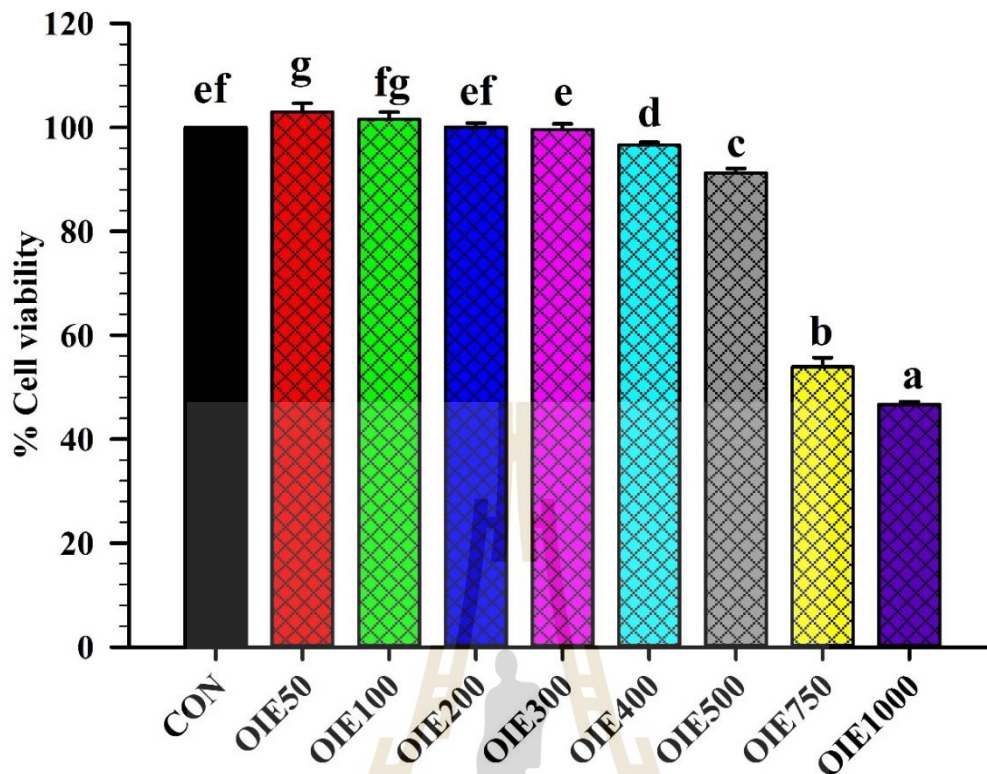
Figure 4.2 Effect of OIE on cell viability in RAW264.7 cells. Cells were treated with different concentrations of OIE for 24 h. Cell viability was determined by the MTT assay. CON = Cells without OIE and OIE50 - OIE1000 = Cells were treated with OIE at concentration ranges of 50-1,000 μg/mL, respectively. Values are expressed as a percentage of the control. The data represent the mean ± SD of three independent experiments. Bars marked with different letters are significantly different at $p < 0.05$ as determined by one-way ANOVA with Tukey post hoc test.

4.1.3 Effects of OIE on intracellular ROS production in LPS plus IFN-γ-induced RAW264.7 cells

In the event of the inflammatory response, the classically activated macrophages respond to intracellular pathogens by secreting proinflammatory cytokines, chemokines, proteases, and the production of reactive oxygen species (Castaneda et al., 2017). These factors are key signaling molecules that play a significant role in host defense and inflammation. ROS overproduction can prompt injury issues that might initiate the inflammation process (Yahfoufi et al., 2018).

Ribeiro et al. (2013) reported that flavonoid compounds possessed anti-inflammatory activity by the modulation of ROS generated through the neutrophils' oxidative burst (Ribeiro et al., 2013). Therefore, a flavonoid-enriched extract from OIE undoubtedly contributes to their anti-inflammatory roles by scavenging intracellular ROS and thus helps prevent the uncontrolled inflammation process.

To investigate whether the protective effects of OIE on the LPS plus IFN-γ induced inflammatory response were due to a blockade of oxidative stress. The intracellular ROS scavenging potential of OIE was evaluated in LPS plus IFN-γ-activated RAW264.7 cells. As presented in Figure 4.3, the treatment of RAW264.7 cells with LPS plus IFN-γ increased ROS accumulation by 1.79-fold compared to unactivated-RAW264.7 cells. Whereas pretreatment with OIE significantly inhibited the ROS generation in a dose-dependent manner. Compared to LPS plus IFN-γ-activated RAW264.7 cells, OIE at a concentration of 50, 100, and 200 µg/mL reduced intracellular ROS accumulation to 81.08±3.44, 68.16±3.34, and 36.35±1.62%, respectively. The inhibitory effects of OIE on ROS accumulation at 35% (IC_{35}), 40% (IC_{40}), and 50% (IC_{50}) were determined to be 106.03±5.71, 122.72±4.94, and 156.10±4.36 µg/mL, respectively. Surprisingly, the intracellular ROS scavenging activity of OIE (IC_{50}, 156.10±4.36 µg/mL) is, therefore, approximately 3 times more effective than a selective ROS scavenger, NAC (IC_{50}, 3 mM or 489.57 µg/mL). The antioxidant compound, vitamin C (VIT.C) at 50 µg/mL inhibited intracellular ROS by 40%inhibition, which is 2.45 times greater than OIE (IC_{40}=122.72±4.94 µg/mL) when compared at the same inhibitory potential. These results suggest that OIE possesses a strong antioxidant activity in scavenging ROS secreted by LPS plus IFN-γ-stimulated in RAW264.7 cells.

Mairuae et al. demonstrated that *O. indicum* treatment attenuated the generation of ROS on Aβ25-35-induced cell injury in human neuroblastoma SH-SY5Y cells (Mairuae et al., 2019). Mohan et al. found that *O. indicum* leaf extract could overcome the oxidative stress induced by 4-NQO in albino Wistar rats when administered orally (Mohan et al., 2016). These findings lead us to believe that flavonoids present in OIE, baicalein, quercetin, luteolin, and apigenin may play an important role in protection against oxidative stress. Based on the LC-MS experiment,

the results indicated that OIE at a 200 µg/mL concentration is composed of baicalein of about 5 µg/mL. In order to clarify whether baicalein could act as an intracellular ROS scavenger or not, baicalein 5 µg/mL was used as a positive control. The result indicated that baicalein decreased LPS plus IFN-γ-induced intracellular ROS levels by approximately 30%. These data suggest that baicalein in OIE can scavenge the ROS production of test cells. Previous investigators demonstrated that baicalein enhanced cellular antioxidant defense capacity in C6 glial cells by inhibiting ROS production and activating the Nrf2 signaling pathway (Choi et al., 2016). Qi et al. (2013) found that baicalein reduced LPS-induced inflammation via suppressing JAK/ STATs activation and ROS production (Qi et al., 2013). In addition, baicalein declined H_2O_2-induced DNA damage due to a decrease of phospho-h2a.x output, DNA tail formation, and lipid peroxidation prevention (K. A. Kang et al., 2012). Our results indicated that the pretreatment of RAW264.7 cells with OIE at a 200 µg/mL concentration significantly decreased the intracellular ROS accumulation by approximately 64%. This finding suggests that OIE at 200 µg/mL, which contains baicalein around 5 µg/mL, shows significantly stronger radical scavenging potency than baicalein alone ($p < 0.05$, Figure 3). The higher potency of OIE may be due to the other bioactive compounds present in OIE such as β-sitosterol, stigmasterol, luteolin, apigenin, and quercetin, which could act as ROS scavenging agents. All compounds above have been shown to possess antioxidant properties. The intracellular ROS scavenging potency of OIE is more than two times stronger compared to baicalein alone which leads us to believe that synergistic activity could take place between baicalein and other flavonoids or volatile compounds (Eumkeb et al., 2017).
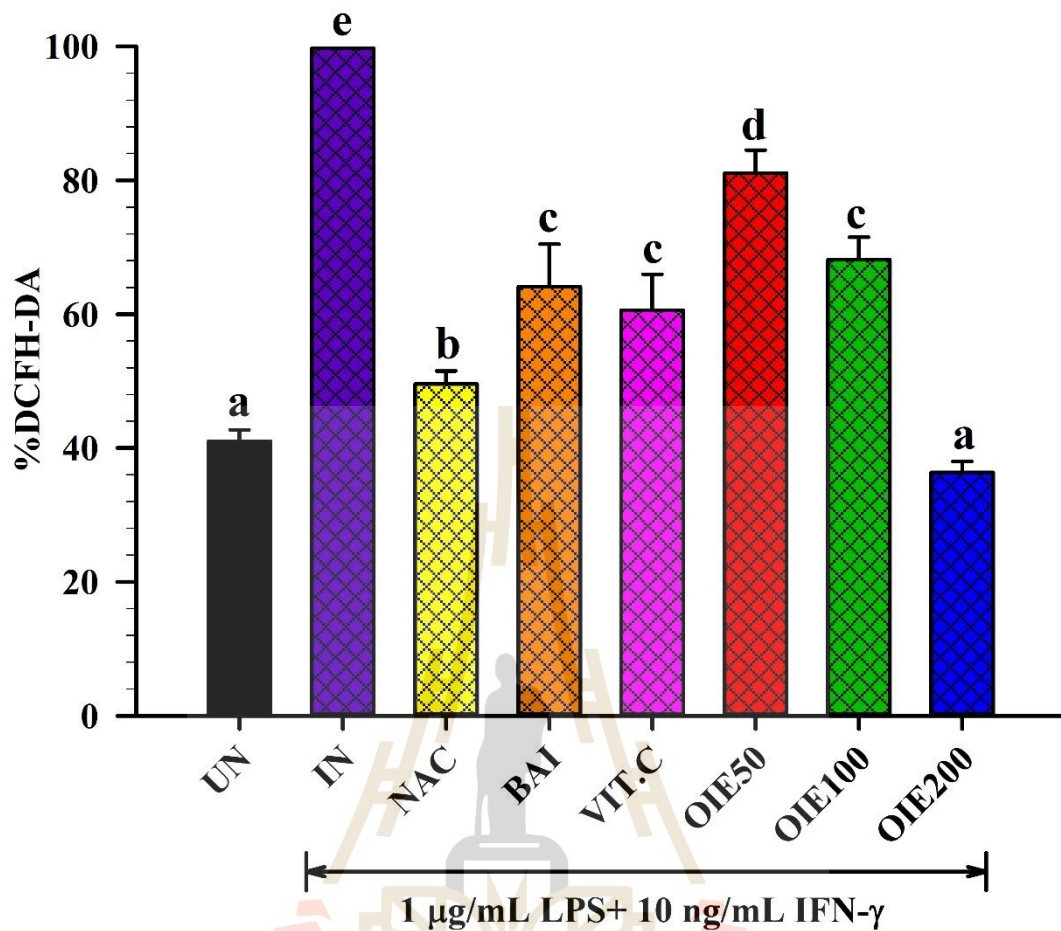
Figure 4.3 Effects of OIE on the intracellular ROS production in LPS plus IFN-γ-induced RAW264.7 cells. Cells were pretreated with different concentrations of OIE for 3 h and then induced with LPS plus IFN-γ for 24 h. UN = Uninduced cells, IN = Untreated LPS plus IFN-γ-induced cells, NAC = Cells were pretreated with NAC 3 mM, BAI = Cells were pretreated with baicalein at 5 µg/mL, VIT.C = Cells were pretreated with vitamin C at 50 µg/mL, and OIE50, OIE100, and OIE200 = Cells were pretreated with OIE at 50, 100, and 200 µg/mL, respectively. The intracellular ROS levels are expressed as a percentage of the control. The data represent the mean ± SD of three independent experiments. Bars marked with different letters are significantly different at $p < 0.05$ as determined by one-way ANOVA with Tukey post hoc test.

4.1.4   Effects of OIE on anti-oxidant mRNA expression in LPS plus IFN-γ-induced RAW264.7 cells

Next, the inhibitory effect of OIE on oxidative stress was investigated by measuring antioxidant mRNA expression in RAW264.7 cells induced by LPS plus IFN-γ. Following stimulation of the cells by LPS plus IFN-γ, SOD2 and NQO1 mRNA expression exhibited a significant increase, along with a considerable decrease in GSTP1 and GCLC mRNA expression (Figure 4.4). Treatment by 200 µg/mL OIE achieved a statistically significant increase in SOD2, GSTP1, NQO1, GCLC, and GCLM mRNA expression in LPS plus IFN-γ-induced cells ($p < 0.05$). These results provide evidence that OIE inhibited ROS production by upregulating the expression of anti-oxidant genes in LPS plus IFN-γ-induced RAW264.7 cells.

The glutathione S-transferase pi gene (GSTP1) is a polymorphic gene encoding active, functionally different GSTP1 variant proteins. Glutathione S-transferase P1 (GSTP1) is a crucial phase II enzyme that can protect cells from oxidative stress in various human cancers. GSTP1 could be up-regulated in response to lipopolysaccharide (LPS) stimulation in RAW264.7 macrophage-like cells and over-expression of GSTP1 prevented LPS-induced excessive production of pro-inflammatory factors in RAW264.7 cells and release of NO (Xue et al., 2005). The literature also reported that GSTP1 down-regulates the iNOS protein level and increased S-nitrosylation and ubiquitination of iNOS (Cao et al., 2015).

SOD2 is one of the primary cellular antioxidant enzymes, which catalyze the dismutation of superoxide anion (O_2^-) to oxygen and hydrogen peroxide (H_2O_2) (Halliwell and Gutteridge, 1990). SOD2 was actively expressed via the NF-kB pathway during the progression of inflammatory conditions. The intracellular SOD2 is protective by suppressing the nucleotide-binding oligomerization domain, leucine-rich repeat, and pyrin domain-containing (NLRP) inflammasome-caspase-1-IL-1β axis under inflammatory conditions (Yoon et al., 2018). Superoxide dismutase (SOD) also acts as an anti-inflammatory due to its inhibitory effects on releasing lipid peroxidation-derived prostaglandins, thromboxane, and leukotrienes (Kirkham and Rahman, 2006). Therefore, OIE elevated levels of SOD2 can be an effective therapeutic strategy in oxidative stress and inflammation.

NAD(P)H:quinone oxidoreductase 1 (NQO1) was originally identified as a flavoenzyme that catalyzes the two-electron reduction of quinones to their hydroquinone forms protecting cells from oxidative stress, redox cycling, and neoplastic lesions (Dinkova-Kostova and Talalay, 2000). However, recent studies have indicated that LPS plus IFN-γ induce NQO1 expression in RAW264.7 cells. This result is in accordance with the results of earlier studies, which found that LPS induces NQO1 expression in human monocytes via Nrf2 (Rushworth et al., 2008). NQO1 promotes the ubiquitin-dependent degradation of I$\varkappa$B-ζ in association with PDLIM2, thereby selectively suppressing IL-6 production induced by TLR ligands (Kimura et al., 2018).

Glutamate-cysteine ligase (GCL), the key regulator of de novo glutathione synthesis, is composed of catalytic (GCLC) and modifier (GCLM) subunits. Glutathione (GSH) is the master antioxidant that maintains redox homeostasis, and it is critically involved in the inflammatory response (Espinosa-Diez et al., 2015; Zhang and Forman, 2012). GCLC down-regulation in the inflammatory response of macrophages is mediated through increased mRNA decay and caspase-5-mediated GCLC protein degradation, and γ-GC is an efficient agent to restore GSH and regulate the inflammatory response (Zhang et al., 2020).

Therefore, OIE activates the anti-oxidant gene expression, reducing inflammation and oxidative stress to contribute to its anti-inflammatory and antioxidant effects.
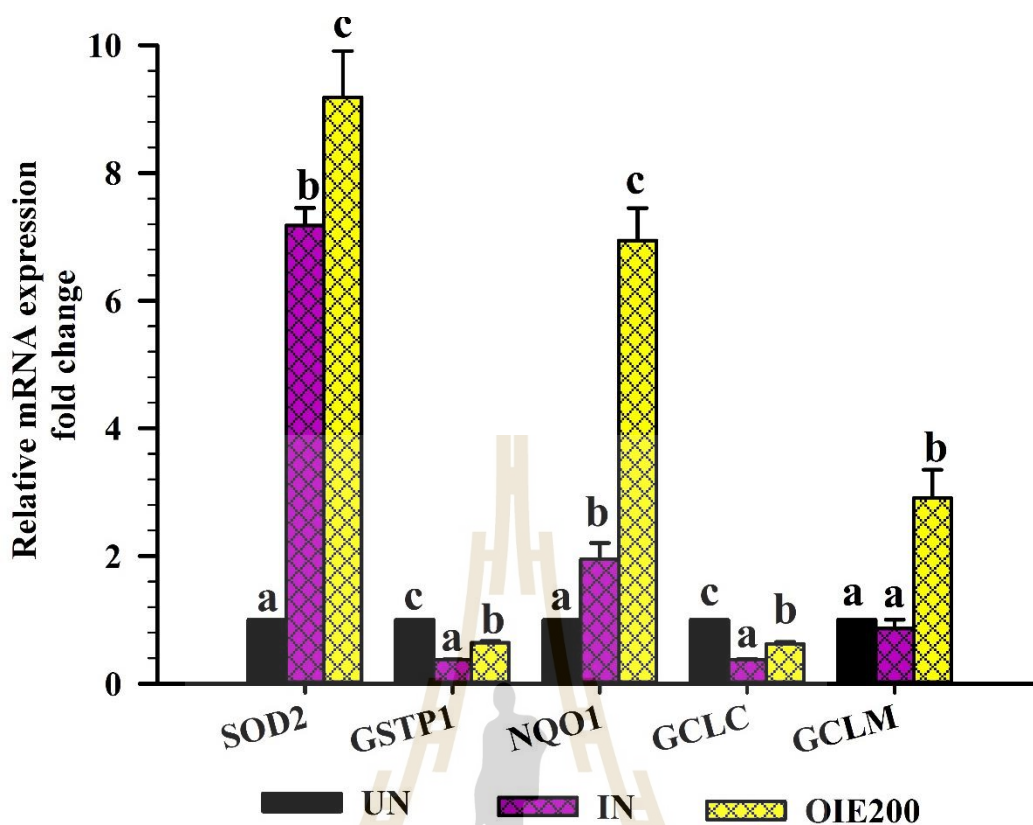
Figure 4.4 Effects of OIE on the antioxidant mRNA expression in LPS plus IFN-γ-induced RAW264.7 cells. Cells were pretreated with different concentrations of OIE 200 μg/mL for 3 h and then induced with LPS plus IFN-γ for 24 h. UN = Uninduced cells, IN = Untreated LPS plus IFN-γ-induced cells, and OIE200 = Cells were pretreated with OIE 200 μg/mL. The data represent the mean ± SD of three independent experiments. Bars marked with different letters are significantly different at $p < 0.05$ as determined by one-way ANOVA with Tukey post hoc test.

4.1.5 Effects of OIE on nitric oxide (NO) production, iNOS, and COX-2 mRNA expression in LPS plus IFN-γ-induced RAW264.7 cells

During inflammation, the macrophages actively participate in the inflammatory response by releasing cytokines (TNF-α, IL-1β, and IL-6), chemokines, and inflammatory mediators (NO, iNOS, PGE2, and COX-2) (Adib-Conquy et al., 2014). The overproduction of these agents contributes to the induction and progression of several inflammatory diseases. Thus, it is crucial to regulate the inflammatory mediators to control the inflammatory progression and treat inflammatory disorders.

Nitric oxide (NO) is synthesized by many cell types involved in immunity and inflammation. NO is vital as a toxic defense molecule against infectious organisms. On the other hand, NO reacts rapidly with superoxide to form the more reactive product, peroxynitrite ($ONOO^-$), which can directly react with various biological targets and components of the cell, including lipids, thiols, amino acid residues, DNA bases, and low-molecular-weight antioxidants (Sharma et al., 2007).

The anti-inflammatory potential of OIE on inhibition of NO production was measured after the treatment of OIE in LPS plus IFN-γ-activated RAW264.7 cells. The anti-inflammatory agent, dexamethasone (DEX), was selected to serve as the reference drug. As shown in Figure 4.5A, upon LPS plus IFN-γ treatment (IN), NO production was increased with the nitrite level peaking to 54.17±0.38 μM. However, pretreatment of cells with the highest concentration (200 μg/mL) of OIE suppressed the production of NO of about 16%, which precisely has the same efficiency as 1 μM DEX, compared to the LPS plus IFN-γ-induced group.

Qi et al. (2013) reported that baicalein suppressed LPS-induced inflammatory responses in RAW264.7 macrophages via attenuating NO synthesis (Qi et al., 2013). Shimizu et al. noted that an equimolar mixture (F-mix) of baicalein, wogonin, and oroxylin A showed a synergistic inhibitory effect on NO production in LPS-treated J774.1 cells (T. Shimizu et al., 2018). Also, a mixture of β-sitosterol and stigmasterol isolated from *Androgrphis paniculata* significantly suppressed NO production in LPS plus IFN-γ stimulated RAW264.7 cells (Chao et al., 2010).

In the inflammatory response, NO and PGE2 are synthesized by iNOS and COX-2, respectively (Karpuzoglu and Ahmed, 2006). To confirm if the suppression of NO production by OIE was related to change in iNOS as well as COX-2 mRNA levels, qRT-PCR was performed. Figures 4.5B and 4.5C showed that iNOS and COX-2 mRNA expression was increased in LPS plus IFN-γ-induced cells (IN). At the same time, pretreated OIE significantly decreased the expression of iNOS and COX-2 mRNA levels in a concentration-dependent manner ($p < 0.05$). The present study indicates that the suppressive effect of OIE on NO production is mediated through the inhibition of iNOS mRNA expression. Therefore, iNOS reduction leads to the lower PGE2 and COX-2 expression in activated macrophages with LPS. There is no doubt that LPS and IFN-

γ also efficiently enhance COX-2 expression in RAW264.7 cells (Jang et al., 2005). Our results demonstrate that OIE can exhibit anti-inflammatory activity by attenuating COX-2 mRNA expression. Thus, OIE might play essential roles in ameliorating inflammation by suppressing NO production and downregulation of iNOS and COX-2 mRNA expression.
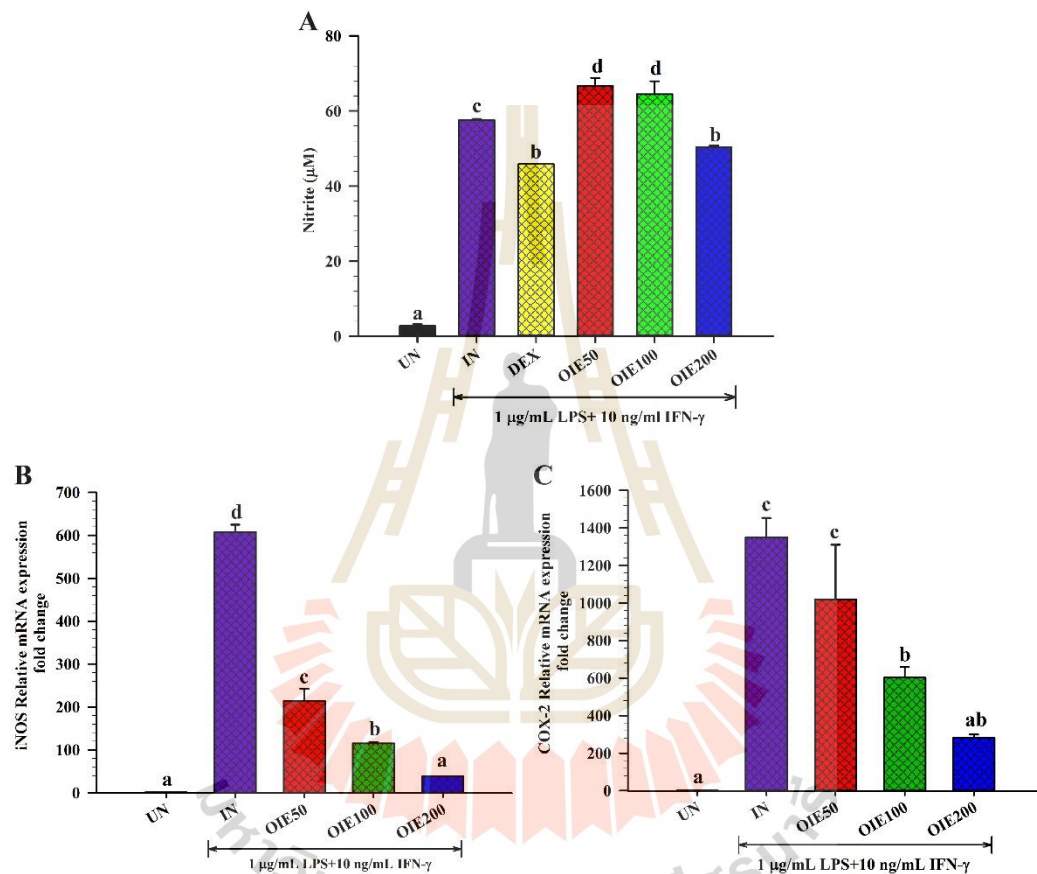
Figure 4.5 Effects of OIE on NO production (A), iNOS (B), and COX-2 (C) mRNA expression in LPS plus IFN-γ-induced RAW264.7 cells. Cells were pretreated with different concentrations of OIE for 3 h and then induced with LPS plus IFN-γ for 24 h. UN = Un-induced cells, IN = Untreated LPS plus IFN-γ-induced cells, and OIE50, OIE100, and OIE200 = Cells were pretreated with OIE at 50, 100, and 200 μg/mL, respectively. The data represent the mean ± SD of three independent experiments. Bars marked with different letters are significantly different at $p < 0.05$ as determined by one-way ANOVA with Tukey post hoc test.

4.1.6 Effects of OIE on anti-inflammatory cytokines (IL-10) and pro-inflammatory cytokines (IL-6 and TNF-α) and mRNA expression in LPS plus IFN-γ-induced RAW264.7 cells

IL-6 and TNF-α are essential proinflammatory cytokines, either of which can serve as an indicator of inflammation. To confirm the anti-inflammatory effect of OIE, we also investigated the effect of OIE on proinflammatory and anti-inflammatory cytokine secretion by measuring IL-6, TNF-α, and IL-10 levels in RAW264.7 cells induced by LPS plus IFN-γ. Exposure of the cells with LPS plus IFN-γ strongly induced the secretion of IL-6, TNF-α, and IL-10 compared to the uninduced group (Figure 4.6A-4.6C). The results showed that DEX markedly reduced the secretion of IL-6 and TNF-α by about 69.34% and 62.02%, respectively, compared to the LPS plus IFN-γ-induced group. Treatment with OIE inhibited the secretion of IL-6 and IL-10 in a dose-dependent manner (Figure 4A), but it did not affect the reduction of TNF-α level ($p > 0.05$, Figure 4B). OIE concentration at 200 µg/mL exerted an IL-6 inhibition by 62.99%, which was practically similar to the reference drug, DEX (69.34% inhibition). qRT-PCR was performed to investigate whether suppression of TNF-α and IL-6 production by OIE was related to a change in mRNA levels for both proinflammatory cytokines. Increasing concentrations of OIE produced a decrease in IL-6 mRNA levels in LPS plus IFN-γ-induced cells (Figure 4.6D). However, OIE slightly decreased TNF-α mRNA levels compared to LPS plus IFN-γ-induced cells (Figure 4.6E). The IL-6 and TNF-α suppression profile by OIE suggests that OIE acts more potent on IL-6 than TNF-α.

Other researchers had demonstrated that the ethyl acetate extract derived from the stem bark of *O. indicum* showed the inhibitory effect on LPS-induced IL-6, IL-1β, and TNF-α release in human monocytes (Siriwatanametanon et al., 2010). *In vivo* study indicated that the aqueous decoction of both stem bark and root bark of *O. indicum* produced anti-inflammatory activity by reducing paw edema formation in the carrageenan-induced paw edema model (Doshi et al., 2012). Furthermore, flavonoids found in this plant, such as baicalein, apigenin, oroxylin A, and luteolin, are known for their anti-inflammatory effects attributed at least partially through the suppression of proinflammatory cytokines, IL-6, IL-1β, and TNF-α (J. Y. Lee and Park,

2016). Moreover, it had been reported that a mixture of β-sitosterol and stigmasterol isolated from *Andrographis paniculata* significantly decreased TNF-α and IL-6 secretion from LPS plus IFN-γ-stimulated RAW264.7 cells (Chao et al., 2010). These findings provide evidence that the main constituents of OIE are flavonoids and phytosterols, which could potentially act as the anti-inflammatory compounds of this plant. Differential effects of OIE on IL-6 and TNF-α production in RAW264.7 cells could be explained by the different mechanisms of OIE on the secretion of IL-6 and those of TNF-α alleviation. Several studies reported that the mechanism, signaling pathways, and transcription factors controlling TNF-α expression were distinct from IL-6 (Greenhill et al., 2011; Horwood et al., 2006; Samavati et al., 2009). It had been reported that the activation of p38 MAPK was required for the LPS/TLR4-induced expression of TNF-α, but not IL-6 (Horwood et al., 2006). It is well known that CREB recognizes a similar DNA binding sequence in the promoter region of the TNF-α gene (O'Donnell and Taffet, 2002). In contrast, similar sequences have not been identified on the IL-6 and IL-1 promoters. Also, the STAT3 tyrosine phosphorylation is a key role to induce IL-6 production in response to inflammation. *In vitro* study revealed that the blocking STAT3 activity preferred to inhibit LPS-mediated production of IL-1β and IL-6, but not TNF-α, in RAW264.7 cells (Samavati et al., 2009). The study of Prele et al. also confirmed that the STAT3 activation did not directly regulate LPS-induced TNF-α production in human monocytes (Prele et al., 2007).
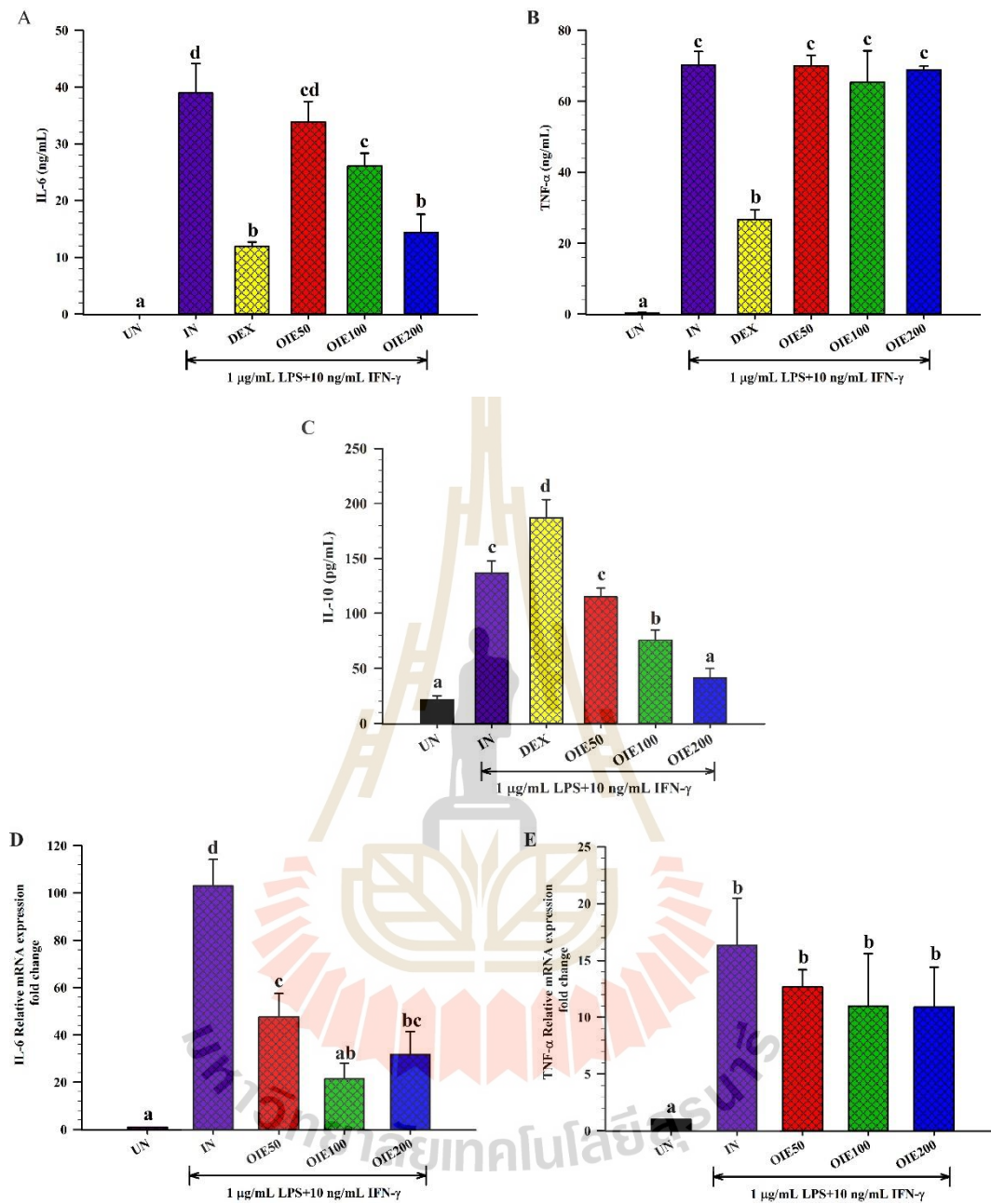
Figure 4.6 Effects of OIE on the secretion of proinflammatory cytokines (A) IL-6, (B) TNF-α, and anti-inflammatory cytokines (C) IL-10 secretion in LPS plus IFN-γ-induced RAW264.7 cells. The effects of OIE on (D) IL-6 and (E) TNF-α mRNA expression. Cells were pretreated with GIE or DEX for 3 h and then induced with LPS plus IFN-γ for 24 h. UN = uninduced cells, IN = untreated LPS plus IFN-γ-induced cells, DEX = cells were pretreated with DEX at 1 μM, and OIE50, OIE100, and OIE200 = Cells were pretreated with OIE at 50, 100, and 200 μg/mL, respectively. The data represent the mean ± SD of two independent experiments. One-way ANOVA performed the

comparison, and Tukey was used as a post hoc test. The degree of significance was denoted with different letters for the comparison between sample groups. $p < 0.05$ was considered as statistically significant.

4.1.7 Effects of OIE on NF-kB p65 nuclear translocation and p-NF-kB p65 (27. Ser 536) protein expression in LPS plus IFN-γ-induced RAW264.7 cells

Given that LPS plus IFN-γ-induced inflammation is through Toll-like receptor (TLR) signaling, NF-kB is activated and translocated into the nucleus to regulate the induced transcription of proinflammatory genes (Tak and Firestein, 2001). As a marker of NF-kB activation, the nuclear translocation of the NF-kB p65 was visualized in LPS plus IFN-γ induced RAW264.7 cells by immunofluorescence confocal microscopy. As shown in Figure 4.7, LPS plus IFN-γ-induced RAW264.7 cells (IN) showed marked NF-kB p65 staining in the nuclei, while uninduced cells (UN) showed weaker nuclear NF-kB expression but stronger staining in the cytoplasm. OIE treatment (OIE200) attenuated LPS plus IFN-γ induced nuclear translocation of NF-kB p65. Based on these findings, OIE can decrease the nuclear translocation of NF-kB, thus further inhibiting the expression of target inflammatory genes. To further investigate whether OIE can regulate NF-kB signaling in LPS plus IFN-γ-induced RAW264.7 cells, the phosphorylation of NF-kB p65 was detected by Western blotting. Stimulation of the uninduced cells by LPS plus IFN-γ (IN) exhibited significantly higher phosphorylation of NF-kB p65 than uninduced cells (UN) ($p < 0.05$, Figures 4.8A and 4.8B). Pretreatment with 1 µM DEX or OIE showed a trend to reduce the phosphorylation of NF-kB p65 proteins, but no significant difference compared to LPS plus IFN-γ induced cells (IN) ($p > 0.05$). This result suggests that OIE exhibits a slight inhibitory effect on the phosphorylation of NF-kB p65 to exert its anti-inflammatory effects.

NF-kB is a transcription factor which regulates multiple aspects of innate and adaptive immune functions and serves as a pivotal mediator of inflammatory responses. Nowadays, inhibition of NF-kB signaling pathway is established as one of most important targets for the treatment of a wide variety of inflammatory diseases, autoimmune diseases as well as cancers. Therefore, OIE could significantly inhibit NF-kB should be exploited for future development of anti-inflammatory drugs.
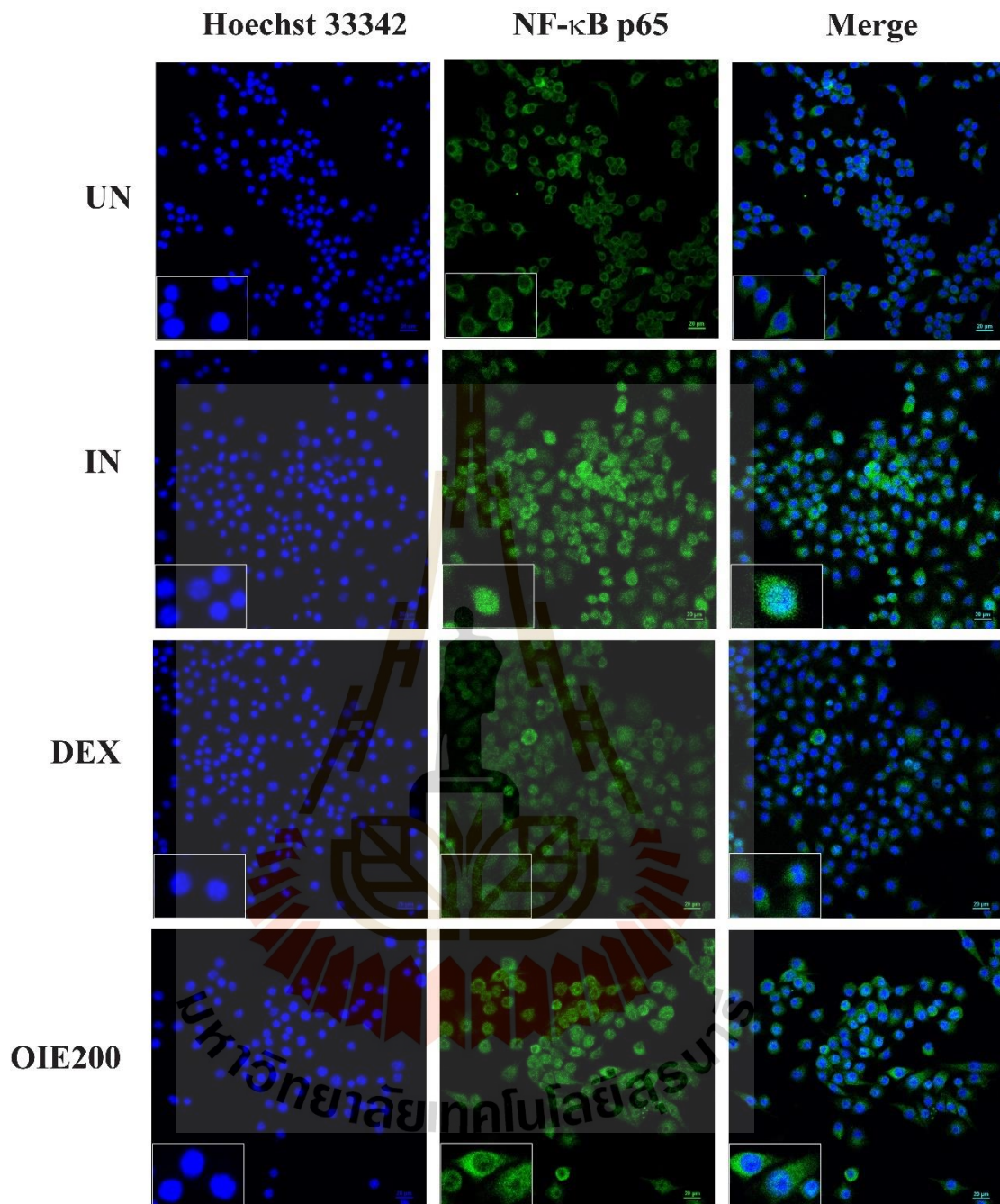
Figure 4.7 Effects of OIE on the nuclear translocation of NF-kB p65 in LPS plus IFN-γ-induced RAW264.7 cells at 24 h. Cells were pretreated with OIE or DEX for 3 h and then incubated with LPS plus IFN-γ for 24 h. The nuclear translocation of NF-kB p65 was detected using an immunofluorescence assay and visualized under confocal microscopy. The figure represents the cell morphology (bright field), the nuclear translocation of NF-kB p65 (green fluorescence), nucleus (blue fluorescence), and co-staining (overlay green and blue fluorescence). Scale bar, 20 μm. UN = Uninduced

cells, IN = Untreated LPS plus IFN-γ-induced cells, DEX = Cells were pretreated with DEX at 1 µM, and OIE200 = Cells were pretreated with OIE 200 µg/mL.
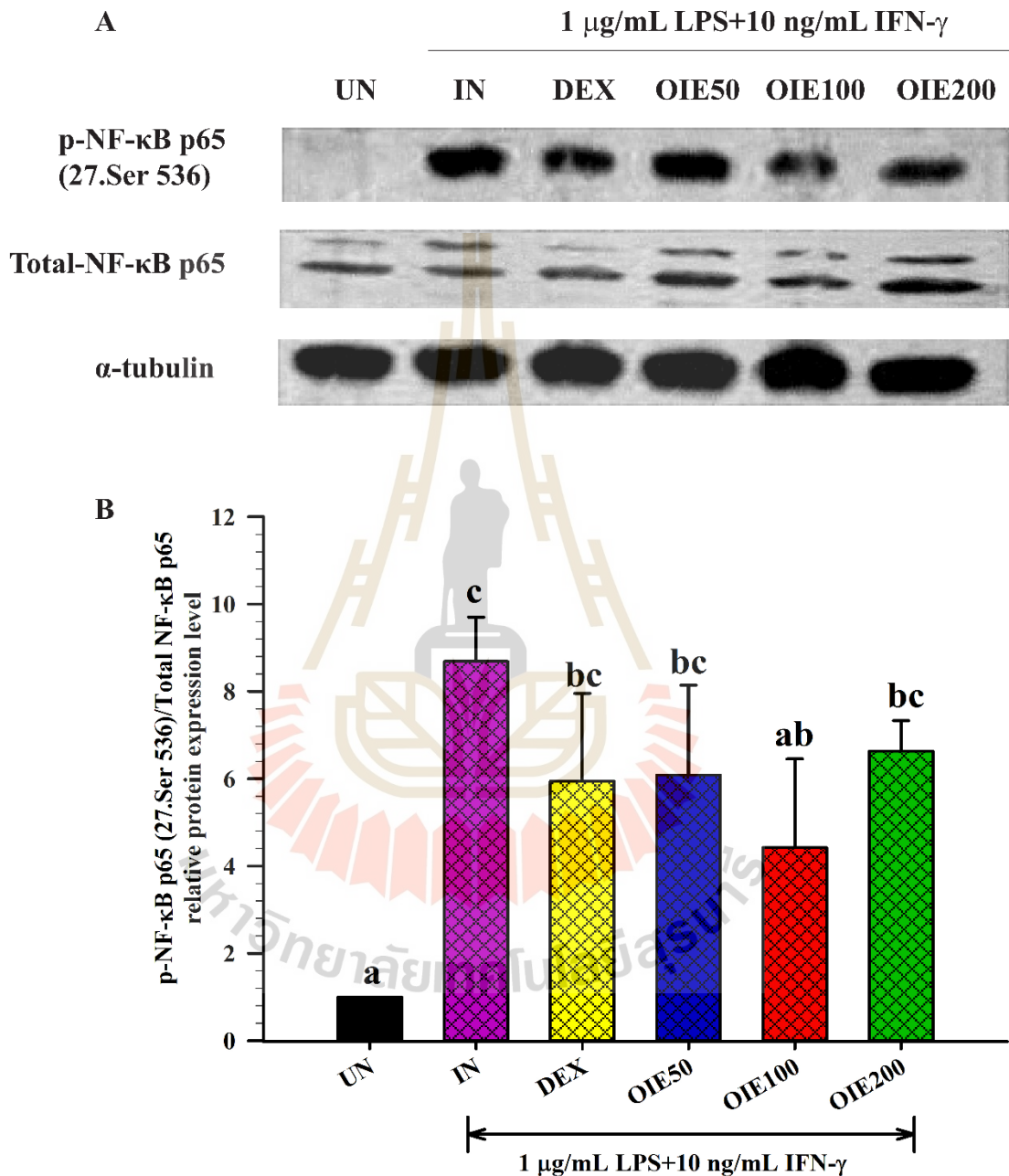
Figure 4.8 Effects of OIE on phosphorylation of NF-kB p65 induced by LPS plus IFN-γ in RAW264.7 cells. Cells were pretreated with OIE or DEX for 3 h and then co-incubated with LPS plus IFN-γ for 24 h. The protein expression was analyzed by Western blotting. (A) The cellular proteins were used to detect the phosphorylated p-NF-kB p65 and total forms of NF-kB with α-tubulin as a housekeeping control

protein. (B) Mean densitometric values are expressed as bar charts. The data represent the mean ± SD of three independent experiments. One-way ANOVA performed the comparison, and Tukey was used as a post hoc test. The degree of significance was denoted with different letters for the comparison between sample groups. $p < 0.05$ was considered as statistically significant. UN = Uninduced cells, IN = Untreated LPS plus IFN-γ-induced cells, DEX = Cells were pretreated with DEX at 1 µM, and OIE50, OIE100, and OIE200 = Cells were pretreated with OIE at 50, 100, and 200 µg/mL, respectively.

4.2 Anti-oxidation and anti-inflammation of *G. inodorum* extract (GIE)

4.2.1 Phytochemicals and antioxidant activity

4.2.1.1 Extraction yield

The dried powder of *G. inodorum* leaves was extracted with 95% ethanol. The ethanol extract was evaporated and lyophilized to obtain a final yield of 17.43% (w/w) *G. inodorum* extract (GIE).

4.2.1.2 GC-MS analysis of volatile oil constituents of GIE

In this study, the phytochemical constituents of GIE were analyzed. GC-MS analysis in GIE reported about 16 compounds, as shown in Table 4.3. The major prevailing compounds were linolenic acid (24.91%), n-Hexadecanoic acid (Palmitic acid) (16.98%), and Methylparaben (11.58%). Besides, it also presented the other chemical compounds, which are known to exhibit important pharmacological activity, in particular, anti-inflammatory and antioxidant activities such as phytol (Jeong, 2018; Silva et al., 2014), squalene (Cárdeno et al., 2015), γ-tocopherol, dl-α-tocopherol (Mathur et al., 2015; Reiter et al., 2007), and stigmasterol (Jimenez-Suarez et al., 2016; Zeb et al., 2017).

Phytol, diterpene alcohol, has been reported to have remarkable anti-inflammatory activity by reducing carrageenan-induced paw edema and inhibiting the recruitment of total leukocytes and neutrophils, a decrease in IL-1β and TNF-α levels and oxidative stress (Silva et al., 2014). Jeong (2018) also reported that phytol suppressed H_2O_2-induced inflammation, as indicated by the reduced expression of

the mRNA levels of TNF-α, IL-6, IL-8, and COX-2 (Jeong, 2018). Squalene, a natural lipid belonging to the terpenoid family, significantly inhibited the secretion of proinflammatory cytokines (TNF-α, IL-1β, IL-6, and IFN-γ), proinflammatory enzymes (iNOS, COX-2, and myeloperoxidase (MPO)), and enhanced expression levels of anti-inflammatory enzymes (heme oxygenase-1 (HO-1)) and transcription factors (Nrf2 and PPARγ) in overactivation of neutrophils, monocytes, and macrophages (Cárdeno et al., 2015). γ-Tocopherol and dl-α-tocopherol exhibited anti-inflammatory activity *in vitro* and *in vivo*, whereas the combination of γ- and α-tocopherols seems to be more potent than supplementation with α-tocopherols alone (Reiter et al., 2007). These results provide evidence that GIE is a source of antioxidants and anti-inflammatory agents, which could benefit treating inflammation-related diseases. However, further studies are needed to clarify pharmacological properties.

Table 4.3 GC-MS analysis of GIE.

No.	Compound Name	Formula	RT	%Area
1	2,3-dihydrobenzofuran	C_8H_8O	4.74	3.76
2	2-Methoxy-5-vinylphenol	$C_9H_{10}O_2$	5.89	1.42
3	Methylparaben	$C_8H_8O_3$	7.71	11.58
4	Tetradecanoic acid	$C_{14}H_{28}O_2$	11.09	2.86
5	n-Hexadecanoic acid	$C_{16}H_{32}O_2$	14.06	16.98
6	Phytol	$C_{20}H_{40}O$	16.73	5.96
7	Linolenic acid	$C_{18}H_{30}O_2$	17.42	24.91
8	Octadecanoic acid	$C_{18}H_{36}O_2$	17.70	2.04
9	Glycerol beta-palmitate	$C_{19}H_{38}O_4$	23.60	5.54
10	beta-Monolinolein	$C_{21}H_{38}O_4$	26.36	6.31
11	9,12,15-Octadecatrienal	$C_{18}H_{30}O$	26.51	9.50
12	Squalene	$C_{30}H_{50}$	28.27	0.93
13	γ-Tocopherol	C28H48O2	31.37	1.80
14	dl-α-Tocopherol	C29H50O2	33.04	2.33
15	Stigmasterol	C29H48O	35.67	2.50
16	Olean-12-ene-3,28-diol, (3beta)-	C30H50O2	46.98	1.57

4.2.1.3 Free radical scavenging and antioxidant activities of GIE

Antioxidants can act via several pathways, therefore, to investigate the antioxidant activity of the GIE, we estimated their reducing antioxidant power and free radical scavenging by using the FRAP and DPPH radical scavenging assays, respectively. Trolox and Vitamin C were used as standard antioxidant compounds. As shown in Table 4.4, GIE exhibited antioxidant activity due to its ability to reduce ferric ion (Fe^{3+}) to ferrous ion (Fe^{2+}) by 24.00±0.69 µg VCEA/mg of dry extract and 28.06±0.78 µg TREA/mg of dry extract. GIE at a concentration of 406.59±0.11 µg/mL displayed the ability to scavenge DPPH radical at 50% (IC_{50}). In contrast, the positive antioxidant controls, Vitamin C and Trolox, exhibited the IC_{50} values of approximately 44.57±0.59 µg/mL and 67.19±4.82 µg/mL, respectively.

Based on GC-MS analysis (Table 4.3), GIE contained many bioactive compounds such as phytol, squalene, γ-tocopherol, dl-α-tocopherol, and stigmasterol, which were reported to have antioxidant activity. Previous studies demonstrated that the phytochemical screening of GIE indicated the presence of phenolic, flavonoids, terpenoids, and glycoside (Chaiyasut et al., 2017; Tiamyom et al., 2019). Numerous studies have shown that plant products' antioxidant capacity is related to their phenolic and flavonoid contents (El Jemli et al., 2016; Loizzo et al., 2012; Youn et al., 2019). The synergistic effect of some substances present in GIE had been reported the antioxidant activity. Previous studies showed that the combination of squalene and α-tocopherol displayed a synergistic effect by reducing the rate of oxidation in a crocin bleaching assay where squalene might act as a competitive compound to α-tocopherol (Finotti et al., 2000). The sunflower seed oil containing total polyphenols and α-tocopherol had a positive Ka/Kc ratio of rate constants for antioxidant and crocin value antioxidant activity. It is possible that the synergistic effect occurs between α-tocopherol and total polyphenols (Perretti et al., 2004). Besides, the presence of α-, β-, γ-tocopherol in sunflower seed oil may contribute to the oil resistance to oxidation (Perretti et al., 2004; Yanishlieva et al., 2002). Therefore, the presence of squalene, α-tocopherol, γ-tocopherol, and phenolic in GIE may provide synergistic effects on antioxidant activity. However, it is also essential to further confirm whether the antioxidant activity of the combination of α-

tocopherol plus squalene or other volatile compounds in GIE is synergistic. Moreover, the synergistic action of such compounds from plants had been calculated by the combination index (CI) (Chou, 2006; K.-R. Kwon et al., 2019; Son et al., 2019).

Table 4.4 The FRAP and DPPH scavenging activities of GIE and standard compounds.

Sample	FRAP values		DPPH scavenging activity
	(µgVCEA/mg)	(µgTREA/mg)	(IC$_{50}$) µg/mL
GIE	24.00±0.69	28.06±0.78	406.59±0.11[c]
Vitamin C	-	-	44.57±0.59[a]
Trolox	-	-	67.19±4.82[b]

Values are mean ± SD (n = 3) and represent three independent experiments with similar results. Different letters within the same column are significantly different at $p < 0.05$.

4.2.2 Effects of GIE on cell viability in RAW264.7 cells

The cytotoxicity of GIE was evaluated by MTT assay. The RAW264.7 cells were treated with various concentrations of the GIE, ranging from 100-500 µg/mL for 24 h. As shown in Figure 4.9, the results demonstrated that GIE at the concentration ranges of 100-400 µg/mL did not show a toxic effect on RAW264.7 cells ($p > 0.05$). At the highest tested concentration (500 µg/mL), the number of livings RAW264.7 cells decreased by up to 71.50% compared to the control group. Based on these results, the non-toxic concentration ranges of GIE (50, 100, 200, and 300 µg/mL) were selected for treating cells in further investigation.
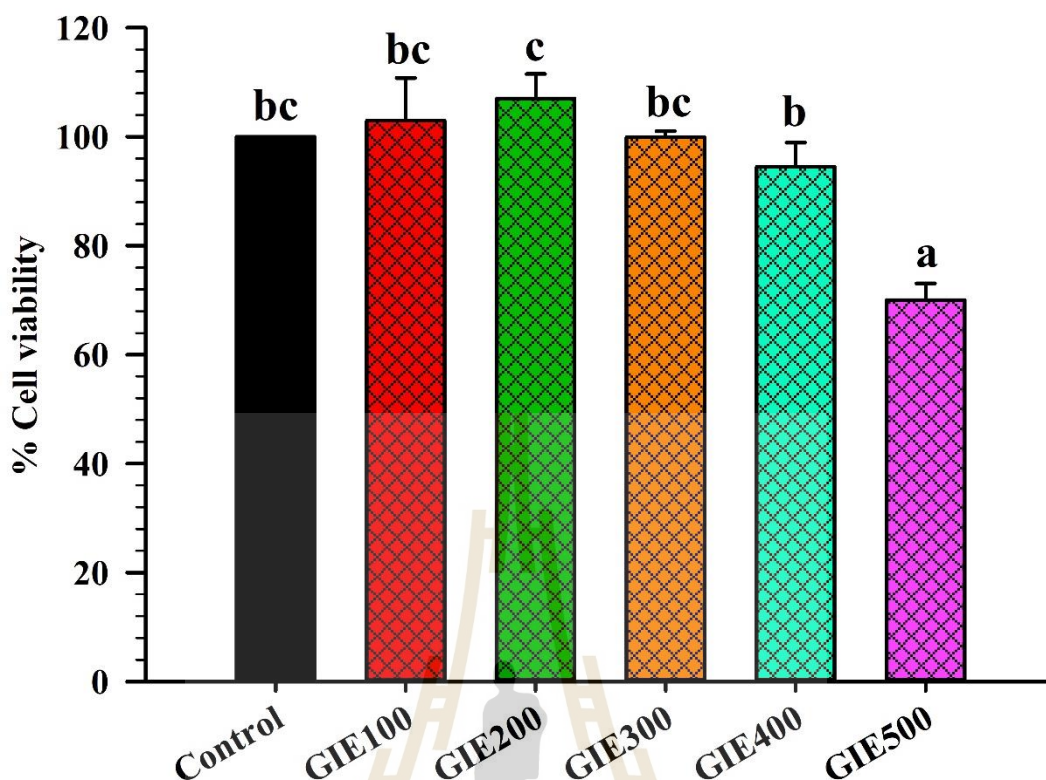
Figure 4.9 Effect of GIE on cell viability in RAW264.7 cells. Cells were treated with different concentrations of GIE for 24 h. Cell viability was determined by the MTT assay. CON = Cells without GIE and GIE100 – GIE500 = Cells were treated with GIE at concentration ranges of 100-500 µg/mL, respectively. Values are expressed as a percentage of the control. The data represent the mean ± SD of three independent experiments. Bars marked with different letters are significantly different at $p < 0.05$ as determined by one-way ANOVA with Tukey post hoc test.

4.2.3 Effects of GIE on intracellular ROS production in LPS plus IFN-γ-induced RAW264.7 cells

ROS generated by inflammatory cells also stimulates pathways that lead to the amplification of inflammation. ROS-induced kinase activation leads to the activation of transcription factors, which triggers the generation of proinflammatory cytokines and chemokine. Therefore, it is possible that the inflammation would be controlled by suppressing intracellular ROS production. Antioxidants are proven that help to protect cells and tissue from damage caused by free radical molecules (Allegra, 2019). According to FRAP and DPPH results, the possibility of GIE to scavenge

intracellular ROS formation was further evaluated using the cell-base assay, DCFH-DA model. LPS and IFN-γ were chosen as inflammatory inducing molecules, which can trigger a series of inflammatory mediators and reactive oxygen. NAC, as a nutritional supplement, was applied as the positive antioxidant control. The cells were pretreated with various concentrations of GIE (50, 100, 200, and 300 µg/mL) for 3 h and then co-incubated with LPS plus IFN-γ for another 24 h. As shown in Figure 4.10, while LPS plus IFN-γ increased ROS formation in RAW264.7 cells (by 1.76-fold compared to uninduced cells), pretreated cells with GIE significantly reduced ROS generation in a concentration-dependent manner. Surprisingly, the highest concentration of GIE showed the efficacy of decreasing the intracellular ROS level to 56.72 ± 3.62%, which was a similar level of the basal intracellular ROS production (56.56 ± 3.18%) in uninduced cells (UN). As expected, the positive antioxidant compound, NAC, possessed a potent free radical scavenging activity by decreasing the intracellular ROS level to 44.07 ± 3.82% compared to untreated LPS plus IFN-γ-induced cells. These results lead us to believe that GIE could inhibit ROS production by scavenging free radicals in cells, which is confirmed by the results of the FRAP and DPPH assay (Table 4.4). Our study was in agreement with other studies, which reported that *G. inodorum* displayed the antioxidant activity measured by various *in vitro* antioxidant assays (Chanwitheesuk et al., 2005; Nanasombat et al., 2019). However, this is the first report of the study, proving the antioxidant effect of this plant in the cell-based assay.
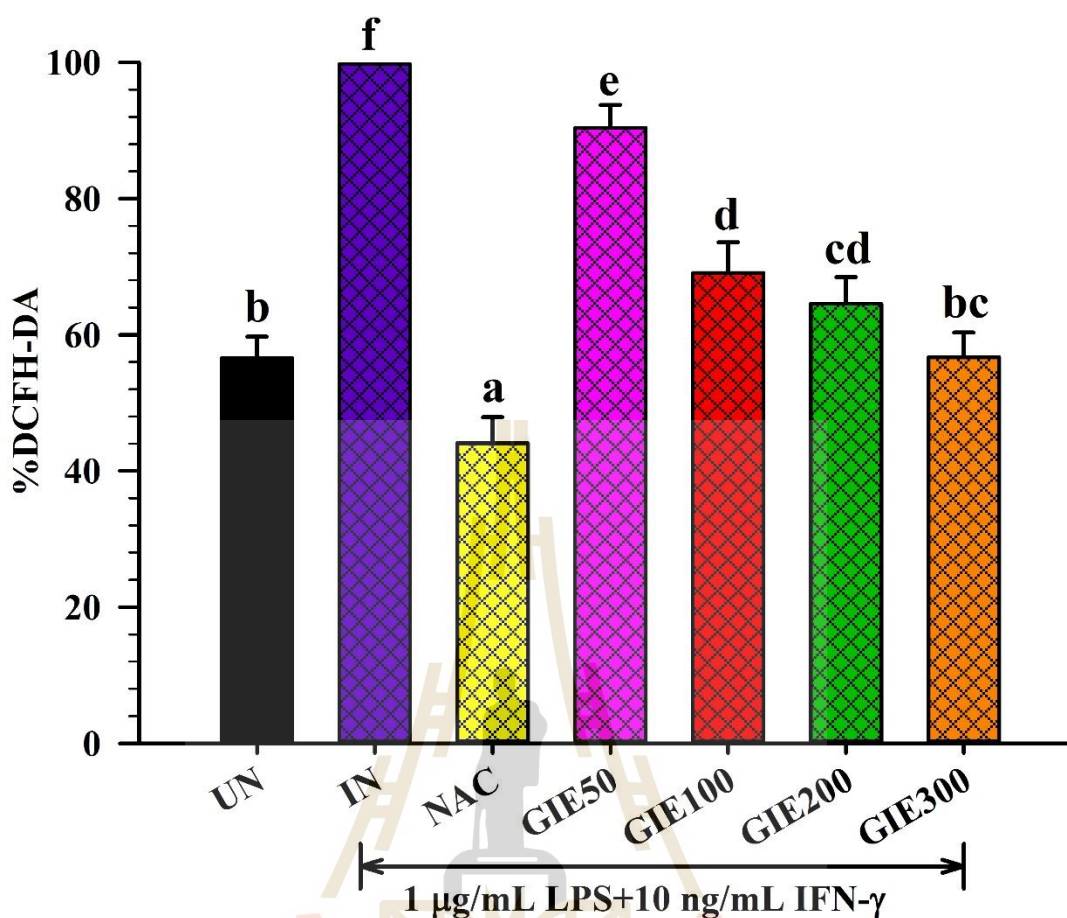
Figure 4.10 Effects of GIE on the intracellular ROS production in LPS plus IFN-γ-induced RAW264.7 cells. Cells were pretreated with different concentrations of GIE for 3 h and then induced with LPS plus IFN-γ for 24 h. UN = Uninduced cells, IN = Untreated LPS plus IFN-γ-induced cells, NAC = Cells were pretreated with NAC 3 mM, and GIE50, GIE100, GIE200, and GIE300 = Cells were pretreated with GIE at 50, 100, 200, and 300 μg/mL, respectively. The intracellular ROS levels are expressed as a percentage of the control. The data represent the mean ± SD of three independent experiments. Bars marked with different letters are significantly different at $p < 0.05$ as determined by one-way ANOVA with Tukey post hoc test.

4.2.4 Effects of GIE on anti-oxidant mRNA expression in LPS plus IFN-γ-induced RAW264.7 cells

Next, the inhibitory effect of GIE on oxidative stress was investigated by measuring antioxidant enzyme mRNA expression in RAW264.7 cells induced by LPS plus IFN-γ. Following stimulation of the cells by LPS plus IFN-γ, SOD2 mRNA

expression exhibited a slight increase, along with a significant decrease in GSTP1, NQO1, GCLC, and GCLM mRNA expression (Figure 4.11). Treatment by 300 µg/mL GIE achieved a statistically significant increase in SOD2 mRNA expression in LPS plus IFN-γ-induced cells ($p < 0.05$). However, with concentrations of 300 µg/mL, there was no statistically significant difference in the mRNA expression of GSTP1, NQO1, GCLC, and GCLM compared to LPS plus IFN-γ-induced cells (IN) ($p > 0.05$). These results provide evidence that GIE inhibited ROS production by upregulating the expression of SOD2 mRNA levels in LPS plus IFN-γ-induced RAW264.7 cells.

ROS is considered to be a causal factor in inflammatory responses. Higher levels of ROS can cause toxicity or act as signaling molecules. The cellular levels of ROS are controlled by low molecular mass antioxidants and antioxidant enzymes. SOD2 is one of the primary cellular antioxidant enzymes, which catalyze the dismutation of superoxide anion (O_2^-) to oxygen and hydrogen peroxide (H_2O_2) (Halliwell and Gutteridge, 1990). SOD2 was actively expressed via the NF-kB pathway during the progression of inflammatory conditions. The intracellular SOD2 has a protective role by suppressing the nucleotide-binding oligomerization domain, leucine-rich repeat, and pyrin domain-containing (NLRP) inflammasome-caspase-1-IL-1β axis under inflammatory conditions (Yoon et al., 2018). Superoxide dismutase (SOD) also acts as an anti-inflammatory due to its inhibitory effects on releasing lipid peroxidation-derived prostaglandins, thromboxane, and leukotrienes (Kirkham and Rahman, 2006). Therefore, GIE elevated the levels of SOD2 can be an effective therapeutic strategy in oxidative stress and inflammation.
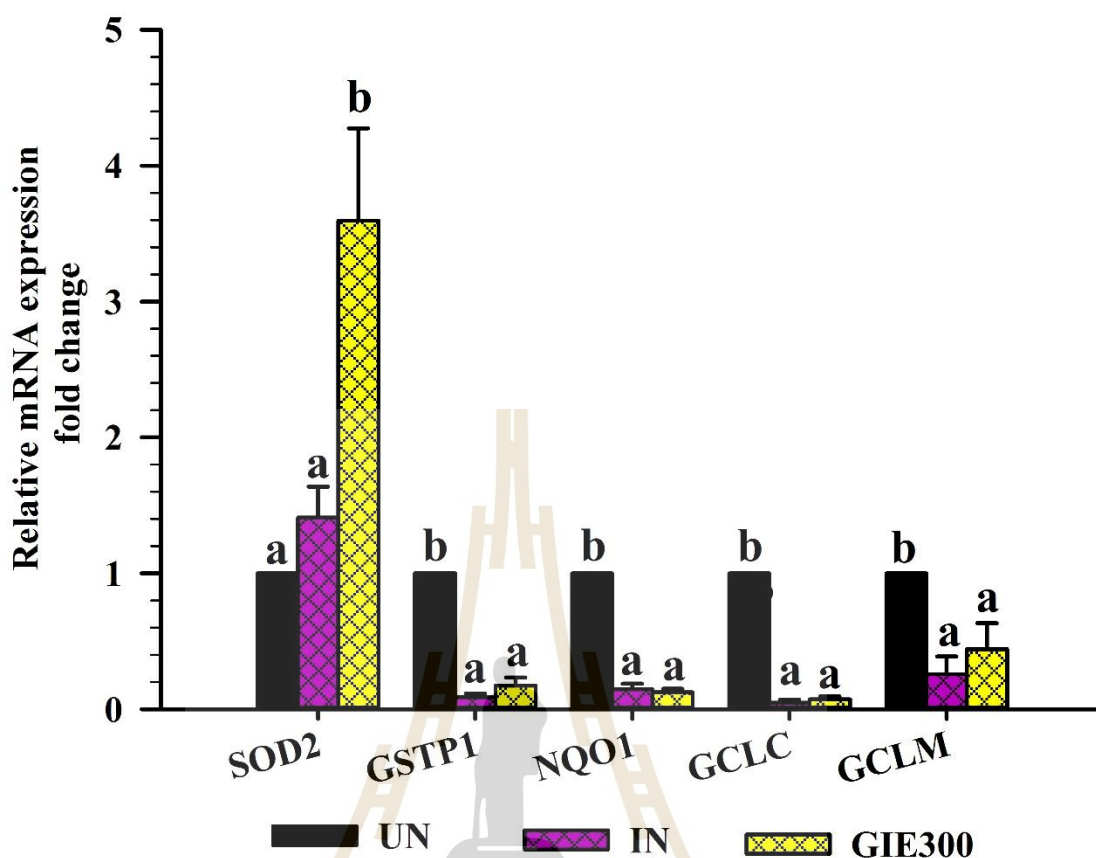
Figure 4.11 Effects of GIE on the antioxidant mRNA expression in LPS plus IFN-γ-induced RAW264.7 cells. Cells were pretreated with different concentrations of GIE 300 μg/mL for 3 h and then induced with LPS plus IFN-γ for 24 h. Values are expressed as a percentage of the control. The data represent the mean ± SD of three independent experiments. Bars marked with different letters are significantly different at $p < 0.05$ as determined by one-way ANOVA with Tukey post hoc test.

4.2.5 Effects of GIE on nitric oxide (NO) production, iNOS, and COX-2 mRNA expression in LPS plus IFN-γ-induced RAW264.7 cells

NO is a reactive nitrogen species (RNS), which also plays essential biology roles, similar to ROS. NO is synthesized by activating macrophages involved in an immune and inflammatory response. Inhibition of NO production was usually used as the necessary pharmacological treatment of inflammation-related diseases. Therefore, this study investigated whether GIE could modulate NO production in LPS plus IFN-γ-induced RAW264.7 cells and measured for NO production using the Griess

assay. The anti-inflammatory agent, dexamethasone (DEX), was used as the reference drug. As shown in Figure 4.12A, the results showed that LPS plus IFN-γ induced significantly increased NO production ($p < 0.05$), reaching 45.68 ± 1.26 µM in untreated LPS plus IFN-γ-induced cells (IN). GIE reduced NO production in a dose-dependent manner. Moreover, the extract at concentrations of 200 and 300 µg/mL significantly suppressed NO production compared to untreated LPS plus IFN-γ-induced cells (IN) ($p < 0.05$). The highest concentration of GIE at 300 µg/mL exhibited NO suppression (12.62% of NO inhibition), approximately the same efficiency as the reference drug, DEX (15.80% of NO inhibition).

In the inflammatory response, NO and PGE2 are synthesized by iNOS and COX-2, respectively (Karpuzoglu and Ahmed, 2006). To confirm if the suppression of NO production by GIE was related to change in iNOS as well as COX-2 mRNA levels, qRT-PCR was performed. Figures 4.12B and 4.12C showed that iNOS and COX-2 mRNA expression was increased in LPS plus IFN-γ-induced cells (IN). At the same time, pretreated GIE significantly decreased the expression of iNOS and COX-2 mRNA levels in a concentration-dependent manner ($p < 0.05$). The present study indicates that the suppressive effect of GIE on NO production is mediated through the inhibition of iNOS mRNA expression. Therefore, iNOS reduction leads to the lower PGE2 and COX-2 expression in activated macrophages with LPS. There is no doubt that LPS and IFN-γ also efficiently enhance COX-2 expression in RAW264.7 cells (Jang et al., 2005). Our results demonstrate that GIE can exhibit anti-inflammatory activity by attenuating COX-2 mRNA expression. Thus, GIE might play essential roles in ameliorating inflammation by suppressing NO production and downregulation of iNOS and COX-2 mRNA expression.

Figure 4.12 Effects of GIE on NO production (A), iNOS (B), and COX-2 (C) mRNA expression in LPS plus IFN-γ-induced RAW264.7 cells. Cells were pretreated with different concentrations of GIE for 3 h and then induced with LPS plus IFN-γ for 24 h. UN = Un-induced cells, IN = Untreated LPS plus IFN-γ-induced cells, and GIE50, GIE100, GIE200, and GIE300 = Cells were pretreated with GIE at 50, 100, 200, and 300 μg/mL, respectively. The data represent the mean ± SD of three independent experiments. Bars marked with different letters are significantly different at $p < 0.05$ as determined by one-way ANOVA with Tukey post hoc test.

4.2.6 Effects of GIE on pro-, anti-inflammatory cytokines (IL-6, TNF-α, and IL-10), and proinflammatory mRNA expression in LPS plus IFN-γ-induced RAW264.7 cells

Inflammation is mediated by cytokines released from immune cells in response to pathogens' molecular components, such as the LPS of gram-negative bacteria. TNF-α in inflammatory processes is an essential proinflammatory mediator,

leading to others using ELISA. The results indicated that GIE at all tested concentrations significantly suppressed LPS plus IFN-γ-induced IL-6 production ($p < 0.05$, Figure 4.32A) and slightly decreased TNF-α production compared to untreated LPS plus IFN-γ-induced cells (IN) (Figure 4.13B). As expected, DEX (a reference drug) could also inhibit LPS plus IFN-γ-induced IL-6 and TNF-α production by 95.38% and 58.88%, respectively. Surprisingly, LPS plus IFN-γ induced the secretion of IL-10 about 6.5-fold compared to uninduced cells. DEX significantly increased the secretion of IL-10 level by almost 36.78% compared to untreated LPS plus IFN-γ-induced cells ($p < 0.05$, Figure 4.13C). While pretreated-GIE only showed a slight increase in IL-10 levels (around 5-10%) but no significant difference compared to untreated LPS plus IFN-γ-induced cells ($p > 0.05$). qRT-PCR was performed to investigate whether suppression of TNF-α and IL-6 production by GIE was related to a change in mRNA levels for both proinflammatory cytokines. Increasing concentrations of GIE produced a decrease in the order of IL-6 mRNA levels in LPS plus IFN-γ-induced cells (Figure 4.13D). However, GIE slightly decreased TNF-α mRNA levels compared to LPS plus IFN-γ-induced cells (Figure 4.13E). The IL-6 and TNF-α suppression profile by GIE suggests that GIE acts more potent on IL-6 than TNF-α.

Based on GC-MS analysis, the volatile oil compounds presenting in GIE, including phytol, squalene, γ-tocopherol, dl-α-tocopherol, and stigmasterol, have been reported to have anti-inflammatory and antioxidant activities. Therefore, the anti-inflammatory effects of the GIE could rely on volatile oil components that may exert synergistic effects. This is the first study concerning the inhibitory activity against proinflammatory cytokines (IL-6 and TNF-α) in LPS plus IFN-γ-induced RAW264.7 cells. The secretion of proinflammatory cytokines, TNF-α and IL-6, is important in upregulating the inflammatory process. The high levels of TNF-α and IL-6 play a critical role in acute and chronic inflammatory diseases; both cytokines are prime targets for intervention by anti-inflammatory therapeutic agents. Therefore, the development of anti-inflammatory substances, which can modulate proinflammatory mediators' production, is an efficient way to manage inflammatory conditions. These results provide evidence that GIE could be a source of anti-inflammatory agents, which may benefit treating inflammation-associated diseases.
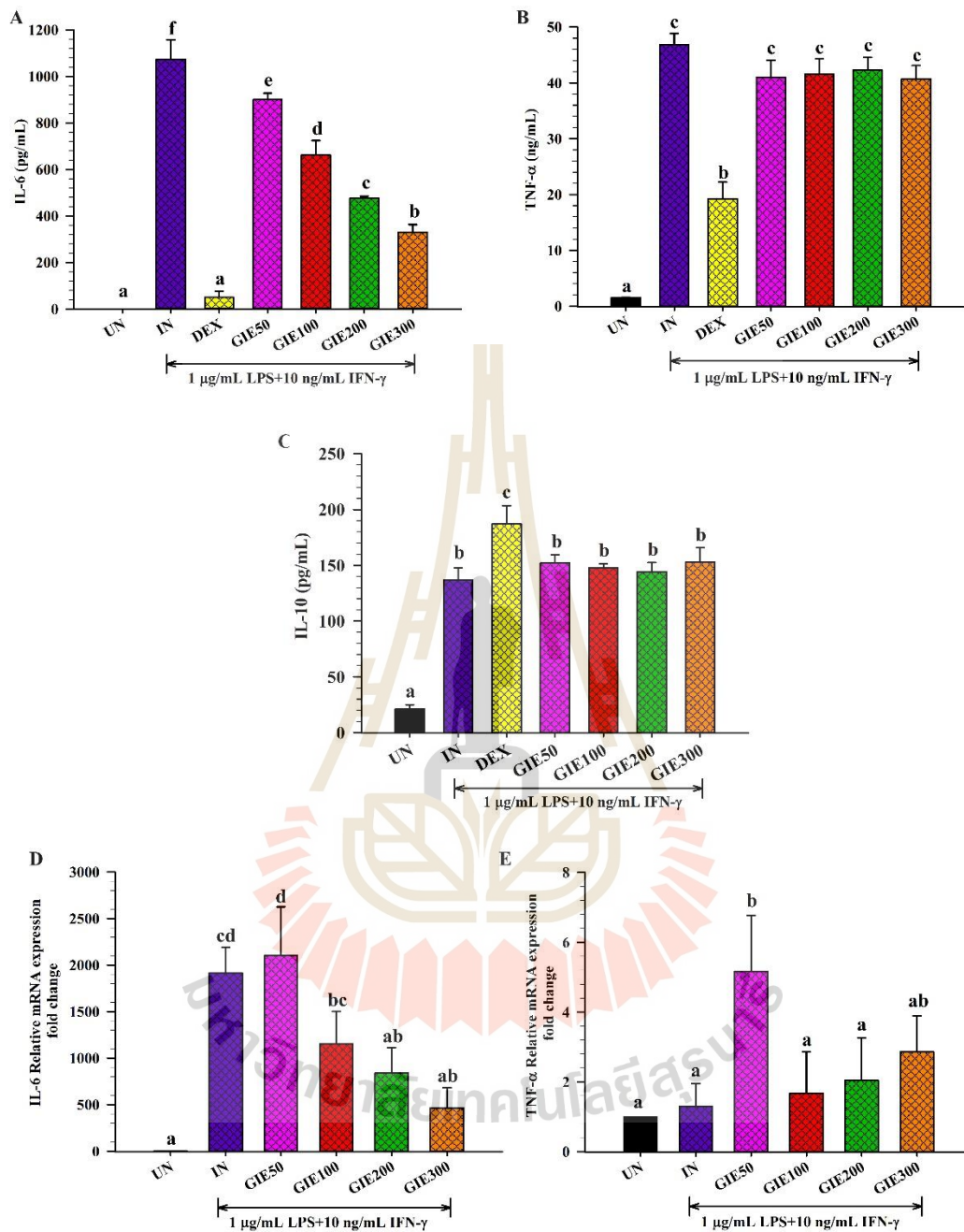
Figure 4.13 Effects of GIE on the secretion of proinflammatory cytokines (A) IL-6, (B) TNF-α, and anti-inflammatory cytokines (C) IL-10 secretion in LPS plus IFN-γ-induced RAW264.7 cells. The effects of GIE on (D) IL-6 and (E) TNF-α mRNA expression. Cells were pretreated with GIE or DEX for 3 h and then induced with LPS plus IFN-γ for 24 h. UN = uninduced cells, IN = untreated LPS plus IFN-γ-induced cells, DEX = cells were pretreated with DEX at 1 μM, and GIE50, GIE100, GIE200, and GIE300 = Cells were pretreated with GIE at 50, 100, 200, and 300 μg/mL, respectively. The data

represent the mean ± SD of two independent experiments. One-way ANOVA performed the comparison, and Tukey was used as a post hoc test. The degree of significance was denoted with different letters for the comparison between sample groups. $p < 0.05$ was considered as statistically significant.

4.2.7 Effects of GIE on NF-kB p65 nuclear translocation and p-NF-kB p65 (27. Ser 536) protein expression in LPS plus IFN-γ-induced RAW264.7 cells

Given that LPS plus IFN-γ-induced inflammation is through Toll-like receptor (TLR) signaling. NF-kB is activated and translocated into the nucleus to regulate the induced transcription of proinflammatory genes (Tak and Firestein, 2001). As a marker of NF-kB activation, the nuclear translocation of the NF-kB p65 was visualized in LPS plus IFN-γ induced RAW264.7 cells by immunofluorescence confocal microscopy. As shown in Figure 4.14, LPS plus IFN-γ-induced RAW264.7 cells (IN) showed marked NF-kB p65 staining in the nuclei, while uninduced cells (UN) showed weaker nuclear NF-kB expression but more vital staining in the cytoplasm. GIE treatment (GIE300) attenuated LPS plus IFN-γ induced nuclear translocation of NF-kB p65. Based on these findings, GIE can decrease the nuclear translocation of NF-kB, thus further inhibiting the expression of target inflammatory genes. To further investigate whether GIE can regulate NF-kB signaling in LPS plus IFN-γ-induced RAW264.7 cells, the phosphorylation of NF-kB p65 was detected by Western blotting. Stimulation of the uninduced cells by LPS plus IFN-γ (IN) exhibited significantly higher phosphorylation of NF-kB p65 than uninduced cells (UN) ($p < 0.05$, Figures 4.15A and 4.15B). Pretreatment with 1 µM DEX or GIE showed a trend to reduce the phosphorylation of NF-kB p65 proteins, but no significant difference compared to LPS plus IFN-γ induced cells (IN) ($p > 0.05$). This result suggests that GIE exhibits a slight inhibitory effect on the phosphorylation of NF-kB p65 to exert its anti-inflammatory effects.

In oxidative stress and anti-inflammation, enhancement of antioxidant gene expression plays an essential role in cell protection. It has been reported that superoxide dismutase (SOD) can modulate ROS-dependent signaling pathways during inflammatory responses (Lee et al., 2009). The activation of the Nrf2 antioxidant pathway prevents LPS-induced transcriptional upregulation of proinflammatory

cytokines (Luo et al., 2018). This research found that GIE increased the antioxidant gene expression, SOD2, and reduced NO and ROS production. Therefore, it is possible that the antioxidant properties of GIE could modulate the inflammation process caused by regulating the ROS levels.

Figure 4.14 Effects of GIE on the nuclear translocation of NF-kB p65 in LPS plus IFN-γ-induced RAW264.7 cells at 24 h. Cells were pretreated with GIE or DEX for 3 h and

then co-incubated with LPS plus IFN-γ for 24 h. The nuclear translocation of NF-kB p65 was detected using an immunofluorescence assay and visualized under confocal microscopy. The figure represents the cell morphology (bright field), the nuclear translocation of NF-kB p65 (green fluorescence), nucleus (blue fluorescence), and co-staining (overlay green and blue fluorescence). Scale bar, 20 μm. UN = Uninduced cells, IN = Untreated LPS plus IFN-γ-induced cells, DEX = Cells were pretreated with DEX at 1 μM, and GIE300 = Cells were pretreated with GIE 300 μg/mL.

Figure 4.15 Effects of GIE on phosphorylation of NF-kB p65 induced by LPS plus IFN-γ in RAW264.7 cells. Cells were pretreated with GIE or DEX for 3 h and then co-

incubated with LPS plus IFN-γ for 24 h. The protein expression was analyzed by Western blotting. (A) The cellular proteins were used to detect the phosphorylated p-NF-kB p65 and total forms of NF-kB with α-tubulin as a housekeeping control protein. (B) Mean densitometric values are expressed as bar charts. The data represent the mean ± SD of three independent experiments. One-way ANOVA performed the comparison, and Tukey was used as a post hoc test. The degree of significance was denoted with different letters for the comparison between sample groups. $p < 0.05$ was considered as statistically significant. UN = Uninduced cells, IN = Untreated LPS plus IFN-γ-induced cells, DEX = Cells were pretreated with DEX at 1 µM, and GIE300 = Cells were pretreated with GIE 300 µg/mL.

CHAPTER V

CONCLUSION

O. indicum has been used as plant-based food and herbal medicine in many Asian countries. The phytochemical compounds in *O. indicum* extract (OIE) were identified by GC-MS and LC-MS/MS. Five flavonoids (luteolin, apigenin, baicalein, oroxylin A, and quercetin) and 27 volatile compounds were found in OIE. These findings provide evidence that OIE could possess the antioxidant and anti-inflammatory effects in LPS plus IFN-γ-induced RAW264.7 cells. OIE presented antioxidant activities by scavenging free radical DPPH and ferric reducing antioxidant power (FRAP). Moreover, OIE also suppressed LPS plus IFN-γ-induced reactive oxygen species generation (ROS) and upregulated the expression of anti-oxidant genes (SOD2, GSTP1, NQO1, GSTP1, and GCLC) in LPS plus IFN-γ-induced RAW264.7 cells. It possessed the potent anti-inflammatory action through suppressing nitric oxide (NO), IL-6, and IL-10 secretion and also downregulation of the expression of cyclooxygenase-2 (COX-2), inducible nitric oxide synthase (iNOS), and IL-6 mRNA levels in LPS plus IFN-γ-induced RAW264.7 cells. Mechanism studies showed that OIE alleviated the NF-kB p65 nuclear translocation and slightly decreased the phosphorylation of the NF-kB p65 (p-NF-kB p65) protein. It possessed the potent anti-inflammatory action through suppressing nitric oxide (NO) and IL-6 secretion, possibly due to its ability to scavenge intracellular ROS and upregulate the antioxidant genes expression.

G. inodorum is widely used in Northern Thai cuisine as local vegetables and commercial herb tea products. In the present study, *G. inodorum* extract (GIE) was evaluated for its antioxidant and anti-inflammatory effects in LPS plus IFN-γ-induced RAW264.7 cells. Major compounds in GIE were evaluated using GC-MS and found 16 volatile compounds presenting in the extract. GIE exhibited antioxidant activity by scavenging the intracellular reactive oxygen species (ROS) production and increasing

superoxide dismutase 2 (SOD2) mRNA expression in LPS plus IFN-γ-induced RAW264.7 cells. GIE showed anti-inflammatory activity through suppressing nitric oxide (NO), proinflammatory cytokine production interleukin 6 (IL-6) and also downregulation of the expression of cyclooxygenase-2 (COX-2), inducible nitric oxide synthase (iNOS), and IL-6 mRNA levels in LPS plus IFN-γ-induced RAW264.7 cells. Mechanism studies showed that GIE suppressed the NF-kB p65 nuclear translocation and slightly decreased the phosphorylation of the NF-kB p65 (p-NF-kB p65) protein. These findings lead us to believe that GIE may prevent oxidative damage by scavenging intracellular ROS production and activating the antioxidant gene, SOD2, expression. Therefore, it is possible that the antioxidant properties of GIE could modulate the inflammation process by regulating the ROS levels, which lead to the suppression of proinflammatory cytokines and genes.

By comparing the antioxidant capacity of OIE and GIE, OIE appeared to have a stronger antioxidant capacity than GIE, which resulted in more potent to scavenge free radical revealed by the DPPH, FRAP, and DCFH-DA cell-based assay. Likewise, OIE were stronger NO inhibitors and more potent suppressor of proinflammatory cytokines (IL-6) and genes (iNOS, COX-2, and IL-6) than GIE.

In summary, both OIE and GIE have significant antioxidant and anti-inflammatory properties and could serve as a potent compound of those activities that warrant further research and development.
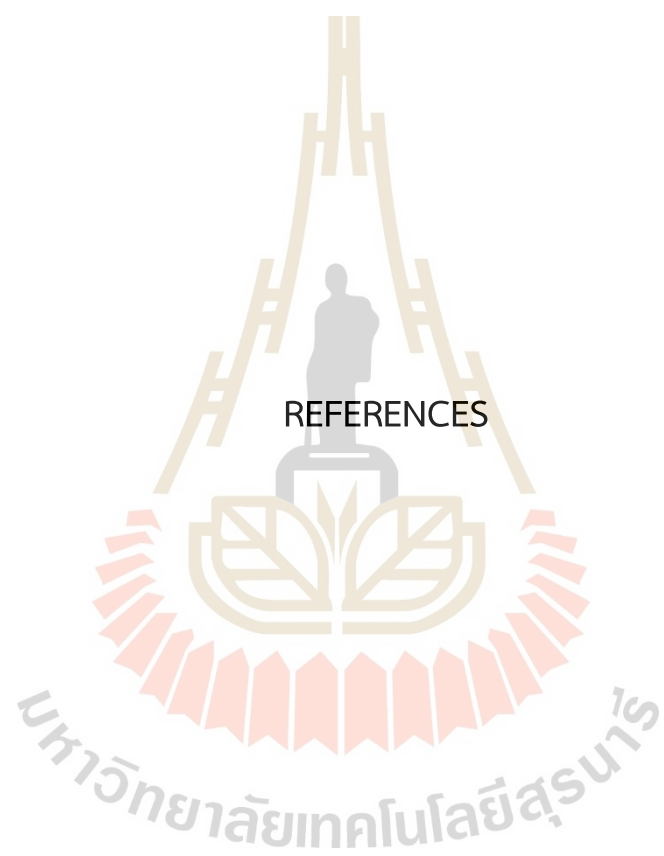
REFERENCES

REFERENCES

Adib‑Conquy, M., Scott-Algara, D., Cavaillon, J. M., and Souza-Fonseca-Guimaraes, F. (2014). TLR-mediated activation of NK cells and their role in bacterial/viral immune responses in mammals. *Immunology and Cell Biology*. *92*(3), 256-262.

Aggarwal, B. B., Vijayalekshmi, R., and Sung, B. (2009). Targeting inflammatory pathways for prevention and therapy of cancer: short-term friend, long-term foe. *Clinical Cancer Research*. *15*(2), 425-430.

Aggrey, A. A., Srivastava, K., Ture, S., Field, D. J., and Morrell, C. N. (2013). Platelet induction of the acute-phase response is protective in murine experimental cerebral malaria. *The Journal of Immunology*. *190*(9), 4685-4691.

Ali, R. M., Houghton, P., Raman, A., and Hoult, J. (1998). Antimicrobial and antiinflammatory activities of extracts and constituents of *Oroxylum indicum* (L.) Vent. *Phytomedicine*. *5*(5), 375-381.

Allegra, M. (2019). Antioxidant and anti-Inflammatory properties of plants extract. *Antioxidants*. *8*(11), 549.

Ames, B. N., and Wakimoto, P. (2002). Are vitamin and mineral deficiencies a major cancer risk? *Nature Reviews Cancer*. *2*(9), 694.

Arisawa, T., Tahara, T., Shibata, T., Nagasaka, M., Nakamura, M., Kamiya, Y., Fujita, H., Hasegawa, S., Takagi, T., and Wang, F.-Y. (2007). The relationship between Helicobacter pylori infection and promoter polymorphism of the Nrf2 gene in chronic gastritis. *International Journal of Molecular Medicine*. *19*(1), 143-148.

Armaka, M., Apostolaki, M., Jacques, P., Kontoyiannis, D. L., Elewaut, D., and Kollias, G. (2008). Mesenchymal cell targeting by TNF as a common pathogenic principle in chronic inflammatory joint and intestinal diseases. *Journal of Experimental Medicine*. *205*(2), 331-337.

Arulselvan, P., Fard, M. T., Tan, W. S., Gothai, S., Fakurazi, S., Norhaizan, M. E., and Kumar, S. S. (2016). Role of antioxidants and natural products in inflammation. *Oxidative Medicine and Cellular Longevity*. *2016*.

Babu, T. H., Manjulatha, K., Kumar, G. S., Hymavathi, A., Tiwari, A. K., Purohit, M., Rao, J. M., and Babu, K. S. (2010). Gastroprotective flavonoid constituents from *Oroxylum indicum* Vent. *Bioorganic & Medicinal Chemistry Letters*. *20*(1), 117-120.

Bespinyowong, R., Pongthananikorn, S., and Chiabchalard, A. (2013). Efficacy and safety of *Gymnema inodorum* tea consumption in type 2 diabetic patients. *Chulalongkorn Medical Journal*. *57*(5), 587-599.

Bhowmik, A., Seemungal, T. A., Sapsford, R. J., and Wedzicha, J. A. (2000). Relation of sputum inflammatory markers to symptoms and lung function changes in COPD exacerbations. *Thorax*. *55*(2), 114-120.

Bhushan, B., and Kumar, M. (2013). Ethnobotanically important medicinal plants of Tehsil Billawar, District Kathua, J&K, India. *Journal of Pharmacognosy and Phytochemistry*. *2*(4), 14-21.

Bradley, J. (2008). TNF-mediated inflammatory disease. *The Journal of Pathology: A Journal of the Pathological Society of Great Britain and Ireland*. *214*(2), 149-160.

Braun, S., Hanselmann, C., Gassmann, M. G., auf dem Keller, U., Born-Berclaz, C., Chan, K., Kan, Y. W., and Werner, S. (2002). Nrf2 transcription factor, a novel target of keratinocyte growth factor action which regulates gene expression and inflammation in the healing skin wound. *Molecular and Cellular Biology*. *22*(15), 5492-5505.

Brusselle, G., and Bracke, K. (2014). Targeting immune pathways for therapy in asthma and chronic obstructive pulmonary disease. *Annals of the American Thoracic Society*. *11*(Supplement 5), S322-S328.

Calandra, T., and Roger, T. (2003). Macrophage migration inhibitory factor: a regulator of innate immunity. *Nature Reviews Immunology*. *3*(10), 791-800.

Cao, X., Kong, X., Zhou, Y., Lan, L., Luo, L., and Yin, Z. (2015). Glutathione S-transferase P1 suppresses iNOS protein stability in RAW264. 7 macrophage-like cells after LPS stimulation. *Free Radical Research*. *49*(12), 1438-1448.

Cárdeno, A., Aparicio-Soto, M., Montserrat-de la Paz, S., Bermudez, B., Muriana, F. J., and Alarcón-de-la-Lastra, C. (2015). Squalene targets pro-and anti-inflammatory mediators and pathways to modulate over-activation of neutrophils, monocytes and macrophages. *Journal of Functional Foods*. *14*, 779-790.

Castaneda, O. A., Lee, S.-C., Ho, C.-T., and Huang, T.-C. (2017). Macrophages in oxidative stress and models to evaluate the antioxidant function of dietary natural compounds. *Journal of Food and Drug Analysis*. *25*(1), 111-118.

Cesari, M., Penninx, B. W., Newman, A. B., Kritchevsky, S. B., Nicklas, B. J., Sutton-Tyrrell, K., Rubin, S. M., Ding, J., Simonsick, E. M., and Harris, T. B. (2003). Inflammatory markers and onset of cardiovascular events: results from the Health ABC study. *Circulation*. *108*(19), 2317-2322.

Chaiyasut, C., Kesika, P., Chaiyasut, K., Sittiyuno, P., Peerajan, S., and Sivamaruthi, B. S. (2017). Total phenolic content and free radical scavenging activity of representative medicinal plants of Thailand. *Asian Journal of Pharmaceutical and Clinical Research*. *10*(11), 137-141.

Chanwitheesuk, A., Teerawutgulrag, A., and Rakariyatham, N. (2005). Screening of antioxidant activity and antioxidant compounds of some edible plants of Thailand. *Food Chemistry*. *92*(3), 491-497.

Chao, W.-W., Kuo, Y.-H., and Lin, B.-F. (2010). Anti-inflammatory activity of new compounds from *Andrographis paniculata* by NF-kB transactivation inhibition. *Journal of Agricultural and Food Chemistry*. *58*(4), 2505-2512.

Chen, L., Deng, H., Cui, H., Fang, J., Zuo, Z., Deng, J., Li, Y., Wang, X., and Zhao, L. (2018). Inflammatory responses and inflammation-associated diseases in organs. *Oncotarget*. *9*(6), 7204-7218.

Chen, T.-L., Chang, C.-C., Lin, Y.-L., Ueng, Y.-F., and Chen, R.-M. (2009). Signal-transducing mechanisms of ketamine-caused inhibition of interleukin-1β gene

expression in lipopolysaccharide-stimulated murine macrophage-like Raw 264.7 cells. *Toxicology and Applied Pharmacology*. *240*(1), 15-25.

Chen, X.-L., Dodd, G., Thomas, S., Zhang, X., Wasserman, M. A., Rovin, B. H., and Kunsch, C. (2006). Activation of Nrf2/ARE pathway protects endothelial cells from oxidant injury and inhibits inflammatory gene expression. *American Journal of Physiology-Heart and Circulatory Physiology*. *290*(5), H1862-H1870.

Chen, Y.-C., Yang, L.-L., and Lee, T. J. (2000). Oroxylin A inhibition of lipopolysaccharide-induced iNOS and COX-2 gene expression via suppression of nuclear factor-$\varkappa$B activation. *Biochemical Pharmacology*. *59*(11), 1445-1457.

Cheng, Z., Garvin, D., Paguio, A., Stecha, P., Wood, K., and Fan, F. (2010). Luciferase reporter assay system for deciphering GPCR pathways. *Current Chemical Genomics*. *4,* 84-91.

Chhetri, D., Parajuli, P., and Subba, G. (2005). Antidiabetic plants used by Sikkim and Darjeeling Himalayan tribes, India. *Journal of Ethnopharmacology*. *99*(2), 199-202.

Choi, E.-O., Jeong, J.-W., Park, C., Hong, S. H., Kim, G.-Y., Hwang, H.-J., Cho, E.-J., and Choi, Y. H. (2016). Baicalein protects C6 glial cells against hydrogen peroxide-induced oxidative stress and apoptosis through regulation of the Nrf2 signaling pathway. *International Journal of Molecular Medicine*. *37*(3), 798-806.

Chou, T.-C. (2006). Theoretical basis, experimental design, and computerized simulation of synergism and antagonism in drug combination studies. *Pharmacological Reviews*. *58*(3), 621-681.

Cuzzocrea, S., Riley, D. P., Caputi, A. P., and Salvemini, D. (2001). Antioxidant therapy: a new pharmacological approach in shock, inflammation, and ischemia/reperfusion injury. *Pharmacological Reviews*. *53*(1), 135-159.

Devanathan, K. (2001). *Oroxylum indicum* (L.) Kurz Bignoniaceae. In Franco F.M. (Ed.), *Ethnobotany of the Mountain Regions of Southeast Asia : hnobotany of Mountain Regions* (p.769-782). Switzerland: Springer, Cham.

Dinda, B., Mohanta, B. C., Arima, S., Sato, N., and Harigaya, V. (2007). Flavonoids from the stem-bark of *Oroxylum indicum. Natural Product Sciences*. *13*(3), 190-194.

Dinkova-Kostova, A. T., and Talalay, P. (2000). Persuasive evidence that quinone reductase type 1 (DT diaphorase) protects cells against the toxicity of electrophiles and reactive forms of oxygen. *Free Radical Biology and Medicine*. *29*(3-4), 231-240.

Doshi, K., Ilanchezhian, R., Acharya, R., Patel, B., and Ravishankar, B. (2012). Anti-inflammatory activity of root bark and stem bark of Shyonaka. *Journal of Ayurveda and Integrative Medicine*. *3*(4), 194–197.

Dubois, R. N., Abramson, S. B., Crofford, L., Gupta, R. A., Simon, L. S., A. Van De Putte, L. B., and Lipsky, P. E. (1998). Cyclooxygenase in biology and disease. *The FASEB Journal*. *12*(12), 1063-1073.

Dunkhunthod, B., Thumanu, K., and Eumkeb, G. (2017). Application of FTIR microspectroscopy for monitoring and discrimination of the anti-adipogenesis activity of baicalein in 3T3-L1 adipocytes. *Vibrational Spectroscopy*. *89*, 92-101.

Durackova, Z. (2010). Some current insights into oxidative stress. *Physiological Research*. *59*(4), 459-469.

El Jemli, M., Kamal, R., Marmouzi, I., Zerrouki, A., Cherrah, Y., and Alaoui, K. (2016). Radical-scavenging activity and ferric reducing ability of *Juniperus thurifera* (L.), *J. oxycedrus* (L.), *J. phoenicea* (L.) and *Tetraclinis articulata* (L.). *Advances in Pharmacological Sciences*. *2016,* 6392656.

Espinosa-Diez, C., Miguel, V., Mennerich, D., Kietzmann, T., Sánchez-Pérez, P., Cadenas, S., and Lamas, S. (2015). Antioxidant responses and cellular adjustments to oxidative stress. *Redox Biology*. *6*, 183-197.

Eumkeb, G., Tanphonkrang, S., Sirichaiwetchakoon, K., Hengpratom, T., and Naknarong, W. (2017). The synergy effect of daidzein and genistein isolated from *Butea superba* Roxb. on the reproductive system of male mice. *Natural Product Research*. *31*(6), 672-675.

Federico, A., Morgillo, F., Tuccillo, C., Ciardiello, F., and Loguercio, C. (2007). Chronic inflammation and oxidative stress in human carcinogenesis. *International Journal of Cancer*. *121*(11), 2381-2386.

Finotti, E., D'AMBROSIO, M., Paoletti, F., Vivanti, V., and Quaglia, G. (2000). Synergistic effects of α-tocopherol, β-sitosterol and squalene on antioxidant activity assayed by crocin bleaching method. *Nahrung (Weinheim)*. *44*(5), 373-374.

Fujiwara, N., and Kobayashi, K. (2005). Macrophages in inflammation. *Current Drug Targets-Inflammation & Allergy*. *4*(3), 281-286.

Gomez, M., Saenz, M., Garcia, M., and Fernandez, M. (1999). Study of the topical anti-inflammatory activity of *Achillea ageratum* on chronic and acute inflammation models. *Zeitschrift für Naturforschung C*. *54*(11), 937-941.

Gordon, S. (1976). Macrophage neutral proteinases and chronic inflammation. *Annals of the New York Academy of Sciences*. *278*(1), 176-189.

Gordon, S., and Martinez, F. O. (2010). Alternative activation of macrophages: mechanism and functions. *Immunity*. *32*(5), 593-604.

Greenhill, C. J., Rose-John, S., Lissilaa, R., Ferlin, W., Ernst, M., Hertzog, P. J., Mansell, A., and Jenkins, B. J. (2011). IL-6 trans-signaling modulates TLR4-dependent inflammatory responses via STAT3. *The Journal of Immunology*. *186*(2), 1199-1208.

Gudkov, A. V., and Komarova, E. A. (2016). p53 and the carcinogenicity of chronic inflammation. *Cold Spring Harbor Perspectives in Medicine*. *6*(11), a026161.

Halliwell, B., and Gutteridge, J. M. (1990). Role of free radicals and catalytic metal ions in human disease: an overview. *Methods in Enzymology*. *186*, 1-85.

Heinrich, P. C., Castell, J. V., and Andus, T. (1990). Interleukin-6 and the acute phase response. *Biochemical Journal*. *265*(3), 621–636.

Hendrayani, S.-F., Al-Harbi, B., Al-Ansari, M. M., Silva, G., and Aboussekhra, A. (2016). The inflammatory/cancer-related IL-6/STAT3/NF-kB positive feedback loop includes AUF1 and maintains the active state of breast myofibroblasts. *Oncotarget*. *7*(27), 41974-41985.

Hengpratom, T., Lowe, G. M., Thumanu, K., Suknasang, S., Tiamyom, K., and Eumkeb, G. (2018). *Oroxylum indicum* (L.) Kurz extract inhibits adipogenesis and lipase activity *in vitro*. *BMC Complementary and Alternative Medicine*. *18*(1), 177.

Hirano, T., Yasukawa, K., Harada, H., Taga, T., Watanabe, Y., Matsuda, T., Kashiwamura, S.-i., Nakajima, K., Koyama, K., and Iwamatsu, A. (1986). Complementary DNA

for a novel human interleukin (BSF-2) that induces B lymphocytes to produce immunoglobulin. *Nature*. *324*(6092), 73-76.

Horwood, N. J., Page, T. H., McDaid, J. P., Palmer, C. D., Campbell, J., Mahon, T., Brennan, F. M., Webster, D., and Foxwell, B. M. (2006). Bruton's tyrosine kinase is required for TLR2 and TLR4-induced TNF, but not IL-6, production. *The Journal of Immunology*. *176*(6), 3635-3641.

Huang, C., Šali, A., and Stevens, R. L. (1998). Regulation and function of mast cell proteases in inflammation. *Journal of Clinical Immunology*. *18*(3), 169-183.

Huang, W. J., Zhang, X., and Chen, W. W. (2016). Role of oxidative stress in Alzheimer's disease. *Biomedical Reports*. *4*(5), 519-522.

Ingram, S., and Diotallevi, M. (2017). Reactive oxygen species: Rapid fire in inflammation. *Biochemist*. *39*, 30-33.

Janeway Jr, C. A., and Medzhitov, R. (2002). Innate immune recognition. *Annual Review of Immunology*. *20*(1), 197-216.

Jang, S. I., Kim, Y.-J., Lee, W.-Y., Kwak, K. C., Baek, S. H., Kwak, G. B., Yun, Y.-G., Kwon, T.-O., Chung, H. T., and Chai, K.-Y. (2005). Scoparone from *Artemisia capillaris* inhibits the release of inflammatory mediators in RAW 264.7 cells upon stimulation cells by interferon-γ plus LPS. *Archives of Pharmacal Research*. *28*(2), 203-208.

Jeong, S. H. (2018). Inhibitory effect of phytol on cellular senescence. *Biomedical Dermatology*. *2*(1), 1-9.

Jimenez-Suarez, V., Nieto-Camacho, A., Jiménez-Estrada, M., and Alvarado Sanchez, B. (2016). Anti-inflammatory, free radical scavenging and alpha-glucosidase inhibitory activities of *Hamelia patens* and its chemical constituents. *Pharmaceutical Biology*. *54*(9), 1822-1830.

Kamata, H., Manabe, T., Oka, S.-i., Kamata, K., and Hirata, H. (2002). Hydrogen peroxide activates I$\varkappa$B kinases through phosphorylation of serine residues in the activation loops. *FEBS Letters*. *519*(1-3), 231-237.

Kaminska, B. (2005). MAPK signalling pathways as molecular targets for anti-inflammatory therapy-from molecular mechanisms to therapeutic benefits.

Biochimica et Biophysica Acta (BBA)-Proteins and Proteomics. 1754(1-2), 253-262.

Kang, B. Y., Chung, S. W., Kim, S. H., Cho, D., and Kim, T. S. (2003). Involvement of nuclear factor-𝜘B in the inhibition of interleukin-12 production from mouse macrophages by baicalein, a flavonoid in *Scutellaria baicalensis. Planta Medica. 69*(08), 687-691.

Kang, K. A., Zhang, R., Piao, M. J., Chae, S., Kim, H. S., Park, J. H., Jung, K. S., and Hyun, J. W. (2012). Baicalein inhibits oxidative stress-induced cellular damage via antioxidant effects. *Toxicology and Industrial Health. 28*(5), 412-421.

Karpuzoglu, E., and Ahmed, S. A. (2006). Estrogen regulation of nitric oxide and inducible nitric oxide synthase (iNOS) in immune cells: implications for immunity, autoimmune diseases, and apoptosis. *Nitric Oxide. 15*(3), 177-186.

Kawai, T., and Akira, S. (2011). Toll-like receptors and their crosstalk with other innate receptors in infection and immunity. *Immunity. 34*(5), 637-650.

Khandhar, M., Shah, M., Santani, D., and Jain, S. (2006). Antiulcer Activity of the root bark of *Oroxylum indicum*. against experimental gastric ulcers. *Pharmaceutical Biology. 44*(5), 363-370.

Khansari, N., Shakiba, Y., and Mahmoudi, M. (2009). Chronic inflammation and oxidative stress as a major cause of age-related diseases and cancer. *Recent Patents on Inflammation & Allergy Drug Discovery. 3*(1), 73-80.

Kimura, A., Kitajima, M., Nishida, K., Serada, S., Fujimoto, M., Naka, T., Fujii-Kuriyama, Y., Sakamato, S., Ito, T., and Handa, H. (2018). NQO1 inhibits the TLR-dependent production of selective cytokines by promoting I𝜘B-ζ degradation. *Journal of Experimental Medicine. 215*(8), 2197-2209.

Kirkham, P., and Rahman, I. (2006). Oxidative stress in asthma and COPD: antioxidants as a therapeutic strategy. *Pharmacology & Therapeutics. 111*(2), 476-494.

Kishimoto, T. (2005). Interleukin-6: from basic science to medicine-40 years in immunology. *Annual Review Immunology*. *23*, 1-21.

Kobayashi, E. H., Suzuki, T., Funayama, R., Nagashima, T., Hayashi, M., Sekine, H., Tanaka, N., Moriguchi, T., Motohashi, H., and Nakayama, K. (2016). Nrf2

suppresses macrophage inflammatory response by blocking proinflammatory cytokine transcription. *Nature Communications*. *7*, 11624.

Koenderman, L., Buurman, W., and Daha, M. R. (2014). The innate immune response. *Immunology Letters*. *162*(2), 95-102.

Korhonen, R., Lahti, A., Kankaanranta, H., and Moilanen, E. (2005). Nitric oxide production and signaling in inflammation. *Current Drug Targets-Inflammation & Allergy*. *4*(4), 471-479.

Kotas, M. E., and Medzhitov, R. (2015). Homeostasis, inflammation, and disease susceptibility. *Cell*. *160*(5), 816-827.

Krishnaiah, D., Sarbatly, R., and Nithyanandam, R. (2011). A review of the antioxidant potential of medicinal plant species. *Food and Bioproducts Processing*. *89*(3), 217-233.

Kwon, K.-R., Alam, M. B., Park, J.-H., Kim, T.-H., and Lee, S.-H. (2019). Attenuation of UVB-induced photo-aging by polyphenolic-rich Spatholobus suberectus stem extract via modulation of MAPK/AP-1/MMPs signaling in human keratinocytes. *Nutrients*. *11*(6), 1341.

Kwon, O. J., Choo, B. K., Lee, J. Y., Kim, M. Y., Shin, S. H., Seo, B.-I., Seo, Y.-B., Rhee, M. H., Shin, M.-R., and Kim, G.-N. (2015). Protective effect of Rhei Rhizoma on reflux esophagitis in rats via Nrf2-mediated inhibition of NF-kB signaling pathway. *BMC Complementary and Alternative Medicine*. *16*(1), 1-12.

Kyriakis, J. M., and Avruch, J. (2001). Mammalian mitogen-activated protein kinase signal transduction pathways activated by stress and inflammation. *Physiological Reviews*. *81*(2), 807-869.

Lampiasi, N., and Montana, G. (2018). An *in vitro* inflammation model to study the Nrf2 and NF-kB crosstalk in presence of ferulic acid as modulator. *Immunobiology*. *223*(4-5), 349-355.

Laupattarakasem, P., Houghton, P., Hoult, J., and Itharat, A. (2003). An evaluation of the activity related to inflammation of four plants used in Thailand to treat arthritis. *Journal of Ethnopharmacology*. *85*(2-3), 207-215.

Lee, J. A., Song, H. Y., Ju, S. M., Lee, S. J., Kwon, H.-J., Eum, W. S., Jang, S. H., Choi, S. Y., and Park, J. (2009). Differential regulation of inducible nitric oxide synthase

and cyclooxygenase-2 expression by superoxide dismutase in lipopolysaccharide stimulated RAW 264.7 cells. *Experimental & Molecular Medicine*. *41*(9), 629-637.

Lee, J. Y., and Park, W. (2016). Anti-inflammatory effects of oroxylin A on RAW 264.7 mouse macrophages induced with polyinosinic-polycytidylic acid. *Experimental and Therapeutic Medicine*. *12*(1), 151-156.

Lee, S. C., Kwon, Y.-W., Park, J.-Y., Park, S. Y., Lee, J.-H., and Park, S.-D. (2017). Antioxidant and anti-Inflammatory effects of herbal formula SC-E3 in lipopolysaccharide-stimulated RAW264.7 Macrophages. *Evidence-Based Complementary and Alternative Medicine*. *2017*.

Levine, S. J. (2006). Tumor necrosis factor alpha (TNF-α). In G. J. Laurent & S. D. Shapiro (Eds.), *Encyclopedia of Respiratory Medicine* (pp. 307-311). Oxford: Academic Press.

Li, W., Wang, L., Huang, W., Skibba, M., Fang, Q., Xie, L., Wei, T., Feng, Z., and Liang, G. (2015). Inhibition of ROS and inflammation by an imidazopyridine derivative X22 attenuate high fat diet-induced arterial injuries. *Vascular Pharmacology*. *72*, 153-162.

Loizzo, M. R., Tundis, R., Bonesi, M., Menichini, F., Mastellone, V., Avallone, L., and Menichini, F. (2012). Radical scavenging, antioxidant and metal chelating activities of *Annona cherimola* Mill. (cherimoya) peel and pulp in relation to their total phenolic and total flavonoid contents. *Journal of Food Composition and Analysis*. *25*(2), 179-184.

Lopresti, A. L., Maker, G. L., Hood, S. D., and Drummond, P. D. (2014). A review of peripheral biomarkers in major depression: the potential of inflammatory and oxidative stress biomarkers. *Progress in Neuro-Psychopharmacology and Biological Psychiatry*. *48*, 102-111.

Lowry, O. H., Rosebrough, N. J., Farr, A. L., and Randall, R. J. (1951). Protein measurement with the Folin phenol reagent. *Journal of Biological Chemistry*. *193*: 265-275.

Lu, Y.-C., Yeh, W.-C., and Ohashi, P. S. (2008). LPS/TLR4 signal transduction pathway. *Cytokine*. *42*(2), 145-151.

Luo, J.-F., Shen, X.-Y., Lio, C. K., Dai, Y., Cheng, C.-S., Liu, J.-X., Yao, Y.-D., Yu, Y., Xie, Y., and Luo, P. (2018). Activation of Nrf2/HO-1 pathway by nardochinoid C inhibits inflammation and oxidative stress in lipopolysaccharide-stimulated macrophages. *Frontiers in Pharmacology*. *9*, 911.

Maiese, K. (2015). New Insights for Oxidative Stress and Diabetes Mellitus. *Oxidative Medicine and Cellular Longevity*. *2015*, 875961.

Mairuae, N., Connor, J. R., Buranrat, B., and Lee, S. Y. (2019). *Oroxylum indicum* (L.) extract protects human neuroblastoma SH-SY5Y cells against β-amyloid-induced cell injury. *Molecular Medicine Reports*. *20*(2), 1933-1942.

Maizels, R. M., Hewitson, J. P., and Smith, K. A. (2012). Susceptibility and immunity to helminth parasites. *Current Opinion in Immunology*. *24*(4), 459-466.

Mathieu, P., Lemieux, I., and Després, J. P. (2010). Obesity, inflammation, and cardiovascular risk. *Clinical Pharmacology & Therapeutics*. *87*(4), 407-416.

Mathur, P., Ding, Z., Saldeen, T., and Mehta, J. L. (2015). Tocopherols in the prevention and treatment of atherosclerosis and related cardiovascular disease. *Clinical Cardiology*. *38*(9), 570-576.

Matteo, V., and Esposito, E. (2003). Biochemical and therapeutic effects of antioxidants in the treatment of Alzheimer's disease, Parkinson's disease, and amyotrophic lateral sclerosis. *Current Drug Targets-CNS & Neurological Disorders*. *2*(2), 95-107.

Matzinger, P. (2002). The danger model: a renewed sense of self. *Science*. *296*(5566), 301-305.

Medzhitov, R. (2010). Inflammation 2010: new adventures of an old flame. *Cell*. *140*(6), 771-776.

Mohan, S., Thiagarajan, K., Sundaramoorthy, B., Gurung, V., Barpande, M., Agarwal, S., and Chandrasekaran, R. (2016). Alleviation of 4-nitroquinoline 1-oxide induced oxidative stress by *Oroxylum indicum* (L.) leaf extract in albino Wistar rats. *BMC Complementary and Alternative Medicine*. *16*(1), 229.

Moon, Y. J., Wang, X., and Morris, M. E. (2006). Dietary flavonoids: effects on xenobiotic and carcinogen metabolism. *Toxicology in Vitro*. *20*(2), 187-210.

Mukherjee, S., Karmakar, S., and Babu, S. P. S. (2016). TLR2 and TLR4 mediated host immune responses in major infectious diseases: a review. *Brazilian Journal of Infectious Diseases*. *20*(2), 193-204.

Murakami, A., and Ohigashi, H. (2007). Targeting NOX, INOS and COX-2 in inflammatory cells: Chemoprevention using food phytochemicals. *International Journal of Cancer*. *121*(11), 2357-2363.

Nanasombat, S., Yansodthee, K., and Jongjaited, I. (2019). Evaluation of Antidiabetic, Antioxidant and Other Phytochemical Properties of Thai Fruits, Vegetables and Some Local Food Plants. *Walailak Journal of Science and Technology (WJST)*. *16*(11), 851-866.

Nathan, C. (2002). Points of control in inflammation. *Nature*. *420*(6917), 846-52.

Nathan, C. (2006). Neutrophils and immunity: challenges and opportunities. *Nature Reviews Immunology*. *6*(3), 173-182.

Nomura, M., Ma, W.-y., Chen, N., Bode, A. M., and Dong, Z. (2000). Inhibition of 12-O-tetradecanoylphorbol-13-acetate-induced NF-kB activation by tea polyphenols,(−)-epigallocatechin gallate and theaflavins. *Carcinogenesis*. *21*(10), 1885-1890.

Noort, A. R., Tak, P. P., and Tas, S. W. (2015). Non-canonical NF-kB signaling in rheumatoid arthritis: Dr Jekyll and Mr Hyde? *Arthritis Research & Therapy*. *17*(1), 15.

O'Donnell, P. M., and Taffet, S. M. (2002). The proximal promoter region is essential for lipopolysaccharide induction and cyclic AMP inhibition of mouse tumor necrosis factor-α. *Journal of Interferon & Cytokine Research*. *22*(5), 539-548.

Oeckinghaus, A., and Ghosh, S. (2009). The NF-kB family of transcription factors and its regulation. *Cold Spring Harbor Perspectives in Biology*. *1*(4), a000034.

Ozinsky, A., Underhill, D. M., Fontenot, J. D., Hajjar, A. M., Smith, K. D., Wilson, C. B., Schroeder, L., and Aderem, A. (2000). The repertoire for pattern recognition of pathogens by the innate immune system is defined by cooperation between toll-like receptors. *Proceedings of the National Academy of Sciences*. *97*(25), 13766-13771.

Palasuwan, A., Soogarun, S., Lertlum, T., Pradniwat, P., and Wiwanitkit, V. (2005). Inhibition of heinz body induction in an *in vitro* model and total antioxidant activity of medicinal Thai plants. *Asian Pacific Journal of Cancer Prevention*. *6*(4), 458-463.

Perretti, G., Finotti, E., Adamuccio, S., Della Sera, R., and Montanari, L. (2004). Composition of organic and conventionally produced sunflower seed oil. *Journal of the American Oil Chemists' Society*. *81*(12), 1119-1123.

Perwez Hussain, S., and Harris, C. C. (2007). Inflammation and cancer: an ancient link with novel potentials. *International Journal of Cancer*. *121*(11), 2373-2380.

Prele, C., Keith-Magee, A., Murcha, M., and Hart, P. (2007). Activated signal transducer and activator of transcription-3 (STAT3) is a poor regulator of tumour necrosis factor-α production by human monocytes. *Clinical & Experimental Immunology*. *147*(3), 564-572.

Qi, Z., Yin, F., Lu, L., Shen, L., Qi, S., Lan, L., Luo, L., and Yin, Z. (2013). Baicalein reduces lipopolysaccharide-induced inflammation via suppressing JAK/STATs activation and ROS production. *Inflammation Research*. *62*(9), *845-855*.

Raetz, C. R., Ulevitch, R. J., Wright, S. D., Sibley, C. H., Ding, A., and Nathan, C. (1991). Gram-negative endotoxin: an extraordinary lipid with profound effects on eukaryotic signal transduction. *The FASEB Journal*. *5*(12), 2652-2660.

Raggatt, L. J., Wullschleger, M. E., Alexander, K. A., Wu, A. C., Millard, S. M., Kaur, S., Maugham, M. L., Gregory, L. S., Steck, R., and Pettit, A. R. (2014). Fracture healing via periosteal callus formation requires macrophages for both initiation and progression of early endochondral ossification. *The American Journal of Pathology*. *184*(12), 3192-3204.

Rajasekaran, S., Sriram, N., Arulselvan, P., and Subramanian, S. (2007). Effect of Aloe vera leaf gel extract on membrane bound phosphatases and lysosomal hydrolases in rats with streptozotocin diabetes. *Die Pharmazie*. *62*(3), 221-225.

Ravipati, A. S., Zhang, L., Koyyalamudi, S. R., Jeong, S. C., Reddy, N., Bartlett, J., Smith, P. T., Shanmugam, K., Münch, G., and Wu, M. J. (2012). Antioxidant and anti-inflammatory activities of selected Chinese medicinal plants and their relation

with antioxidant content. *BMC Complementary and Alternative Medicine*. *12*(1), 173.

Reiter, E., Jiang, Q., and Christen, S. (2007). Anti-inflammatory properties of α-and γ-tocopherol. *Molecular Aspects of Medicine*. *28*(5-6), 668-691.

Reuter, S., Gupta, S. C., Chaturvedi, M. M., and Aggarwal, B. B. (2010). Oxidative stress, inflammation, and cancer: how are they linked? *Free Radical Biology and Medicine*. *49*(11), 1603-1616.

Ribeiro, D., Freitas, M., Tomé, S. M., Silva, A. M., Porto, G., and Fernandes, E. (2013). Modulation of human neutrophils' oxidative burst by flavonoids. *European Journal of Medicinal Chemistry*. *67*, 280-292.

Ricciotti, E., and FitzGerald, G. A. (2011). Prostaglandins and inflammation. *Arteriosclerosis, Thrombosis, and Vascular Biology*. *31*(5), 986-1000.

Rinnerthaler, M., Bischof, J., Streubel, M., Trost, A., and Richter, K. (2015). Oxidative stress in aging human skin. *Biomolecules*. *5*(2), 545-589.

Ripunjoy, S. (2013). Indigenous knowledge on the utilization of medicinal plants by the Sonowal Kachari tribe of Dibrugarh district in Assam, North-East India. *International Research Journal of Biological Sciences*. *2*(4), 44-50.

Roy, M. K., Nakahara, K., Thalang, V. N., Trakoontivakorn, G., Takenaka, M., Isobe, S., and Tsushida, T. (2007). Baicalein, a flavonoid extracted from a methanolic extract of *Oroxylum indicum* inhibits proliferation of a cancer cell line *in vitro via induction of apoptosis. Pharmazie. 62(2), 149-153*.

Rupasinghe, H. V., Wang, L., Huber, G. M., and Pitts, N. L. (2008). Effect of baking on dietary fibre and phenolics of muffins incorporated with apple skin powder. *Food Chemistry*. *107*(3), 1217-1224.

Rushworth, S. A., MacEwan, D. J., and O'Connell, M. A. (2008). Lipopolysaccharide-induced expression of NAD (P) H: quinone oxidoreductase 1 and heme oxygenase-1 protects against excessive inflammatory responses in human monocytes. *The Journal of Immunology*. *181*(10), 6730-6737.

Saha, P., Choudhury, P. R., Das, S., Talukdar, A. D., and Choudhury, M. D. (2017). *In vitro* antioxidant activity of bark extracts of *Oroxylum indicum* (L) vent. *Asian Journal of Pharmaceutical and Clinical Research*. *10*(8), 263-266.

Sala, E., Guasch, L., Iwaszkiewicz, J., Mulero, M., Salvadó, M.-J., Bladé, C., Ceballos, M., Valls, C., Zoete, V., and Grosdidier, A. (2011). Identification of human IKK-2 inhibitors of natural origin (Part II), In Silico prediction of IKK-2 inhibitors in natural extracts with known anti-inflammatory activity. *European Journal of Medicinal Chemistry*. *46*(12), 6098-6103.

Samavati, L., Rastogi, R., Du, W., Hüttemann, M., Fite, A., and Franchi, L. (2009). STAT3 tyrosine phosphorylation is critical for interleukin 1 beta and interleukin-6 production in response to lipopolysaccharide and live bacteria. *Molecular Immunology*. *46*(8-9), 1867-1877.

Sánchez-Moreno, C. (2002). Methods used to evaluate the free radical scavenging activity in foods and biological systems. *Food Science and Technology International*. *8*(3), 121-137.

Schulze-Osthoff, K., Bauer, M., Vogt, M., and Wesselborg, S. (1997). Oxidative stress and signal transduction. *International Journal for Vitamin and Nutrition Research*. *67*(5), 336-342.

Segal, B. H., Leto, T. L., Gallin, J. I., Malech, H. L., and Holland, S. M. (2000). Genetic, biochemical, and clinical features of chronic granulomatous disease. *Medicine*. *79*(3), 170-200.

Seong, S.-Y., and Matzinger, P. (2004). Hydrophobicity: an ancient damage-associated molecular pattern that initiates innate immune responses. *Nature Reviews Immunology*. *4*(6), 469-478.

Sharma, J., Al-Omran, A., and Parvathy, S. (2007). Role of nitric oxide in inflammatory diseases. *Inflammopharmacology*. *15*(6), 252-259.

Shimizu, K., Ozeki, M., Iino, A., Nakajyo, S., Urakawa, N., and Atsuchi, M. (2001). Structure-activity relationships of triterpenoid derivatives extracted from *Gymnema inodorum* leaves on glucose absorption. *The Japanese Journal of Pharmacology*. *86*(2), 223-229.

Shimizu, T., Shibuya, N., Narukawa, Y., Oshima, N., Hada, N., and Kiuchi, F. (2018). Synergistic effect of baicalein, wogonin and oroxylin A mixture: multistep inhibition of the NF-kB signalling pathway contributes to an anti-inflammatory

effect of Scutellaria root flavonoids. *Journal of Natural Medicines*. *72*(1), 181-191.

Shin, E. K., Kwon, H.-S., Kim, Y. H., Shin, H.-K., and Kim, J.-K. (2009). Chrysin, a natural flavone, improves murine inflammatory bowel diseases. *Biochemical and Biophysical Research Communications*. *381*(4), 502-507.

Siewert, E., Bort, R., Kluge, R., Heinrich, P. C., Castell, J., and Jover, R. (2000). Hepatic cytochrome P450 down-regulation during aseptic inflammation in the mouse is interleukin 6 dependent. *Hepatology*. *32*(1), 49-55.

Silva, R. O., Sousa, F. B. M., Damasceno, S. R., Carvalho, N. S., Silva, V. G., Oliveira, F. R. M., Sousa, D. P., Aragão, K. S., Barbosa, A. L., and Freitas, R. M. (2014). Phytol, a diterpene alcohol, inhibits the inflammatory response by reducing cytokine production and oxidative stress. *Fundamental & Clinical Pharmacology*. *28*(4), 455-464.

Singh, J., and Kakkar, P. (2013). Modulation of liver function, antioxidant responses, insulin resistance and glucose transport by *Oroxylum indicum* stem bark in STZ induced diabetic rats. *Food and Chemical Toxicology*. *62*, 722-731.

Siriwatanametanon, N., Fiebich, B. L., Efferth, T., Prieto, J. M., and Heinrich, M. (2010). Traditionally used Thai medicinal plants: *in vitro* anti-inflammatory, anticancer and antioxidant activities. *Journal of Ethnopharmacology*. *130*(2), 196-207.

Sittisart, P., and Chitsomboon, B. (2014). Intracellular ROS scavenging activity and downregulation of inflammatory mediators in RAW264. 7 macrophage by fresh leaf extracts of *Pseuderanthemum palatiferum*. *Evidence-Based Complementary and Alternative Medicine*. *2014*.

Son, H.-U., Yoon, E.-K., Yoo, C.-Y., Park, C.-H., Bae, M., Kim, T.-H., Lee, C. H., Lee, K. W., Seo, H., and Kim, K.-J. (2019). Effects of synergistic inhibition on α-glucosidase by phytoalexins in soybeans. *Biomolecules*. *9*(12), 828.

Stamler, J. S., Lamas, S., and Fang, F. C. (2001). Nitrosylation: the prototypic redox-based signaling mechanism. *Cell*. *106*(6), 675-683.

Steer, P., Millgård, J., Sarabi, D. M., Basu, S., Vessby, B., Kahan, T., Edner, M., and Lind, L. (2002). Cardiac and vascular structure and function are related to lipid peroxidation and metabolism. *Lipids*. *37*(3), 231-236.

Stramer, B. M., Mori, R., and Martin, P. (2007). The inflammation-fibrosis link? A Jekyll and Hyde role for blood cells during wound repair. *Journal of Investigative Dermatology*. *127*(5), 1009-1017.

Subramanian, S., Kumar, D. S., Arulselvan, P., and Senthilkumar, G. (2006). In vitro antibacterial and antifungal activities of ethanolic extract of *Aloe vera* leaf gel. *Journal of Plant Sciences*. *1*(4), 348-355.

Subramanian, S. S. (1972). Flavonoids of the leaves of *Oroxylum indicum* and *Pajanelia longifolia. Phytochemistry*. *11*(1), 439-440.

Sun, J., Zhang, X., Broderick, M., and Fein, H. (2003). Measurement of nitric oxide production in biological systems by using Griess reaction assay. *Sensors*. *3*(8), 276-284.

Suzuki, K., Meguro, K., Nakagomi, D., and Nakajima, H. (2017). Roles of alternatively activated M2 macrophages in allergic contact dermatitis. *Allergology International*. *66*(3), 392-397.

Tak, P. P., and Firestein, G. S. (2001). NF-kB: a key role in inflammatory diseases. *The Journal of Clinical Investigation*. *107*(1), 7-11.

Tan, H.-Y., Wang, N., Li, S., Hong, M., Wang, X., and Feng, Y. (2016). The reactive oxygen species in macrophage polarization: reflecting its dual role in progression and treatment of human diseases. *Oxidative Medicine and Cellular Longevity*. *2016*.

Tanaka, T., and Kishimoto, T. (2012). Targeting interleukin-6: all the way to treat autoimmune and inflammatory diseases. *International Journal of Biological sciences*. *8*(9), 1227-1236.

Taniguchi, K., and Karin, M. (2018). NF-kB, inflammation, immunity and cancer: coming of age. *Nature Reviews Immunology*. *18*(5), 309-324.

Tenpe, C., Upaganlawar, A., Burle, S., and Yeole, Y. (2009). *In vitro* antioxidant and preliminary hepatoprotective activity of *Oroxylum indicum* Vent leaf extracts. *Pharmacologyonline*. 1, 35-43.

Tiamyom, K., Sirichaiwetchakoon, K., Hengpratom, T., Kupittayanant, S., Srisawat, R., Thaeomor, A., and Eumkeb, G. (2019). The effects of *Cordyceps sinensis* (Berk.) Sacc. and *Gymnema inodorum* (Lour.) Decne. extracts on adipogenesis and

lipase activity *in vitro*. *Evidence-Based Complementary and Alternative Medicine*. *2019*.

Tilley, S. L., Coffman, T. M., and Koller, B. H. (2001). Mixed messages: modulation of inflammation and immune responses by prostaglandins and thromboxanes. *The Journal of Clinical Investigation*. *108*(1), 15-23.

Tran, T. V. A., Malainer, C., Schwaiger, S., Hung, T., Atanasov, A. G., Heiss, E. H., Dirsch, V. M., and Stuppner, H. (2015). Screening of Vietnamese medicinal plants for NF-kB signaling inhibitors: Assessing the activity of flavonoids from the stem bark of *Oroxylum indicum. Journal of Ethnopharmacology*. *159*, 36-42.

Trang, D. H. T., Son, H. L., and Trung, P. V. (2018). Investigation on the *in vitro* antioxidant capacity of methanol extract, fractions and flavones from *Oroxylum indicum* Linn bark. *Brazilian Journal of Pharmaceutical Sciences*. *54*(1), e17178.

Tripathy, B. N., Panda, S., Sahoo, S., Mishra, S., and Nayak, L. (2011). Phytochemical analysis and hepatoprotective effect of stem bark of *Oroxylum indicum* (L) Vent. on carbon tetrachloride induced hepatotoxicity in rat. *International Journal of Pharmaceutical & Biological Archives*. *2*(6), 1714-1717.

Van Linthout, S., Miteva, K., and Tschöpe, C. (2014). Crosstalk between fibroblasts and inflammatory cells. *Cardiovascular Research*. *102*(2), 258-269.

Wynn, T. A., Chawla, A., and Pollard, J. W. (2013). Macrophage biology in development, homeostasis and disease. *Nature*. *496*(7446), 445-455.

Xue, B., Wu, Y., Yin, Z., Zhang, H., Sun, S., Yi, T., and Luo, L. (2005). Regulation of lipopolysaccharide-induced inflammatory response by glutathione S-transferase P1 in RAW264. 7 cells. *FEBS Letters*. *579*(19), 4081-4087.

Yahfoufi, N., Alsadi, N., Jambi, M., and Matar, C. (2018). The immunomodulatory and anti-inflammatory role of polyphenols. *Nutrients*. *10*(11), 1618.

Yan, R.-y., Cao, Y.-y., Chen, C.-y., Dai, H.-q., Yu, S.-x., Wei, J.-l., Li, H., and Yang, B. (2011). Antioxidant flavonoids from the seed of *Oroxylum indicum*. *Fitoterapia*. *82*(6), 841-848.

Yanishlieva, N. V., Kamal‑Eldin, A., Marinova, E. M., and Toneva, A. G. (2002). Kinetics of antioxidant action of α-and γ-tocopherols in sunflower and soybean

triacylglycerols. *European Journal of Lipid Science and Technology*. *104*(5), 262-270.

Ye, M., Wang, Q., Zhang, W., Li, Z., Wang, Y., and Hu, R. (2014). Oroxylin A exerts anti-inflammatory activity on lipopolysaccharide-induced mouse macrophage via Nrf2/ARE activation. *Biochemistry and Cell Biology*. *92*(5), 337-348.

Yoon, Y., Kim, T. J., Lee, J. M., and Kim, D. Y. (2018). SOD2 is upregulated in periodontitis to reduce further inflammation progression. *Oral Diseases*. *24*(8), 1572-1580.

Youn, J. S., Kim, Y.-J., Na, H. J., Jung, H. R., Song, C. K., Kang, S. Y., and Kim, J. Y. (2019). Antioxidant activity and contents of leaf extracts obtained from *Dendropanax morbifera* LEV are dependent on the collecting season and extraction conditions. *Food Science and Biotechnology*. *28*(1), 201-207.

Zeb, M., Khan, S., Rahman, T., Sajid, M., and Seloni, S. (2017). I Isolation and biological activity of β-sitosterol and stigmasterol from the roots of *Indigofera heterantha*. *Pharmacy & Pharmacology International Journal*. *5*(5), 204-207.

Zhang, H., and Forman, H. J. (2012). Glutathione synthesis and its role in redox signaling. *In Seminars in Cell & Developmental Biology*. *23*(7), 722–728.

Zhang, H., and Sun, S.-C. (2015). NF-kB in inflammation and renal diseases. *Cell & Bioscience*. *5*(1), 1-12.

Zhang, H., Zhang, S. J., Lyn, N., Florentino, A., Li, A., Davies, K. J., and Forman, H. J. (2020). Down regulation of glutathione and glutamate cysteine ligase in the inflammatory response of macrophages. *Free Radical Biology and Medicine*. *158*, 53-59.

APPENDICES
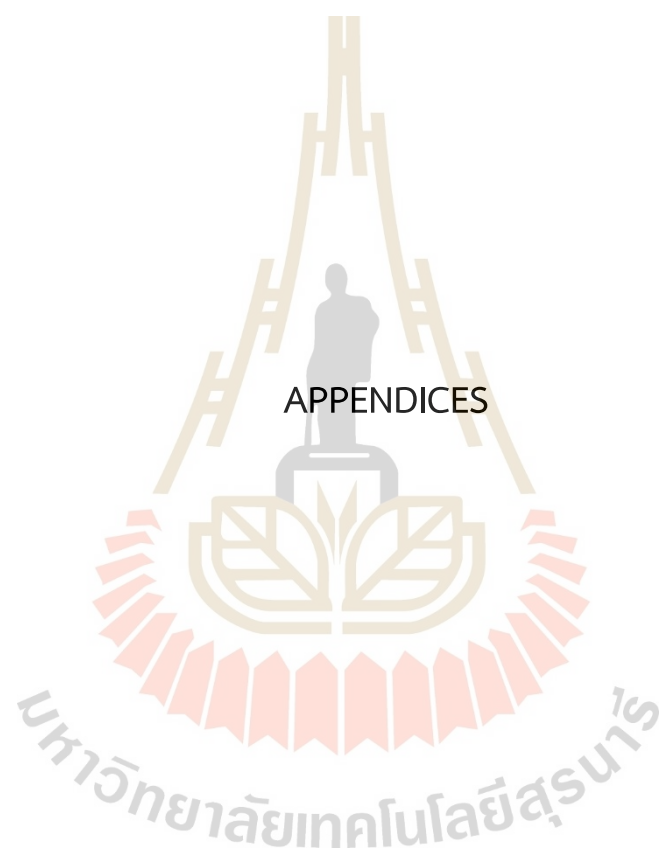
APPENDIX A

PREPARATION OF REAGENTS FOR CHEMICAL

A.1 Western blot

- RIPA buffer

- PBS (1X)	100	mL
- NP-40	1	mL
- Sodium dodecyl sulfate (SDS)	0.1	g

  (Store at 4 °C)

- Lysis buffer

- RIPA buffer	1	mL
- Phenylmethanesulfonyl fluoride (PMSF, 200 mM)	10	μL
- Leupeptin (2 mM)	1	μL
- E-64 (1 mM)	1	μL

  (Freshly prepared)

- Lowry reagents

  - Reagent A (2% Na_2CO_3 in 0.1 N NaOH)

▪ Na_2CO_3	5	g
▪ NaOH (0.1 N)	250	mL

    (Store at 4 °C)

  - Reagent B (0.5% $CuSO_4 5H_2O$ in 1% sodium citrate)

▪ $CuSO_4 5H_2O$	0.05	g
▪ Sodium citrate	0.1	g
▪ DI water	10	mL

  - Reagent C (1 N Folin phenol reagent)

    - ▪ 2 N Folin phenol reagent diluted with DI water (1:1, v/v)

    (Freshly prepared)

- Reagent D
  - Reagent A : Reagent B (50 : 1) (Freshly prepared)

- Sample buffer (6X)
  - Tris-base   0.59   g
  - DI water   8.5   mL
  - SDS   1.5   g
  - 2-Mercaptoethanol (2ME)   0.6   mL
  - Glycerol   7.5   mL
  - Bromophenol blue   7.5   mg
  (Store at 4 ℃)

- SDS (10%, w/v)
  - SDS   10   g
  - DI water   100   mL
  (Store at RT)

- Ammonium persulfate (Aps) solution (10%, w/v)
  - Aps   0.1   g
  - DI water   1   mL

- Acrylamide (30%, w/v)
  - Acrylamide   30   g
  - Bis-acrylamide   0.8   g
  - DI water   100   mL
  (Filtrate, store at 4 ℃)

- Tris-Cl (1.5 M, pH 8.8)
  - Tris-base   18.165 g
  - DI water   80   mL
  Adjust pH to 8.8 with HCl and bring to 100 mL with DI water.
  (Filtrate, store at 4 ℃)

- Tris-Cl (0.5 M, pH 6.8)
  - Tris-base   6   g

- DI water   80   mL

  Adjust pH to 6.8 with HCl and bring to 100 mL with DI water.

  (Filtrate, store at 4 ℃)

- Running buffer (10X)

  - Tris-base   30   g
  - Glycine   14.4   g
  - SDS   10   g
  - DI water   1   L

    (Filtrate, store at 4 ℃)

- Running buffer (1X)

  - Running buffer (10X)   100   mL
  - DI water   900   mL

- Blotting buffer (1X)

  - Tris-base   3   g
  - Glycine   14.4   g
  - Methanol   200   mL

    Adjust volume to 1 L with DI water, and filter (store at 4 ℃).

- TPBS 0.1% Tween 20

  - PBS (1X)   1000   mL
  - Tween 20   1   mL

    (Filtrate, store at 4 ℃)

- Nonfat milk (5%, w/v)

  - Nonfat milk   0.75   g
  - TPBS 0.1% Tween 20   15   mL

    (Freshly prepared)

- Coomassie blue solution

  - Coomassie blue   0.05   g
  - Methanol   80   mL
  - Glacial acetic acid   14   mL

Adjust volume to 100 mL with DI water (store at RT).

- Destaining solution

    - Methanol   5   mL

    - Glacial acetic acid   7   mL

    Adjust volume to 100 mL with DI water (store at RT).

- Resolving gel (7.5%) (for 2 gels)

    - DI water   4.84 mL

    - 1.5 M Tris-Cl (pH 8.8)   2.5   mL

    - Acrylamide (30%, w/v)   2.5   mL

    - SDS (10%, w/v)   100   µL

    - Aps (10%, w/v)   50   µL

    - Tetramethylethylenediamine (TEMED)   10   µL

- Resolving gel (10%) (for 2 gels)

    - DI water   4   mL

    - Tris-Cl (1.5 M, pH 8.8)   2.5   mL

    - Acrylamide (30%, w/v)   3.3   mL

    - SDS (10%, w/v)   100   µL

    - Aps (10%, w/v)   50   µL

    - TEMED   10   µL

- Stacking gel (4%) (for 2 gels)

    - DI water   3   mL

    - Tris-Cl (0.5 M, pH 6.8)   1.25 mL

    - Acrylamide (30%, w/v)   665   µL

    - SDS (10%, w/v)   50   µL

    - Aps (10%, w/v)   25   µL

    - TEMED   10   µL

A.2 ELISA

- Citric-phosphate buffer (pH 5.0)

    - Diabasic sodium phosphate (0.2 M)   25.7 mL

-	Ctric acid (0.1 M)	24.3	mL
-	DI water	50	mL

(Adjust pH to 5.0)

- 3, 3', 5, 5'-tetramethyl-benzidine stock solution (6 mg/mL)

-	3, 3', 5, 5'-tetramethyl-benzidine (TMB)	30	mg
-	DMSO	5	mL

(Stock solution can be store up to 1 month at RT)

- H_2O_2 (1%)

-	H_2O_2 (30%)	0.1	mL
-	DI water	2.9	mL

- TMB substrate

-	Citric-phosphate buffer pH 5.0	12.5	mL
-	TMB stock solution (6 mg/mL)	200	μL
-	H_2O_2 (1%)	50	μL

(Freshly prepared)

- H_2SO_4 (6 N)

-	H_2SO_4 (18 M)	166.67	mL

Adjust volume to 1 L with DI water

APPENDIX B

PREPARATION OF REAGENTS FOR CELL CULTURE

B.1 Phosphate buffer saline (PBS), 1X, pH 7.4

- KH2PO4   0.144   g
- $Na_2HPO_4.7H_2O$ 0.795   g
- NaCl   9.0   g
- DI water   1   L

Adjust pH to 7.2 ± 0.1 and filter sterile (store at 4 ℃).

B.2 Culture media preparation

- FBS (heat-inactivated)
    - Slowly thaw the frozen FBS in a beaker filled with water.
    - Put in a water bath at 37 ℃ till completely thaw.
    - Heat inactivate (56 ℃, 30 min), gentle mix every 15 min.
    (Store at -20 ℃).
- RPMI 1640, 1X (incomplete medium)
    - RPMI 1640, 1X with L-glutamine and phenol red   1   pack
    - $NaHCO_3$ 9.0   g
    - DI water   1   L
    Adjust pH to 7.2-7.4 and filter sterile (Store at 4 ℃).
- RPMI 1640, 1X (complete medium)
    - Inactivated FBS   20   mL
    - Penicillin/Streptomycin   2   mL
    - HEPES buffer, 1M   3   mL
    Adjust volume to 200 ml with RPMI 1640, 1X (incomplete medium, s
    4 ℃).

APPENDIX C
STANDARD CURVE

C.1 DPPH assay

- DPPH radical scavenging activity of OIE and positive controls (Vitamin C and Trolox)
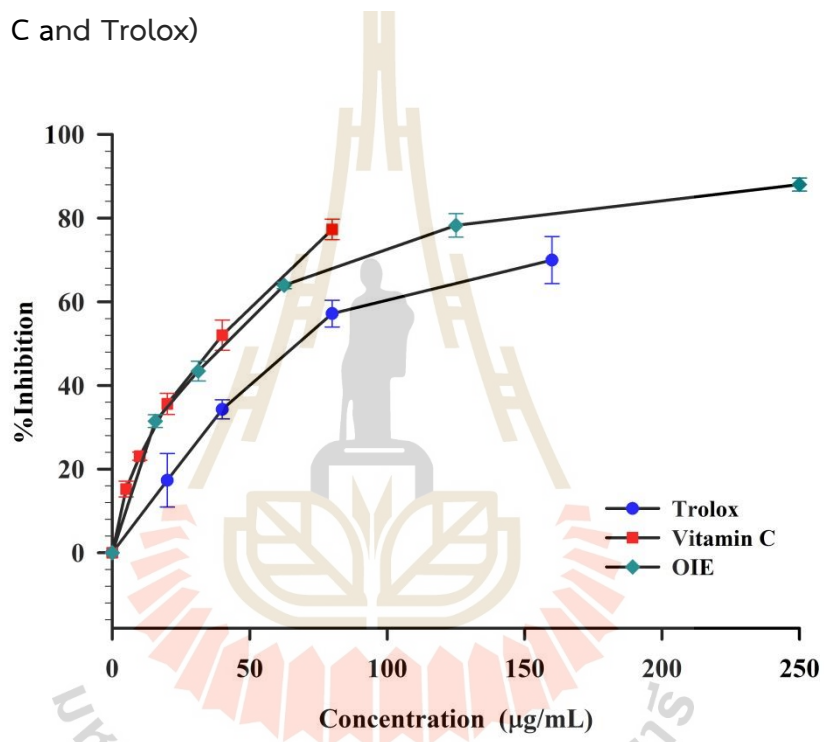
- DPPH radical scavenging activity of GIE and positive controls (Vitamin C and Trolox)
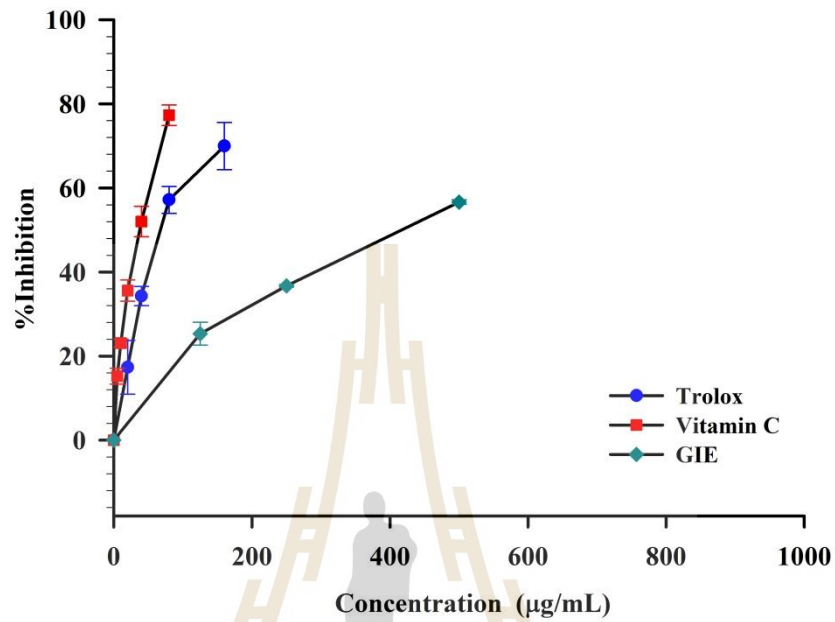
C.2   FRAP assay

•   Standard curve of Trolox

Standard curve of Trolox. $y = 0.0109x + 0.1068$, $R^2 = 0.984$. Absorbance at 595 nm versus Trolox concentration (μg/mL).

•   Standard curve of Vitamin C

Standard curve of Vitamin C. $y = 0.0124x + 0.1151$, $R^2 = 0.9994$. Absorbance at 595 nm versus Vitamin C concentration (μg/mL).
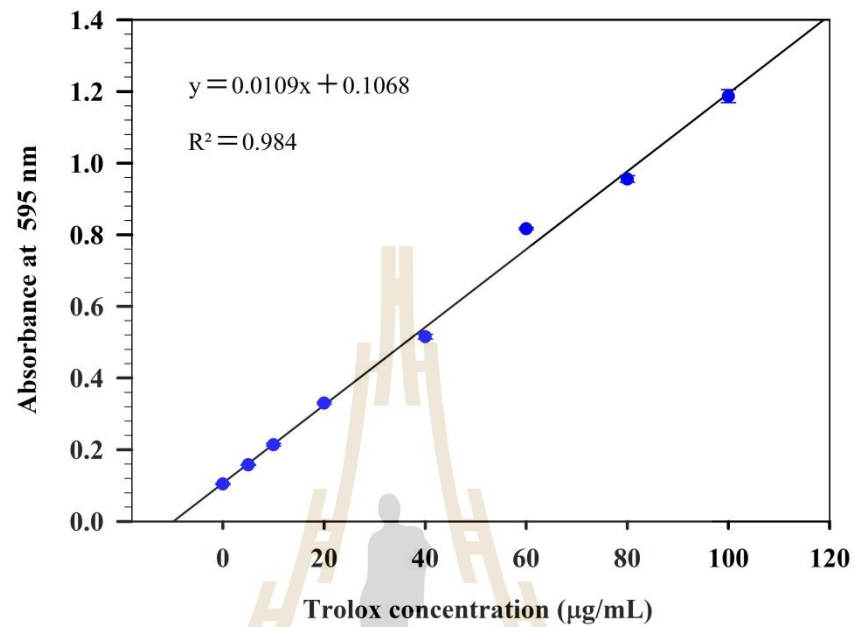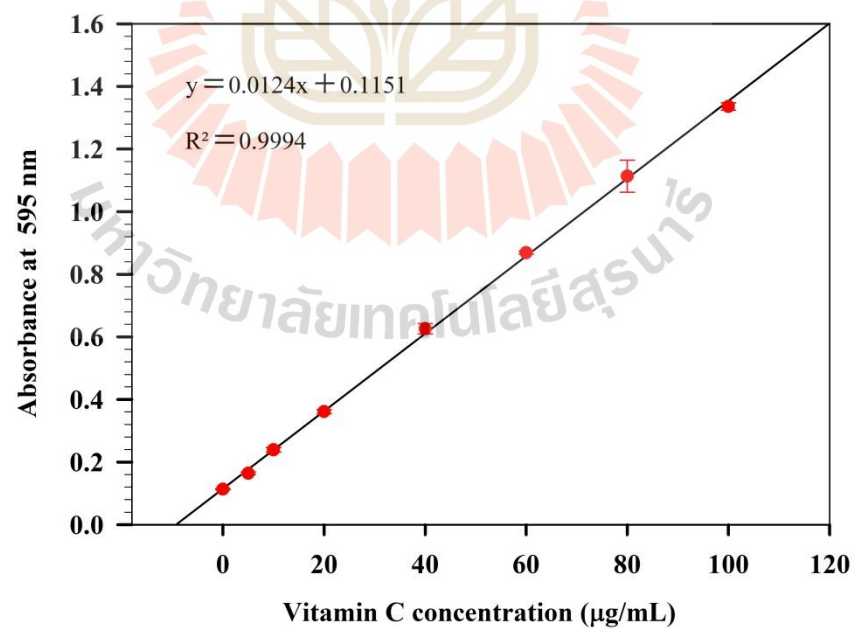
C.3   ELISA

- Standard curve of IL-6
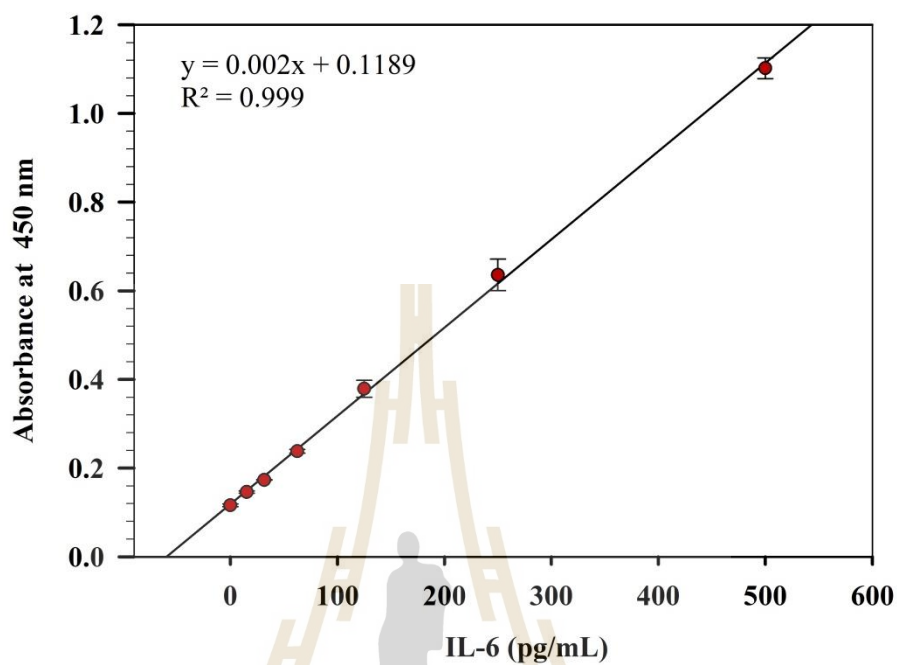
- Standard curve of TNF-α
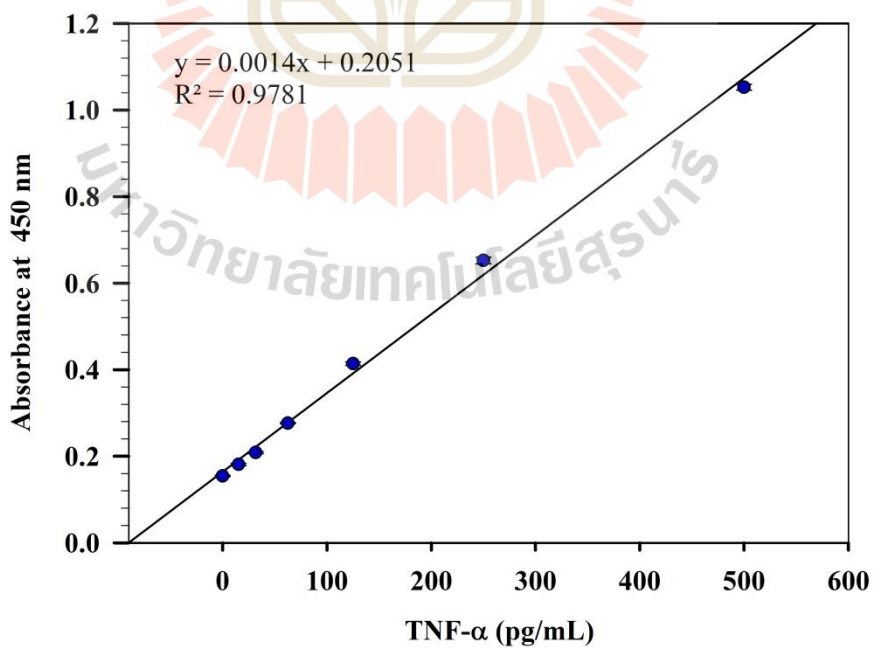
- Standard curve of IL-10

y = 0.0018x + 0.2406
R² = 0.998
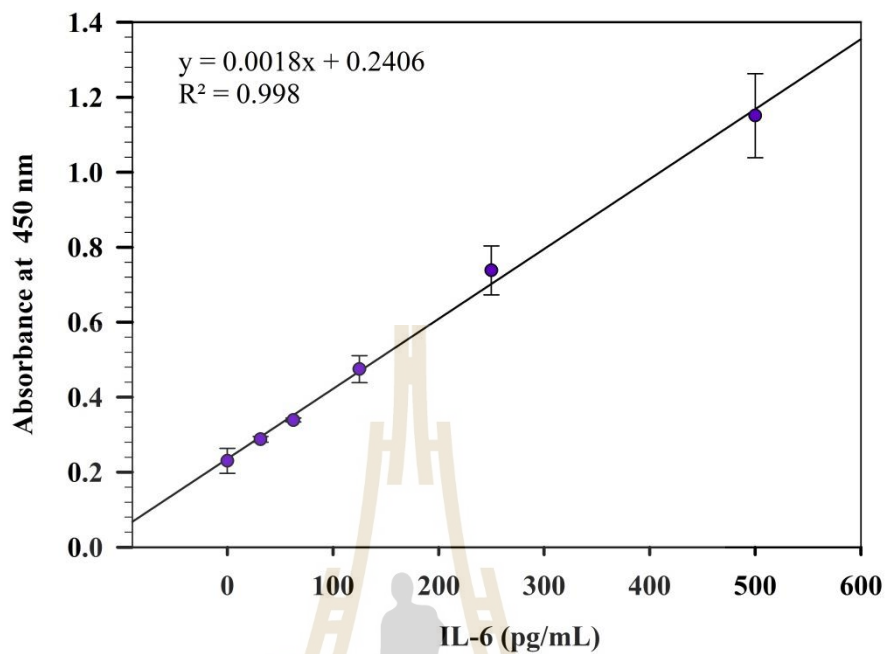
C.4   Western blotting

- Standard curve of BSA

y = 0.0006x + 0.1134
R² = 0.9847
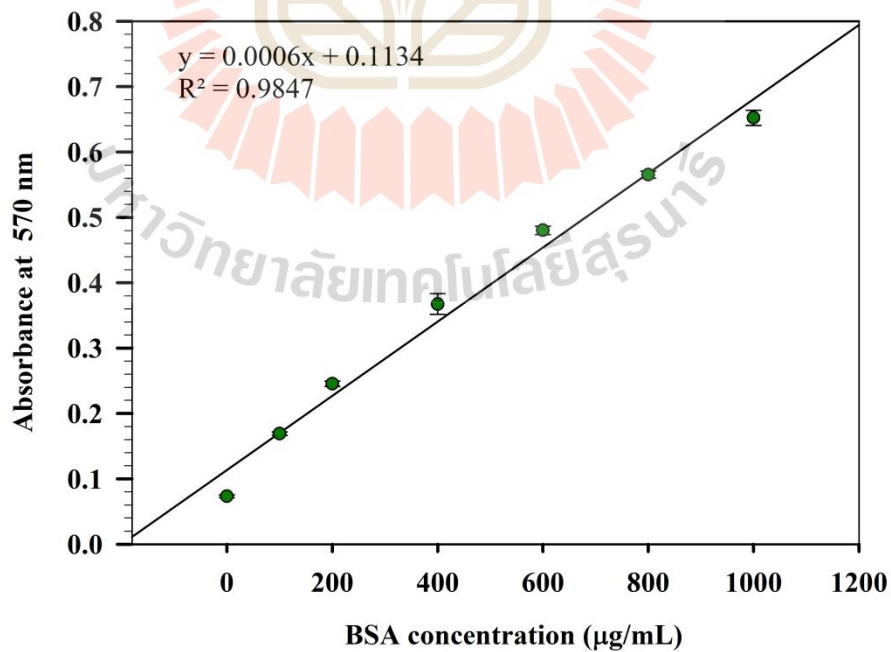
APPENDIX D

PUBLICATIONS

Dunkhunthod, B., Talabnin, C., Murphy, M., Thumanu, K., Sittisart, P., and Eumkeb, G. (2021). *Gymnema inodorum* (Lour.) Decne. Extract Alleviates Oxidative Stress and Inflammatory Mediators Produced by RAW264. 7 Macrophages. *Oxidative Medicine and Cellular Longevity*. *2021*: 8658314. (Impact Factor 2020 = 5.60; SCOPUS SJR 2020 = Q1, Web of Sci JCR 2020 = Q2).

Dunkhunthod, B., Talabnin, C., Murphy, M., Thumanu, K., Sittisart, P., Hengpratom, T., and Eumkeb, G. (2020). Intracellular ROS scavenging and anti-Inflammatory activities of *Oroxylum indicum* Kurz (L.) extract in LPS plus IFN-γ-activated RAW264.7 macrophages. *Evidence-Based Complementary and Alternative Medicine*. *2020*: 7436920. (Impact Factor 2020 = 2.40; SCOPUS SJR 2020 = Q1, Web of Sci JCR 2020 = Q3).

Research Article

Gymnema inodorum (Lour.) Decne. Extract Alleviates Oxidative Stress and Inflammatory Mediators Produced by RAW264.7 Macrophages

Benjawan Dunkhunthod,[1] **Chutima Talabnin,**[2] **Mark Murphy,**[3] **Kanjana Thumanu,**[4] **Patcharawan Sittisart,**[5] **and Griangsak Eumkeb** [ID][1]

[1]*School of Preclinical Sciences, Institute of Science, Suranaree University of Technology, Nakhon Ratchasima 30000, Thailand*
[2]*School of Chemistry, Institute of Science, Suranaree University of Technology, Nakhon Ratchasima 30000, Thailand*
[3]*School of Biomolecular Science, Liverpool John Moores University, Liverpool L3 3AF, UK*
[4]*Synchrotron Light Research Institute (Public Organization), Nakhon Ratchasima 30000, Thailand*
[5]*Division of Environmental Science, Faculty of Liberal Arts and Science, Sisaket Rajabhat University, Sisaket 33000, Thailand*

Correspondence should be addressed to Griangsak Eumkeb; griang@sut.ac.th

Gymnema inodorum (Lour.) Decne. (*G. inodorum*) is widely used in Northern Thai cuisine as local vegetables and commercial herb tea products. In the present study, *G. inodorum* extract (GIE) was evaluated for its antioxidant and anti-inflammatory effects in LPS plus IFN-γ-induced RAW264.7 cells. Major compounds in GIE were evaluated using GC-MS and found 16 volatile compounds presenting in the extract. GIE exhibited antioxidant activity by scavenging the intracellular reactive oxygen species (ROS) production and increasing superoxide dismutase 2 (SOD2) mRNA expression in LPS plus IFN-γ-induced RAW264.7 cells. GIE showed anti-inflammatory activity through suppressing nitric oxide (NO), proinflammatory cytokine production interleukin 6 (IL-6) and also downregulation of the expression of cyclooxygenase-2 (COX-2), inducible nitric oxide synthase (iNOS), and IL-6 mRNA levels in LPS plus IFN-γ-induced RAW264.7 cells. Mechanism studies showed that GIE suppressed the NF-κB p65 nuclear translocation and slightly decreased the phosphorylation of NF-κB p65 (p-NF-κB p65) protein. Our studies applied the synchrotron radiation-based FTIR microspectroscopy (SR-FTIR), supported by multivariate analysis, to identify the FTIR spectral changes based on macromolecule alterations occurring in RAW264.7 cells. SR-FTIR results demonstrated that the presence of LPS plus IFN-γ in RAW264.7 cells associated with the increase of amide I/amide II ratio (contributing to the alteration of secondary protein structure) and lipid content, whereas glycogen and other carbohydrate content were decreased. These findings lead us to believe that GIE may prevent oxidative damage by scavenging intracellular ROS production and activating the antioxidant gene, SOD2, expression. Therefore, it is possible that the antioxidant properties of GIE could modulate the inflammation process by regulating the ROS levels, which lead to the suppression of proinflammatory cytokines and genes. Therefore, GIE could be developed into a novel antioxidant and anti-inflammatory agent to treat and prevent diseases related to oxidative stress and inflammation.

1. Introduction

Inflammation is the immune system's response to harmful stimuli, such as infection and tissue injury [1]. Macrophages are a diverse group of white blood cells known for eliminating pathogens through phagocytosis. Macrophages play a central role in promoting inflammatory lesions, which cause pathological tissue damage in various inflammatory diseases [2]. It is well known that interferon-gamma (IFN-γ) or lipopolysaccharide (LPS) is sufficient to induce classically activated macrophages [3]. The nuclear factor kappa light chain enhancer of activated B cells (NF-κB) is an important

transcription factor playing crucial roles in the inflammatory response [4]. In response to inflammatory stimuli, the nuclear localization signal of cytosolic NF-κB into the nucleus binds to a consensus sequence in the promoters of target genes including proinflammatory cytokines, chemokines, adhesion proteins, and inducible enzymes (COX-2 and iNOS) [5]. Due to the response with the existence of cellular stimuli, activated macrophages produce high levels of proinflammatory cytokines, including IL-6, interleukin 1β (IL-1β), TNF-α, and prostaglandin (PGE$_2$) [6]. These cytokines are involved in the process of pathological pain. During inflammation, free radical molecules such as NO and reactive oxygen intermediates (ROI) are also generated by inflammatory cells. Free radicals are involved in an imbalance of the redox system and damaging cells and tissues [7]. The link between oxidative stress and inflammation has extensively been demonstrated that the mechanism by which continued oxidative stress can lead to chronic inflammation. This mechanism leads to various inflammatory diseases such as diabetes, cardiovascular diseases, cancer, degenerative diseases, ischemia, and anemia [8]. Currently, the available drug in treating inflammatory disorders is often not successful, lacking availability, high cost, and causes of undesirable side effects [9, 10]. Based on these, the necessity for exploring a better anti-inflammatory therapeutic agent is always in need.

Herbs' use as traditional medicine has a long history in treating various diseases, including inflammatory diseases. It is currently well known that many bioactive compounds derived from natural products play an essential role in a wide range of therapeutic effects [11]. The World Health Organization (WHO) recognizes the vital role of traditional medicines and continues to support the integration of conventional medicine into each country's health system [12].

G. inodorum is one of the local Thai vegetables belonging to the family Asclepiadaceae. It is found ubiquitously in Southeastern Asia, including Thailand, especially in the northern region. In Thailand, its local name is "Phak chin da" or "Phak chiang da." It has been known to have therapeutic effects in curing certain diseases, including diabetes mellitus, rheumatic arthritis, and gout. The literature survey reported that the leaves of *G. inodorum* had many phytochemical compounds such as phenolics, flavonoids, terpenoids, and glycoside [13, 14]. Moreover, its antioxidant, antiadipogenesis, antidiabetic, and hypoglycemic effects were also reported [14–16]. Therefore, the phytochemical constituents presented in *G. inodorum* may contribute to its biological activity. Numerous studies exhibited that the phytochemical compounds, especially flavonoids and phenolic content, had contributed to the redox-modulating properties of natural compounds, which had also been shown to modulate the inflammatory response virtually [15–17]. Along this line, it is possible that *G. inodorum* may exert a beneficial effect on alleviating intracellular ROS and inflammation. However, to the best of our knowledge, this plant's antioxidant and anti-inflammatory activities have not earlier been reported, especially for the research study in cell-based assays.

Fourier-transform infrared spectroscopy (FTIR) is an analytical technique widely applied for studying the vibrational fingerprint for organic compounds [17]. This technique was previously applied to study biomedical research to investigate biomolecule profiles (lipid, protein, nucleic acids, and carbohydrate) in various biological samples without the need for probe molecules [18–20]. Synchrotron light is exceptionally bright. When a synchrotron light (SR) source, FTIR spectroscopy, and microscopy are combined together, it is called "Synchrotron radiation-based FTIR microspectroscopy (SR-FTIR)." This technique takes advantage of synchrotron light brightness, making it possible to record high-quality spectra and explore the biochemical changes within biological samples' microstructures without destruction's inherent structures of its [21].

The present study is aimed at investigating the anti-inflammatory and the antioxidant effect of GIE on LPS plus IFN-γ-induced RAW264.7 cells. The SR-FTIR was applied to detect biomolecule changes in RAW264.7 cells induced by LPS plus IFN-γ and their response to GIE treatment.

2. Materials and Methods

2.1. Preparation of GIE. *G. inodorum* (dried leaves) was purchased from commercial products (Chiangda organic company garden, Chiangmai, Thailand). The voucher specimens were deposited at the botanical garden of Suranaree University of Technology (SUT) Herbarium and authenticated by Dr. Santi Wattatana, a lecturer and a plant biologist at the Institute of Science, SUT, Thailand. The plant extractions were conducted following the method of Tiamyom et al. [14]. Briefly, the dried powder of *G. inodorum* was soaked in 95% ethanol with a ratio of 1 : 3 (g : mL) at room temperature for 7 days. The pooled extract was filtered through Whatman No. 1 filter paper. The ethanolic extract was concentrated using a vacuum rotary evaporator at 50°C and lyophilized to obtain the powder of GIE. The crude extract was stored at -20°C till use in subsequent experiments. GIE was dissolved in dimethyl sulfoxide (DMSO) and diluted to 0.1% (*v/v*) in the cell culture medium.

2.2. Identification of Phytochemical Constituents of GIE Gas Chromatography-Mass Spectrometry (GC-MS) Analysis. GC-MS analysis of GIE was performed using a Bruker 450-GC/Bruker 320-MS equipped with Rtx-5MS fused silica capillary column (30 m length × 250 μm diameter × 0.25 μm film thickness). For GC-MS detection, an electron ionization system was operated in the electron impact mode with ionization energy of 70 eV. The injector temperature was maintained at 250°C, and the ion-source temperature was 200°C. The oven temperature was programmed from 110°C (2 min), with an increase of 10°C/min to 200°C (3 min), then 5°C/min to 280°C, ending with a 20 min isothermal at 280°C. The MS scan range was 45-500 atomic mass units (amu), and helium was used as the carrier gas with a flow rate of 1.0 mL/min. The chemical components were identified by matching their mass spectra with those recorded in the NIST mass spectral library 2008.

2.3. Ferric Reducing/Antioxidant Power (FRAP) Assay. The ferric reducing capacity of GIE was determined by using the colorimetric method as described by Rupasinghe et al. [22]. Briefly, 20 μL of each of the samples and 180 μL of

FRAP reagent (300 mM acetate buffer (pH 3.6), 10 mM 2, 4, 6-tripyridyl-s-triazine (TPTZ), and 20 mM $FeCl_3 \bullet 6H_2O$ solution) were mixed in a 96-well plate for 6 min. The absorbance was recorded at 595 nm using a microplate reader (Bio-Rad Laboratories, Inc., Hercules, CA, USA). The different concentrations of Trolox (Cat. No. 238813, Sigma-Aldrich, St. Louis, USA) and vitamin C (Cat. No. 95210, Fluka Chemie GmbH, Buchs, Switzerland) were used to develop the standard calibration curve. FRAP values were expressed as a milligram of Trolox equivalent antioxidant capacity (TREA) or vitamin C equivalent antioxidant capacity (VCEA) per gram of dry extract.

2.4. 2,2-Diphenyl-1-Picryl-Hydrazyl (DPPH) Radical-Scavenging Activity Assay. The ability of GIE to scavenge the DPPH radical was estimated according to the method of Yang et al. [23]. Briefly, an aliquot of 100 μL of the sample at different concentrations was added to 100 μL of 0.2 mM DPPH solution (Cat. No. D9132, Sigma-Aldrich, St. Louis, USA) in a 96-well plate. The reaction mixture was kept in the dark for 15 min, and the absorbance was measured at 517 nm using a microplate reader (Bio-Rad Laboratories, Inc., Hercules, CA, USA). The positive standards (Trolox and vitamin C) were prepared using the same procedure. A lesser absorbance rate demonstrated higher radical scavenging activity. The percentage inhibition of free radical was calculated using the following equation: %Inhibition = $[(A_{control} - A_{sample})/A_{control}] \times 100$. The sample concentration providing 50% inhibition (IC_{50}) was determined from a dose-response curve using linear regression analysis.

2.5. Cell Culture. The murine macrophage cell line RAW264.7 (CLS Cell Lines Service GmbH., Eppelheim, Germany) was cultured in RPMI-1640 medium (Cat. No. 1IVG1-31800022) supplemented with 10% heat-inactivated fetal bovine serum (FBS, Cat. No. 1IVG7-10270-106) and 100 U/mL penicillin-streptomycin (Cat. No. 1IVG7-15140-122) (GIBCO, Grand Island, NY, USA). Cells were maintained at 37°C in 95% humidified with 5% of the CO_2 atmosphere.

2.6. Measurement of Cell Proliferation by the 3-(4,5-Dimethylthiazol-2-yl)-2,5-Diphenyl-Tetrazolium Bromide (MTT) Assay. The effect of GIE on cell viability was evaluated by using a tetrazolium dye colorimetric assay as described by Tiamyom et al. [14] and Dunkhunthod et al. [24]. Briefly, RAW264.7 cells were seeded in a 96-well plate (2×10^4 cells/well) and cultured for 24 h. Cells were treated with different concentrations of GIE for 24 h. Following treatment, the culture medium was removed, the MTT solution (0.5 mg/mL) (Cat. No. M6494, Invitrogen, Carlsbad, CA, USA) was added and further incubated at 37°C for 4 h. Subsequently, 150 μL DMSO was added to dissolve formazan crystal formed by viable cells, and absorbance was measured at 540 nm with a microplate spectrophotometer (Bio-Rad Laboratories, Inc., Hercules, CA, USA).

2.7. Detection of Intracellular ROS by $2',7'$-Dichlorofluorescein-Diacetate (DCFH-DA) Assay. Relative changes of intracellular ROS in RAW264.7 cells were monitored using the fluorescent probe DCFH-DA (Cat. No.

D6883, Sigma-Aldrich, St. Louis, USA) as previously described by Sittisart and Chitsomboon [25]. Briefly, RAW264.7 cells were seeded onto a 96-well black plate at 2.0×10^4 cells/well and cultured for 24 h. After removing the medium, the cells were pretreated with GIE at the concentration of 50, 100, 200, or 300 μg/mL or a selective ROS scavenger, N-acetyl-cysteine 3 mM (NAC, Cat. No. A9165, Sigma-Aldrich, St. Louis, USA) for 3 h prior to exposing them to 1 μg/mL lipopolysaccharide (LPS) (LPS from *Escherichia coli* O111:B4, Cat. No. L2630, Sigma-Aldrich, St. Louis, USA) plus 10 ng/mL IFN-γ (Cat. No. 200-16, Shenandoah Biotechnology Inc., Warwick, PA, USA) for 24 h. After removing the medium and washing the cells with PBS twice, 20 μM DCFH-DA in Hank's Balanced Salt Solution (HBSS, Cat. No. TFS-CB-14175095, GIBCO, Grand Island, NY, USA) was then added, and the cells were incubated for 30 min at 37°C. The cells were washed twice with phosphate-buffered saline (PBS), and fluorescence intensity was measured using a Gemini EM fluorescence microplate reader (Molecular Devices, Sunnyvale, CA, USA) with an excitation wavelength of 485 nm and an emission wavelength of 535 nm. Data were expressed as the percentage of $2'$-$7'$-dichlorofluorescein (DCF) fluorescence intensity that was calculated according to the following formula: DCF fluorescence intensity (%) = (DCF fluorescence intensity$_{test group}$/DCF fluorescence intensity$_{control group}$) $\times$ 100.

2.8. Cell Treatment. The RAW 264.7 cells (6×10^5 cells/well) were seeded in a 6-well plate and cultured for 24 h. The cells were pretreated with GIE at the concentration of 50, 100, 200, or 300 μg/mL or 1 μM dexamethasone (DEX, Cat. No. API-04, G Bioscience, St. Louis, MO, USA) or 300 μg/mL of vitamin E (Vit.E, Cat. No. 95240, Fluka Chemie GmbH, Buchs, Switzerland) for 3 h prior to exposing them to 1 μg/mL LPS plus 10 ng/mL IFN-γ for 24 h.

2.9. Observation of Morphological Changes by Hematoxylin Staining. The phenotype feature of RAW264.7 cells was observed by staining with hematoxylin solution described by Dunkhunthod et al. [24] and visualized under the inverted fluorescence microscope (Olympus Corporation, Shinjuku, TYO, Japan).

2.10. Determination of NO by Griess Reagents. After treatment, the culture supernatants were collected for analysis of NO using Griess reagents. The accumulation of nitrite in culture supernatants as an indicator of NO production by RAW264.7 cells was evaluated using Griess reagent (Cat. No. 109023, Merck KGaA, Darmstadt, Germany) as described by Sittisart and Chitsomboon [25]. The amount of nitrite in the samples was calculated using the linear sodium nitrite calibration curves at a concentration range of 2.5-100 μM.

2.11. Determination of Proinflammatory Cytokines (IL-6 and TNF-α) and Anti-inflammatory Cytokines (IL-10) by ELISA. After treatment, the supernatants containing antigens were collected. The levels of IL-6, TNF-α, and IL-10 were quantified by DuoSet® ELISA Kits (IL-6; Cat. No. DY406-05, TNF-α; Cat. No. DY410-05, and IL-10; Cat. No. DY417-05,

R & D systems Inc., Minneapolis, MN, USA) according to the manufacturer's instructions. The *optical density* of each well was measured at 450 nm with a microplate reader (Bio-Rad Laboratories, Inc., Hercules, CA, USA). The number of cytokines in the samples was calculated using standard cytokine linear calibration curves at indicated concentration ranges.

2.12. Detection of mRNA Expression by Quantitative Real-Time Polymerase Chain Reaction (qRT-PCR). To determine the level of mRNA expression of inflammatory genes (iNOS and COX-2) and antiantioxidant genes, including SOD2, glutathione S-transferase pi 1 (GSTP1), NAD(P)H quinone dehydrogenase 1 (NQO1), cysteine ligase catalytic subunit (GCLC), and glutamate-cysteine ligase regulatory subunit (GCLM) in RAW264.7 macrophage cells after treating with GIE. Total RNA was isolated using TRIzol reagent (Cat. No. 15-596-026, Invitrogen, Carlsbad, CA, USA), and $2\,\mu g$ of total RNA was reverse transcribed to single-stranded cDNA using the SuperScript VILO cDNA Synthesis Kit (Cat. No. 11754-050, Invitrogen™, California, USA) at 42°C for 1 h. qPCR was performed in a LightCycler® 480 Real-Time PCR System (Roche Diagnostics, Mannheim, Germany) using SYBR green master mix. The PCR was performed in a final volume of $20\,\mu L$ containing $1\,\mu L$ of primer mixture ($10\,\mu M$), $10\,\mu L$ of 2X SYBR Green Master Mix (Cat. No. 04707516001, Roche Diagnostics, Mannheim, Germany), $5\,\mu L$ of cDNA template ($5\,\mu g$), and $4\,\mu L$ of nuclease-free distilled water. Real-time PCR cycles included initial denaturation at 95°C for 5 min, 95°C for 10 s, annealing at 60°C for 20 s, and extension at 72°C for 30 s through 40 cycles. The specificity of each of the PCR products was confirmed by melting curve analysis. The fold change in mRNA expression was calculated by comparing the GAPDH normalized threshold cycle numbers (Ct) in the untreated- and GIE treated-LPS plus IFN-γ-induced cells compared to the uninduced cells using the $2^{-\Delta\Delta Ct}$ method. Triplicate wells were run for each experiment, and two independent experiments were performed. The primer sequences designed for qRT-PCR analysis are listed in Table 1.

2.13. Western Blotting Analysis. The expression of NF-κB p65 and p-NF-κB p65 in RAW264.7 macrophage cells after treating with GIE for 24 h was examined. After incubation, the cells were washed three times with PBS and placed in $150\,\mu L$ of ice-cold lysis buffer (1 mL RIPA buffer supplemented with 2 mM phenylmethylsulfonyl fluoride (PMSF), $2\,\mu M$ leupeptin, and $1\,\mu M$ E-64) for 20 min. The disrupted cells were then transferred to microcentrifuge tubes and centrifuged at 14,000 g at 4°C for 30 min. The supernatant was collected, and the protein concentration of cell lysate was estimated by the Lowry method [26]. Thirty micrograms of cellular proteins were separated by sodium dodecyl sulfate-polyacrylamide gel electrophoresis (SDS-PAGE) using 10% polyacrylamide gels (125 volts, 120 min). The proteins in the gel were then transferred onto a nitrocellulose membrane (Amersham, Pittsburgh, PA, USA) at 80 volts for 1 h. The membrane was blocked with 5% bovine serum albumin (BSA) in 0.1% Tween 20 in a PBS buffer (0.1% PBST) at room temperature for 1 h. The membranes were then incubated

with a 1 : 1,000 dilution of the mouse monoclonal anti-NF-κB p65 antibody (F-6, Cat. No. sc-8008), anti-p-NF-κB p65 (27.Ser 536, Cat. No. sc136548), and α-tubulin (B-7, Cat. No. sc-5286) (Santa Cruz Biotechnology, Inc., Dallas, TX, USA) at 4°C overnight. After extensive washing with 0.1% PBST, the membranes were incubated with a 1 : 5,000 dilution of the secondary antibody mouse IgGκ light chain binding protein conjugated to horseradish peroxidase (m-IgGκ BP-HRP, Cat. No. sc-516102, Santa Cruz Biotechnology, Inc., Dallas, TX, USA) at room temperature for 1 h. The membranes were washed three times for 5 min each time, with 0.1% PBST. The membranes were incubated for 3 min in SuperSignal™ West Pico Chemiluminescent Substrate (Cat. No. 34079, Thermo Scientific, Waltham, MA, USA) and exposed to film. The relative expression of NF-κB p65 and p-NF-κB p65 proteins was quantified densitometrical using the software image J. The α-tubulin was used as a housekeeping protein.

2.14. Immunofluorescence Staining. As a marker of NF-κB activation, the NF-κB p65 subunit's nuclear translocation was visualized in RAW264.7 cells by immunofluorescence microscopy. Cells were seeded at a density of 6×10^4 cells/well in an 8-well cell culture slide. After 24 h of incubation, cells were pretreated with $300\,\mu g$/mL GIE or $1\,\mu M$ of DEX for 3 h. Then, cells were coincubated with $1\,\mu g$/mL LPS +10 ng/mL IFN-γ for another 24 h. After incubation, cells were fixed with 4% paraformaldehyde for 15 min and then permeabilized with 0.1%Triton-X100 for 10 min at room temperature. After washing with PBS, the samples were blocked in 0.1% PBST containing 4% BSA and then incubated overnight at 4°C with the mouse monoclonal anti-NF-κB p65 antibody (F-6, Cat. No. sc-8008, Santa Cruz Biotechnology, Inc., Dallas, TX, USA) diluted 1 : 200 in 0.1% PBST containing 1% BSA. After washing with 0.1% PBST, each reaction was followed by incubation for 1 h with anti-mouse conjugated to Alexa 488-conjugated goat anti-mouse IgG (Cat. No. ab150113, Abcam, Cambridge, UK) diluted 1 : 250 in 0.1% PBST containing 1% BSA. After washing with 0.1% PBST, the cells were incubated with 10 mg/mL Hoechst 33258 diluted 1 : 2000 in 0.1% PBST (Cat. No. H3569, Invitrogen, Waltham, MA, USA) for 10 min at room temperature and then washed with 0.1% PBST. Slides were mounted with Bio Mount HM mounting medium (Cat. No. 05-BMHM100, Bio-Optica Milano S.p.a., Milano, Italy). Images of the fixed RAW264.7 cells were taken with confocal microscopy (Nikon, Melville, NY, USA).

2.15. Detection of Biomolecule Changing by SR-FTIR Microspectroscopy. FTIR experiments were conducted using a spectroscopy facility at the Synchrotron Light Research Institute (Public Organization), Nakhon Ratchasima, Thailand. Sample preparation was performed, as previously described by Dunkhunthod et al. [24]. FTIR spectra were acquired in transmission mode with a Vertex 70 FTIR spectrometer coupled with an IR microscope Hyperion 2000 (Bruker Optics, Ettlingen, Germany), using synchrotron radiation as an IR source. The microscope was equipped with a 64×64 element MCT, FPA detector, which allowed

TABLE 1: Oligomeric nucleotide primer sequence of qRT-PCR.

Gene	Forward primer (5′-3′)	Reverse primer (5′-3′)
iNOS	CAGCACAGGAAATGTTTCAGC	TAGCCAGCGTACCGGATGA
COX-2	TTTGGTCTGGTGCCTGGTC	CTGCTGGTTTGGAATAGTTGCTC
IL-6	CTGCAAGAGACTTCCATCCAG	AGTGGTATAGACAGGTCTGTTGG
TNF-α	CAGGCGGTGCCTATGTCTC	CGATCACCCCGAAGTTCAGTAG
SOD2	TTAACGCGCAGATCATGCA	GGTGGCGTTGAGATTGTTCA
GSTP1	TGGGCATCTGAAGCCTTTTG	GATCTGGTCACCCACGATGAA
NQO1	TTCTGTGGCTTCCAGGTCTT	AGGCTGCTTGGAGCAAAATA
GCLC	GATGATGCCAACGAGTCTGA	GACAGCGGAATGAGGAAGTC
GCLM	CTGACATTGAAGCCCAGGAT	GTTCCAGACAACAGCAGGTC
GAPDH	AACGACCCCTTCATTGAC	TCCACGACATACTCAGCAC

simultaneous spectral data acquisition with a 36× objective. The measurements were performed using an aperture size of $10\,\mu m \times 10\,\mu m$ with a spectral resolution of $4\,cm^{-1}$, with 64 scans coadded. FTIR spectrum was recorded within a spectral range of $4000\text{-}600\,cm^{-1}$ using OPUS software (Bruker Optics Ltd., Ettlingen, Germany).

Unsupervised explorative multivariate data analysis by Principal Component Analysis (PCA) was conducted using variables within a spectral range of $3,000\text{-}2,800\,cm^{-1}$ and $1,800\text{-}950\,cm^{-1}$. Data manipulations were processed following the method of Tiamyom et al. [14] with slight modification. Briefly, the data were preprocessed by taking the second derivative using the Savitzky-Golay algorithm (with 15 points of smoothing), followed by normalization with extended multiplicative signal correction (EMSC) (Unscrambler® X software version 10.5, CAMO Software AS, Oslo, Norway). The outcome of the analysis could be presented as 2D score plots and loading plots. The integrated peak areas of the second derivative FTIR spectra were calculated using OPUS 7.2 software (Bruker Optics, Ettlingen, Germany) in the lipid regions ($3000\text{-}2800\,cm^{-1}$), nucleic acids regions ($1257\text{-}1204\,cm^{-1}$ and $1125\text{-}1074\,cm^{-1}$), and glycogen and other carbohydrates regions ($1181\text{-}1164\,cm^{-1}$ and $1063\text{-}1032\,cm^{-1}$). The band area ratio of amide I to amide II was obtained by calculating the ratio of the amide I ($1670\text{-}1627\,cm^{-1}$) area to the area under the amide II ($1558\text{-}1505\,cm^{-1}$) regions.

2.16. Statistical Analysis. All data are expressed as the means ± S.D. from at least three independent experiments. The statistical significances (Statistical Package for the Social Sciences, version 19) were determined by performing a one-way analysis of variance (ANOVA). Tukey's test was used as a *post hoc* test. $p < 0.05$ was considered as statistically significant difference, which was indicated by the different superscript letters.

3. Results and Discussion

3.1. GC-MS Analysis of Volatile Oil Constituents of GIE. In this study, the phytochemical constituents of GIE were analyzed. GC-MS analysis in GIE reported about 16 compounds (as shown in Table 2). The major prevailing compounds were

linolenic acid (24.91%), n-Hexadecanoic acid (Palmitic acid) (16.98%), and Methylparaben (11.58%). Besides, it also presented the other chemical compounds, which are known to exhibit important pharmacological activity, in particular, anti-inflammatory and antioxidant activities such as phytol [27, 28], squalene [29], γ-tocopherol, dl-α-tocopherol [30, 31], and stigmasterol [32, 33].

Phytol, diterpene alcohol, has been reported to have remarkable anti-inflammatory activity by reducing carrageenan-induced paw edema and inhibiting the recruitment of total leukocytes and neutrophils, a decrease in IL-1β and TNF-α levels and oxidative stress [27]. Jeong [28] also reported that phytol suppressed H_2O_2-induced inflammation, as indicated by the reduced expression of the mRNA levels of TNF-α, IL-6, IL-8, and COX-2. Squalene, a natural lipid belonging to the terpenoid family, significantly inhibited the secretion of proinflammatory cytokines (TNF-α, IL-1β, IL-6, and IFN-γ), proinflammatory enzymes (iNOS, COX-2, and myeloperoxidase (MPO)), and enhanced expression levels of anti-inflammatory enzymes (heme oxygenase-1 (HO-1)) and transcription factors (Nrf2 and PPARγ) in overactivation of neutrophils, monocytes, and macrophages [29]. γ-Tocopherol and dl-α-tocopherol exhibited anti-inflammatory activity *in vitro* and *in vivo*, whereas the combination of γ- and α-tocopherols seems to be more potent than supplementation with α-tocopherols alone [30]. These results provide evidence that GIE is a source of antioxidants and anti-inflammatory agents, which could have beneficial effects on treating inflammation-related diseases. However, further studies are needed to clarify pharmacological properties.

3.2. Antioxidant Capacity of GIE. Antioxidants can act via several pathways. Therefore, to investigate the antioxidant activity of the GIE, we estimated their reducing antioxidant power and free radical scavenging by using the FRAP and DPPH radical scavenging assays, respectively. Trolox and vitamin C were used as standard antioxidant compounds. As shown in Table 3, GIE exhibited antioxidant activity due to its ability to reduce ferric ion (Fe^{3+}) to ferrous ion (Fe^{2+}) by $24.00 \pm 0.69\,\mu g$ VCEA/mg of dry extract and $28.06 \pm 0.78\,\mu g$ TREA/mg of dry extract. GIE at a concentration of $406.59 \pm 0.11\,\mu g/mL$ displayed the ability to scavenge DPPH

Table 2: GC-MS analysis of GIE.

No.	Peak name	Formula	Molecular weight (g/mol)	RT (min)	%Area
1	2,3-Dihydrobenzofuran	C_8H_8O	120.15	4.74	3.76
2	2-Methoxy-5-vinylphenol	$C_9H_{10}O_2$	150.17	5.89	1.42
3	Methylparaben	$C_8H_8O_3$	152.15	7.71	11.58
4	Tetradecanoic acid	$C_{14}H_{28}O_2$	228.37	11.09	2.86
5	n-Hexadecanoic acid	$C_{16}H_{32}O_2$	256.43	14.06	16.98
6	Phytol	$C_{20}H_{40}O$	128.17	16.73	5.96
7	Linolenic acid	$C_{18}H_{30}O_2$	278.43	17.42	24.91
8	Octadecanoic acid	$C_{18}H_{36}O_2$	284.48	17.70	2.04
9	Glycerol beta-palmitate	$C_{19}H_{38}O_4$	330.50	23.60	5.54
10	Beta-Monolinolein	$C_{21}H_{38}O_4$	354.52	26.36	6.31
11	9,12,15-Octadecatrienal	$C_{18}H_{30}O$	262.43	26.51	9.50
12	Squalene	$C_{30}H_{50}$	410.72	28.27	0.93
13	γ-Tocopherol	$C_{28}H_{48}O_2$	416.68	31.37	1.80
14	dl-α-Tocopherol	$C_{29}H_{50}O_2$	430.72	33.04	2.33
15	Stigmasterol	$C_{29}H_{48}O$	412.69	35.67	2.50
16	Olean-12-ene-3,28-diol, (3beta)-	$C_{30}H_{50}O_2$	442.73	46.98	1.57

Table 3: The FRAP and DPPH scavenging activities of GIE and standard compounds.

| Sample | FRAP values | | DPPH scavenging activity (IC$_{50}$) μg/mL |
	(μg VCEA/mg of dry extract)	(μg TREA/mg of dry extract)	
GIE	24.00 ± 0.69	28.06 ± 0.78	406.59 ± 0.11[c]
Vitamin C	—	—	44.57 ± 0.59[a]
Trolox	—	—	67.19 ± 4.82[b]

Values are mean ± S.D. ($n = 3$) and are representative of three independent experiments with similar results. One-way ANOVA performed the comparison, and Tukey was used as a *post hoc* test. The degree of significance was denoted with different letters for the comparison between sample groups. $p < 0.05$ was considered as statistically significant.

radical at 50% (IC$_{50}$). In contrast, the positive antioxidant controls, vitamin C, and Trolox exhibited the IC$_{50}$ values of approximately 44.57 ± 0.59 μg/mL and 67.19 ± 4.82 μg/mL, respectively.

Based on GC-MS analysis (Table 2), GIE contained many bioactive compounds such as phytol, squalene, γ-tocopherol, dl-α-tocopherol, and stigmasterol, which were reported to have antioxidant activity. Previous studies demonstrated that the phytochemical screening of GIE indicated the presence of phenolic, flavonoids, terpenoids, and glycoside [14, 15]. Numerous studies have shown that plant products' antioxidant capacity is related to their phenolic and flavonoid contents [34–36]. The synergistic effect of some substances present in GIE had been reported the antioxidant activity. Previous studies showed that the combination of squalene and α-tocopherol displayed a synergistic effect by reducing the rate of oxidation in a crocin bleaching assay where squalene might act as a competitive compound to α-tocopherol [37]. The sunflower seed oil containing total polyphenols and α-tocopherol had a positive K_a/K_c ratio of rate constants

for antioxidant and crocin value antioxidant activity. It is possible that the synergistic effect occurs between α-tocopherol and total polyphenols [38]. Besides, the presence of α-, β-, γ-tocopherol in sunflower seed oil may contribute to the oil resistance to oxidation [38, 39]. Therefore, the presence of squalene, α-tocopherol, γ-tocopherol, and phenolic in GIE may provide synergistic effects on antioxidant activity. However, it is also essential to further confirm whether the antioxidant activity of the combination of α-tocopherol plus squalene or other volatile compounds in GIE is synergistic. Moreover, the synergistic action of such compounds from plants had been calculated by the combination index (CI) [40–42].

3.3. Cytotoxic Effects of GIE on RAW264.7 Cells. The cytotoxicity of GIE was evaluated by MTT assay. The RAW264.7 cells were treated with various concentrations of the GIE, ranging from 100 to 500 μg/mL for 24 h. As shown in Figure 1(a), the results demonstrated that GIE at the concentration ranges of 100-400 μg/mL did not show a toxic effect on RAW264.7 cells ($p > 0.05$). At the highest tested concentration (500 μg/mL), the number of living RAW264.7 cells decreased by up to 71.50% compared to the control group. Based on these results, the nontoxic concentration ranges of GIE (50, 100, 200, and 300 μg/mL) were selected for treating cells in further investigation.

3.4. GIE Attenuated the Intracellular ROS Generation and Increased SOD2 mRNA Expression in LPS plus IFN-γ-Induced RAW264.7 Cells. ROS generated by inflammatory cells also stimulates pathways that lead to the amplification of inflammation. ROS-induced kinase activation leads to the activation of transcription factors, which triggers the generation of proinflammatory cytokines and chemokine. Therefore, it is possible that the inflammation would be controlled by suppressing intracellular ROS production.
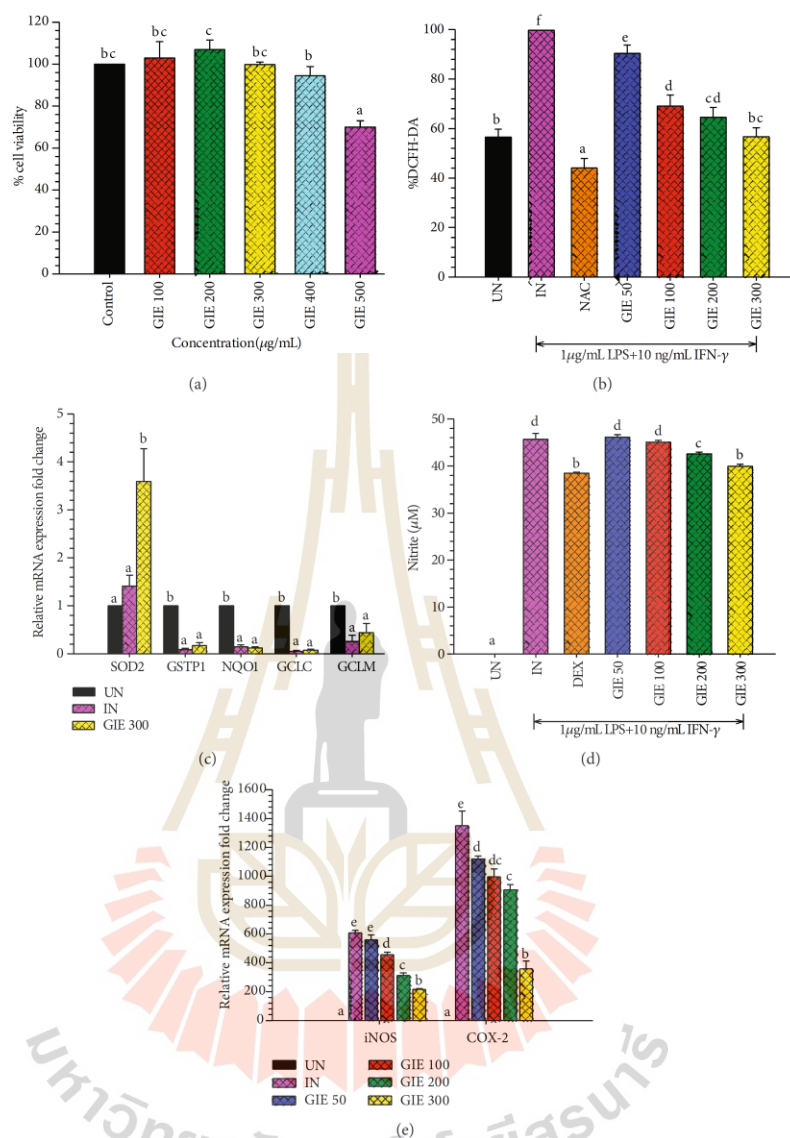
Figure 1: (a) Cytotoxic effects of GIE on RAW264.7 cells. Cells were treated with different concentrations of GIE (100-500 μg/mL) for 24 h. MTT assay was used to determine cell viability. Values are expressed as a percentage of the control. (b) GIE attenuated the intracellular ROS production in LPS plus IFN-γ-induced RAW264.7 cells. The intracellular ROS levels are expressed as a percentage of the control. (c) The effects of GIE on antioxidant mRNA expression in LPS plus IFN-γ-induced RAW264.7 cells. (d) GIE suppressed NO production in LPS plus IFN-γ-induced RAW264.7 cells. Nitrite concentration was determined from a sodium nitrite standard curve, and the results are expressed as a concentration (μM) of nitrite in a culture medium. (e) The effects of GIE on COX-2 and iNOS mRNA expression in LPS plus IFN-γ-induced RAW264.7 cells. The data represent the mean ± S.D. of two independent experiments. Cells were pretreated with GIE, NAC, or DEX for 3 h and then coincubated with LPS plus IFN-γ for 24 h. UN: uninduced cells; IN: untreated LPS plus IFN-γ-induced cells; NAC: cells were pretreated with NAC at 3 mM; DEX: cells were pretreated with DEX at 1 μM; GIE (50, 100, 200, and 300): cells were pretreated with GIE at concentrations range of 50, 100, 200, and 300 μg/mL, respectively. One-way ANOVA performed the comparison, and Tukey was used as a *post hoc* test. The degree of significance was denoted with different letters for the comparison between sample groups. $p < 0.05$ was considered as statistically significant.

120

Antioxidants are proved that help to protect cells and tissue from damage caused by free radical molecules [43]. According to FRAP and DPPH results, the possibility of GIE to scavenge intracellular ROS formation was further evaluated using the cell-base assay, DCFH-DA model. LPS and IFN-γ were chosen as an inflammatory inducing molecule, which can trigger the generation of a series of inflammatory mediators and reactive oxygen. NAC, as a nutritional supplement, was applied as the positive antioxidant control. The cells were pretreated with various concentrations of GIE (50, 100, 200, and 300 μg/mL) for 3 h and then coincubated with LPS plus IFN-γ for another 24 h. As shown in Figure 1(b), while LPS plus IFN-γ increased ROS formation in RAW264.7 cells (by 1.76-fold compared to uninduced cells), pretreated cells with GIE significantly reduced ROS generation in a concentration-dependent manner. Surprisingly, the highest concentration of GIE showed the efficacy of decreasing the intracellular ROS level to $56.72 \pm 3.62\%$, which was a similar level of the basal intracellular ROS production ($56.56 \pm 3.18\%$) in uninduced cells (UN). As expected, the positive antioxidant compound, NAC, possessed a potent free radical scavenging activity by decreasing the intracellular ROS level to $44.07 \pm 3.82\%$ compared to untreated LPS plus IFN-γ-induced cells. These results lead us to believe that GIE could inhibit ROS production by scavenging free radicals in cells, which is confirmed by the results of the FRAP and DPPH assay (Table 3). Our study was in agreement with other studies, which reported that *G. inodorum* displayed the antioxidant activity measuring by various *in vitro* antioxidant assays [13, 44]. However, this is the first report of the study, proving the antioxidant effect of this plant in the cell-based assay. Next, the inhibitory effect of GIE on oxidative stress was investigated by measuring antioxidant enzyme mRNA expression in RAW264.7 cells induced by LPS plus IFN-γ. Following stimulation of the cells by LPS plus IFN-γ, SOD2 mRNA expression exhibited a slight increase, along with a significant decrease in GSTP1, NQO1, GCLC, and GCLM mRNA expression (Figure 1(c)). Treatment by 300 μg/mL GIE achieved a statistically significant increase in SOD2 mRNA expression in LPS plus IFN-γ-induced cells ($p < 0.05$). However, with concentrations of 300 μg/mL, there was no statistically significant difference in the mRNA expression of GSTP1, NQO1, GCLC, and GCLM compared to LPS plus IFN-γ-induced cells (IN) ($p > 0.05$). These results provide evidence that GIE inhibited ROS production by upregulating the expression of SOD2 mRNA levels in LPS plus IFN-γ-induced RAW264.7 cells.

ROS is considered to be a causal factor in inflammatory responses. Higher levels of ROS can cause toxicity or act as signaling molecules. The cellular levels of ROS are controlled by low molecular mass antioxidants and antioxidant enzymes. SOD2 is one of the primary cellular antioxidant enzymes, which catalyze the dismutation of superoxide anion (O_2^-) to oxygen and hydrogen peroxide (H_2O_2) [45]. SOD2 was actively expressed via the NF-κB pathway during the progression of inflammatory conditions. The intracellular SOD2 has a protective role by suppressing the nucleotide-binding oligomerization domain, leucine-rich repeat, and pyrin domain-containing (NLRP) inflammasome-caspase-

1-IL-1β axis under inflammatory conditions [46]. Superoxide dismutase (SOD) also acts as an anti-inflammatory due to its inhibitory effects on the release of lipid peroxidation-derived prostaglandins, thromboxane, and leukotrienes [47]. Therefore, GIE elevated the levels of SOD2 can be an effective therapeutic strategy in oxidative stress and inflammation.

3.5. GIE Suppressed the Production of NO and Attenuated iNOS and COX-2 mRNA Expression in LPS plus IFN-γ-Induced RAW264.7 Cells. NO is a reactive nitrogen species (RNS), which also plays essential biology roles, similar to ROS. NO is synthesized by activating macrophages involved in an immune and inflammatory response. Inhibition of NO production was usually used as the necessary pharmacological treatment of inflammation-related diseases. Therefore, in this study, we investigated whether GIE could modulate NO production in LPS plus IFN-γ-induced RAW264.7 cells and measured for NO production using the Griess assay. The anti-inflammatory agent, dexamethasone (DEX), was used as the reference drug. As shown in Figure 1(d), the results showed that LPS plus IFN-γ induced significantly increased NO production ($p < 0.05$), reaching $45.68 \pm 1.26 \mu$M in untreated LPS plus IFN-γ-induced cells (IN). GIE reduced NO production in a dose-dependent manner. Moreover, the extract at concentrations of 200 and 300 μg/mL significantly suppressed NO production compared to untreated LPS plus IFN-γ-induced cells (IN) ($p < 0.05$). The highest concentration of GIE at 300 μg/mL exhibited the NO suppression (12.62% of NO inhibition), approximately the same efficiency as the reference drug, DEX (15.80% of NO inhibition).

In the inflammatory response, NO and PGE$_2$ are synthesized by iNOS and COX-2, respectively [48]. To confirm if the suppression of NO production by GIE was related to change in iNOS as well as COX-2 mRNA levels, qRT-PCR was performed. Figure 1(e) showed that iNOS and COX-2 mRNA expression was increased in LPS plus IFN-γ-induced cells (IN). At the same time, pretreated GIE significantly decreased the expression of iNOS and COX-2 mRNA levels in a concentration-dependent manner ($p < 0.05$). The present study indicates that the suppressive effect of GIE on NO production is mediated through the inhibition of iNOS mRNA expression. Therefore, iNOS reduction leads to the lower of PGE$_2$ and COX-2 expression in activated macrophages with LPS. There is no doubt that LPS and IFN-γ also efficiently enhance COX-2 expression in RAW264.7 cells [49]. Our results demonstrate that GIE can exhibit anti-inflammatory activity by attenuating COX-2 mRNA expression. Thus, GIE might play essential roles in ameliorating inflammation by suppressing NO production and downregulation of iNOS and COX-2 mRNA expression.

3.6. GIE Suppressed Proinflammatory Cytokines (IL-6 and TNF-α), Proinflammatory mRNA Expression, and Slightly Increased Anti-inflammatory Cytokines (IL-10) in LPS plus IFN-γ-Induced RAW264.7 Cells. Inflammation is mediated by cytokines released from immune cells in response to pathogens' molecular components, such as the LPS of gram-negative bacteria. TNF-α in inflammatory processes is an essential proinflammatory mediator, leading to other
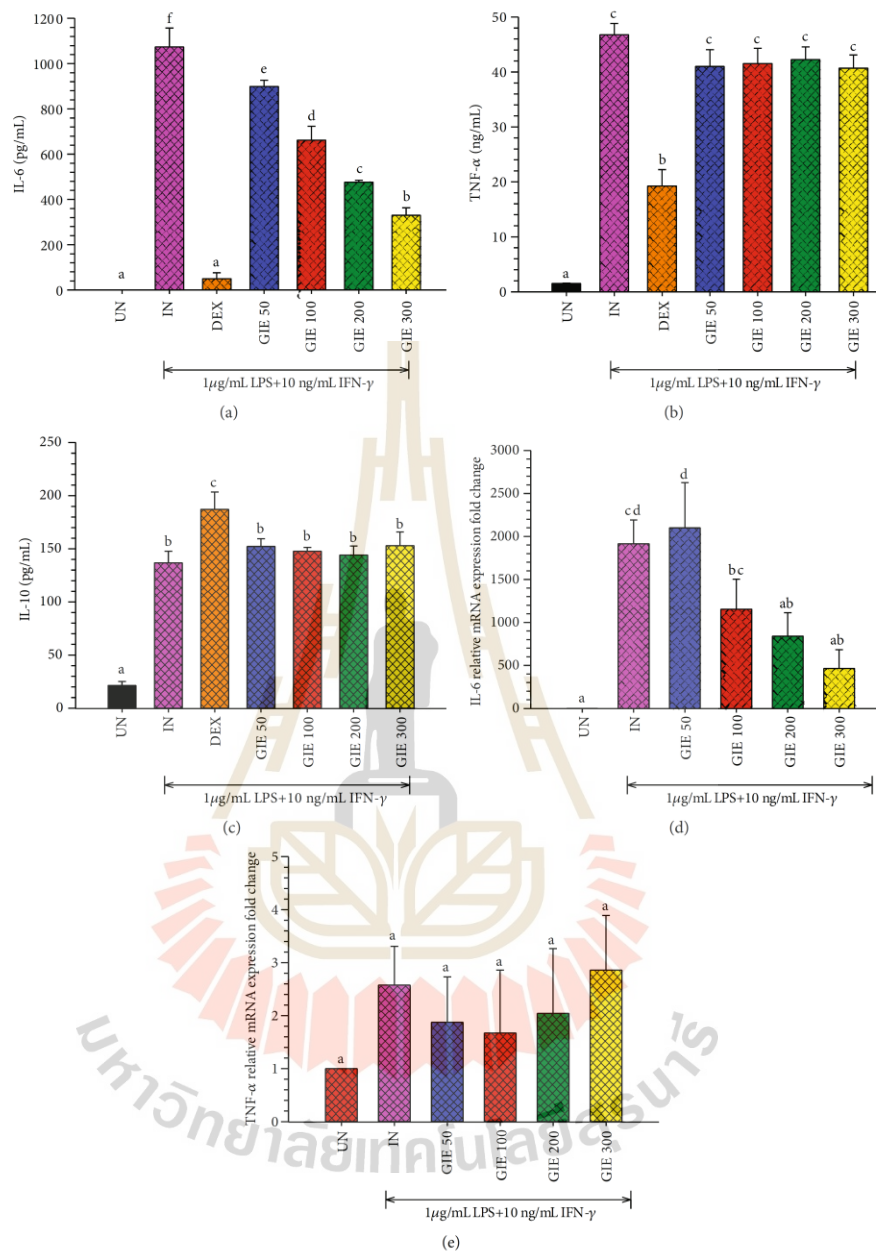
Figure 2: GIE suppressed the secretion of (a) proinflammatory cytokines IL-6, (b) TNF-α, and slightly increased (c) anti-inflammatory cytokines IL-10 secretion in LPS plus IFN-γ-induced RAW264.7 cells. The effects of GIE on (d) IL-6 and (e) TNF-α mRNA expression. Cells were pretreated with GIE or DEX for 3 h and then coincubated with LPS plus IFN-γ for 24 h. UN: uninduced cells; IN: untreated LPS plus IFN-γ-induced cells; DEX: cells were pretreated with DEX at 1 μM; GIE (50, 100, 200, and 300): cells were pretreated with GIE at concentrations range of 50, 100, 200, and 300 μg/mL, respectively. The data represent the mean ± S.D. of two independent experiments. One-way ANOVA performed the comparison, and Tukey was used as a *post hoc* test. The degree of significance was denoted with different letters for the comparison between sample groups. $p < 0.05$ was considered as statistically significant.

Figure 3: Effects of GIE on the morphology of LPS plus IFN-γ-induced RAW264.7 cells. Cells were stained with hematoxylin staining: (a) uninduced RAW264.7 cells, (b) untreated LPS plus IFN-γ-induced cells, (c) cells were pretreated with DEX at $1\,\mu$M, (d), (e), (f), and (g) cells were pretreated with GIE at concentrations range of 50, 100, 200, and $300\,\mu$g/mL, respectively (original magnification at $\times 600$, scale bar; $10\,\mu$m).

inflammatory molecular expressions as IL-6 and COX-2. However, IL-10 is a key anti-inflammatory cytokine with immunomodulatory effects, causing the inhibition of another proinflammatory cytokine such as TNF-α [50]. In order to confirm the anti-inflammatory activity of the GIE, the effects of the extract on proinflammatory cytokine (IL-6 and TNF-α) and anti-inflammatory cytokine (IL-10) production were evaluated in LPS plus IFN-γ-induced RAW264.7 cells by

FIGURE 4: Effects of GIE on the nuclear translocation of NF-κB p65 in LPS plus IFN-γ-induced RAW264.7 cells at 24 h. Cells were pretreated with GIE or DEX for 3 h and then coincubated with LPS plus IFN-γ for 24 h. The nuclear translocation of NF-κB p65 was detected using an immunofluorescence assay and visualized under confocal microscopy. The figure represents the cell morphology (bright field), the nuclear translocation of NF-κB p65 (green fluorescence), nucleus (blue fluorescence), and costaining (overlay green and blue fluorescence). Scale bar, 20 μm. UN: uninduced cells; IN: untreated LPS plus IFN-γ-induced cells; DEX: cells were pretreated with DEX at 1 μM; GIE300: cells were pretreated with GIE 300 μg/mL.

using ELISA. The results indicated that GIE at all tested-concentration significantly suppressed LPS plus IFN-γ-induced IL-6 production ($p < 0.05$; Figure 2(a)) and slightly decreased TNF-α production compared to untreated LPS plus IFN-γ-induced cells (IN) (Figure 2(b)). As expected, DEX (a reference drug) could also inhibit LPS plus IFN-γ-induced IL-6 and TNF-α production by 95.38% and 58.88%, respectively. Surprisingly, LPS plus IFN-γ induced the secretion of IL-10 about 6.5-fold compared to uninduced cells. DEX significantly increased the secretion of IL-10 level by almost 36.78% compared to untreated LPS plus IFN-γ-induced cells ($p < 0.05$; Figure 2(c)). While pretreated-GIE only showed a slight increase in IL-10 levels (around 5-10%) but no significant difference compared to untreated LPS plus IFN-γ-induced cells ($p > 0.05$). qRT-PCR was performed to investigate whether suppression of TNF-α and IL-6 production by GIE was related to a change in mRNA levels for both proinflammatory cytokines. Increasing concentrations of GIE produced a decrease in the order of IL-6 mRNA levels in LPS plus IFN-γ-induced cells (Figure 2(d)). However, GIE slightly decreased TNF-α mRNA levels compared to LPS plus IFN-γ-induced cells (Figure 2(e)). The profile of IL-6 and TNF-α suppression by GIE suggests that GIE acts more potent on IL-6 than TNF-α.

Base on GC-MS analysis, the volatile oil compounds presenting in GIE, including phytol, squalene, γ-tocopherol, dl-α-tocopherol, and stigmasterol, have been reported to have anti-inflammatory and antioxidant activities. Therefore, the anti-inflammatory effects of the GIE could simply rely on volatile oil components that may exert synergistic effects. This is the first study concerning the inhibitory activity against proinflammatory cytokines (IL-6 and TNF-α) in LPS plus IFN-γ-induced RAW264.7 cells. The secretion of proinflammatory cytokines, TNF-α and IL-6, is an important factor in upregulating the inflammatory process. The high levels of TNF-α and IL-6 play a critical role in acute and chronic inflammatory diseases; both cytokines are prime targets for intervention by anti-inflammatory therapeutic agents. Therefore, the development of anti-inflammatory substances, which can modulate proinflammatory mediators' production, is an efficient way to manage inflammatory conditions. These results provide evidence that GIE could be a source of anti-inflammatory agents, which may have a beneficial effect on treating inflammation-associated diseases.
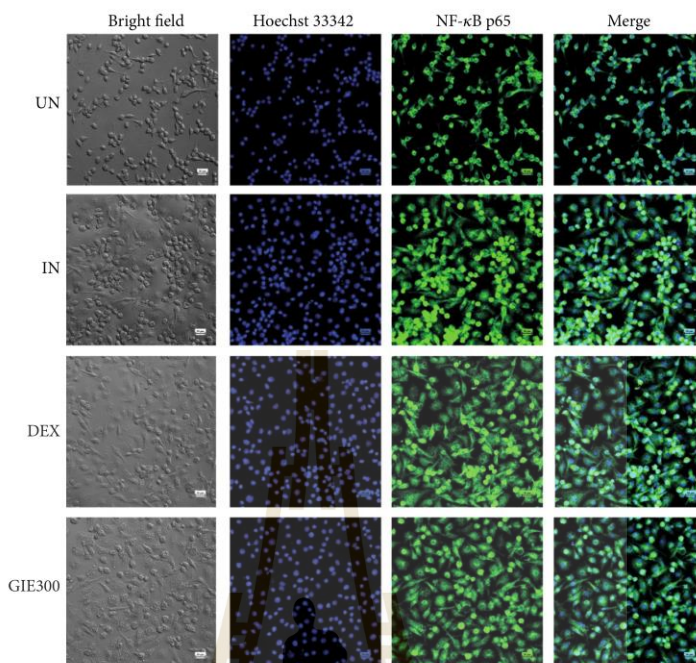
3.7. Effects of GIE on the Morphology of LPS plus IFN-γ-Induced RAW264.7 Cells. The morphological alteration in LPS plus IFN-γ-induced RAW264.7 cells in the presence or
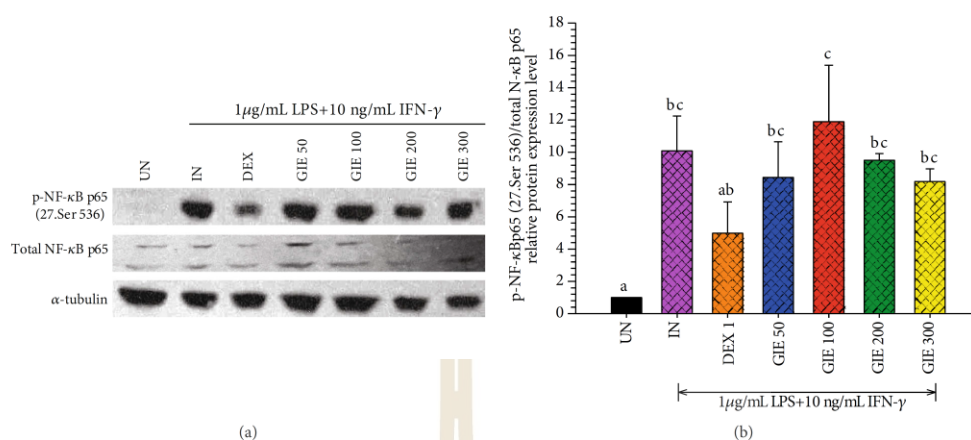
(a)

(b)

FIGURE 5: Effects of GIE on phosphorylation of NF-κB p65 induced by LPS plus IFN-γ in RAW264.7 cells. Cells were pretreated with GIE or DEX for 3 h and then coincubated with LPS plus IFN-γ for 24 h. The protein expression was analyzed by Western blotting. (a) The cellular proteins were used to detect the phosphorylated NF-κB p65 and total form of NF-κB with α-tubulin as a housekeeping control protein. (b) Mean densitometric values are expressed as bar charts. The data represent the mean ± S.D. of three independent experiments. One-way ANOVA performed the comparison, and Tukey was used as a *post hoc* test. The degree of significance was denoted with different letters for the comparison between sample groups. $p < 0.05$ was considered as statistically significant. UN: uninduced cells; IN: untreated LPS plus IFN-γ-induced cells; DEX: cells were pretreated with DEX at 1 μM; GIE300: cells were pretreated with GIE 300 μg/mL.

absence of GIE were also observed (as seen in Figures 3(a)–3(g)). The results demonstrated that LPS and IFN-γ caused cell morphology to change into a pseudopodia formation, spreading, and pancake-like shape within 24 h of stimulation (Figure 3(b)). The phenotypic polarization of macrophages allows the macrophage to engulf lipids, dead cells, other substances perceived as danger signals and secrete a large number of inflammatory molecules [51, 52]. In contrast, uninduced cells (UN) displayed a circular shape, a common form of RAW264.7 cells (Figure 3(a)). The pretreatment with GIE decreased the degree of cell spreading and pseudopodia formation, which was obviously observed in cells after pretreated with GIE 300 μg/mL (Figure 3(g)). Our results are in substantial agreement with a previous study of Kang et al. that the cotreatment of LPS with the crude methanol extract of *Citrus aurantium* L. reduces the level of cell spreading and pseudopodia formation by suppressing cell differentiation [53].

3.8. Effects of GIE on NF-κB p65 Nuclear Translocation and p-NFκB p65 (27.Ser 536) Protein Expression in LPS plus IFN-γ-Induced RAW264.7 Cells. Given that LPS plus IFN-γ-induced inflammation is through Toll-like receptor (TLR) signaling, NF-κB is activated and translocate into the nucleus to regulate the induced transcription of proinflammatory genes [54]. As a marker of NF-κB activation, the nuclear translocation of the NF-κB p65 was visualized in LPS plus IFN-γ-induced RAW264.7 cells by immunofluorescence confocal microscopy. As shown in Figure 4, LPS plus IFN-γ-induced RAW264.7 cells (IN) showed marked NF-κB p65 staining in the nuclei, while uninduced cells (UN) showed weaker nuclear NF-κB expression but stronger staining in the cyto-

plasm. GIE treatment (GIE300) attenuated LPS plus IFN-γ-induced nuclear translocation of NF-κB p65. Based on these findings, GIE can decrease the nuclear translocation of NF-κB, thus further inhibiting the expression of target inflammatory genes.

To further investigate whether GIE can regulate NF-κB signaling in LPS plus IFN-γ-induced RAW264.7 cells, the phosphorylation of NF-κB p65 was detected by Western blotting. Stimulation of the uninduced cells by LPS plus IFN-γ (IN) exhibited significantly higher phosphorylation of NF-κB p65 than uninduced cells (UN) ($p < 0.05$; Figures 5(a) and 5(b)). Pretreatment with 1 μM DEX or GIE showed a trend to reduce the phosphorylation of NF-κB p65 proteins, but no significant difference compared to LPS plus IFN-γ-induced cells (IN) ($p > 0.05$). This result suggests that GIE exhibits a slight inhibitory effect on the phosphorylation of NF-κB p65 to exert its anti-inflammatory effects.

In oxidative stress and anti-inflammation, enhancement of antioxidant gene expression plays an essential role in cell protection. It has been reported that superoxide dismutase (SOD) can modulate ROS-dependent signaling pathways during inflammatory responses [55]. The activation of Nrf2 antioxidant pathway prevents LPS-induced transcriptional upregulation of proinflammatory cytokines [56]. This research found that GIE increased the antioxidant gene expression, SOD2, and reduced NO and ROS production. Therefore, it is possible that the antioxidant properties of GIE could modulate the inflammation process caused by regulating the ROS levels.

3.9. Vitamin E Exhibited Anti-inflammatory Activities by Suppressing iNOS, COX-2, and IL-6 mRNA Expression in
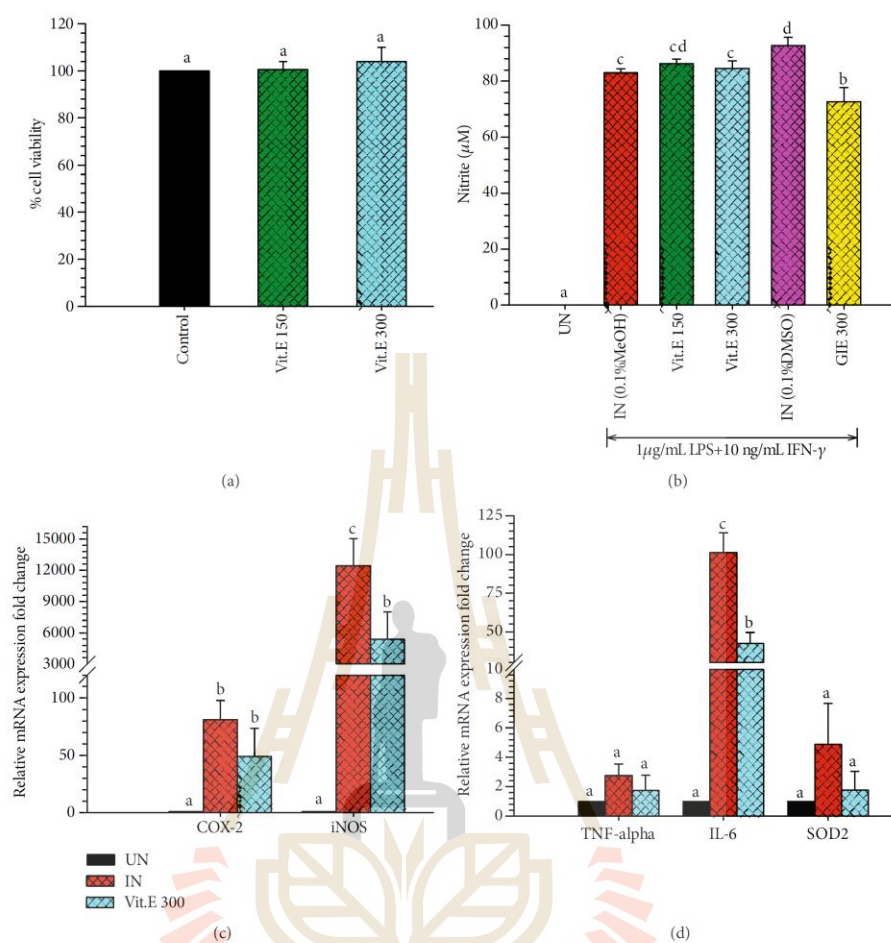
FIGURE 6: (a) Cytotoxic effects of Vit.E on RAW264.7 cells for 24 h. MTT assay was used to determine cell viability. Values are expressed as a percentage of the control. (b) The effect of Vit.E compared to GIE on NO production in LPS plus IFN-γ-induced RAW264.7 cells. Nitrite concentration was determined from a sodium nitrite standard curve, and the results are expressed as a concentration (μM) of nitrite in a culture medium. The data represent the mean ± S.D. of three independent experiments. (c) The effects of Vit.E on COX-2 and iNOS mRNA expression in LPS plus IFN-γ-induced RAW264.7 cells. (d) The effects of Vit.E on TNF-α, IL-6, and SOD2 mRNA expression in LPS plus IFN-γ-induced RAW264.7 cells. The data represent the mean ± S.D. of two independent experiments. Cells were pretreated with GIE or DEX for 3 h and then coincubated with LPS plus IFN-γ for 24 h. UN: uninduced cells; IN: untreated LPS plus IFN-γ-induced cells; DEX: cells were pretreated with DEX at 1 μM; GIE 300: cells were pretreated with GIE 300 μg/mL; Vit.E (150 and 300): cells were pretreated with Vit.E 150 and 300 μg/mL, respectively. One-way ANOVA performed the comparison, and Tukey was used as a *post hoc* test. The degree of significance was denoted with different letters for the comparison between sample groups. $p < 0.05$ was considered as statistically significant.

LPS plus IFN-γ-Induced RAW264.7 Cells. GIE has been reported to have antioxidant and anti-inflammatory activities in LPS plus IFN-γ-induced RAW264.7 cells in this research. Based on GC-MS analysis, we found that GIE consisted of many volatile oil compounds, including phytol, squalene, γ-tocopherol, dl-α-tocopherol, and stigmasterol. The antioxidant and anti-inflammatory activities of these active constituents have been demonstrated in several studies. Therefore, it is essential to confirm whether the active ingredients contributed to the antioxidant and anti-inflammatory abilities of GIE. The dl-alpha-tocopherol or Vit.E was *chosen* to elucidate the anti-inflammation and anti-oxidative activities in LPS plus IFN-γ-induced RAW264.7 cells. The cytotoxicity of Vit.E was evaluated. The results

TABLE 4: Band assignments of major absorptions in FTIR spectra in 3000-950 cm^{-1} regions.

Band position of 2nd derivative spectra (cm^{-1})	Assignments
2962	CH_3 stretching (antisymmetric) due to the methyl terminal of membrane phospholipids
2923	CH_2 antisymmetric stretching of methylene group of membrane phospholipids
2875	CH_3 symmetric stretching: lipids and proteins
2852	CH_2 symmetric stretching: mainly lipids
1655	Amide I: C=O (80%) and C–N (10%) stretching, N–H (10%) bending vibrations: proteins α-helix
1544	Amide II: N–H (60%) bending and C–N (40%) stretching vibrations: proteins α-helix
1515	CO_2 antisymmetric stretching
1463	CH_2 bending vibrations: mainly lipids with little contributions from proteins
1452	CH_2 bending vibrations: mainly lipids with little contributions from proteins
1394	COO^- symmetric stretching: fatty acids and amino acids
1243	PO_2^- asymmetric stretching vibrations: RNA, DNA, and phospholipids
1176	C–O vibrations from glycogen and other carbohydrates
1087	PO_2^- asymmetric stretching vibrations: RNA, DNA, and phospholipids
1047	C–O vibrations from glycogen and other carbohydrates
963	C–C/C–O is stretching of deoxyribose vibration

exhibited that Vit.E at 150 and 300 μg/mL did not reduce the cell viability compared to RAW264.7 cells (Figure 6(a)). Then, the noncytotoxic concentration of Vit.E at 300 μg/mL was chosen to perform subsequent experiments. Vit.E did not suppress NO production induced by LPS plus IFN-γ in RAW264.7 cells (Figure 6(b)). The results indicated that Vit.E showed a significantly suppressed iNOS and IL-6 mRNA expression lower than untreated LPS plus IFN-γ-induced cells (IN) ($p < 0.05$; Figures 6(c) and 6(d)), whereas COX-2, TNF-α, and SOD2 were lower than IN but no significant difference ($p > 0.05$; Figures 6(c) and 6(d)). Therefore, these results imply that Vit.E exhibits the inhibitory effect on the inflammatory gene expression, which is related to the anti-inflammatory effects of GIE. As mentioned above, GIE consists of many volatile oils; therefore, the antioxidant and anti-inflammatory activities of it may cause by other chemical compositions found in this plant. Moreover, phenolic, flavonoids, terpenoids, and glycoside in GIE were reported in previous studies [14, 15]. The presence of flavonoids had been reported to be associated with the antioxidant and anti-inflammatory activities of several plant extracts [25, 57, 58]. Thus, it is possible that phenolic and flavonoid compounds in GIE could provide substantial antioxidant and anti-inflammatory activities. In order to compare the inhibitory effect of Vit.E and GIE, GIE at 300 μg/mL contains Vit.E approximately 6.99 μg/mL. The results indicated that GIE at 300 μg/mL had inhibitory effect on COX-2 (73.48% inhibition, Figure 1(e)), iNOS (64.58% inhibition, Figure 1(e)), and IL-6 (75.72% inhibition, Figure 2(d)) mRNA levels higher than Vit.E alone at 300 μg/mL, which inhibited COX-2 (40.74% inhibition, Figure 6(c)), iNOS (56.86% inhibition, Figure 6(c)), and IL-6 (58.42% inhibition, Figure 6(d)). These results imply that the anti-inflammatory effect of GIE on these cells may have synergistic activities that cause by the combination of compounds presenting in GIE.

3.10. SR-FTIR Detected Biomolecule Alterations in RAW264.7 Cells. SR-FTIR was applied to detect the effects of GIE on biomolecule alterations such as lipids, proteins, nucleic acids, and carbohydrates based on their specific vibrational fingerprints. The detailed spectral band assignments of samples are given in Table 4. As shown in Figure 7(a), the representative FTIR spectra acquired in the 3800-900 cm^{-1} from four individuals of sample groups, including uninduced RAW264.7 cells, untreated LPS plus IFN-γ-induced RAW264.7 cells, 1 μM of DEX-, and 300 μg/mL GIE-treated LPS plus IFN-γ-induced RAW264.7 cells. The second derivative analysis in spectral regions ranges from 3,000 to 2800 cm^{-1} for lipid regions and 1800 to 950 cm^{-1} for protein regions, nucleic acid, and other carbohydrate regions (as shown in Figures 7(b) and 7(c)) respectively. The 2nd spectral revealed the prominent differences between the average spectra belonging to the different groups. The spectral differences were clearly observed mainly in lipid regions centered at 2962 cm^{-1}, 2923 cm^{-1}, and 2852 cm^{-1}, protein regions centered at 1655 cm^{-1} and 1544 cm^{-1}, nucleic acid and other carbohydrates regions centered at 1243 cm^{-1}, 1176 cm^{-1}, 1087 cm^{-1}, and 1047 cm^{-1}. The integral area of 2nd derivative FTIR spectral regions in each region was calculated to analyze the differences between lipid regions (2972-2951 cm^{-1}, 2934-2910 cm^{-1}, 2878-2870 cm^{-1}, and 2856-2843 cm^{-1}), nucleic acids (1257-1204 cm^{-1} and 1125-1074 cm^{-1}), glycogen, and other carbohydrates (1181-1164 cm^{-1} and 1063-1032 cm^{-1}) as shown in Figure 8(a). The level of lipid content was significantly increased in all test groups compared to the uninduced group ($p < 0.05$), whereas the highest level of lipid was found in DEX- and GIE-treated groups. This increase in lipid content might be due to the changing of the cell membrane and lipid accumulation in RAW264.7 cells. According to the results of cell morphological changes stained by hematoxylin staining, the
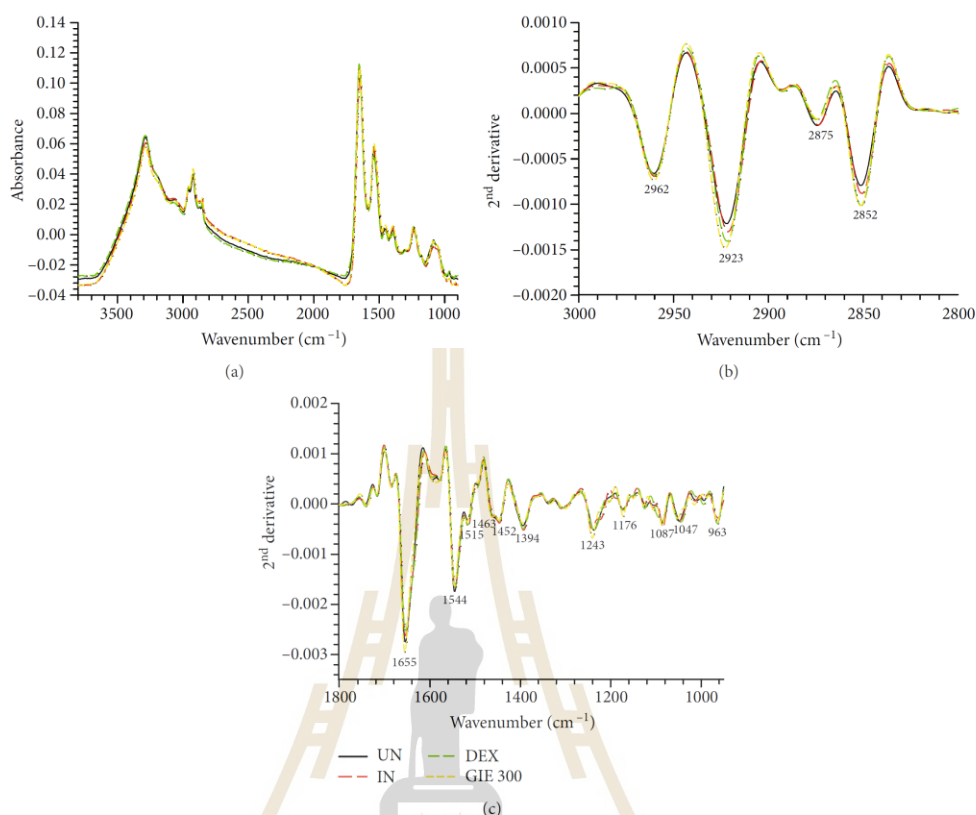
FIGURE 7: FTIR spectra obtained using SR-FTIR and processed with a second derivative. (a) Average original FTIR spectra (3800-900 cm^{-1}), (b) average the second derivative spectra of lipid regions (3000-2800 cm^{-1}), and (c) average the 2nd derivative spectra of protein and nucleic acid and other carbohydrate regions (1800-950 cm^{-1}). The data obtained from uninduced cells (UN, $n = 70$), untreated LPS plus IFN-γ-induced cells (IN, $n = 70$), 1 μM of DEX-treated cells (DEX, $n = 70$), and 300 μg/mL of GIE-treated LPS plus IFN-γ-induced cells (GIE300, $n = 70$).

phenotypic changes of RAW264.7 cells are induced by LPS and IFN-γ (Figures 3(b)–3(g)). The increasing lipid content may be related to the inflammatory phenotype of macrophages in which they are able to engulf lipids, dead cells, and other substances perceived as danger signals via phagocytosis [52]. All ingested lipids are then processed by acid lipases within the lysosomes, leading to free fatty acids and cholesterol generation [59]. Nevertheless, our data indicated that nucleic acid content seemed to increase in the DEX-treated cells and decrease in GIE-treated cells. However, the differences were not statistically significant from both uninduced cells and untreated LPS plus IFN-γ-induced cells ($p > 0.05$). According to these findings, the present data showed that the selected GIE concentration did not affect the cells' nucleic acids, consistent with the cytotoxic effect of GIE obtained from MTT assay. These results are confirmed by the study of Machana et al. [60], which reported the DNA content in apoptotic cell death, by contrast, to increase during necrotic cell death. As shown in Figure 8(a), the glycogen and other carbohydrate content

of the untreated LPS plus IFN-γ-induced cells were significantly decreased compared to the uninduced cells ($p < 0.05$). Upon DEX and GIE treatment, the glycogen and other carbohydrate contents were increased compared to the untreated LPS plus IFN-γ-induced cells. The band area ratio of amide I (1670-1627 cm^{-1})/amide II regions (1558-1505 cm^{-1}) was calculated to obtain information about changes in protein composition and structure (Figure 8(b)). There was a significant increase in the ratio of amide I to amide II bands in untreated LPS plus IFN-γ-induced RAW264.7 cells compared to the uninduced RAW264.7 cells ($p < 0.05$), revealing an alteration in the structures of proteins. In comparison, the GIE treating group showed a significant decrease in amide I/amide II ratio compared to untreated LPS plus IFN-γ-induced RAW264.7 cells ($p < 0.05$). According to amide I and amide II profiles depending on the protein structural composition, the changing of amide I/amide II ratio suggests that there are some alterations in protein structure and conformation in LPS plus IFN-γ-induced RAW264.7 cells [18].
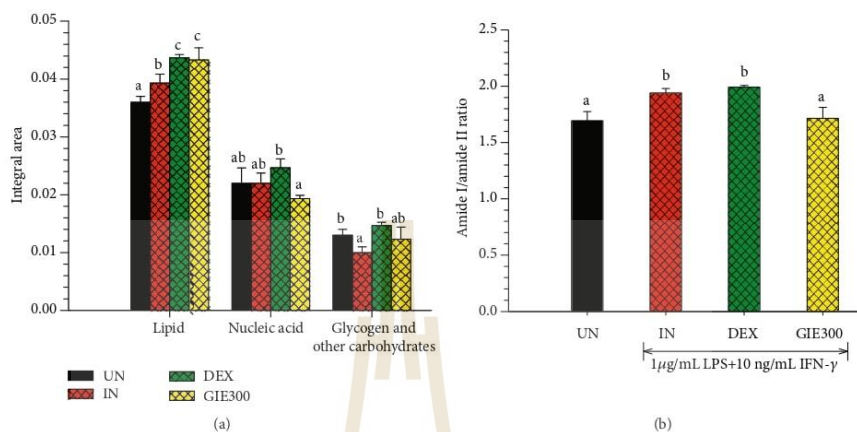
(a)

(b)

FIGURE 8: Bar graph shows (a) integrated areas of remarkable lipid, nucleic acid, glycogen, and other carbohydrate regions and (b) the amide I/amide II ratio of 2nd derivative spectra. Data are represented as means ± S.D. for three replicates. The data obtained from uninduced cells (UN, $n = 70$), untreated LPS plus IFN-γ-induced cells (IN, $n = 70$), 1 μM of DEX-treated cells (DEX, $n = 70$), and 300 μg/mL of GIE-treated LPS plus IFN-γ-induced cells (GIE300, $n = 70$). One-way ANOVA performed the comparison, and Tukey was used as a *post hoc* test. The degree of significance was denoted with different letters for the comparison between sample groups. $p < 0.05$ was considered as statistically significant.

Based on the spectral differences, the PCA analysis was applied to confirm any possible discrepancies between four sample groups in spectral ranges of 3000-2800 cm^{-1} and 1800-950 cm^{-1}. Four clusters of spectra were distinctly visualized in two-dimensional score plots, including PC1 vs. PC2, PC1 vs. PC3, and PC1 vs. PC4 score plot as shown in Figures 9(a)–9(c), respectively. PCA loading plots were used to indicate the contribution of variables between sample groups (as shown in Figures 9(d) and 9(e)). The PCA analysis obviously illustrated that the clusters of untreated LPS plus IFN-γ-induced RAW264.7 cells (IN) and DEX-treated cells (DEX) were separated from the cluster of GIE-treated cells (GIE300) along PC1 (33%). They were also separated from the group of uninduced RAW264.7 cells (UN) along with the PC2 score (9%) as shown in Figure 9(a). The amide I band from protein at 1629 cm^{-1} and 1623 cm^{-1} (assigned to the β-sheet structure) were heavily loaded for negative PC1 and positive PC2 loading, respectively (Figure 9(d)), which were responsible for discriminating the untreated LPS plus IFN-γ-induced RAW264.7 cells and DEX-treated cells, respectively. These data indicated that the amide I protein of the untreated LPS plus IFN-γ-induced RAW264.7 cells and DEX-treated cells were higher than the uninduced and GIE-treated cells. The cluster of DEX-treated cells was discriminated from uninduced and untreated LPS plus IFN-γ-induced RAW264.7 cells along PC3 (8%) (Figure 9(b)) in correlation with the positive loading centered at 2960 cm^{-1}, 2925 cm^{-1}, and 2854 cm^{-1}, assigned to the C-H stretching vibration of lipid in the cells (Figure 9(e)). Moreover, the cluster of uninduced and DEX-treated cells could be distinguished from untreated LPS plus IFN-γ-induced

RAW264.7 cells by their having positive PC4 scores (5%) (Figure 9(c)), which were associated with the negative loading plot centered at 1232 cm^{-1}, 1201 cm^{-1}, and 998 cm^{-1}, attributing to C–C from nucleic acid and C–O from a glycoprotein and other carbohydrates. This data displayed that the glycogen and other carbohydrates in uninduced and DEX-treated cells were higher than untreated LPS plus IFN-γ-induced RAW264.7 cells. These results provide evidence that PCA analysis has corresponded to the integrated peak areas obtained from 2nd derivative spectra (Figures 8(a) and 8(b)).

4. Conclusions

To our knowledge, the present study is the first report of the antioxidant and anti-inflammatory effects of GIE in LPS plus IFN-γ-induced RAW264.7 cells. GIE exerted an antioxidative effect based on its ROS scavenging properties and elevating the antioxidant gene expressions. GIE possesses anti-inflammatory effects by suppressing both proinflammatory mediators and gene expression in LPS plus IFN-γ-induced RAW264.7 cells. The data from SR-FTIR spectroscopy exhibited that LPS plus IFN-γ could affect the biochemical profile of RAW264.7 cells. SR-FTIR analysis was able to evaluate the effect of GIE on the changing of macromolecules, including lipid, protein structure, nucleic acid, glycogen, and other carbohydrates. These findings provide evidence that GIE has significant antioxidant and anti-inflammatory properties and could serve as a potent compound of those activities that warrant further research and development.
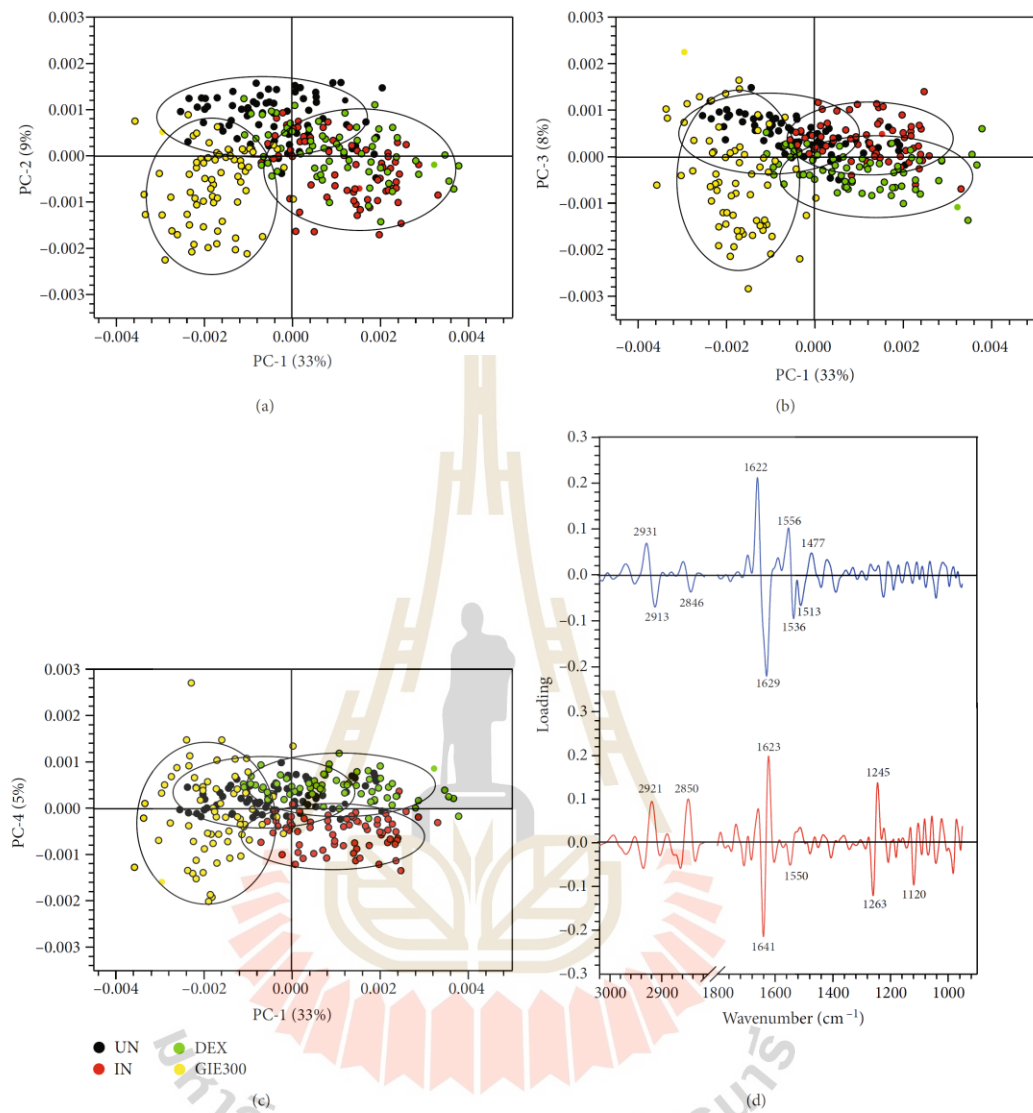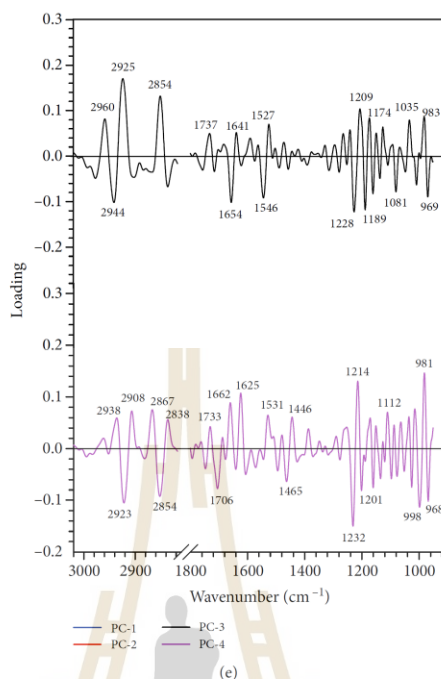
FIGURE 9: Continued.

FIGURE 9: PCA analysis of the FTIR spectra of uninduced cells (UN, $n = 70$), untreated LPS plus IFN-γ-induced cells (IN, $n = 70$), 1 μM of DEX-treated cells (DEX, $n = 70$), and 300 μg/mL of GIE-treated LPS plus IFN-γ-induced cells (GIE300, $n = 70$) in the spectral range of 3000-2800 cm^{-1} and 1800-950 cm^{-1} regions. PCA 2D score plot of (a) PC1 versus PC2, (b) PC1 versus PC3, and (c) PC1 versus PC4. PCA loading plot of (d) PC1 and PC2 and (e) PC3 and PC4.

Data Availability

The datasets used and analyzed during this study are available from the corresponding author on reasonable request.

Conflicts of Interest

The authors declare that there are no conflicts of interest regarding the publication of this manuscript.

Authors' Contributions

B.D. performed experiments and data analysis and drafted the manuscript. C.T. designed the study and revised the manuscript. M.M. contributed and designed the experiments and critical discussion. K.T. performed the SR-FTIR microspectroscopy. P.S. investigated ROS by DCFH-DA, proinflammatory cytokines (IL-6 and TNF-α), and anti-inflammatory cytokines (IL-10) by ELISA. G.E. supervised, coordinated, and improved quality and proofread the manuscript. All authors have read and approved the submission.

Acknowledgments

References

[1] S. Watanabe, M. Alexander, A. V. Misharin, and G. R. S. Budinger, "The role of macrophages in the resolution of inflammation," *The Journal of Clinical Investigation*, vol. 129, no. 7, pp. 2619–2628, 2019.

[2] D. L. Laskin, V. R. Sunil, C. R. Gardner, and J. D. Laskin, "Macrophages and tissue injury: agents of defense or destruction?," *Annual Review of Pharmacology and Toxicology*, vol. 51, no. 1, pp. 267–288, 2011.

[3] F. O. Martinez and S. Gordon, "The M1 and M2 paradigm of macrophage activation: time for reassessment," *F1000Prime Reports*, vol. 6, 2014.

[4] J. B. Calixto, M. F. Otuki, and A. R. Santos, "Anti-inflammatory compounds of plant origin. Part I. Action on arachidonic acid pathway, nitric oxide and nuclear factor κ B (NF-κB)," *Planta Medica*, vol. 69, no. 11, pp. 973–983, 2003.

[5] A. D. Politis, K. Ozato, J. E. Coligan, and S. N. Vogel, "Regulation of IFN-gamma-induced nuclear expression of IFN

consensus sequence binding protein in murine peritoneal macrophages," *The Journal of Immunology*, vol. 152, no. 5, pp. 2270–2278, 1994.

[6] J.-M. Zhang and J. An, "Cytokines, inflammation and pain," *International Anesthesiology Clinics*, vol. 45, no. 2, pp. 27–37, 2007.

[7] S. Reuter, S. C. Gupta, M. M. Chaturvedi, and B. B. Aggarwal, "Oxidative stress, inflammation, and cancer: how are they linked?," *Free Radical Biology and Medicine*, vol. 49, no. 11, pp. 1603–1616, 2010.

[8] P. Arulselvan, M. T. Fard, W. S. Tan et al., "Role of antioxidants and natural products in inflammation," *Oxidative Medicine and Cellular Longevity*, vol. 2016, Article ID 5276130, 15 pages, 2016.

[9] R. E. Sevinsky, D. W. Stewart, and S. Harirforoosh, "Nonsteroidal anti-inflammatory drugs: is there a link between cardiovascular and renal adverse effects?," *Journal of Integrative Nephrology and Andrology*, vol. 4, no. 1, p. 1, 2017.

[10] S. Wongrakpanich, A. Wongrakpanich, K. Melhado, and J. Rangaswami, "A comprehensive review of non-steroidal anti-inflammatory drug use in the elderly," *Aging and Disease*, vol. 9, no. 1, pp. 143–150, 2018.

[11] T. Charoonratana, T. Songsak, C. Monton et al., "Quantitative analysis and formulation development of a traditional Thai antihypertensive herbal recipe," *Phytochemistry Reviews*, vol. 13, no. 2, pp. 511–524, 2014.

[12] World Health Organization, *WHO Medicines Strategy 2004-2007: Countries at the Core*, World Health Organization, 2004.

[13] A. Chanwitheesuk, A. Teerawutgulrag, and N. Rakariyatham, "Screening of antioxidant activity and antioxidant compounds of some edible plants of Thailand," *Food Chemistry*, vol. 92, no. 3, pp. 491–497, 2005.

[14] K. Tiamyom, K. Sirichaiwetchakoon, T. Hengpratom et al., "The effects of Cordyceps sinensis (Berk.) Sacc. and Gymnema inodorum (Lour.) Decne. Extracts on adipogenesis and lipase activity in vitro," *Evidence-based Complementary and Alternative Medicine*, vol. 2019, Article ID 5370473, 13 pages, 2019.

[15] C. Chaiyasut, P. Kesika, K. Chaiyasut, P. Sittiyuno, S. Peerajan, and B. S. Sivamaruthi, "Total phenolic content and free radical scavenging activity of representative medicinal plants of Thailand," *Asian Journal of Pharmaceutical and Clinical Research*, vol. 10, no. 11, pp. 137–141, 2017.

[16] K. Shimizu, M. Ozeki, A. Iino, S. Nakajyo, N. Urakawa, and M. Atsuchi, "Structure-activity relationships of triterpenoid derivatives extracted from *Gymnema inodorum* leaves on glucose absorption," *Japanese Journal of Pharmacology*, vol. 86, no. 2, pp. 223–229, 2001.

[17] S. Sabbatini, C. Conti, G. Orilisi, and E. Giorgini, "Infrared spectroscopy as a new tool for studying single living cells: is there a niche?," *Biomedical Spectroscopy and Imaging*, vol. 6, no. 3-4, pp. 85–99, 2017.

[18] O. Bozkurt, S. Haman Bayari, M. Severcan, C. Krafft, J. Popp, and F. Severcan, "Structural alterations in rat liver proteins due to streptozotocin-induced diabetes and the recovery effect of selenium: Fourier transform infrared microspectroscopy and neural network study," *Journal of Biomedical Optics*, vol. 17, no. 7, article 076023, 2012.

[19] S. Siriwong, Y. Teethaisong, K. Thumanu, B. Dunkhunthod, and G. Eumkeb, "The synergy and mode of action of quercetin plus amoxicillin against amoxicillin-resistant Staphylococcus

[20] epidermidis," *BMC Pharmacology and Toxicology*, vol. 17, no. 1, p. 39, 2016.

[20] P. Pocasap, N. Weerapreeyakul, and K. Thumanu, "Alyssin and iberin in cruciferous vegetables exert anticancer activity in HepG2 by increasing intracellular reactive oxygen species and tubulin depolymerization," *Biomolecules & Therapeutics*, vol. 27, no. 6, pp. 540–552, 2019.

[21] P. Yu, "Synchrotron IR microspectroscopy for protein structure analysis: potential and questions," *Spectroscopy*, vol. 20, no. 5,6, pp. 229–251, 2006.

[22] H. V. Rupasinghe, L. Wang, G. M. Huber, and N. L. Pitts, "Effect of baking on dietary fibre and phenolics of muffins incorporated with apple skin powder," *Food Chemistry*, vol. 107, no. 3, pp. 1217–1224, 2007.

[23] H. Yang, Y. Dong, H. Du, H. Shi, Y. Peng, and X. Li, "Antioxidant compounds from propolis collected in Anhui, China," *Molecules*, vol. 16, no. 4, pp. 3444–3455, 2011.

[24] B. Dunkhunthod, K. Thumanu, and G. Eumkeb, "Application of FTIR microspectroscopy for monitoring and discrimination of the anti-adipogenesis activity of baicalein in 3T3-L1 adipocytes," *Vibrational Spectroscopy*, vol. 89, pp. 92–101, 2017.

[25] P. Sittisart and B. Chitsomboon, "Intracellular ROS scavenging activity and downregulation of inflammatory mediators in RAW264.7 macrophage by fresh leaf extracts of Pseuderanthemum palatiferum," *Evidence-based Complementary and Alternative Medicine*, vol. 2014, Article ID 309095, 11 pages, 2014.

[26] O. H. Lowry, N. J. Rosebrough, A. L. Farr, and R. J. Randall, "Protein measurement with the Folin phenol reagent," *Journal of Biological Chemistry*, vol. 193, no. 1, pp. 265–275, 1951.

[27] R. O. Silva, F. B. M. Sousa, S. R. Damasceno et al., "Phytol, a diterpene alcohol, inhibits the inflammatory response by reducing cytokine production and oxidative stress," *Fundamental & Clinical Pharmacology*, vol. 28, no. 4, pp. 455–464, 2014.

[28] S. H. Jeong, "Inhibitory effect of phytol on cellular senescence," *Biomedical Dermatology*, vol. 2, no. 1, 2018.

[29] A. Cárdeno, M. Aparicio-Soto, S. Montserrat-de la Paz, B. Bermudez, F. J. Muriana, and C. Alarcón-de-la-Lastra, "Squalene targets pro- and anti-inflammatory mediators and pathways to modulate over-activation of neutrophils, monocytes and macrophages," *Journal of Functional Foods*, vol. 14, pp. 779–790, 2015.

[30] E. Reiter, Q. Jiang, and S. Christen, "Anti-inflammatory properties of α\- and γ-tocopherol," *Molecular Aspects of Medicine*, vol. 28, no. 5-6, pp. 668–691, 2007.

[31] P. Mathur, Z. Ding, T. Saldeen, and J. L. Mehta, "Tocopherols in the prevention and treatment of atherosclerosis and related cardiovascular disease," *Clinical Cardiology*, vol. 38, no. 9, pp. 570–576, 2015.

[32] V. Jimenez-Suarez, A. Nieto-Camacho, M. Jiménez-Estrada, and B. Alvarado Sanchez, "Anti-inflammatory, free radical scavenging and alpha-glucosidase inhibitory activities of Hamelia patens and its chemical constituents," *Pharmaceutical Biology*, vol. 54, no. 9, pp. 1822–1830, 2016.

[33] M. Zeb, S. Khan, T. Rahman, M. Sajid, and S. Seloni, "Isolation and biological activity of β-sitosterol and stigmasterol from the roots of Indigofera heterantha," *Pharmacy & Pharmacology International Journal*, vol. 5, no. 5, p. 139, 2017.

[34] M. R. Loizzo, R. Tundis, M. Bonesi et al., "Radical scavenging, antioxidant and metal chelating activities of *Annona cherimola* Mill. (cherimoya) peel and pulp in relation to their total

phenolic and total flavonoid contents," *Journal of Food Composition and Analysis*, vol. 25, no. 2, pp. 179–184, 2012.

[35] M. El Jemli, R. Kamal, I. Marmouzi, A. Zerrouki, Y. Cherrah, and K. Alaoui, "Radical-scavenging activity and ferric reducing ability of Juniperus thurifera (L.), J. oxycedrus (L.), J. phoenicea (L.) and Tetraclinis articulata (L.)," *Advances in Pharmacological Sciences*, vol. 2016, Article ID 6392656, 6 pages, 2016.

[36] J. S. Youn, Y.-J. Kim, H. J. Na et al., "Antioxidant activity and contents of leaf extracts obtained from Dendropanax morbifera LEV are dependent on the collecting season and extraction conditions," *Food Science and Biotechnology*, vol. 28, no. 1, pp. 201–207, 2019.

[37] E. Finotti, M. D'Ambrosio, F. Paoletti, V. Vivanti, and G. Quaglia, "Synergistic effects of α-tocopherol, β-sitosterol and squalene on antioxidant activity assayed by crocin bleaching method," *Nahrung (Weinheim)*, vol. 44, no. 5, pp. 373-374, 2000.

[38] G. Perretti, E. Finotti, S. Adamuccio, R. Della Sera, and L. Montanari, "Composition of organic and conventionally produced sunflower seed oil," *Journal of the American Oil Chemists' Society*, vol. 81, no. 12, pp. 1119–1123, 2004.

[39] N. V. Yanishlieva, A. Kamal-Eldin, E. M. Marinova, and A. G. Toneva, "Kinetics of antioxidant action of α- and γ-toco-pherols in sunflower and soybean triacylglycerols," *European Journal of Lipid Science and Technology*, vol. 104, no. 5, pp. 262–270, 2002.

[40] T.-C. Chou, "Theoretical basis, experimental design, and computerized simulation of synergism and antagonism in drug combination studies," *Pharmacological Reviews*, vol. 58, no. 3, pp. 621–681, 2006.

[41] K.-R. Kwon, M. B. Alam, J.-H. Park, T.-H. Kim, and S.-H. Lee, "Attenuation of UVB-induced photo-aging by polyphenolic-rich Spatholobus suberectus stem extract via modulation of MAPK/AP-1/MMPs signaling in human keratinocytes," *Nutrients*, vol. 11, no. 6, p. 1341, 2019.

[42] H.-U. Son, E.-K. Yoon, C.-Y. Yoo et al., "Effects of synergistic inhibition on α-glucosidase by phytoalexins in soybeans," *Biomolecules*, vol. 9, no. 12, p. 828, 2019.

[43] M. Allegra, *Antioxidant and Anti-Inflammatory Properties of Plants Extract*, Multidisciplinary Digital Publishing Institute, 2019.

[44] S. Nanasombat, K. Yansodthee, and I. Jongjaited, "Evaluation of antidiabetic, antioxidant and other phytochemical properties of Thai fruits, vegetables and some local food plants," *Walailak Journal of Science and Technology (WJST)*, vol. 16, no. 11, pp. 851–866, 2018.

[45] B. Halliwell and J. M. Gutteridge, "Role of free radicals and catalytic metal ions in human disease: an overview," in *Methods in Enzymology*, pp. 1–85, Elsevier, 1990.

[46] Y. Yoon, T. J. Kim, J. M. Lee, and D. Y. Kim, "SOD2 is upregulated in periodontitis to reduce further inflammation progression," *Oral Diseases*, vol. 24, no. 8, pp. 1572–1580, 2018.

[47] P. Kirkham and I. Rahman, "Oxidative stress in asthma and COPD: antioxidants as a therapeutic strategy," *Pharmacology & Therapeutics*, vol. 111, no. 2, pp. 476–494, 2006.

[48] E. Karpuzoglu and S. A. Ahmed, "Estrogen regulation of nitric oxide and inducible nitric oxide synthase (iNOS) in immune cells: implications for immunity, autoimmune diseases, and apoptosis," *Nitric Oxide*, vol. 15, no. 3, pp. 177–186, 2006.

[49] S. I. Jang, Y.-J. Kim, W.-Y. Lee et al., "Scoparone from Artemisia capillaris inhibits the release of inflammatory mediators in RAW 264.7 cells upon stimulation cells by interferon-γ plus LPS," *Archives of Pharmacal Research*, vol. 28, no. 2, pp. 203–208, 2005.

[50] R. Sundaram, P. Shanthi, and P. Sachdanandam, "Tangeretin, a polymethoxylated flavone, modulates lipid homeostasis and decreases oxidative stress by inhibiting NF-κB activation and proinflammatory cytokines in cardiac tissue of streptozotocin-induced diabetic rats," *Journal of Functional Foods*, vol. 16, pp. 315–333, 2015.

[51] F. Y. McWhorter, T. Wang, P. Nguyen, T. Chung, and W. F. Liu, "Modulation of macrophage phenotype by cell shape," *Proceedings of the National Academy of Sciences*, vol. 110, no. 43, pp. 17253–17258, 2013.

[52] I. Tabas and K. E. Bornfeldt, "Macrophage phenotype and function in different stages of atherosclerosis," *Circulation Research*, vol. 118, no. 4, pp. 653–667, 2016.

[53] S.-R. Kang, D.-Y. Han, K.-I. Park et al., "Suppressive effect on lipopolysaccharide-induced proinflammatory mediators by Citrus aurantium L. in macrophage RAW 264.7 cells via NF-B signal pathway," *Evidence-based Complementary and Alternative Medicine*, vol. 2011, Article ID 248592, 12 pages, 2011.

[54] P. P. Tak and G. S. Firestein, "NF-κB: a key role in inflammatory diseases," *The Journal of Clinical Investigation*, vol. 107, no. 1, pp. 7–11, 2001.

[55] J. A. Lee, H. Y. Song, S. M. Ju et al., "Differential regulation of inducible nitric oxide synthase and cyclooxygenase-2 expression by superoxide dismutase in lipopolysaccharide stimulated RAW 264.7 cells," *Experimental & Molecular Medicine*, vol. 41, no. 9, pp. 629–637, 2009.

[56] J.-F. Luo, X.-Y. Shen, C. K. Lio et al., "Activation of Nrf2/HO-1 pathway by nardochinoid C inhibits inflammation and oxidative stress in lipopolysaccharide-stimulated macrophages," *Frontiers in Pharmacology*, vol. 9, p. 911, 2018.

[57] C.-l. Lu, W. Zhu, M. Wang, X.-j. Xu, and C.-j. Lu, "Antioxidant and anti-inflammatory activities of phenolic-enriched extracts of Smilax glabra," *Evidence-based Complementary and Alternative Medicine*, vol. 2014, Article ID 910438, 8 pages, 2014.

[58] J. C. Ruiz-Ruiz, A. J. Matus-Basto, P. Acereto-Escoffié, and M. R. Segura-Campos, "Antioxidant and anti-inflammatory activities of phenolic compounds isolated from Melipona beecheii honey," *Food and Agricultural Immunology*, vol. 28, no. 6, pp. 1424–1437, 2017.

[59] S. C.-C. Huang, B. Everts, Y. Ivanova et al., "Cell-intrinsic lysosomal lipolysis is essential for alternative activation of macrophages," *Nature Immunology*, vol. 15, no. 9, pp. 846–855, 2014.

[60] S. Machana, N. Weerapreeyakul, S. Barusrux, K. Thumanu, and W. Tanthanuch, "FTIR microspectroscopy discriminates anticancer action on human leukemic cells by extracts of *Pinus kesiya*; *Cratoxylum formosum* ssp. *pruniflorum* and melphalan," *Talanta*, vol. 93, pp. 371–382, 2012.

Research Article

Intracellular ROS Scavenging and Anti-Inflammatory Activities of *Oroxylum indicum* Kurz (L.) Extract in LPS plus IFN-γ-Activated RAW264.7 Macrophages

Benjawan Dunkhunthod,[1] Chutima Talabnin,[2] Mark Murphy,[3] Kanjana Thumanu,[4] Patcharawan Sittisart,[5] Tanaporn Hengpratom [ID],[1] and Griangsak Eumkeb [ID][1]

[1]*School of Preclinic, Institute of Science, Suranaree University of Technology, Nakhon Ratchasima 30000, Thailand*
[2]*School of Chemistry, Institute of Science, Suranaree University of Technology, Nakhon Ratchasima 30000, Thailand*
[3]*School of Biomolecular Science, Liverpool John Moores University, Liverpool L3 3AF, UK*
[4]*Synchrotron Light Research Institute (Public Organization), Nakhon Ratchasima 30000, Thailand*
[5]*Division of Environmental Science, Faculty of Liberal Arts and Science, Sisaket Rajabhat University, Sisaket 33000, Thailand*

Correspondence should be addressed to Griangsak Eumkeb; griang@sut.ac.th

Oroxylum indicum (L.) Kurz has been used as plant-based food and herbal medicine in many Asian countries. The aim of the present study was to examine the antioxidant and anti-inflammatory activities of *O. indicum* extract (*O. indicum*) in RAW264.7 cells activated by LPS plus IFN-γ. The phytochemical compounds in *O. indicum* were identified by GC-MS and LC-MS/MS. Five flavonoids (luteolin, apigenin, baicalein, oroxylin A, and quercetin) and 27 volatile compounds were found in *O. indicum*. *O. indicum* presented antioxidant activities, including reducing ability by FRAP assay and free radical scavenging activity by DPPH assay. Moreover, *O. indicum* also suppressed LPS plus IFN-γ-activated reactive oxygen species generation in RAW264.7 macrophages. It possessed the potent anti-inflammatory action through suppressing nitric oxide (NO) and IL-6 secretion, possibly due to its ability to scavenge intracellular ROS. The synchrotron radiation-based Fourier transform infrared (SR-FTIR) spectroscopy results showed the alteration of signal intensity and integrated areas relating to lipid and protein of the activated RAW264.7 macrophages compared to unactivated cells. This is the first report of an application of the SR-FTIR technique to evaluate biomolecular changes in activated RAW264.7 cells. Our results indicate that *O. indicum* may be used as a potential source of nutraceutical for the development of health food supplement or a novel anti-inflammatory herbal medicine.

1. Introduction

Inflammation is a response of the immune system to injury, irritation, or infection caused by invading pathogens, radiation exposure, very high or low temperatures, or autoimmune processes. Lipopolysaccharide (LPS), an outer membrane component of Gram-negative bacteria, has been reported as one of the major causes of septic shock [1]. In response to endotoxin stimulation, a variety of immune cells can be activated. In the innate immunity system, macrophages play pivotal roles in the cellular host's defense against

infection and tissue injury [2]. Inflammation is considered to be beneficial when it is short term and under control within the immune system (acute inflammation). However, if the inflammatory process has been going on for too long (chronic inflammation) or if the inflammatory response occurs in places where it is not needed, it can become problematic.

During inflammation responses, mast cells, monocytes, macrophages, lymphocytes, and other immune cells are first activated. The cells are recruited to the site of damage, resulting in the generation of reactive oxygen species that

damage macromolecules, including DNA. At the same time, these inflammatory cells also produce large amounts of inflammatory mediators such as metabolites of arachidonic acid, nitric oxide (NO), proinflammatory cytokines, chemokines, prostaglandins, inducible enzymes, and growth factors [3]. Excessive production of intracellular ROS can cause oxidative stress associated with redox unbalance [4]. This imbalance leads to damage of essential biomolecules and cells, with potential impact on the whole organism. Accordingly, excessive oxidative stress and chronic inflammation can cause chronic diseases such as cancer, aging, diabetes, obesity, cardiovascular diseases, Alzheimer's, and Parkinson's disease. Therefore, oxidative stress and inflammation must be adequately controlled to prevent the progressions of chronic diseases.

Over the past few decades, studies have investigated the possible protective role of plant foods against chronic diseases. Several epidemiological studies have revealed that higher consumption of fruits and vegetables is associated with a lower risk of chronic diseases [5]. The usage of herbs or traditional herbal medicines that are complementary and alternative medicines for the management of inflammation has increased because of the concerns about the adverse side effects of nonsteroidal anti-inflammatory drugs [6]. These indigenous vegetables can be readily available in the local area. Consequently, the consumption of these vegetables would be appropriate to control and also reduce the cost of inflammatory management.

Oroxylum indicum (L.) Kurz is a species of flowering plant belonging to the Bignoniaceae family. Fruit pods of this plant have been used in many Asian countries as a plant-based food and herbal medicine for thousands of years without any known adverse effects [7–9]. Numerous scientific studies showed that *O. indicum* was not toxic even in experimental animals, even up to high doses [10–12]. The fruit pods of this plant are rich in nutrients concerning dietary fiber, essential amino acids, minerals, and fatty acids [8]. Every part of this tree is also an essential source of several medicinally essential flavonoids, including baicalein, chrysin, and oroxylin A, which have contributed to many of the biological activities. The crude extracts and its isolated compounds exhibit a broad spectrum of *in vitro* and *in vivo* pharmacological activities involving antioxidant, antidiabetic, anti-adipogenesis, hepatoprotective, and anti-inflammatory activities [7, 11, 13, 14].

Currently, Fourier transform infrared (FTIR) microspectroscopy is widely used as a tool to monitor the changes in various biological samples such as bacteria, apoptotic and necrotic cell death, stem cell differentiation, and adipocyte cells [14–17]. FTIR technique is based on the absorption of infrared (IR) light of chemical bonds by vibrational transitions. This is a label-free and nondestructive technique that enables the analysis of biological samples with no need for staining and without sample destruction [18]. However, infrared microspectroscopy of cellular samples is not a single-molecule detection technique because of the limited spatial resolution when working on individual cells and the lack of sensitivity of the detectors while analyzing thick tissue sections [19]. In this context, the use of synchrotron

radiation-based Fourier transform infrared (SR-FTIR) microspectroscopy was considered to explore the molecular chemistry within microstructures of individual single cells with a high signal [20]. To date, there are no studies available for SR-FTIR microspectroscopy to detect molecular changes in LPS plus IFN-γ-activated RAW264.7 cells. There is considerable interest in applying SR-FTIR microspectroscopy to identify biochemical changes in LPS plus IFN-γ-activated RAW264.7 cells.

Therefore, this study aimed to investigate the antioxidant and anti-inflammatory activities of *O. indicum* in RAW264.7 cells activated by LPS plus IFN-γ. We also examined the biochemical alteration in LPS plus IFN-γ-activated RAW264.7 cells upon treatment with *O. indicum* by using SR-FTIR microspectroscopy.

2. Materials and Methods

2.1. Chemicals and Reagents. Vitamin C (VIT.C) was purchased from Fluka Chemie GmbH (Buchs, Switzerland). 2,2-Diphenyl-1-picryl-hydrazyl (DPPH), sodium nitrite, LPS (Escherichia coli; O111 : B4), $2',7'$-dichlorofluorescein-diacetate (DCFH-DA), and N-acetyl-cysteine (NAC) were purchased from Sigma-Aldrich (St. Louis, USA). Dimethyl sulfoxide (DMSO) was bought from Amresco Inc. (Solon, USA). 6-Hydroxy-2,5,7,8-tetramethylchroman-2-carboxylic acid (Trolox) was obtained from Sigma-Aldrich Chemie GmbH (Steinheim, Germany). Dexamethasone (DEX) was obtained from G Bioscience (St. Louis, USA). 3-(4,5-Dimethylthiazol-2-yl)-2,5-diphenyl-tetrazolium bromide (MTT), Roswell Park Memorial Institute (RPMI) 1640, fetal bovine serum (FBS), penicillin-streptomycin, and N-2-hydroxyethylpiperazine-N-2-ethane sulfonic acid (HEPES) were obtained from Gibco Invitrogen (Grand Island, NY, USA). Griess-Ilosvay's reagent was purchased from Merck KGaA (Darmstadt, Germany). Mouse interferon-gamma (mIFN-γ) was purchased from Pierce Protein Research Products (Rockford, USA). TMB substrate: $3,3',5,5'$ tetramethylbenzidine was purchased from PanReac AppliChem ITW Reagents (Darmstadt, Germany). Elisa kits for IL-6 and TNF-α were obtained from R&D Systems, Inc. (Minneapolis, USA). Baicalein and all other chemical standards for LC-MS/MS analysis were obtained from INDOFINE Chemical Company, Inc. (Hillsborough, NJ, USA). Other reagents used were all of analytical grade.

2.2. Preparation of Plant Extract. The fresh fruit pods of *O. indicum* were purchased from the local market at Wang Nam Khiao District, Nakhon Ratchasima province, Thailand. The plant samples were identified by a botanist at the Institute of Science, Suranaree University, Thailand, and the voucher specimens were kept at the flora of Suranaree University of Technology Herbarium (SOI0808U). Fresh fruit pods were washed and cut into small pieces and then dried in the oven at 40°C for 2 days. The dried pieces were pulverized using a mechanical grinder. *O. indicum* dry powder (500 g) was extracted with 95% ethanol by a soxhlation for 8 h and then filtered through Whatman filter

paper. The ethanolic extract was concentrated and lyophilized to obtain the powder of *O. indicum*. The crude extracts were stored at −20°C till use in subsequent experiments. *O. indicum* was dissolved in 100% DMSO and diluted to 0.06% (v/v) in the cell culture medium.

2.3. GC-MS Analysis. The phytoconstituents present in the extract of *O. indicum* were analyzed by gas chromatography-mass spectrometry (GC-MS) using a Bruker 450-GC/Bruker 320-MS equipped with Rtx-5MS fused silica capillary column (30 m × 0.25 mm; 0.25 μm in the thickness of film). Helium was used as the carrier gas with a flow rate of 1 mL min^{-1}. The injector temperature was operated at 250°C, and the oven temperature was programmed from 110°C (2 min), 200°C (3 min), and 280°C (20 min) with rates of 0, 10, and 5°C min^{-1}, respectively. The mass spectral data were taken with an electron energy of 70 eV. The ion source and transfer line temperature were kept at 200°C. The mass spectra were obtained by a centroid scan of the mass range from 45 to 500 atomic mass units. Interpretation of the mass spectrum of GC-MS was made by using NIST mass spectral library 2008.

2.4. Liquid Chromatography-Mass Spectrometer (LC-MS/MS) Quantification of the Selected Phenols and Flavonoids. The analyses were performed on the Dionex Ultimate 3000 UHPLC system (Dionex, USA) coupled with electrospray ionization (ESI) tandem mass spectrometer (micro-TOF-Q II) (Bruker, Germany). The injection volume of all samples was 5 μL. The separation was achieved using a Zorbax SB-C18 (250 mm × 4.6 mm × 3.5 μm (Agilent Technologies, USA)) and thermostat at 35°C, with a flow rate of 0.8 mL min^{-1} of the mobile phase, which included deionized water containing 0.1% formic acid (FA) as solvent A and acetonitrile containing 0.1% formic acid as solvent B. The gradient elution was performed using the following solvent gradient: starting with 30% B, reaching 80% B at 30 min, and holding until 38 min, reducing to 30% B in 2 min and holding until the run ending at 45 min. Detection of eluted components, ionized by ESI, was performed in the mass scanning mode in the range of 50 m/z to 1,500 m/z at negative ion polarity. The nebulizer gas (N$_2$) was 2 Bar, drying gas was 8 L min^{-1}, the dryer heater temperature was 180°C, and the capillary voltage was 4.5 kV. The LC-QTOF data were collected and processed by Compass 1.3 software (Bruker, Germany). The target phenolic and flavonoid compounds were identified and quantified with Bruker Quant Analysis Version 2.0 SP 5 software.

The calibration curves were constructed from peak areas of different concentrations of the reference standard (from 0.5 μg mL^{-1} to 250 μg mL^{-1}), and the concentration of targeted compounds was calculated based on the equation for linear regression obtained from the calibration curves.

2.5. Ferric-Reducing/Antioxidant Power (FRAP) Assay. FRAP is based on the detection of the sample capacity to reduce ferric ions, which is measured as a change in the absorbance of the ferrous TPTZ complex. The assay was carried out, according to Rupasinghe et al. [21]. Briefly, the working FRAP reagent was prepared by mixing 300 mM acetate buffer (pH 3.6), a solution of 10 mM 2,4,6-tripyridyl-s-triazine (TPTZ) in 10 mM hydrochloric acid and 20 mM ferric chloride at 10 : 1:1 (v/v/v). The working FRAP reagent (180 μL) and sample solutions (20 μL) were mixed in a 96-well plate for 6 min. The absorbance was measured at 595 nm by using a microplate reader (Bio-Rad Laboratories, Inc., USA). The standard calibration curve was developed using different concentrations of Trolox and VIT.C. FRAP values were expressed as a milligram of Trolox equivalent antioxidant capacity (TREA) or ascorbic equivalent antioxidant capacity (VCEA) per gram of dry extract.

2.6. DPPH Radical Scavenging Activity Assay. The total free radical scavenging capacity of *O. indicum* was estimated according to the method of Yang et al. [22]. Briefly, one hundred microliters of the sample at different concentrations were added to 100 μL of DPPH solution (0.2 mM) in a 96-well plate. The mixture was shaken vigorously at room temperature for 15 min in the dark and measured the absorbance at 517 nm by using a microplate reader (Bio-Rad Laboratories, Inc, USA). Trolox and VIT.C were used as a positive control. The free radical scavenging activity was calculated as follows:

$$\text{scavenging rate} \, (\%) = \left[\frac{A_{\text{control}} - A_{\text{sample}}}{A_{\text{control}}} \right] \times 100. \qquad (1)$$

The IC$_{50}$ of DPPH was determined from a dose-response curve using linear regression analysis. Decreasing DPPH solution absorption indicates an increase of DPPH radical scavenging activity.

2.7. Cell Culture. The RAW264.7 macrophage cells (Cell Lines Service, Eppelheim, Germany) were cultured at 37°C, 5% CO$_2$ in RPMI-1640 medium supplemented with 10% heat-inactivated FBS and 100 U mL^{-1} penicillin-streptomycin.

2.8. In Vitro Cytotoxic Test (MTT Assay). The cytotoxic effect of *O. indicum* on cell viability was determined by using a tetrazolium dye (MTT) colorimetric assay [23]. Briefly, the cells were seeded in a 96-well plate at a density of 2×10^4 cells/well and allowed to adhere for 24 h. Cells were treated with different concentrations of *O. indicum* for 24 h. After incubation, the culture medium was removed, and 0.5 mg mL^{-1} (final concentration) MTT was added. Then, the cells were further incubated for 4 h at 37°C. Formazan crystal formed by viable cells was dissolved in DMSO and absorbance was measured at 540 nm with a microplate spectrophotometer (Bio-Rad Laboratories, Inc., USA).

2.9. Assessment of Intracellular ROS Scavenging Activity. The intracellular ROS scavenging capacity of *O. indicum* in RAW264.7 cells induced by LPS plus IFN-γ was measured using a DCFH-DA fluorescent probe, according to the

method described by Sittisart and Chitsomboon [23]. Briefly, RAW264.7 cells were seeded in a 96-well black plate at 2.0×10^4 cells/well and incubated overnight. Then, the culture medium was removed, and the cells were pretreated with *O. indicum* at the concentration of 50, 100, or $200 \, \mu g \, mL^{-1}$, VIT.C $50 \, \mu g \, mL^{-1}$, baicalein $5 \, \mu g \, mL^{-1}$, or a selective ROS scavenger, NAC, for 3 h. Then, the cells were activated with $1 \, \mu g \, mL^{-1}$ LPS plus $10 \, ng \, mL^{-1}$ IFN-γ and another 24-hour incubation. After removing the medium, the cells were treated with 20 M DCFH-DA in Hank's Balanced Salt Solution (HBSS) for 30 min and then washed with PBS twice. The fluorescence intensity was measured using a Gemini EM fluorescence microplate reader (Molecular Devices, Sunnyvale, CA) with an excitation wavelength of 485 nm and an emission wavelength of 535 nm. The percentage of DCF fluorescence intensity was calculated by the following formula: DCF fluorescence intensity (%) = (DCF fluorescence intensity$_{test \, group}$/DCF fluorescence intensity$_{control \, group}$) $\times$ 100. The IC$_{35}$, IC$_{40}$, and IC$_{50}$ of *O. indicum* were also calculated from a dose-response curve using linear regression analysis.

2.10. Determination of Nitric Oxide (NO) and Proinflammatory Cytokines (IL-6 and TNF-α) Production. The anti-inflammatory activities of *O. indicum* were evaluated by measuring the level of NO and proinflammatory cytokines (IL-6 and TNF-α) production in LPS plus IFN-γ-activated RAW264.7 cells. The cells were seeded at a density of 6×10^5 cells/well in a 6-well plate and then incubated overnight. After incubation, the culture medium was removed, and the cells were pretreated with different concentrations of *O. indicum* (50, 100, and $200 \, \mu g \, mL^{-1}$) or the anti-inflammatory agent, DEX ($1 \, \mu M$), for 3 h. Then, the cells were activated with $1 \, \mu g \, mL^{-1}$ LPS plus $10 \, ng \, mL^{-1}$ IFN-γ and incubated for 24 h. The supernatant was collected for further analysis of NO using Griess reagent and determined the level of TNF-α and IL-6 with the ELISA kits.

The level of NO in the culture media was detected as nitrite, a major stable product of NO, using Griess reagent as described by Sittisart et al. [24]. Briefly, $100 \, \mu L$ of cell culture medium was mixed with an equal volume of Griess reagent in a 96-well plate and incubated at room temperature for 10 min in the dark. The intensity of the pink color of the samples was measured at 540 nm using a microplate reader (Bio-Rad Laboratories, Inc.). The amount of nitrite in the samples was determined using the linear sodium nitrite calibration curves at a concentration range of $2.5–100 \, \mu M$.

Proinflammatory cytokine levels (IL-6 and TNF-α) were quantified by Mouse IL-6 or Mouse TNF-α DuoSet® ELISA Kits (R&D systems Inc., Minneapolis, USA) according to the manufacturer's instructions. Optical density was measured at 450 nm with a microplate reader (Benchmark Plus, Bio-Rad, Japan). By preparing the standards of known cytokine concentrations, the number of cytokines in the samples was quantified from a standard curve.

2.11. Haematoxylin Staining. The macrophage cells were activated by LPS plus IFN-γ for 24 h and then stained with a

haematoxylin solution to observe the phenotype feature as described by Dunkhunthod et al. [13] with some modification. Shortly, the cells were washed with PBS twice and fixed with 10% formaldehyde in PBS for 1 h. Then, cells were washed with distilled water twice and stained with haematoxylin solution for 10 min at room temperature. The stained cells were visualized under the inverted fluorescence microscope (Olympus Corporation, Japan).

2.12. FTIR Measurement Using Synchrotron IR Source. The sample was collected and dropped onto a barium fluoride (BaF$_2$) optical window (Crystran, Crystran Ltd.) as previously described by Dunkhunthod et al. [13]. FTIR experiments were conducted using a spectroscopy facility at the Synchrotron Light Research Institute (Public Organization), Thailand. FTIR spectra were acquired in transmission mode with a Vertex 70 FTIR spectrometer coupled with a Bruker Hyperion 2000 microscope (Bruker Optics Inc., Ettlingen, Germany), using synchrotron radiation as an IR source. The microscope was equipped with 64×64 element MCT, FPA detector, which allowed simultaneous spectral data acquisition with a 36 × objective. FTIR spectrum was recorded within a spectral range of $4000–600 \, cm^{-1}$ using an aperture size of $10 \, \mu m \times 10 \, \mu m$ with a spectral resolution $4 \, cm^{-1}$, with 64 scans being coadded. OPUS software (Bruker Optics Ltd., Ettlingen, Germany) was used for spectral measurement and instrument control.

The preprocessing of the spectra was performed by second derivative transformations using the Savitzky-Golay algorithm (nine smoothing points) and normalized with extended multiplicative signal correction (EMSC) using the spectral regions from 3000 to $2800 \, cm^{-1}$ and 1800 to $1400 \, cm^{-1}$. A principal component analysis (PCA) was performed using the Unscrambler® 10.5 software packages (CAMO Software AS., Oslo, Norway). Score plots (3D) and loading plots were used to represent the different classes of data and relations among variables of the data set, respectively. The integrated peak areas of FTIR spectra were analyzed using OPUS 7.2 software (Bruker) in the lipid regions ($3000–2800 \, cm^{-1}$) and protein regions ($1800–1400 \, cm^{-1}$) and demonstrated on a histogram.

2.13. Statistical Analysis. All data are expressed as the means $\pm$ SD from at least three independent experiments. The statistical significance (Statistical Package for the Social Sciences, version 19) was determined by performing a one-way analysis of variance (ANOVA) with Tukey's post hoc analysis to determine the differences among each treated group. Statistical significance was considered at $p < 0.05$.

3. Results and Discussion

3.1. GC/MS Analysis of Volatile Oils Obtained from O. indicum. GC/MS analysis of *O. indicum* enabled the identification of 27 volatile compounds, as shown in Table 1. The data in Table 1 illustrate retention time, chemical formula, and the relative amount of each component detected in *O. indicum*. Based on abundance, the top five major

TABLE 1: GC-MS analysis of *O. indicum*.

No.	Compound name	Formula	RT	%area
1	2-Furancarboxaldehyde, 5-(hydroxymethyl)-	$C_6H_6O_3$	4.88	4.86
2	Nonanoic acid	$C_9H_{18}O_2$	5.30	2.28
3	n-Decanoic acid	$C_{10}H_{20}O_2$	6.55	2.82
4	2-Cyclohexen-1-one, 2-methyl-	$C_7H_{10}O$	7.13	15.28
5	2-Dodecenoic acid	$C_{12}H_{22}O_2$	7.30	1.33
6	Benzeneethanol, 4-hydroxy-	$C_8H_{10}O_2$	7.54	13.33
7	3-Hydroxy-2-methylbenzaldehyde	$C_8H_8O_2$	7.88	11.18
8	Cyclobutanecarboxylic acid, decyl ester	$C_{17}H_{28}O_2$	8.89	8.82
9	Dodecanoic acid	$C_{12}H_{24}O_2$	8.98	1.15
10	Ethyl N-(o-anisyl)formimidate	$C_{10}H_{13}NO_2$	9.59	0.40
11	1,6-Dihydro-5-(2-hydroxyethyl)-4-methyl-6-oxopyrimidine	$C_7H_{10}N_2O_2$	10.99	1.39
12	Tetradecanoic acid	$C_{14}H_{28}O_2$	11.26	0.21
13	Hexadecanoic acid, methyl ester	$C_{17}H_{34}O_2$	13.58	0.28
14	n-Hexadecanoic acid	$C_{16}H_{32}O_2$	14.28	0.66
15	Hexadecanoic acid, ethyl ester	$C_{18}H_{36}O_2$	14.82	0.99
16	Phytol	$C_{20}H_{40}O$	17.09	0.39
17	Linoleic acid ethyl ester	$C_{20}H_{36}O_2$	17.95	0.58
18	Linolenic acid ethyl ester	$C_{20}H_{34}O_2$	18.08	0.57
19	Glycerol 1,3-dipalmitate	$C_{35}H_{68}O_5$	20.36	1.13
20	Linolelaidic acid, methyl ester	$C_{19}H_{34}O_2$	23.30	0.79
21	9,12,15-Octadecatrienoic acid, 2-phenyl-1,3-dioxan-5-yl ester	$C_{28}H_{42}O_4$	23.44	0.52
22	Dotriacontane	$C_{32}H_{66}$	23.67	1.29
23	Glycerol 1-monopalmitate	$C_{19}H_{38}O_4$	23.93	4.37
24	β-Monolinolein	$C_{21}H_{38}O_4$	26.70	4.09
25	Campesterol	$C_{28}H_{48}O$	35.57	2.48
26	Stigmasterol	$C_{29}H_{48}O$	36.33	1.48
27	γ-Sitosterol	$C_{29}H_{52}O_2$	37.88	17.19

compounds present in *O. indicum* were γ-sitosterol (17.19%), 2-cyclohexen-1-one, 2-methyl- (15.28%), benzeneethanol, 4-hydroxy- (13.33%), 3-hydroxy-2-methylbenzaldehyde (11.18%), and cyclobutanecarboxylic acid, decyl ester (8.82%). These compounds are known to exhibit important pharmacological activity, such as antidiabetic, antioxidant, anticancer, and anti-inflammatory activities. The sterol compounds, namely, stigmasterol and β-sitosterol, isolated from the methanol extract of *Achillea ageratum* have been shown to possess anti-inflammatory activity against 12-0-tetradecanoylphorbol acetate- (TPA-) induced mouse ear edema [25]. The presence of phytosterols in *O. indicum* is, therefore, considered to be of great importance for the curing of diseases.

3.2. LC-MS/MS Analysis of Selected Flavonoids in O. indicum. The LC-MS chromatograms obtained from *O. indicum* are shown in Figure 1. Corresponding standards of scutellarin, daidzein, luteolin, apigenin, genistein, baicalein, and oroxylin A were used to identify and quantify the flavonoids composition in *O. indicum*. The predominant compounds were identified in *O. indicum*, namely, luteolin (peaks 14, RT 11.4 min) at $m/z = 285$, apigenin (peaks 16, RT 14.6 min) at $m/z = 269$, baicalein (peaks 19, RT 16.2 min) at $m/z = 269$, and oroxylin A (peaks 23, RT 22.0 min) $m/z = 283$. The identified compounds were quantified by comparisons of their retention time to known amounts of authentic standard. The largest amount of baicalein was detected in *O. indicum* with a concentration of $25,498.16 \mu g\,g^{-1}$ while

oroxylin A, luteolin, and apigenin were estimated in *O. indicum* at the level of 266.70, 209.98, and $77.54 \mu g\,g^{-1}$, respectively. The previous investigation reported that *O. indicum* also contained quercetin as another flavonoid [14]. Many studies have shown high biological and pharmacological activity of flavonoid compounds. Baicalein, oroxylin, luteolin, apigenin, and quercetin, the flavonoid compounds, which were found in *O. indicum*, contributed to the antiadipogenesis, anticancer, antioxidant, and anti-inflammatory proprieties of plants [26].

3.3. Free Radical Scavenging and Antioxidant Activities of O. indicum. The antioxidative potential of *O. indicum* was assessed *in vitro* by DPPH and FRAP assays. The obtained results are shown in Table 2. In this study, the free radical scavenging activity of *O. indicum* and standard compound, VIT.C and Trolox, were determined using the DPPH-based method. The results showed that the DPPH scavenging ability of *O. indicum* and standard compound, VIT.C, were comparable and both significantly stronger than Trolox ($p < 0.05$). The ferric reducing antioxidant power (FRAP) was used to assess whether *O. indicum* had an electron-donating capacity. *O. indicum* exhibited a degree of electron-donating capacity by 57.14 ± 4.39 μgVCEA mg^{-1} and $65.77 \pm 4.99 \mu$gTREA mg^{-1} of dry extract. These results indicate that *O. indicum* displays an antioxidant activity based on the reducing ability to reduce ferric ion (Fe^{3+}) to ferrous ion (Fe^{2+}). Therefore, it could be concluded that *O. indicum* displays strong antioxidant activity in the assay used in this
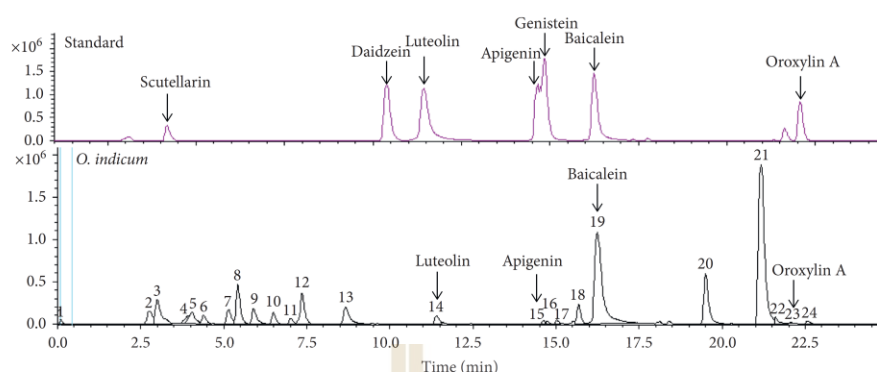
FIGURE 1: LC-MS chromatograms of *O. indicum* and standard compounds (scutellarin, daidzein, luteolin, apigenin, naringenin, genistein, baicalein, and oroxylin (A)).

TABLE 2: Total antioxidant (FRAP) and DPPH scavenging activities of *O. indicum* and standard compounds.

Sample	FRAP values		DPPH scavenging activity (IC$_{50}$) μg mL^{-1}
	(μgVCEA mg^{-1})	(μgTREA mg^{-1})	
O. indicum	57.14 ± 4.39	65.77 ± 4.99	43.28 ± 0.67[a]
VIT.C	—	—	44.57 ± 0.59[a]
Trolox	—	—	67.19 ± 4.82[b]

Values are mean ± SD ($n = 3$) and are representative of three independent experiments with similar results. Different letters within the same column are significantly different at $p < 0.05$.

study. This finding is in accordance with several studies that the antioxidant activity of *O. indicum* is caused by scavenging free radical DPPH and ferric reducing antioxidant power (FRAP) [7,27,28].

3.4. Effects of O. indicum on Cell Viability in RAW264.7 Cells. The effects of *O. indicum* on cell viability in RAW264.7 cells were comprehensively investigated, as shown in Figure 2. The cell viability of RAW264.7 cells treated with *O. indicum* at a concentration range of 50–1,000 μg mL^{-1} was evaluated by using MTT assay. The viability of RAW264.7 cells was not affected by *O. indicum* when the concentrations of *O. indicum* were not greater than 300 μg mL^{-1} ($p > 0.05$). This result suggests further investigation to proceed with *O. indicum* at concentrations of 50, 100, and 200 μg mL^{-1} in all subsequent experiments.

3.5. Effects of O. indicum on Intracellular ROS Production in LPS plus IFN-γ-Activated RAW264.7 Cells. In the event of the inflammatory response, the classically activated macrophages respond to intracellular pathogens by secreting proinflammatory cytokines, chemokines, proteases, and the production of reactive oxygen species [29]. These factors are key signaling molecules that play a significant role in host defense and inflammation. The overproduction of ROS can prompt injury issues that might initiate the inflammation process [30]. Ribeiro et al. reported that flavonoid compounds possessed anti-inflammatory activity by the
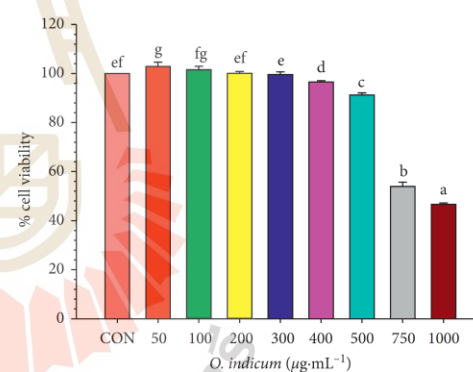

FIGURE 2: Effects of *O. indicum* on cell viability in RAW264.7 cells. Cells were treated with different concentrations of *O. indicum* for 24 h. Cell viability was determined by the MTT assay. CON: cells without *O. indicum*; 50–1,000: cells were treated with *O. indicum* at the concentration range of 50–1,000 μg mL^{-1}. Values are expressed as a percentage of the control. The data represent the mean ± SD of three independent experiments. Bars marked with different letters are significantly different at $p < 0.05$ as determined by one-way ANOVA with Tukey's post hoc test.

modulation of ROS generated through the neutrophils' oxidative burst [31].

Therefore, a flavonoid-enriched extract from *O. indicum* undoubtedly contributes to their anti-inflammatory roles by

scavenging intracellular ROS and thus be useful for preventing the uncontrolled inflammation process. To investigate whether the protective effects of *O. indicum* on the LPS plus IFN-γ-induced inflammatory response were due to a blockade of oxidative stress, the intracellular ROS scavenging potential of *O. indicum* was evaluated in LPS plus IFN-γ-activated RAW264.7 cells. As presented in Figure 3, the treatment of RAW264.7 cells with LPS plus IFN-γ increased ROS accumulation by 1.79-fold compared to unactivated RAW264.7 cells whereas the pretreatment with *O. indicum* significantly inhibited the ROS generation in a dose-dependent manner. Compared to LPS plus IFN-γ-activated RAW264.7 cells, *O. indicum* at a concentration of 50, 100, and 200 μg mL^{-1} reduced intracellular ROS accumulation to 81.08 ± 3.44, 68.16 ± 3.34, and $36.35 \pm 1.62\%$, respectively. The inhibitory effects of *O. indicum* on ROS accumulation at 35% (IC$_{35}$), 40% (IC$_{40}$), and 50% (IC$_{50}$) were determined to be 106.03 ± 5.71, 122.72 ± 4.94, and 156.10 ± 4.36 μg mL^{-1}, respectively. Surprisingly, the intracellular ROS scavenging activity of *O. indicum* (IC$_{50}$, 156.10 ± 4.36 μg mL^{-1}) is, therefore, approximately 3 times more effective than a selective ROS scavenger, NAC (IC$_{50}$, 3 mM or 489.57 μg mL^{-1}). The antioxidant compound, VIT.C, inhibited intracellular ROS by 40% inhibition (IC$_{40}$) at 50 μg mL^{-1}, which was 2.45 times greater than *O. indicum* (IC$_{40}$ = 122.72 ± 4.94 μg mL^{-1}) when compared to the same inhibitory activity. These results suggest that *O. indicum* possesses a vigorous antioxidant activity in scavenging ROS secreted by LPS plus IFN-γ-stimulated in RAW264.7 cells.

Mairuae et al. demonstrated that *O. indicum* treatment attenuated the generation of ROS on Aβ25-35-induced cell injury in human neuroblastoma SH-SY5Y cells [32]. Mohan et al. found that *O. indicum* leaf extract could overcome the oxidative stress induced by 4-NQO in albino Wistar rats when administered orally [33]. These findings lead us to believe that flavonoids present in *O. indicum*, baicalein, quercetin, luteolin, and apigenin may play an important role in protection against oxidative stress.

Base on the LC-MS experiment, the results indicated that *O. indicum* at a concentration of 200 μg mL^{-1} is composed of baicalein of about 5 μg mL^{-1}. In order to clarify whether baicalein could act as an intracellular ROS scavenger or not, baicalein 5 μg mL^{-1} was used as a positive control. The result indicated that baicalein decreased LPS plus IFN-induced intracellular ROS levels by approximately 30%. These data suggest that baicalein in *O. indicum* can scavenge the ROS production of test cells.

Previous investigators demonstrated that baicalein enhanced cellular antioxidant defense capacity in C6 glial cells by inhibiting ROS production and activating the Nrf2 signaling pathway [34]. Qi et al. [35] found that baicalein reduced LPS-induced inflammation via suppressing JAK/STATs activation and ROS production. In addition, baicalein reduced H$_2$O$_2$-induced DNA damage as a result of a decrease in phospho-H2A.X production, DNA tail formation, and lipid peroxidation prevention [36]. Our results indicated that the pretreatment of RAW264.7 cells with *O. indicum* at a concentration of 200 μg mL^{-1} significantly decreased the intracellular ROS accumulation by
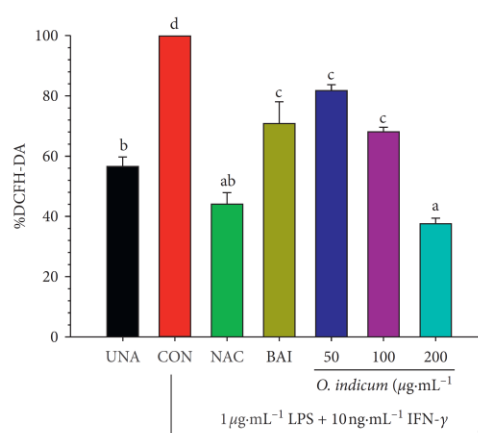

FIGURE 3: Effects of *O. indicum* on the intracellular ROS production in LPS plus IFN-γ-activated RAW264.7 cells. Cells were pretreated with different concentrations of *O. indicum* for 3 h and then activated with LPS plus IFN-γ for 24 h. Cell viability and ROS intensity are expressed as a percentage of the control. UNA: unactivated cells; CON: cells without *O. indicum*; NAC: cells were pretreated with NAC at 3 mM; VIT.C: cells were pretreated with VIT.C at 50 μg mL^{-1}; and 50, 100, and 200: cells were pretreated with *O. indicum* at 50, 100, and 200 μg mL^{-1}, respectively. Values are expressed as a percentage of the control. The data represent the mean ± SD of three independent experiments. Bars marked with different letters are significantly different at $p < 0.05$ as determined by one-way ANOVA with Tukey's post hoc test.

approximately 64%. This finding indicates that *O. indicum* at 200 μg mL^{-1}, which contains baicalein around 5 μg mL^{-1}, shows significantly stronger radical scavenging potency than baicalein alone ($p < 0.05$, Figure 3). The higher potency of *O. indicum* may be due to the other bioactive compounds present in *O. indicum* such as γ-sitosterol, stigmasterol, luteolin, apigenin, and quercetin, which could act as ROS scavenging agents. All compounds above have been shown to possess antioxidant properties. The intracellular ROS scavenging potency of *O. indicum* is more than two times stronger compared to baicalein alone which leads us to believe that synergistic activity could take place between baicalein and other flavonoids or volatile compounds [37].

3.6. Effects of O. indicum on Nitric Oxide (NO) and Proinflammatory Cytokine (IL-6 and TNF-α) Production in LPS plus IFN-γ-Activated RAW264.7 Cells. During inflammation, the macrophages actively participate in the inflammatory response by releasing cytokines (TNF-α, IL-1β, and IL-6), chemokines, and inflammatory mediators (NO, iNOS, PGE$_2$, and COX-2) [38]. The overproduction of these agents contributes to the induction and progression of several inflammatory diseases. Thus, it is crucial to regulate the inflammatory mediators in controlling the inflammatory progression and treating inflammatory disorders.

Nitric oxide (NO) is synthesized by many cell types involved in immunity and inflammation. NO is vital as a toxic defense molecule against infectious organisms. On the other hand, NO reacts rapidly with superoxide to form the more reactive product, peroxynitrite ($ONOO^-$), which can directly react with various biological targets and components of the cell, including lipids, thiols, amino acid residues, DNA bases, and low-molecular-weight antioxidants [39].

Therefore, the anti-inflammatory potential of *O. indicum* on inhibition of NO production was measured after the treatment of *O. indicum* in LPS plus IFN-γ-activated RAW264.7 cells. The anti-inflammatory agent, DEX, was selected to serve as the reference drug. As shown in Figure 4(a), upon LPS plus IFN-γ treatment (CON), NO production was increased with the nitrite level peaking to $54.17 \pm 0.38\,\mu M$. However, pretreatment of cells with the highest concentration ($200\,\mu g\,mL^{-1}$) of *O. indicum* suppressed the production of NO of about 16%, which is precisely the same efficiency as $1\,\mu M$ DEX, compared to the LPS plus IFN-γ-activated group.

Qi et al. reported that baicalein suppressed LPS-induced inflammatory responses in RAW264.7 macrophages via attenuating NO synthesis [35]. Shimizu et al. noted that an equimolar mixture (F-mix) of baicalein, wogonin, and oroxylin A showed a synergistic inhibitory effect on the production of NO in LPS-treated J774.1 cells [40]. Also, a mixture of β-sitosterol and stigmasterol isolated from *Andrographis paniculata* significantly suppressed NO production in LPS/IFN-γ stimulated RAW264.7 cells [41].

Both IL-6 and TNF-α are essential proinflammatory cytokines, either of which can serve as an indicator of inflammation. To confirm the anti-inflammatory effect of *O. indicum,* we also investigated the inhibitory effect of *O. indicum* on proinflammatory cytokine secretion by measuring IL-6 and TNF-α levels in RAW264.7 cells activated by LPS plus TNF-α. Exposure of the cells with LPS plus IFN-γ strongly activated the secretion of IL-6 and TNF-α compared to the unactivated group (Figures 4(b) and 4(c)) [42]. The results showed that DEX markedly reduced the secretion of IL-6 and TNF-α of about 69.34% and 62.02%, respectively, compared to the LPS plus IFN-γ-activated group. Treatment with *O. indicum* inhibited the secretion of IL-6 in a dose-dependent manner (Figure 4(b)), but it did not affect the reduction of TNF-α level ($p > 0.05$, Figure 4(c)). The concentration of *O. indicum* at $200\,\mu g\,mL^{-1}$ exerted an IL-6 inhibition by 62.99%, which was practically similar to the reference drug, DEX (69.34% inhibition).

Other researchers had demonstrated that the ethyl acetate extract derived from the stem bark of *O. indicum* showed the inhibitory effect on LPS-induced IL-6, IL-1β, and TNF-α release in human monocytes [7]. *In vivo* study indicated that the aqueous decoction of both stem bark and root bark of *O. indicum* produced anti-inflammatory activity by reducing paw edema formation in the carrageenan-induced paw edema model [42]. Furthermore, flavonoids found in this plant, such as baicalein, apigenin, oroxylin A, and luteolin, are known for their anti-inflammatory effects attributed at least partially through the suppression of proinflammatory cytokines, IL-6, IL-1β, and TNF-α [43].

Moreover, it had been reported that a mixture of β-sitosterol and stigmasterol isolated from *Andrographis paniculata* significantly decreased TNF-α and IL-6 secretion from LPS/IFN-γ-stimulated RAW264.7 cells [41]. These findings provide evidence that the main constituents of *O. indicum* are flavonoids and phytosterols, which could potentially act as the anti-inflammatory compounds of this plant.

Differential effects of *O. indicum* on IL-6 and TNF-α production in RAW264.7 cells could be explained by the different mechanisms of *O. indicum* on the secretion of IL-6 and those of TNF-α alleviation. Several studies reported that the mechanism, signaling pathways, and transcription factors controlling TNF-α expression were distinct from those of IL-6 [44–46]. It had been reported that the activation of p38 MAPK was required for the LPS/TLR4-induced expression of TNF-α, but not IL-6 [44]. It is well known that CREB recognizes a similar DNA binding sequence in the promoter region of the TNF-α gene [47]. In contrast, similar sequences have not been identified on the IL-6 and IL-1 promoters. Also, the STAT3 tyrosine phosphorylation is a key role to induce IL-6 production in response to inflammation. *In vitro* study revealed that the blocking STAT3 activity preferred to inhibit LPS-mediated production of IL-1β and IL-6, but not TNF-α, in RAW264.7 cells [46]. The study of Prêle et al. also confirmed that the STAT3 activation did not directly regulate LPS-induced TNF-α production in human monocytes [48].

3.7. Effects of O. indicum on the Morphology of LPS plus IFN-γ-Activated RAW264.7 Cells.

RAW264.7 cells were pretreated with different concentrations of *O. indicum* for 3 h and then activated by LPS plus IFN-γ for another 24 h. Morphology change of RAW264.7 cells was observed under microscopy, as shown by haematoxylin staining (Figure 5). The unactivated RAW264.7 cells showed the round morphology, whereas LPS plus IFN-γ-activated RAW264.7 cells showed enlargement, dendritic, spindle, and spheres, which were the phenotype features of activated macrophages [49]. The previous study indicated that the morphological changes of adherent macrophages were associated with their secretion of inflammatory cytokines [50]. These cells treated with *O. indicum* at $200\,\mu g\,mL^{-1}$ displayed less activated macrophage phenotypes than activated RAW264.7 cells, DEX- and *O. indicum* treated at 50 and $100\,\mu g\,mL^{-1}$.

3.8. Effects of O. indicum on Biomolecular Changing Detected by SR-FTIR.

We found that the extract of *O. indicum* possessed antioxidant potential by scavenging intracellular ROS, anti-inflammatory activity, and suppressing proinflammatory mediators (NO) and cytokine secretion (IL-6) in LPS plus IFN-γ-activated RAW264.7 cells. The SR-FTIR investigation was conducted to determine the effect of *O. indicum* on the cellular biochemical alterations in LPS plus IFN-γ-activated RAW264.7 cells.

The average original FTIR spectrum bands of unactivated RAW264.7 cells, activated RAW264.7 cells, and activated RAW264.7 cells treated with *O. indicum* ($200\,\mu g\,mL^{-1}$) or DEX ($1\,\mu M$) are displayed in Figure 6(a).
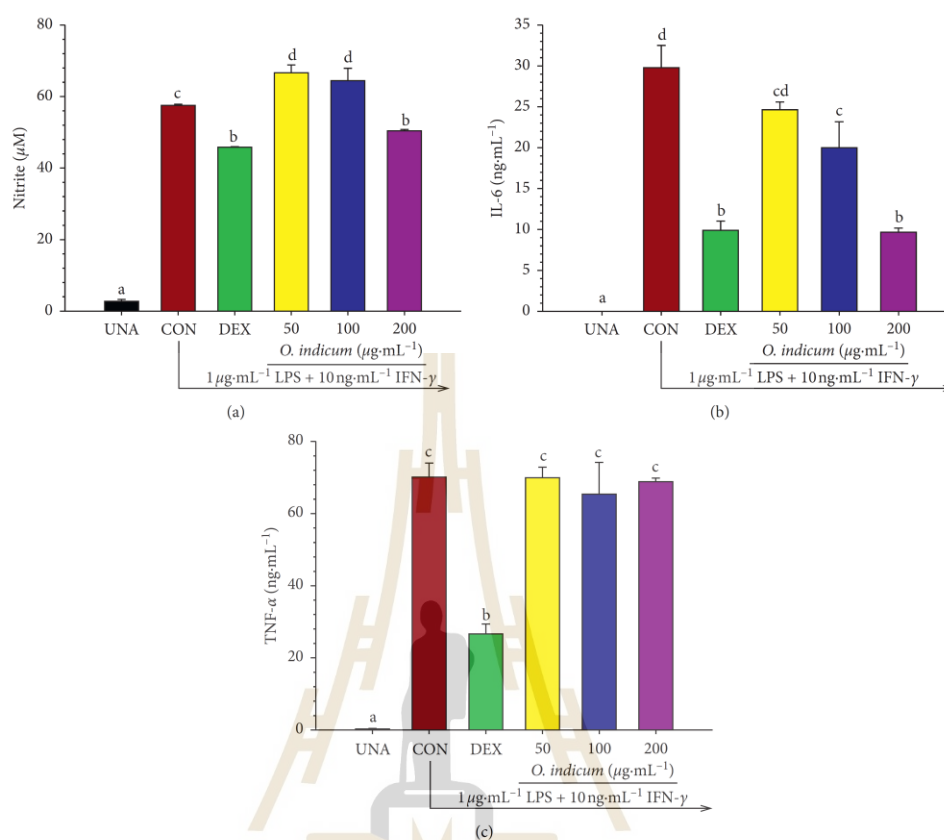
FIGURE 4: Effects of *O. indicum* on (a) NO production, (b) proinflammatory cytokines IL-6, and (c) TNF-α secretion in LPS plus IFN-γ-activated RAW264.7 cells. Cells were pretreated with different concentrations of *O. indicum* for 3 h and then activated with LPS plus IFN-γ for 24 h UNA: unactivated cells; CON: cells without *O. indicum*; DEX: cells were pretreated with DEX at 1 μM; 50, 100, and 200: cells were pretreated with *O. indicum* at 50, 100, and 200 μg mL^{-1}, respectively. The data represent the mean ± SD of three independent experiments. Bars marked with different letters are significantly different at $p < 0.05$ as determined by one-way ANOVA with Tukey's post hoc test.

The raw spectrum was more useful to perform the second derivative analysis in spectral regions ranging from 3,000 to 2800 cm^{-1} for lipid regions and from 1800 to 1400 cm^{-1} for protein regions, as shown in Figure 6(b). The signal intensity and area of the peaks of protein and lipid regions of these groups are calculated and shown in Figure 6(c). Moreover, the FTIR band assignments are shown in Table 3.

The change in cellular lipid was observed in the mainly lipid region (3000–2800 cm^{-1}). The average second derivative spectra of RAW264.7 cells under different experimental conditions exhibited three specific regions at 2960 cm^{-1}, 2921 cm^{-1}, and 2850 cm^{-1}, which are assigned to the asymmetrical stretching vibrations of the CH$_3$ and CH$_2$ groups of the phospholipids membrane and CH$_2$ symmetric stretching, respectively (Figure 6(b)). The relative absorbance at 2960 cm^{-1}, 2921 cm^{-1}, and 2850 cm^{-1} in activated RAW264.7 cells, DEX-, or *O. indicum*-treated activated

RAW264.7 cells was higher than that in the unactivated RAW264.7 cells. The integrated areas of lipid regions of the second derivative spectra were calculated for unactivated and treated activated RAW264.7 cells in order to quantify the lipid content [49]. The results exhibited that the integrated area of the lipid region was significantly increased in activated RAW264.7 cells, DEX-, and *O. indicum*-treated activated RAW264.7 cells compared to the unactivated RAW264.7 cells ($p < 0.05$). The increase of lipid regions in LPS plus IFN-γ-activated RAW264.7 cells under three different experimental conditions could be related to cell membrane changes. The changes in the membrane are due to phenotype features of activated macrophage, including enlargement, dendritic, and spherical features (Figure 5), which developed in response to the inflammatory inducer during inflammation [49]. Moreover, these results are consistent with Funk et al.'s study [51] showing that the
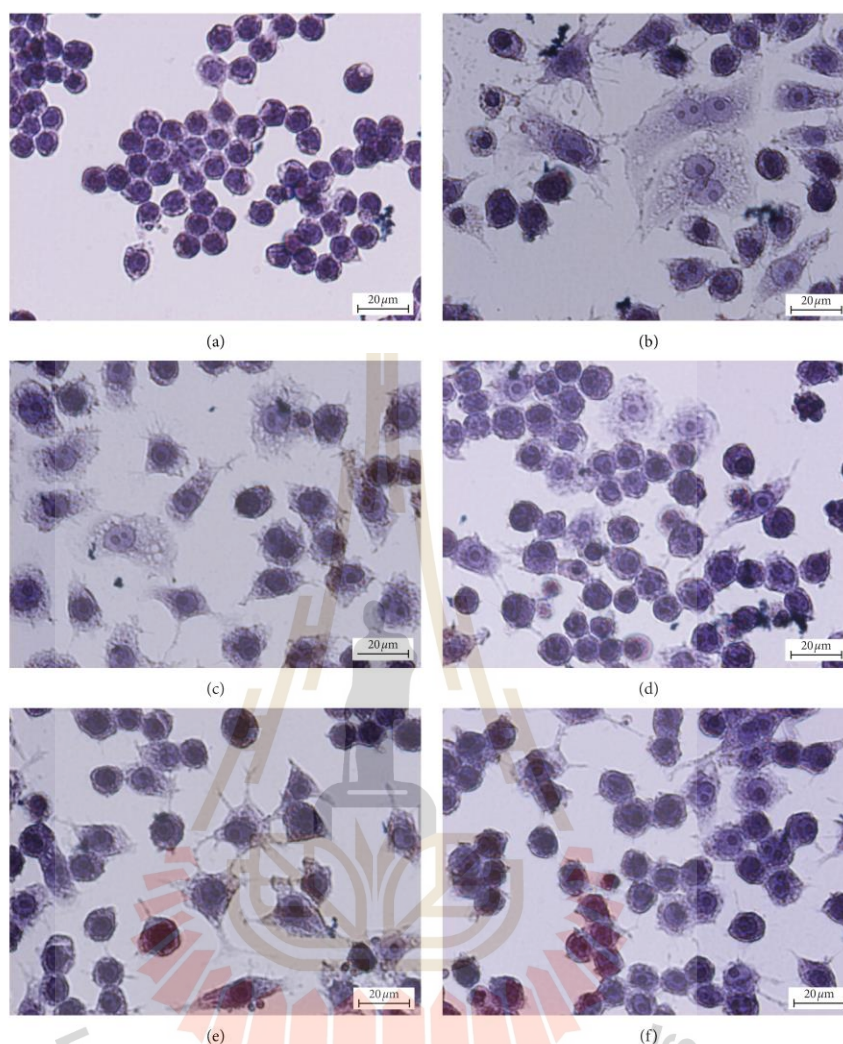
Figure 5: Effects of *O. indicum* on the morphology of LPS plus IFN-γ-activated RAW264.7 cells. Haematoxylin staining of 6 different groups of the sample. a: unactivated RAW264.7 cells; b: activated RAW264.7 cells (cells without *O. indicum*); c: cells were pretreated with DEX at $1\,\mu$M; d, e, and f: cells were pretreated with *O. indicum* at 50, 100, and $200\,\mu$g mL^{-1}, respectively (original magnification at ×400, scale bar; $20\,\mu$m).

activation of RAW264.7 macrophages enhances their ability to accumulate lipid from a variety of lipid molecules and to become foam cells.

The cellular protein change was observed within $1800\,\text{cm}^{-1}$ and $1400\,\text{cm}^{-1}$ interval, reflecting the vibrations of the amide I (1700–$1600\,\text{cm}^{-1}$) and amide II (1600–$1400\,\text{cm}^{-1}$) (Figure 6(b)). In unactivated RAW264.7 cells, a strong peak at $1655\,\text{cm}^{-1}$ and $1545\,\text{cm}^{-1}$ assigned to stretching vibrations of α-helix secondary protein structure displayed higher signal intensity than other groups. These

results are in accordance with the integrated areas of the protein regions where the protein content in unactivated RAW264.7 cells is significantly greater than that in the activated RAW264.7 cells and DEX- or *O. indicum*-treated activated RAW264.7cells ($p < 0.05$, Figure 6(c)). Thus, these results reflect the altered cellular protein profile in all treated groups of LPS plus IFN-γ-activated RAW264.7 cells compared to unactivated RAW264.7 cells. Upon treatment of cells with *O. indicum*, the protein content was significantly increased compared to LPS plus IFN-γ-activated RAW264.7
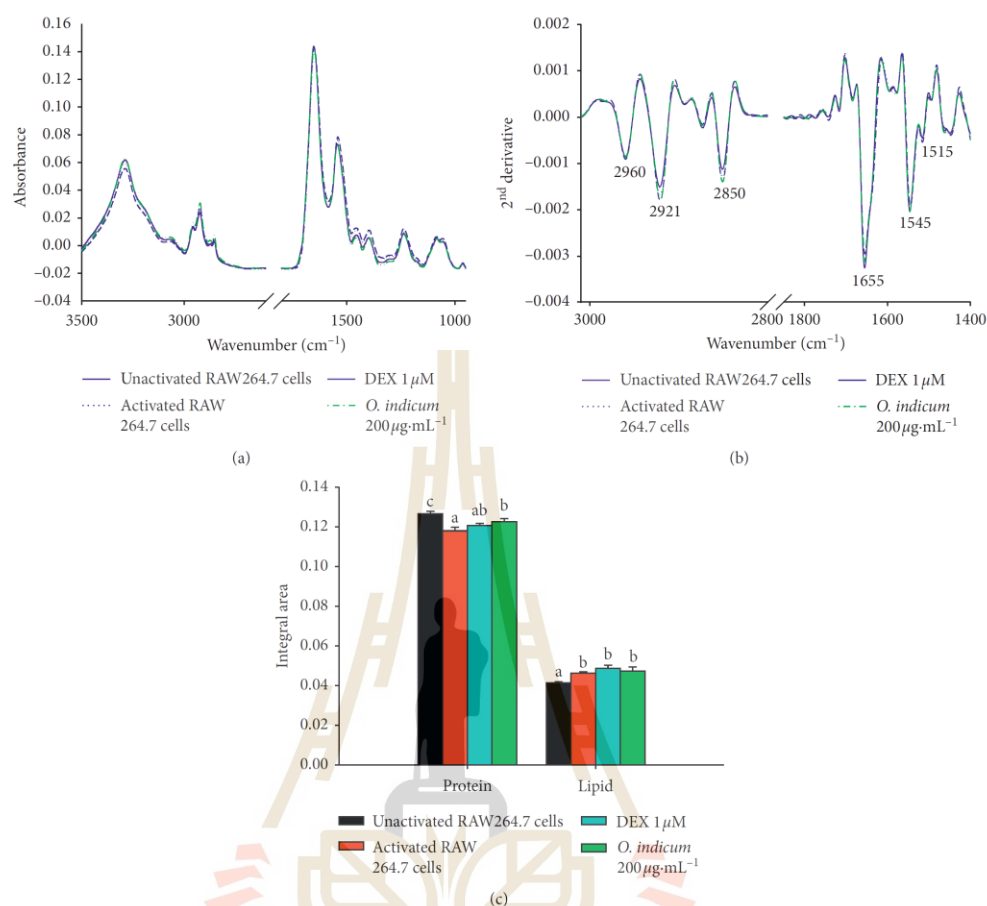
Evidence-Based Complementary and Alternative Medicine 11

FIGURE 6: Effects of *O. indicum* on biomolecular changes detected by FTIR. (a) Average original FTIR spectra (3500–950 cm^{-1}). (b) Average the secondary derivative spectra of lipid regions (3000–2800 cm^{-1}) and protein regions (1800–1400 cm^{-1}). (c) The bar graph of integrated areas of lipid regions (3000–2800 cm^{-1}) and protein regions (1800–1400 cm^{-1}). The data obtained from unactivated RAW264.7 cells ($n = 120$), activated RAW264.7 (LPS plus IFN-γ) ($n = 120$), and activated RAW264.7 (LPS plus IFN-γ) exposed to 1 μM DEX ($n = 157$) or 200 μg mL^{-1} of *O. indicum* ($n = 135$). Data are represented as means ± SD for three replicates. Bars marked with different letters are significantly different at $p < 0.05$ as determined by one-way ANOVA with Tukey's post hoc test.

TABLE 3: FTIR band assignments.

Band position of 2nd derivative spectra (cm^{-1})	Assignments
2960	CH$_3$ stretch (antisymmetric) due to methyl terminal of membrane phospholipids
2921	CH$_2$ antisymmetric stretch of methylene group of membrane phospholipids
2850	CH$_2$ symmetric stretching: mainly lipids
1655	Amide I: C=O (80%) and C–N (10%) stretching, N–H (10%) bending vibrations: Proteins α-helix
1545	Amide II: N–H (60%) bending and C–N (40%) stretching vibrations: proteins α-helix

cells ($p < 0.05$). These results suggest that *O. indicum* treatment could protect the molecule of proteins, probably because of their antioxidant potential. Excessive production of reactive oxygen species is frequently observed during the inflammatory response, causing the oxidation of proteins, lipid peroxidation, nucleic acid destruction, and enzyme
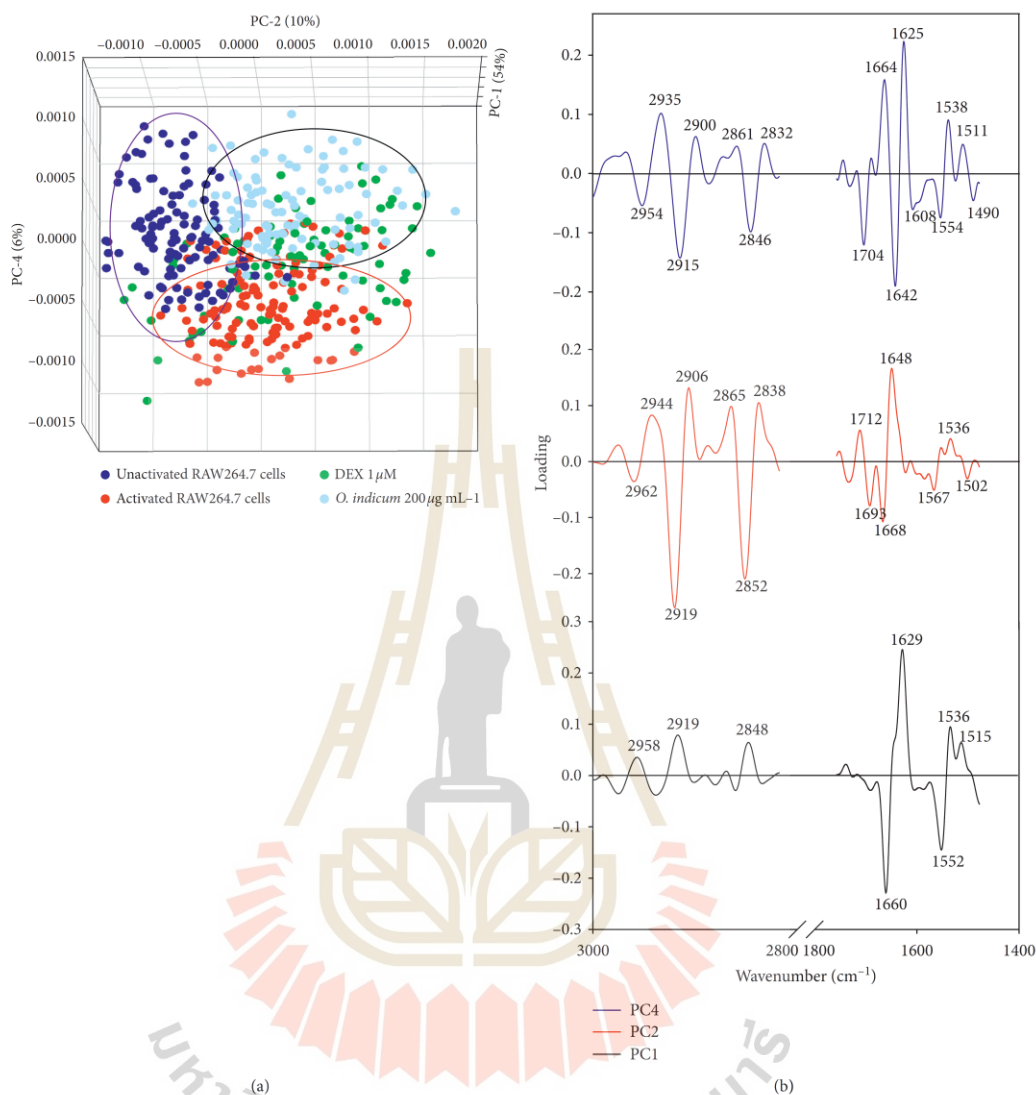
Figure 7: PCA analysis of FTIR spectral range 3000–2800 cm^{-1} and 1800–1400 cm^{-1} giving (a) PCA 3D score plot and (b) PCA loading plot. PCA score plots showed distinct clustering between unactivated RAW264.7 cells ($n = 120$), activated RAW264.7 (LPS plus IFN-γ) ($n = 120$), and activated RAW264.7 (LPS plus IFN-γ) exposed to $1\,\mu$M DEX ($n = 157$) or $200\,\mu$g mL^{-1} of *O. indicum* ($n = 135$). PCA loading plots identify biomarker differences over a spectral range of samples.

inhibition [52]. Accordingly, the oxidized proteins thus become better targets for proteolytic digestion by the 20S proteasomes and, consequently, decrease the levels of the proteins in general [53]. Flavonoids play an important role as a ROS scavenger by locating and neutralizing radicals before they damage the cell structure [54]. Therefore, the flavonoid-enriched extract from *O. indicum* could protect proteins from oxidation under oxidative stress, and

proteolytic digestion leads to an increase in cellular protein contents.

However, there was no significant difference between the FTIR spectra of unactivated RAW264.7 cells and other groups in nucleic acid regions (1,300–900 cm^{-1}) (data are not shown). The data indicated that the selected concentration of *O. indicum* did not produce any effect on nucleic acids (DNA and RNA base) of the cells, which was consistent with

its cytotoxicity evaluation by using MTT assay. Supporting our results, Zelig et al. reported that a decrease in DNA absorbance was associated with apoptotic cell death, by contrast, to increase during necrotic cell death [55].

In order to discriminate the distinct clustering of spectra from the four cell populations, PCA analysis was performed to identify which wavenumbers in the FTIR spectra complex showed the largest spectral variation within the sample. The 3-dimensional PCA clustering results from FTIR spectral data of unactivated RAW264.7 cells, activated RAW264.7 cells, and activated RAW264.7 cells after treatment with DEX or *O. indicum* are displayed in Figure 7(a). The PCA score plot demonstrated that the clusters of unactivated RAW264.7 cells and *O. indicum*-treated activated RAW264.7 cells were separated from activated RAW264.7 cells and DEX-treated activated RAW264.7 cells along PC1 (54%) and PC4 (6%) whereas the clusters of unactivated RAW264.7 cells were distinguished from *O. indicum*-treated activated RAW264.7 cells along PC2 (10%). The PCA loading plots (Figure 7(b)) were used to identify the regions of the spectrum, which most contributed to the clustering. The positive score of the spectra of the unactivated RAW264.7 cells and *O. indicum*-treated activated RAW264.7 cells was clearly separated from the negative score of the spectra of the other two groups along with PC1 score plot, which displayed remarkably high negative PC1 loadings at $1660\,cm^{-1}$ and $1552\,cm^{-1}$ (suggesting an α-helix protein structure of amide I and amide II, respectively). PC2 loading plot was discriminated by the negative loading spectra at $2919\,cm^{-1}$ and $2852\,cm^{-1}$ caused by the C-H stretching assigned to the lipids and at $1693\,cm^{-1}$ and $1668\,cm^{-1}$ resulting from the α-helix protein structure of amide I, which separated the positive score of DEX-treated activated RAW264.7 cells from the negative score of the unactivated RAW264.7 cells. The amide I band from proteins at $1642\,cm^{-1}$ (assigned to the α-helix structure) and the C-H stretching region (assigned to the lipids) were heavily loaded for PC4 which separated the positive score of the spectra of the unactivated RAW264.7 cells and *O. indicum*-treated activated RAW264.7 cells from the negative score of the spectra of the activated RAW264.7 cells and DEX-treated activated RAW264.7 cells. These results are consistent with its second derivative spectra and the integrated areas of protein and lipid regions.

4. Conclusions

In conclusion, these findings provide evidence that *O. indicum* could possess the antioxidant and anti-inflammatory effects in LPS plus IFN-γ-activated RAW264.7 cells by scavenging intracellular ROS, reducing NO and IL-6 secretion, respectively. These pharmacological properties of *O. indicum* may occur from the synergistic interaction between its flavonoids and phytosterol components. These results also provide the first evidence of the potential use of SR-FTIR microspectroscopy to evaluate the biochemical profile alteration of activated RAW264.7 macrophages. Therefore, *O. indicum* may be used as a potential source of nutraceutical for the development of health food supplement or a novel

anti-inflammatory herbal medicine to alleviate the excessive inflammatory response.

Data Availability

The datasets used and analyzed during this study are available from the corresponding author upon reasonable request.

Conflicts of Interest

The authors declare that there are no conflicts of interest regarding the publication of this manuscript.

Acknowledgments

References

[1] C. R. H. Raetz, R. I. Ulevitch, S. D. Wright, C. H. Sibley, A. Ding, and C. F. Nathan, "Gram-negative endotoxin: an extraordinary lipid with profound effects on eukaryotic signal transduction 1," *The FASEB Journal*, vol. 5, no. 12, pp. 2652–2660, 1991.

[2] T.-L. Chen, C.-C. Chang, Y.-L. Lin, Y.-F. Ueng, and R.-M. Chen, "Signal-transducing mechanisms of ketamine-caused inhibition of interleukin-1β gene expression in lipopolysaccharide-stimulated murine macrophage-like Raw 264.7 cells," *Toxicology and Applied Pharmacology*, vol. 240, no. 1, pp. 15–25, 2009.

[3] J. B. Calixto, M. F. Otuki, and A. R. Santos, "Anti-inflammatory compounds of plant origin. Part I. Action on arachidonic acid pathway, nitric oxide and nuclear factor κB (NF-κB)," *Planta Medica*, vol. 69, no. 11, pp. 973–983, 2003.

[4] M. Ye, Q. Wang, W. Zhang, Z. Li, Y. Wang, and R. Hu, "Oroxylin A exerts anti-inflammatory activity on lipopolysaccharide-induced mouse macrophage via Nrf2/ARE activation," *Biochemistry and Cell Biology*, vol. 92, no. 5, pp. 337–348, 2014.

[5] B. N. Ames and P. Wakimoto, "Are vitamin and mineral deficiencies a major cancer risk?" *Nature Reviews Cancer*, vol. 2, no. 9, pp. 694–704, 2002.

[6] N. Khansari, Y. Shakiba, and M. Mahmoudi, "Chronic inflammation and oxidative stress as a major cause of age-related diseases and cancer," *Recent Patents on Inflammation & Allergy Drug Discovery*, vol. 3, no. 1, pp. 73–80, 2009.

[7] N. Siriwatanametanon, B. L. Fiebich, T. Efferth, J. M. Prieto, and M. Heinrich, "Traditionally used Thai medicinal plants: in vitro anti-inflammatory, anticancer and antioxidant activities," *Journal of Ethnopharmacology*, vol. 130, no. 2, pp. 196–207, 2010.

[8] R. Bhat, N. A. Shaharuddin, and Y. T. Kuang, "A promising approach toward exploring nutritional and functional qualities of beko (oroxylum indicum L. Benth. Ex Kurz) pods for potential food applications," *Journal of Food Processing and Preservation*, vol. 39, no. 1, pp. 47–55, 2015.

[9] B. Dinda, I. SilSarma, M. Dinda, and P. Rudrapaul, "*Oroxylum indicum* (L.) Kurz, an important Asian traditional medicine: from traditional uses to scientific data for its commercial exploitation," *Journal of Ethnopharmacology*, vol. 161, pp. 255–278, 2015.

[10] S. V. Joshi, B. A. Vyas, P. D. Shah, D. R. Shah, S. A. Shah, and T. R. Gandhi, "Protective effect of aqueous extract of *Oroxylum indicum* Linn.(root bark) against DNBS-induced colitis in rats," *Indian Journal of Pharmacology*, vol. 43, no. 6, p. 656, 2011.

[11] J. Singh and P. Kakkar, "Modulation of liver function, antioxidant responses, insulin resistance and glucose transport by *Oroxylum indicum* stem bark in STZ induced diabetic rats," *Food and Chemical Toxicology*, vol. 62, pp. 722–731, 2013.

[12] S. Menon, L. Lawrence, V. P. Sivaram, and J. Padikkala, "*Oroxylum indicum* root bark extract prevents doxorubicin-induced cardiac damage by restoring redox balance," *Journal of Ayurveda and Integrative Medicine*, vol. 10, no. 3, pp. 159–165, 2019.

[13] B. Dunkhunthod, K. Thumanu, and G. Eumkeb, "Application of FTIR microspectroscopy for monitoring and discrimination of the anti-adipogenesis activity of baicalein in 3T3-L1 adipocytes," *Vibrational Spectroscopy*, vol. 89, pp. 92–101, 2017.

[14] T. Hengpratom, G. M. Lowe, K. Thumanu, S. Suknasang, K. Tiamyom, and G. Eumkeb, "*Oroxylum indicum* (L.) Kurz extract inhibits adipogenesis and lipase activity *in vitro*," *BMC Complementary and Alternative Medicine*, vol. 18, no. 1, p. 177, 2018.

[15] S. Siriwong, T. Pimchan, W. Naknarong, and G. Eumkeb, "Mode of action and synergy of ceftazidime and baicalein against *Streptococcus pyogenes*," *Tropical Journal of Pharmaceutical Research*, vol. 14, no. 4, pp. 641–648, 2015.

[16] S. Machana, N. Weerapreeyakul, S. Barusrux, K. Thumanu, and W. Tanthanuch, "FTIR microspectroscopy discriminates anticancer action on human leukemic cells by extracts of *Pinus kesiya; Cratoxylum formosum* ssp. pruniflorum and melphalan," *Talanta*, vol. 93, pp. 371–382, 2012.

[17] J. K. Pijanka, D. Kumar, T. Dale et al., "Vibrational spectroscopy differentiates between multipotent and pluripotent stem cells," *The Analyst*, vol. 135, no. 12, pp. 3126–3132, 2010.

[18] A. Marcelli and G. Cinque, "Synchrotron Radiation InfraRed microspectroscopy and imaging in the characterization of archaeological materials and cultural heritage artefacts," *The Contribution of Mineralogy to Cultural Heritage*, vol. 20, pp. 411–444, 2019.

[19] L. Vaccari, G. Birarda, G. Grenci, S. Pacor, and L. Businaro, "Synchrotron radiation infrared microspectroscopy of single living cells in microfluidic devices: advantages, disadvantages and future perspectives," *Journal of Physics: Conference Series*, vol. 359, no. 1, Article ID 012007, 2012.

[20] S. Sabbatini, C. Conti, G. Orilisi, and E. Giorgini, "Infrared spectroscopy as a new tool for studying single living cells: is there a niche?" *Biomedical Spectroscopy and Imaging*, vol. 6, no. 3-4, pp. 85–99, 2017.

[21] H. V. Rupasinghe, L. Wang, G. M. Huber, and N. L. Pitts, "Effect of baking on dietary fibre and phenolics of muffins incorporated with apple skin powder," *Food Chemistry*, vol. 107, no. 3, pp. 1217–1224, 2008.

[22] H. Yang, Y. Dong, H. Du, H. Shi, Y. Peng, and X. Li, "Antioxidant compounds from propolis collected in Anhui, China," *Molecules*, vol. 16, no. 4, pp. 3444–3455, 2011.

[23] P. Sittisart and B. Chitsomboon, "Intracellular ROS scavenging activity and downregulation of inflammatory mediators in RAW264. 7 macrophage by fresh leaf extracts of *Pseuderanthemum palatiferum*," *Evidence-Based Complementary and Alternative Medicine*, vol. 2014, Article ID 309095, 11 pages, 2014.

[24] P. Sittisart, B. Chitsomboon, and N. E. Kaminski, "Pseuderanthemum palatiferum leaf extract inhibits the proinflammatory cytokines, TNF-α and IL-6 expression in LPS-activated macrophages," *Food and Chemical Toxicology*, vol. 97, pp. 11–22, 2016.

[25] M. A. Gómez, M. T. Sáenz, M. D. García, and M. A. Fernández, "Study of the topical anti-inflammatory activity of *Achillea ageratum* on chronic and acute inflammation models," *Zeitschrift für Naturforschung C*, vol. 54, no. 11, pp. 937–941, 1999.

[26] Y. J. Moon, X. Wang, and M. E. Morris, "Dietary flavonoids: effects on xenobiotic and carcinogen metabolism," *Toxicology in Vitro*, vol. 20, no. 2, pp. 187–210, 2006.

[27] P. Saha, P. R. Choudhury, S. Das, A. D. Talukdar, and M. D. Choudhury, "*In vitro* antioxidant activity of bark extracts of *Oroxylum indicum* (L) vent," *Asian Journal of Pharmaceutical and Clinical Research*, vol. 10, no. 8, pp. 263–266, 2017.

[28] D. H. T. Trang, H. L. Son, and P. V. Trung, "Investigation on the *in vitro* antioxidant capacity of methanol extract, fractions and flavones from *Oroxylum indicum* Linn bark," *Brazilian Journal of Pharmaceutical Sciences*, vol. 54, no. 1, 2018.

[29] O. A. Castaneda, S.-C. Lee, C.-T. Ho, and T.-C. Huang, "Macrophages in oxidative stress and models to evaluate the antioxidant function of dietary natural compounds," *Journal of Food and Drug Analysis*, vol. 25, no. 1, pp. 111–118, 2017.

[30] N. Yahfoufi, N. Alsadi, M. Jambi, and C. Matar, "The immunomodulatory and anti-inflammatory role of polyphenols," *Nutrients*, vol. 10, no. 11, p. 1618, 2018.

[31] D. Ribeiro, M. Freitas, S. M. Tomé, A. M. S. Silva, G. Porto, and E. Fernandes, "Modulation of human neutrophils' oxidative burst by flavonoids," *European Journal of Medicinal Chemistry*, vol. 67, pp. 280–292, 2013.

[32] N. Mairuae, J. R. Connor, B. Buranrat, and S. Y. Lee, "*Oroxylum indicum* (L.) extract protects human neuroblastoma SH-SY5Y cells against β-amyloid-induced cell injury," *Molecular Medicine Reports*, vol. 20, no. 2, pp. 1933–1942, 2019.

[33] S. Mohan, K. Thiagarajan, B. Sundaramoorthy et al., "Alleviation of 4-nitroquinoline 1-oxide induced oxidative stress by *Oroxylum indicum* (L.) leaf extract in albino Wistar rats," *BMC Complementary and Alternative Medicine*, vol. 16, no. 1, p. 229, 2016.

[34] E.-O. Choi, J.-W. Jeong, C. Park et al., "Baicalein protects C6 glial cells against hydrogen peroxide-induced oxidative stress and apoptosis through regulation of the Nrf2 signaling pathway," *International Journal of Molecular Medicine*, vol. 37, no. 3, pp. 798–806, 2016.

[35] Z. Qi, F. Yin, L. Lu et al., "Baicalein reduces lipopolysaccharide-induced inflammation via suppressing JAK/STATs activation and ROS production," *Inflammation Research*, vol. 62, no. 9, pp. 845–855, 2013.

[36] K. A. Kang, R. Zhang, M. J. Piao et al., "Baicalein inhibits oxidative stress-induced cellular damage via antioxidant effects," *Toxicology and Industrial Health*, vol. 28, no. 5, pp. 412–421, 2012.

[37] G. Eumkeb, S. Tanphonkrang, K. Sirichaiwetchakoon, T. Hengpratom, and W. Naknarong, "The synergy effect of daidzein and genistein isolated from *Butea superba* Roxb. on

the reproductive system of male mice," *Natural Product Research*, vol. 31, no. 6, pp. 672–675, 2017.

[38] M. Adib-Conquy, D. Scott-Algara, J. M. Cavaillon, and F. Souza-Fonseca-Guimaraes, "TLR-mediated activation of NK cells and their role in bacterial/viral immune responses in mammals," *Immunology and Cell Biology*, vol. 92, no. 3, pp. 256–262, 2014.

[39] J. N. Sharma, A. Al-Omran, and S. S. Parvathy, "Role of nitric oxide in inflammatory diseases," *Inflammopharmacology*, vol. 15, no. 6, pp. 252–259, 2007.

[40] T. Shimizu, N. Shibuya, Y. Narukawa, N. Oshima, N. Hada, and F. Kiuchi, "Synergistic effect of baicalein, wogonin and oroxylin A mixture: multistep inhibition of the NF-κB signalling pathway contributes to an anti-inflammatory effect of Scutellaria root flavonoids," *Journal of Natural Medicines*, vol. 72, no. 1, pp. 181–191, 2018.

[41] W.-W. Chao, Y.-H. Kuo, and B.-F. Lin, "Anti-inflammatory activity of new compounds from Andrographis paniculata by NF-κB transactivation inhibition," *Journal of Agricultural and Food Chemistry*, vol. 58, no. 4, pp. 2505–2512, 2010.

[42] K. Doshi, R. Ilanchezhian, R. Acharya, B. Patel, and B. Ravishankar, "Anti-inflammatory activity of root bark and stem bark of Shyonaka," *Journal of Ayurveda and Integrative Medicine*, vol. 3, no. 4, p. 194, 2012.

[43] J. Y. Lee and W. Park, "Anti-inflammatory effects of oroxylin A on RAW 264.7 mouse macrophages induced with poly-inosinic-polycytidylic acid," *Experimental and Therapeutic Medicine*, vol. 12, no. 1, pp. 151–156, 2016.

[44] N. J. Horwood, T. H. Page, J. P. McDaid et al., "Bruton's tyrosine kinase is required for TLR2 and TLR4-induced TNF, but not IL-6, production," *The Journal of Immunology*, vol. 176, no. 6, pp. 3635–3641, 2006.

[45] C. J. Greenhill, S. Rose-John, R. Lissilaa et al., "IL-6 trans-signaling modulates TLR4-dependent inflammatory responses via STAT3," *The Journal of Immunology*, vol. 186, no. 2, pp. 1199–1208, 2011.

[46] L. Samavati, R. Rastogi, W. Du, M. Hüttemann, A. Fite, and L. Franchi, "STAT3 tyrosine phosphorylation is critical for interleukin 1 beta and interleukin-6 production in response to lipopolysaccharide and live bacteria," *Molecular Immunology*, vol. 46, no. 8-9, pp. 1867–1877, 2009.

[47] P. M. O'Donnell and S. M. Taffet, "The proximal promoter region is essential for lipopolysaccharide induction and cyclic AMP inhibition of mouse tumor necrosis factor-α," *Journal of Interferon & Cytokine Research*, vol. 22, no. 5, pp. 539–548, 2002.

[48] C. M. Prêle, A. L. Keith-Magee, M. Murcha, and P. H. Hart, "Activated signal transducer and activator of transcription-3 (STAT3) is a poor regulator of tumour necrosis factor-α production by human monocytes," *Clinical & Experimental Immunology*, vol. 147, no. 3, pp. 564–572, 2007.

[49] J. L. Shepard and L. I. Zon, "Developmental derivation of embryonic and adult macrophages," *Current Opinion in Hematology*, vol. 7, no. 1, pp. 3–8, 2000.

[50] H.-S. Lee, S. J. Stachelek, N. Tomczyk, M. J. Finley, R. J. Composto, and D. M. Eckmann, "Correlating macrophage morphology and cytokine production resulting from biomaterial contact," *Journal of Biomedical Materials Research Part A*, vol. 101A, no. 1, pp. 203–212, 2013.

[51] J. L. Funk, K. R. Feingold, A. H. Moser, and C. Grunfeld, "Lipopolysaccharide stimulation of RAW 264.7 macrophages induces lipid accumulation and foam cell formation," *Atherosclerosis*, vol. 98, no. 1, pp. 67–82, 1993.

[52] H. A. H. M. A. El-Aal, "Lipid peroxidation end-products as a key of oxidative stress: effect of antioxidant on their production and transfer of free radicals," in *Lipid Peroxidation: IntechOpen in the Fields of Science, Technology and Medicine*, vol. 3, pp. 63–68, IntechOpen, London, UK, 2012.

[53] F. Di Domenico, E. Head, D. A. Butterfield, and M. Perluigi, "Oxidative stress and proteostasis network: culprit and casualty of Alzheimer's-like neurodegeneration," *Advances in Geriatrics*, vol. 2014, 2014.

[54] P. Kovacic and R. Somanathan, "Cell signaling and receptors with resorcinols and flavonoids: redox, reactive oxygen species, and physiological effects," *Journal of Receptors and Signal Transduction*, vol. 31, no. 4, pp. 265–270, 2011.

[55] U. Zelig, J. Kapelushnik, R. Moreh, S. Mordechai, and I. Nathan, "Diagnosis of cell death by means of infrared spectroscopy," *Biophysical Journal*, vol. 97, no. 7, pp. 2107–2114, 2009.

CURRICULUM VITAE

Name   Miss Benjawan Dunkhunthod

Date of Birth   December, 20 1987

Place of Birth Nakhon Ratchasima, Thailand

Education

2010-2014: Master of Science (Biomedical Sciences), Suranaree University of Technology, Nakhon Ratchasima, Thailand

2006-2009: Bachelor of Science (Environmental Health) (First Class Honors), Suranaree University of Technology, Nakhon Ratchasima, Thailand

Scholarships

2017-Present: The Royal Golden Jubilee Ph.D. Program, The Thailand Research Fund, Thailand

Publications

Dunkhunthod, B., Talabnin, C., Murphy, M., Thumanu, K., Sittisart, P., and Eumkeb, G. (2021). *Gymnema inodorum* (Lour.) Decne. Extract Alleviates Oxidative Stress and Inflammatory Mediators Produced by RAW264. 7 Macrophages. *Oxidative medicine and cellular longevity. 2021*: *8658314*. (Impact Factor 2020 = 5.60; SCOPUS SJR 2020 = Q1, Web of Sci JCR 2020 = Q2).

Dunkhunthod, B., Talabnin, C., Murphy, M., Thumanu, K., Sittisart, P., Hengpratom, T., and Eumkeb, G. (2020). Intracellular ROS scavenging and anti-Inflammatory activities of *Oroxylum indicum* Kurz (L.) extract in LPS plus IFN-γ-activated RAW264.7 macrophages. *Evidence-Based Complementary and Alternative Medicine. 2020*: 7436920. (Impact Factor 2020 = 2.40; SCOPUS SJR 2020 = Q1, Web of Sci JCR 2020 = Q3).